The Role of CS1 Fibronectin in HIV-1 Infection of $\alpha_4\beta_7^+$ T Lymphocytes

David Alan Plotnik

A dissertation

submitted in partial fulfillment of the

requirements for the degree of

Doctor of Philosophy

University of Washington

2018

Reading Committee:

Shiu-Lok Hu, Chair

Edward J. Kelly

Kelly K. Lee

Program authorized to offer degree:

Pharmaceutics

University of Washington

Abstract

The Role of CS1 Fibronectin in HIV-1 Infection of $\alpha_4\beta_7^+$ T Lymphocytes

David Alan Plotnik

Chair of the Supervisory Committee:

Shiu-Lok Hu, Ph.D.

Department of Pharmaceutics

A hallmark of Human Immunodeficiency Virus type 1 (HIV-1) pathogenesis is the profound depletion of $CD4^+$ T lymphocytes within gut-associated lymphoid tissues (GALT), and persistent immune dysfunction at mucosal sites. It has been demonstrated that gut-homing $CD4^+$ T cells expressing the $\alpha_4\beta_7$ integrin are preferentially targeted by HIV and play key roles in GALT pathology. Binding between the gp120 subunit of HIV envelope protein and $\alpha_4\beta_7$ has been described and is hypothesized to mediate preferential infection of $\alpha_4\beta_7^+$ T cells. However, it has also been reported that many HIV envelopes do not bind to $\alpha_4\beta_7$, and the role of gp120-$\alpha_4\beta_7$ interaction in HIV pathogenesis is controversial.

In this dissertation, I investigated the basis for HIV-$\alpha_4\beta_7$ interaction in detail. I discovered that gp120 does not bind to $\alpha_4\beta_7$ as previously reported. Instead, I discovered that

mammalian cell lines used to express recombinant gp120 also produced $\alpha_4\beta_7$–reactive isoforms of the extracellular matrix protein fibronectin. These fibronectins co-purified with gp120, and I characterized a method for separating gp120 from fibronectins. Furthermore, I showed that highly purified gp120 bound to CD4 but not to $\alpha_4\beta_7$. Significantly, I also discovered that fibronectins bound to both $\alpha_4\beta_7$ and gp120, and thus mediated indirect gp120-$\alpha_4\beta_7$ binding. These findings resolved the controversy regarding the biochemical basis of gp120-$\alpha_4\beta_7$ interaction, but also suggested that matrix-associated fibronectins may mediate HIV infection of $\alpha_4\beta_7^+$ T cells. Based on this, I developed *in vitro* assays to investigate the role of fibronectins in HIV infection. I discovered that fibronectins captured and delivered HIV preferentially to $\alpha_4\beta_7^+$ T cells, and also facilitated T cell activation and efficient cell-to-cell virus transmission. Finally, because $\alpha_4\beta_7$–reactive fibronectins are oncofetal proteins expressed in inflammation but not in healthy tissue, I investigated their expression in the context of infection. Using immunohistochemistry, I provided evidence that $\alpha_4\beta_7$–reactive fibronectins are expressed *in vivo* in GALT of SIV-infected macaques.

Collectively, these studies clarified the nature of HIV interactions with $\alpha_4\beta_7$, identified a novel role for fibronectins in HIV pathogenesis, and provided insight into how these interactions may be targeted therapeutically.

Table of Contents

List of Figures

List of Tables

List of Abbreviations

AIDS: Acquired Immune Deficiency Syndrome

APC: allophycocyanin

APTS: 9-Aminopyrene-1,4,6-trisulfonic acid

BSA: Bovine serum albumin

cART: combination anti-retroviral therapy

CE: Capillary electrophoresis

CHO: Chinese hamster ovary (cell line)

CCR5: C-C chemokine receptor type 5

CS1: connecting segment 1 (of fibronectin)

CXCR4: C-X-C chemokine receptor type 4

DC-SIGN: dendritic cell-specific intercellular adhesion molecule-3 grabbing non-integrin

DEAE: Diethylaminoethyl

DNA: Deoxyribonucleic acid

DPM: Decays per minute

DTT: Diothiothreitol

EDTA: Ethylenediaminetetraacetic acid

EdU: 5-ethynyl-2'-deoxyuridine

ELISA: Enzyme-linked immunosorbent assay

ER: Endoplasmic reticulum

FBS: Fetal bovine serum

FITC: Fluorescein Isothiocyanate

GALT: Gut-associated lymphoid tissues

GNA: *Galanthus nivalis*-conjugated agarose

GP120: "120 kilodalton glycoprotein", major subunit of HIV Envelope protein

HEK293: Human embryonic kidney 293 cells

HEPES: 4-(2-hydroxyethyl)-1-piperazineethanesulfonic acid

HIV: Human Immunodeficiency Virus-1

HRP: Horseradish peroxidase

IC_{50}: Half-maximal inhibitory concentration

ICAM-1: Intercellular adhesion molecule 1

LC: Liquid chromatography

LFA-1: lymphocyte function associated antigen-1

LTR: long terminal repeat

mAb: monoclonal antibody

MAdCAM: Mucosal Vascular Addression Cell Adhesion Molecule

MS: Mass spectrometry

MOI: Multiplicity of Infection

MMP: methyl-α-D-mannopyranoside

NHS: N-hydroxysuccinimide

PBMC: Peripheral blood mononuclear cell

PBS: Phosphate-buffered saline

PE: Phycoerythrin

PVDF: polyvinylidene difluoride

RNA: Ribonucleic Acid

rVV: Recombinant vaccinia virus

SDS-PAGE: Sodium-dodecyl sulfate polyacrylamide gel electrophoresis

SEC: Size-exclusion chromatography

SHIV: SIV/HIV chimeric virus

SIV: Simian Immunodeficiency Virus

$TCID_{50}$: Half-maximal tissue culture infective dose

T/F: Transmitted-founder viruses

TGFβ-1: Transforming growth factor β-1

TK: Thymidine kinase

V2: Second variable loop of the gp120 subunit of HIV envelope protein

VCAM-1: vascular cell adhesion molecule 1

Acknowledgements

I would first like to thank my advisor and mentor, Shiu-Lok. You invested so much of your time and effort in teaching me how to think about science. Our conversations and the lessons I've learned have had a profound impact on me, and will stay with me throughout my career.

I would additionally like to thank Jeffrey Schwartz, whom I worked with for seven years prior to graduate school. Thank you for giving me a start in science, and for the experiences and opportunities you afforded me. You also played a major part in shaping who I am as a scientist.

Thank you to the members of my committee: Rodney Ho, Nina Isoherranen, Ed Kelly, Kelly Lee, and Rheem Totah. Thank you for your guidance throughout my project, and for always pushing me to do better work. A special thanks to Ed Kelly and Kelly Lee for serving on my reading committee and investing the time to help me with this dissertation.

Thank you to all members of the Hu lab: Brad Cleveland, Wenjin Guo, Deborah Diamond, Rajesh Thippeshappa, Lifei Yang, Yun Li, Samantha Townsley, Patricia Firpo, Modou Mbowe, Heather Mack, Bing Mei, Baoping Tian, Taryn Urion, and Ryan Wallerstedt. Thank you for making the lab a great work environment and for helping me hone my skills.

Thank you to all of my other friends and colleagues from UW Radiation Biology and Radiology: Rob Jordan, Jason Rockhill, Ken Krohn, Kevin Yagle, Mark Muzi, Don Hamlin, Scott Wilbur, Bob Miyaoka, and Barb Lewellen. I learned so much from working with all of you throughout the years.

I would like to thank everybody from the Department of Pharmaceutics, both faculty and fellow students. I have learned something valuable from everyone, and feel privileged to have been part of such a talented group. Special thanks to my cohort for your friendship and support: Alenka Chapron, Jing Jing, Mike Liao, Eli Weber, and Vineet Kumar.

Thank you to friends and colleagues within the Medicinal Chemistry Department who contributed to this project: Dale Whittington and John Scott Edgar in the Mass Spectrometry facility, and to members of the Lee lab for allowing me use of your space and for teaching me analytical techniques. Special thanks to James Williams and Yu Liang for your help. Thanks as well to Miklos Guttman for the many discussions that contributed to this work.

Thank you to the lab of James Arthos at the National Institutes of Health. I sincerely appreciate the time you took to host me in your lab and teach me techniques, and for the many follow-up conversations that followed. Thank you to James Arthos, Claudia Cicala, Danlan Wei, Don Van Ryk, and Joe Hiatt.

Finally, I would like to thank my family. I could not have completed this project without the love and support of my wife Amy and my three boys Noah, Caleb, and Jacob. We have all made sacrifices in order to get me through graduate school. Thank you for all of your patience and understanding, and the accommodations you've made throughout the years.

Chapter 1

Introduction

HIV origins and epidemiology

In 1981 multiple cases of *Pneuomocystis carinii pneumonia* and Kaposi's sarcoma were documented in previously-healthy homosexual males in the United States[1, 2]. The following year, after the discovery of hundreds of similar cases, the Centers for Disease Control first described this disease as "Acquired Immune Deficiency Syndrome" (AIDS)[3]. In 1983, two retroviruses were identified as potential causes of AIDS: lymphadenopathy-associated virus (LAV)[4] and Human T-Cell Lymphotropic Virus-III (HTLV-III)[5]. Subsequently, LAV and HTLV-III were shown to be the same virus and the etiologic agent of AIDS[6], and the virus was renamed to "Human Immunodeficiency Virus" (HIV).

The origins of HIV have been traced to Simian Immunodeficiency Viruses (SIV), which are endemic in African non-human primates. Zoonotic transmissions of SIV into humans are believed to have occurred in the early 20th century in central Africa, in Cameroon and what is now the Democratic Republic of the Congo[7]. Through multiple independent cross-species introductions, different HIV lineages became established in human populations[8]. HIV-1 is the predominant lineage, and is further subdivided into four groups: M, N, O, and P[9]. Group M and N viruses have been traced to chimpanzees[10], while group O and P viruses have been traced to gorillas[11, 12]. HIV-2 is a separate lineage that is believed to have originated from sooty mangabeys[13]. HIV-2 and HIV-1 groups N, O, and P are mostly restricted to countries in central and West Africa, and account for approximately 5% of worldwide infections. HIV-1

group M is the lineage that has disseminated globally and is responsible for the current HIV epidemic.

After its introduction into human populations, HIV transmission was geographically restricted. In the period from 1920 to 1960, several factors contributed to the spread of HIV throughout central Africa, including the rapid growth of population centers, expanded railways, and an active sex trade[7]. Throughout this time, migrant labor likely contributed to the spread of HIV to South and Eastern Africa[14]. In the period from 1950 to 1980, increased international travel between Africa and other countries facilitated the global dissemination of HIV. While the exact details of HIV spread during this time are unclear, HIV likely reached the Western hemisphere by at least the 1960's. One interesting case in the medical literature that demonstrates this is the case of Robert Rayford, a teenager from Missouri who likely died of HIV/AIDS in 1969. Mr. Rayford was admitted to St. Louis City Hospital in 1968 with a severe immunosuppressive disorder, presenting with lymphedema, chlamydia, and Kaposi's sarcoma, and after a lengthy course of treatment his white blood cell levels declined and he died from pneumonia. Nearly two decades later, after the discovery of HIV, archived autopsy specimens from Mr. Rayford were analyzed and found to contain HIV-specific antibodies[15].

One consequence of the global spread of group M HIV-1 has been the diversification of this lineage into 9 distinct subtypes (A, B, C, D, F, G, H, J, and K)[16]. Circulating recombinant forms have also emerged, resulting from individuals co-infected with multiple HIV subtypes. Subtype C HIV-1 circulates primarily in sub-Saharan Africa and India, and accounts for nearly half of all global infections [17, 18]. Subtype B predominates in North and South America, Western Europe, and Australia[19], and subtype A is largely found throughout Russia and Eastern Europe[20]. Subtype A and B together account for roughly one-quarter of all global

infections. The circulating recombinant form CRF01_AE accounts for 5% of global infections, but has been extensively studied in the context of vaccine trials in Southeast Asia where this virus is prevalent[21]. Subtypes G, D, and CRF02_AG account for approximately 15% of global infections, and are largely restricted to central Africa. Each of the remaining subtypes and recombinant forms are relatively rare, and are also predominantly found in Africa.

From the 1980s to the present, the HIV epidemic has developed into one of the most serious threats to human health worldwide. By the end of 2015, approximately 78 million people had become infected with HIV, and AIDS-related illness claimed the lives of 35 million people (statistics from UNAIDS: [22]). Thus, research towards an HIV vaccine or cure remains a top global health priority.

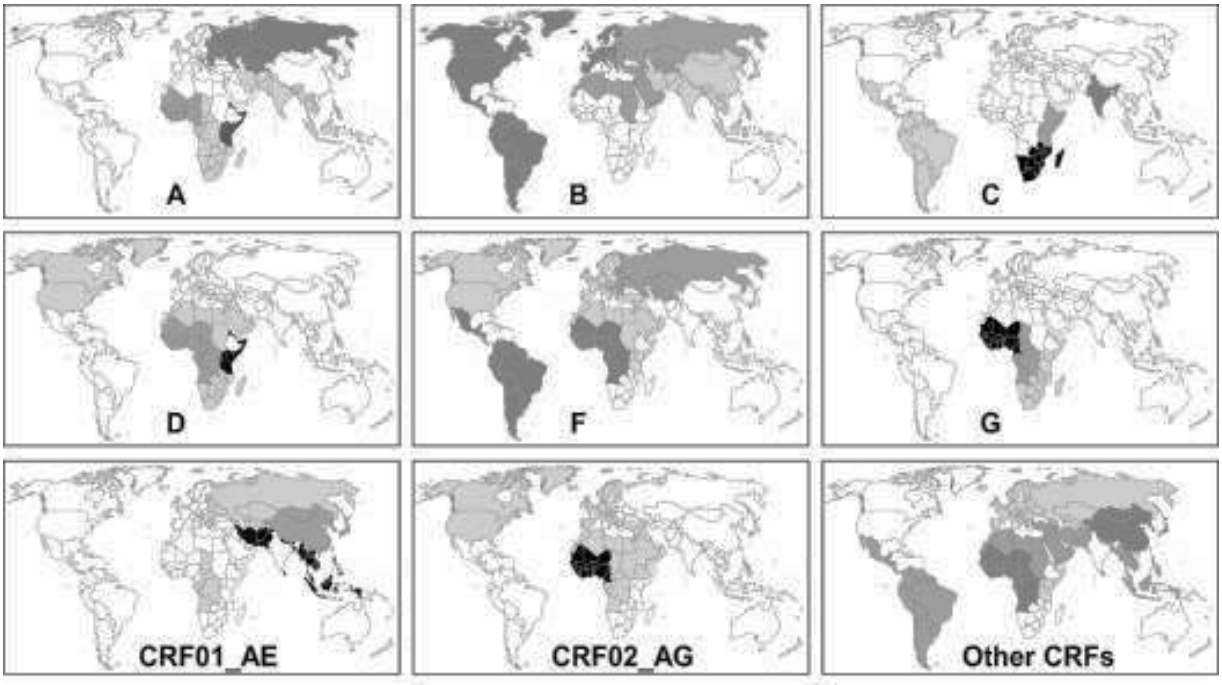

Figure 1-1: Global distribution of HIV-1 group M subtypes and recombinant forms 2004-2007. The degree of shading in each map indicates the proportion of global infections caused by each subtype or recombinant virus, with darker shading indicating a greater proportion. Adapted with permission from Hemelaar et al.[20].

HIV transmission and pathogenesis

HIV is transmitted by exposure to virus-containing blood or body fluids from an infected individual. There are two basic routes of transmission: mucosal and intravenous. Mucosal transmission occurs in a variety of scenarios, including sexual contact and exposure at cervico-vaginal, penile, and rectal sites[23, 24], maternal-fetal transmission during labor and delivery[25], or transmission to infants through breastfeeding by an infected mother[26]. The majority of HIV transmissions worldwide occur through sexual contact. The second most common route of transmission is through the use of contaminated needles by intravenous drug users[27]. Historically, blood transfusions were also a potential source of intravenous transmission, but this has been eliminated by modern blood bank screening practices[28].

The time between virus transmission and the appearance of detectable HIV ribonucleic acid (RNA) in the blood lasts approximately 5-10 days, and is termed the "eclipse phase". During this time viral genetic diversity is restricted. Mucosal transmission imposes a significant population bottleneck on HIV, because mucosal barriers block all but a few viruses from penetrating into tissue and seeding infection. This model of transmission is supported by single genome amplification studies of transmitted viruses, which found approximately 80% of infections resulted from a single virus[29]. It is also supported by studies of couples discordant for HIV infection status, which found low frequencies of transmission associated with mucosal exposures (infection in 0.08% of vaginal exposures and 1.4% of rectal exposures)[30, 31]. The main cells targeted by HIV are T lymphocytes expressing the CD4 receptor ($CD4^+$ T cells), and these are present at low numbers in mucosal portals of entry. For this reason, initial expansion of the virus population is limited and viruses develop into localized founder populations. This phenomenon has been experimentally observed in SIV infection of macaques, in which viruses

were primarily contained in small foci in the reproductive tract for 3-5 days following vaginal transmission[32]. The viruses during this early phase are collectively called "transmitted/founder" (T/F) viruses, and the biology of T/F viruses is believed to be important for vaccine development. Consequently, the genotypic and phenotypic signatures of T/F viruses correlated with transmission fitness has been a subject of intensive study[33-38].

At the end of the eclipse period, HIV disseminates through draining lymph nodes and invades lymphoid tissues throughout the body[39]. These include the gut-associated lymphoid tissues (GALT), which contain the majority of the body's $CD4^+$ T cells within Peyer's patches and lymphoid follicles[40-42]. Upon accessing large pools of activated $CD4^+$ T cells, HIV replication occurs at a high level, leading to rapid expansion and genetic diversification of the virus population. In the process, the virus depletes 80 to 90% of $CD4^+$ T cells within GALT, and 40 to 50% of peripheral $CD4^+$ T cells[43, 44]. The intestinal epithelium is also damaged through bystander effects, resulting in translocation of gut microbes into the intestinal lamina propria and the blood[45]. The combined effects of massive $CD4^+$ T cell depletion, immune dysregulation, and damage to intestinal epithelium all contribute to systemic immune activation. Collectively, the events described above encompass the acute phase, and occur during the first 2 to 4 weeks of infection. Acute infection is defined clinically by the sequential appearance of viral antigens and HIV-specific antibodies in the blood[46], a precipitous drop in peripheral $CD4^+$ T cells, and flu-like symptoms including fever, headache, sore throat, nausea, vomiting, and diarrhea[47, 48].

The second phase of HIV disease is the chronic phase, and is characterized by asymptomatic infection and slow progressive decline of peripheral $CD4^+$ T cells[49]. At the end of acute infection, the immune system gains a degree of control over the virus and establishes

quasi-equilibrium between virus replication and clearance. Consequently, plasma HIV stabilizes at a level referred to as the "viral set point". The set point varies between patients, and is partially correlated with clinical disease progression[50]. Peripheral $CD4^+$ T cells rebound, whereas intestinal $CD4^+$ T cells recover only minimally[47]. The failure of intestinal T cells to repopulate indicates that their regenerative capacity is either inherently slow, or that their regenerative capacity is severely damaged during the acute infection. While T cell levels and viremia stabilize, the systemic inflammation triggered during the acute phase fails to resolve and progressively worsens[51]. This persistent immune activation is thought to sustain virus replication by stimulating T cell proliferation, and is believed to be the primary factor driving loss of T cells through activation-mediated cell killing. Importantly, these effects contribute to the loss of central memory T cells, which are critical for replenishing effector T cell populations. The loss of central memory T cells over time erodes the regenerative capacity of the immune system and underpins the progressive decline of overall T cell levels. Activation-mediated cell death and low-level virus replication are factors that likely also contribute to the failure of intestinal $CD4^+$ T cells to repopulate, in addition to other factors including dysregulation of cytokines including IL-17.

The final stage of the disease occurs with the development of clinical AIDS. AIDS is defined by $CD4^+$ T cell counts of 200cells/mm^3 or less in peripheral blood, or the appearance of opportunistic infections. HIV viral load significantly escalates in the time leading to the onset of AIDS, and $CD4^+$ T cells are quickly depleted[49]. At this point, the immune system is exhausted and unable to control virus replication or replenish T cells. Immunodeficiency results, and leads to opportunistic infections including tuberculosis, pneumonia, candidiasis, toxoplasmosis, and cryptosporidiosis, as well as increased incidence of cancers including Kaposi's sarcoma,

leiomyosarcoma, and hematological malignancies[52-54]. HIV also mediates direct pathogenic effects, including central nervous system damage and AIDS-related dementia, wasting syndrome, and disorders of blood clotting[55-57]. Within a period of time ranging from several months to a few years, these opportunistic infections and complications lead to death.

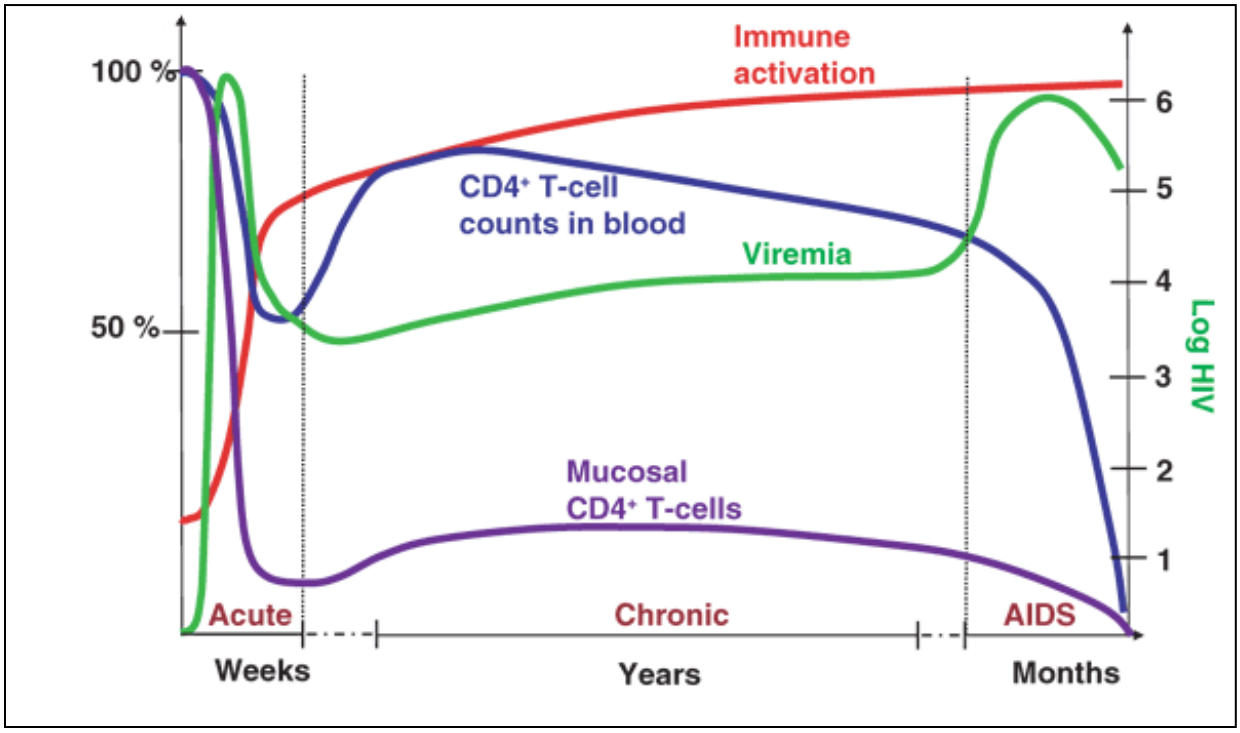

Figure 1-2. HIV-1 disease progression. The interplay between plasma viremia (green), immune activation (red), peripheral $CD4^+$ T cells (blue) and mucosal $CD4^+$ T cells (purple) throughout HIV-1 infection. Reproduced with permission from Grossman et al.[47].

The natural history of SIV infection in non-human primate species supports the hypothesis that persistent and elevated immune activation and GALT T cell depletion play key roles in HIV pathogenesis. In African non-human primate species that are natural hosts of SIV, including sooty mangabeys and African green monkeys, infection frequently does not result in AIDS[58-60]. Systemic inflammation in these animals resolves after 4 to 6 weeks of infection, and immune regenerative capacity remains intact, allowing for repopulation of $CD4^+$ T cells in peripheral and mucosal compartments. After the acute infection, these animals remain latently

infected but live normal lifespans without developing AIDS or SIV-related comorbidities. This non-pathogenic mode of infection is thought to be the result of millennia of co-existence between SIV and these animals, and – according to this hypothesis – HIV is highly pathogenic is because it was recently introduced into human populations. One key piece of evidence supporting this hypothesis is the AIDS-like pathogenesis observed after experimental introduction of SIV from their natural host (sooty mangabeys) to Asian macaques, including rhesus and pigtail macaques. Macaques are not natural hosts of SIV, and SIV in these animals produces highly pathogenic infection that resembles HIV disease in humans. Significantly, this includes severe depletion of intestinal $CD4^+$ T cells and chronic immune activation[61-64]. Thus, mucosal T cell depletion and immune activation are key features that distinguish pathogenic and non-pathogenic SIV infection, and are primary drivers HIV disease.

The HIV-1 lifecycle

In the current model of the HIV-1 replication cycle, the virus first attaches to specific receptors on the surface of $CD4^+$ T cells. All HIV viruses bind with high affinity to the CD4 receptor[65, 66]. In addition, HIV must bind to one of two co-receptors: C-C chemokine receptor type 5 (CCR5)[67-69] or C-X-C chemokine receptor type 4 (CXCR4)[70]. Based on co-receptor tropism, HIV-1 strains are designated as either R5-HIV-1 (CCR5-tropic) or X4-HIV-1 (CXCR4-tropic). Fusion of the virus and cell membranes is accomplished by conformational changes of envelope protein triggered by receptor binding. Following fusion, the virion uncoats and releases the viral capsid into the cell. Within the cytoplasm, the virus RNA genome is reverse-transcribed into double-stranded DNA by the virally-encoded enzyme reverse

transcriptase. Reverse transcriptase has a low degree of accuracy, and introduces approximately one mutation in every 1,700 nucleotides[71]. Because of this, HIV mutates significantly with each round of replication. After reverse transcription, the DNA genome complexes with virus and host cell proteins to form the pre-integration complex (PIC), and utilizes host cell nuclear import machinery to translocate into the nucleus[72]. This feature of the HIV lifecycle allows it to productively infect both resting and proliferating cells. Following nuclear import, the HIV genome permanently integrates into host cell DNA through the activity of the virally-encoded enzyme integrase. Host cell transcription machinery is then exploited to generate messenger RNA (mRNA) from the HIV genome, and viral mRNAs are exported to the cytoplasm to be translated. Viral proteins and genomic RNA assemble at the plasma membrane into new virions, which are released from the infected cell by budding. In the final step of the replication cycle after the release of immature virions from the cell, virally-encoded proteases cleave the precursor viral capsid proteins into their mature forms. The complete HIV-1 lifecycle is illustrated in Figure 1-3.

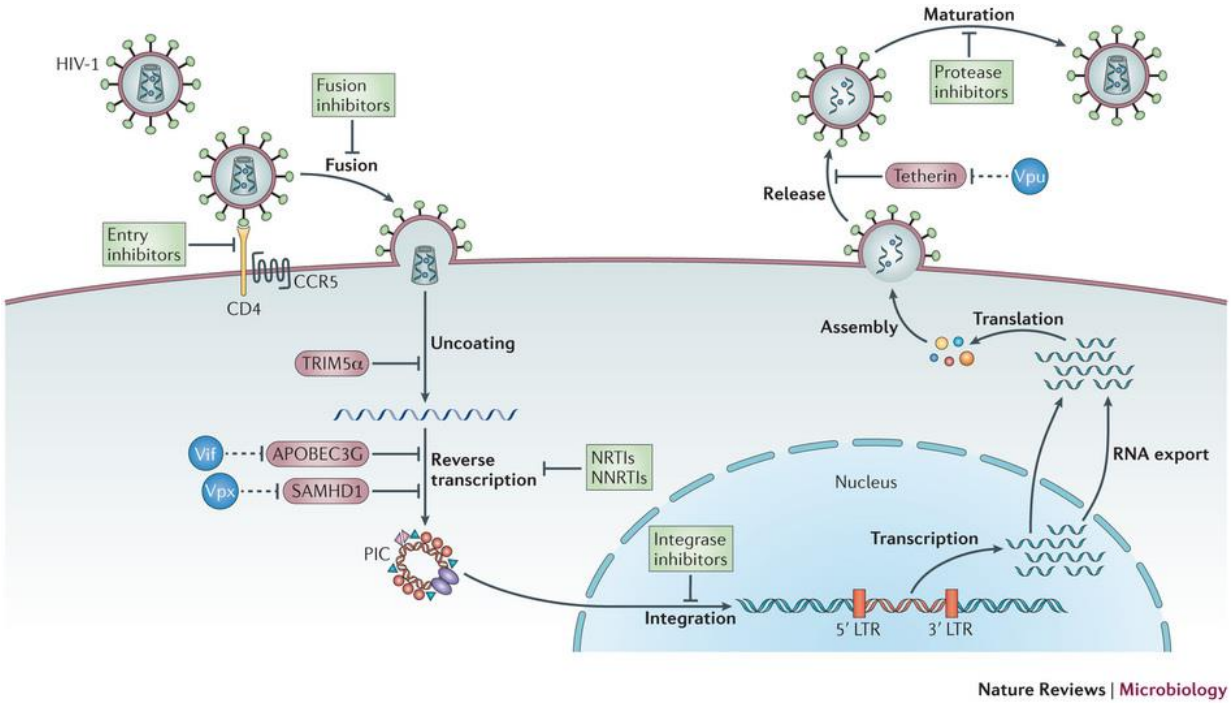

Figure 1-3. The HIV-1 lifecycle. The main steps of the HIV-1 lifecycle are illustrated. Green boxes indicate steps of the lifecycle targeted by antiviral drugs, and red boxes indicate steps targeted by host cell antiviral factors. Blue circles show viral accessory proteins that antagonize cellular antiviral factors. Adapted with permission from Barre-Sinoussi et al.[73].

In addition to initiating infection through cell-free viruses, direct transmission between HIV-infected and uninfected T cells has been described. In this mode of transmission, a virological synapse forms between an infected and uninfected T cell and facilitates the passage of viruses into the uninfected cell[74]. Virological synapse formation involves engagement of CD4 and chemokine co-receptors on the uninfected cell by HIV envelope protein expressed on the surface of the infected cell. Cellular factors involved in normal immunological synapse formation are then recruited to the site of cell-cell contact. These include the integrin receptor lymphocyte function associated antigen-1 (LFA-1) and its binding partner intercellular adhesion molecule 1 (ICAM-1). Through the LFA-1/ICAM-1 interaction, rearrangements of the actin cytoskeleton take place and the secretory apparatus of the infected cell polarizes to the

synapse[75]. Progeny viruses then bud into the synapse and are efficiently internalized by the uninfected cell[76]. The structure of a virological synapse is illustrated in Figure 1-4.

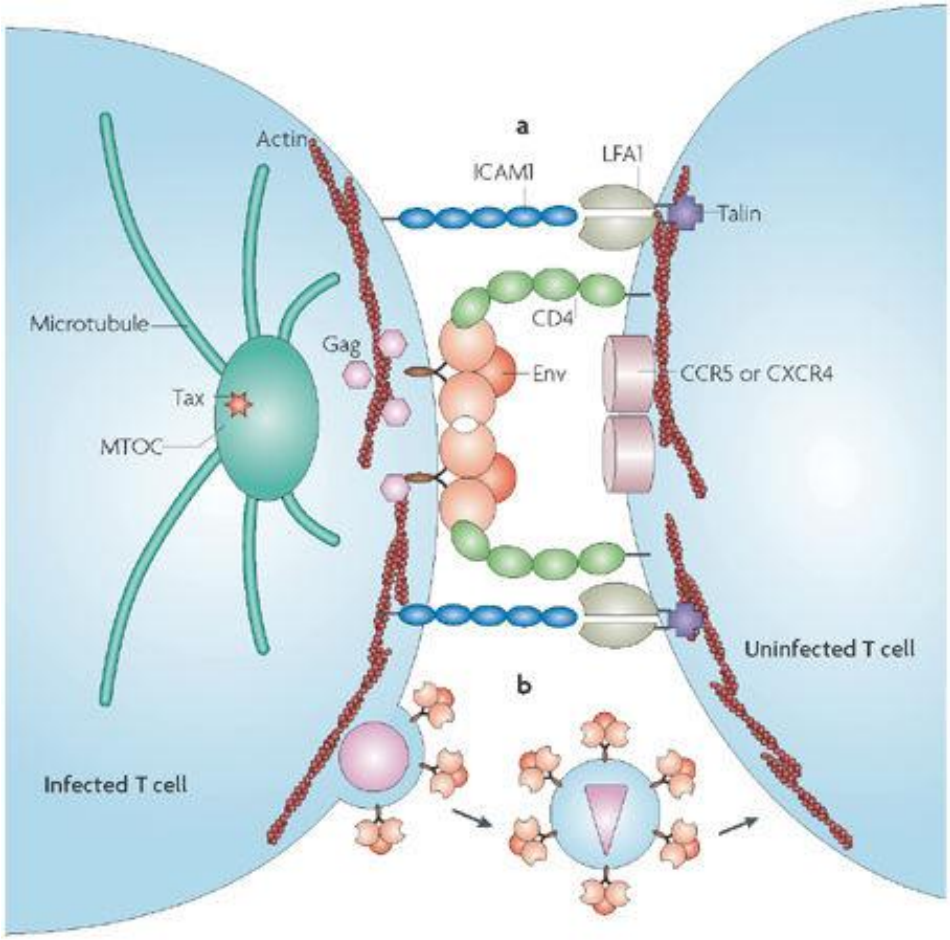

Figure 1-4. Structure of a virological synapse. A hypothetic synapse between an infected cell (left) and uninfected cell (right). The synapse is stabilized by HIV envelope interactions with CD4 and coreceptors, as well as LFA-1/ICAM-1 interactions. Rearrangements of the actin cytoskeleton polarize the secretory apparatus, including the microtubule organizing center (MTOC) to the synapse. Adapted with permission from Sattentau[77].

Cell to cell virus transmission differs from cell-free transmission in several important ways. Cell to cell transmission is estimated to be 10- to 100-fold more efficient, and may be the predominant mode of viral spread in lymphoid tissues[78-80]. Cell to cell transmission is also resistant to neutralizing antibodies and some antiviral drugs, which may contribute to the ability

of HIV-1 to replicate in the presence of these agents[81-84]. Cell to cell transmission frequently results in cell killing instead of productive infection, and this may be a primary cause of rapid T cell depletion in lymphoid tissues. The mechanism for cell killing is attributed to a high multiplicity of infection (MOI) in cell to cell transmission, which triggers cytosolic sensors of viral genetic material and leads to pyroptosis[85]. In support of this, pyroptosis has been identified as a key pathway activated during acute infection that mediates T cell depletion and systemic inflammation[86, 87].

Current HIV treatment relies on the use of combination antiretroviral therapy (cART), targeting multiple stages of the virus lifecycle with different classes of drugs (summarized in Table 1-1 and Figure 1-3). Current cART regimens contain three drugs from two or more classes, with the clinical goal of long-term viral suppression without generating drug-resistant HIV strains. Regardless of the treatment regimen, no known combination of drugs is able to fully clear an established HIV infection. This is partially due to latent reservoirs of virus that persist in long-lived central memory T cells, or other physiological compartments including the male reproductive tract and central nervous system[88]. Additionally, cART regimens do not resolve systemic inflammation or lead to replenishment of mucosal $CD4^+$ T cell populations, and these two factors are linked with viral persistence[44, 89].

Table 1-1. Summary of Antiretroviral Drugs.

Drug Class	Representative Drugs
Fusion and Entry inhibitors	enfuvirtide, maraviroc
Nucleoside/ Nucleotide reverse transcriptase inhibitors (NRTI)	zidovudine, lamivudine, abacavir, tenofovir, emtricitabine
Non-nucleoside reverse transcriptase inhibitors (NNRTI)	nevirapine, delavirdine, efavirenz, etravirine, rilpivirine
Integrase inhibitors	raltegravir, dolutegravir, elvitegravir
Protease inhibitors	ritonavir, saquinavir, nelfinavir, amprenavir, fosamprenavir, tipranivir, darunavir

Classes of antiretroviral drugs targeting different phases of the HIV-1 lifecycle are summarized with representative drugs from each class (reviewed by Cihlar and Fordyce[90]).

Structure and regulation of the HIV-1 genome

The genome of HIV-1 consists of two copies of single-stranded positive-sense RNA. The genome is relatively small (approximately 9,800 nucleotides), and encodes nine genes divided into three functional categories. These are the structural genes *gag* (group specific antigens), *po1* (polymerase), and *env* (envelope glycoprotein); regulatory genes *tat* (trans-activator of transcription) and *rev* (regulator of virion); and the accessory genes *nef* (negative factor), *vif* (viral infectivity factor), *vpu* (viral protein U), and *vpr* (viral protein R)[91]. These genes are organized into overlapping reading frames, and flanked by long-terminal repeats (LTRs) at either end of the genome (Figure 1-5). Transcription is initiated at the 5' LTR, and alternative splicing generates a variety of mRNA molecules, including both fully spliced and partially spliced transcripts. The interplay between these transcripts and host cell nuclear export machinery regulates the time-course of viral gene expression. Early after integration, intron-containing precursor mRNA is prevented by host cell control mechanisms from exporting to the cytoplasm. Thus, only fully-spliced transcripts encoding *tat*, *rev*, and *nef* are exported after integration. Tat

and Rev proteins accumulate in the cell first, and then enter the nucleus. Tat binds to the 5' LTR and initiates high-level transcription, while Rev binds to a structure called the Rev-response element (RRE) on intron-containing viral RNA. Rev-RNA complexes are able to bypass nuclear export controls, which allows partially-spliced and unspliced RNA to enter the cytoplasm[92]. Subsequently, during later stages of infection, the remaining HIV proteins are translated from these larger RNA molecules, and unspliced RNA is packaged as new genomes into progeny virions.

All three structural genes *gag*, *pol*, and *env* encode polypeptides which are further processed into functional proteins by cellular and viral proteases. The Gag polypeptide is translated from unspliced RNA, and becomes packaged into budding virions. Maturation proteases cleave Gag into MA (matrix, p17), CA (capsid, p24), NC (nucleocapsid, p9), and p6. These proteins form the internal structure of the virus, direct packaging of the genome within the capsid, and associate with the genome to facilitate reverse transcription and nuclear import in subsequent infection cycles. A Gag-Pol precursor protein is also translated from unspliced RNA, and arises from a ribosomal frame-shift that occurs in approximately 5% of translation events. Proteins encoded by *pol* are therefore 20 times less abundant than *gag* gene products[93]. Pol is cleaved to produce the virally-encoded enzymes Pro (protease, p10), RT (reverse transcriptase, p50), RNAse H (p15), and IN (integrase, p31). The RT and RNAse H enzymes are frequently not cleaved, and linked together in a functional polyprotein (p65). The Env precursor protein (gp160) is produced from singly-spliced RNA, and encodes the virus envelope protein. Env is translated in the endoplasmic reticulum (ER) and processed through the Golgi complex, where it is cleaved by the cellular protease furin into a transmembrane protein (gp41) and a surface antigen (gp120). Heterodimers of transmembrane protein and surface antigen are formed

through non-covalent interactions, and mature envelope proteins are composed of a trimeric arrangement of these heterodimers. Envelope protein is expressed on the cellular plasma membrane, where it becomes incorporated into the envelopes of budding viruses.

The accessory genes *nef*, *vif*, *vpu*, and *vpr* all encode virulence factors that are necessary for HIV-1 replication *in vivo*. Nef protein is translated from fully-spliced transcripts, and appears early in infection. Nef downregulates cellular CD4 expression in order to facilitate virus assembly and budding, and also downregulates expression of class I major histocompatibility complex (MHC) to protect the cell from attack by cytotoxic T lymphocytes[94]. The remaining accessory proteins are translated from singly-spliced transcripts and appear later in infection. Vpr binds to the viral genome and facilitates nuclear import of the PIC in subsequent rounds of infection[95]. Vif plays an important role in degrading and eliminating the cellular antiviral protein apolipoprotein B mRNA editing enzyme (APOBEC), which is a cytidine deaminases that introduces lethal levels of mutations into viral RNA. Vpu antagonizes another cellular antiviral protein called tetherin, which normally prevents the release of budding viruses from the cell[96]. Vpx is an additional accessory protein encoded by HIV-2 and SIV, but not by HIV-1. Analogous to the Vif-APOBEC interaction, Vpx triggers the degradation of the cellular antiviral protein SAMHD1. The function of SAMHD1 is to reduce pools of cytoplasmic nucleotides needed to support virus replication[97].

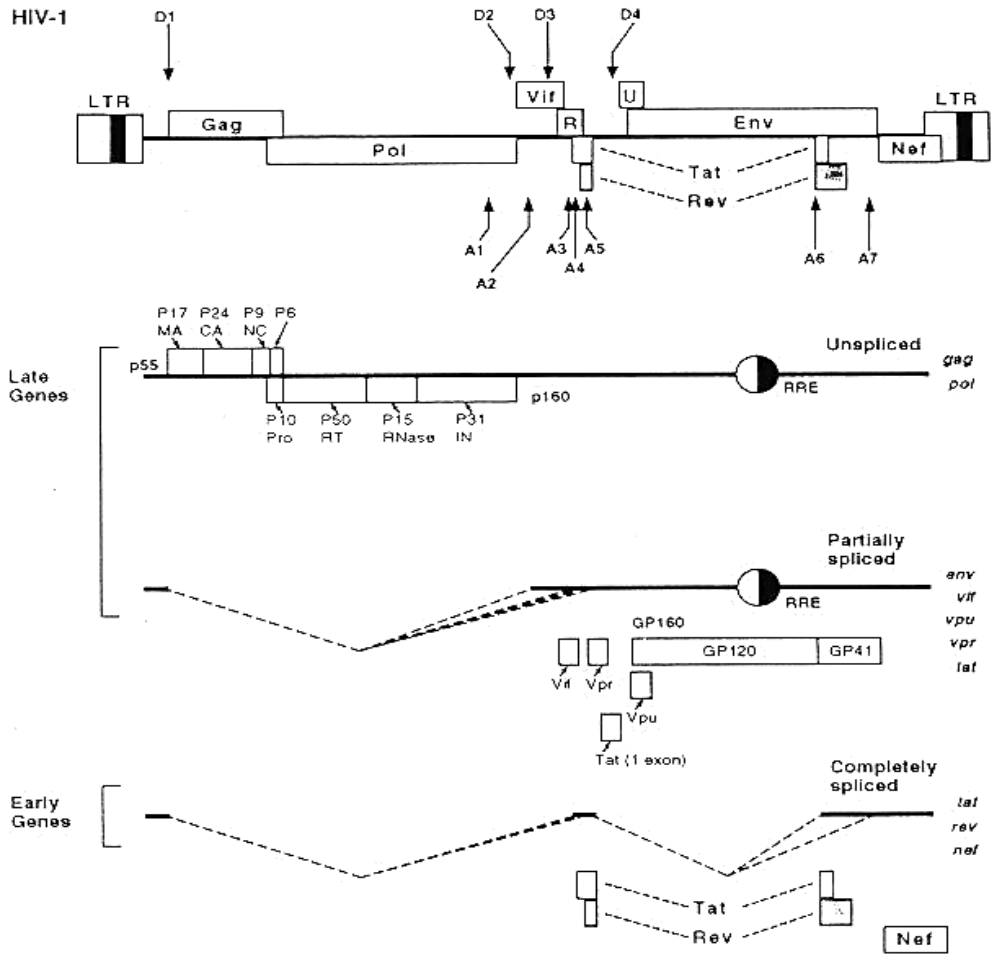

Figure 1-5. Structure and regulation of the HIV-1 genome. The HIV-1 genome is composed of overlapping reading frames (top). Splice donor (D1-4) and acceptor (A1-7) sites are indicated. RNA processing into unspliced, partially spliced, or completely spliced transcripts results in temporal regulation of gene expression, as indicated. Reproduced with permission from the University of California San Francisco HIV InSite Webpage[98].

HIV envelope protein – structure and function

HIV envelope is the only virally-encoded protein present on the surface of virions, and mediates the first critical steps of the virus lifecycle – attachment and entry into target cells. Mature HIV envelopes are commonly referred to as "envelope spikes", and are composed of a trimer of gp120-gp41 heterodimers. As summarized above, the envelope protein precursor gp160 is synthesized in the ER and further processed in the Golgi complex. Within the Golgi,

cellular furin and furin-like enzymes cleave gp160 at the K/R-X-K/R-R amino acid motif into the soluble gp120 subunit and membrane-associated gp41 subunit[99, 100]. While gp120 and gp41 are separate, they remain associated through noncovalent protein-protein interactions. In addition to proteolytic cleavage, substantial glycosylation and disulfide bonding occur within the ER-Golgi.

Glycans account for approximately half of the molecular weight of HIV envelope protein, and are required for infectivity[101]. Within the ER, 25 to 30 N-linked and O-linked glycans are added to Env. N-linked glycans are added at sites of the canonical glycosylation sequon N-X-S/T (where X is any amino acid other than proline)[102]. The ER transfers immature high-mannose (oligomannose) glycans to these sites, which are then modified into complex and hybrid glycans by enzymes in the Golgi. Because of steric constraints imposed by high glycan density and Env trimerization, some sites are not accessible to Golgi enzymes and remain in oligomannose form[103]. The utilization of any particular glycosylation site (i.e. whether or not a glycan is added) and the types of glycans present are partially controlled by rates of protein trafficking through the ER-Golgi system and the pools of carbohydrates available within the Golgi[104]. In general, rapid rates of protein synthesis and conditions of cellular stress result in a higher frequency of oligomannose glycans, and slower rates of synthesis produce more processed glycans. Several studies have shown that the majority of glycans on virus-associated envelopes are oligomannose[105, 106]. Collectively, the glycans form a "shield" around envelope protein, and restrict the immune system from accessing conserved epitopes such as the CD4 or co-receptor binding sites[107]. Consistent with this, exposure of epitopes including the CD4 binding site can be modulated by removing individual glycans[108, 109]. Additionally,

while glycans generally protect Env from immune attack, some oligomannose glycans are themselves immunogenic and targeted by neutralizing antibodies[110, 111].

Along with the glycan shield, hypervariable loops at the surface of Env contribute to immune evasion. Envelope protein is divided into 5 variable (V1 to V5) and 5 conserved (C1 to C5) domains[112, 113] (Figure 1-6). Most of the variable domains form into loops through intramolecular disulfide bonds[114]. The variable loops tolerate large changes in length, glycan content, and amino acid composition without adversely impacting Env function. They are also highly immunogenic and elicit large amounts of non-neutralizing antibodies, and thereby 'distract' the immune system from generating neutralizing antibodies. The variable loops 1 to 3 (V1, V2, and V3, respectively) associate together at the apex of the Env trimer, and play roles in occluding both the CD4 and co-receptor binding sites[115]. The CD4 binding site is a conformational epitope, formed by portions of the C1, C3, and C4 domains[116, 117]. The co-receptor binding sites are located within the V3 loop, and are masked by the V1/V2 loops in the unliganded Env trimer[118, 119]. During virus attachment, the V1/V2 and V3 loops rearrange to allow for sequential binding to CD4 and co-receptor[120]. Subsequently, the gp41 subunit becomes exposed and the gp41 fusion peptide is inserted into the host cell membrane. This triggers the refolding of gp41 into a stable intermediate, called the six-helix bundle formation, which drives fusion of virus and cell membranes[121].

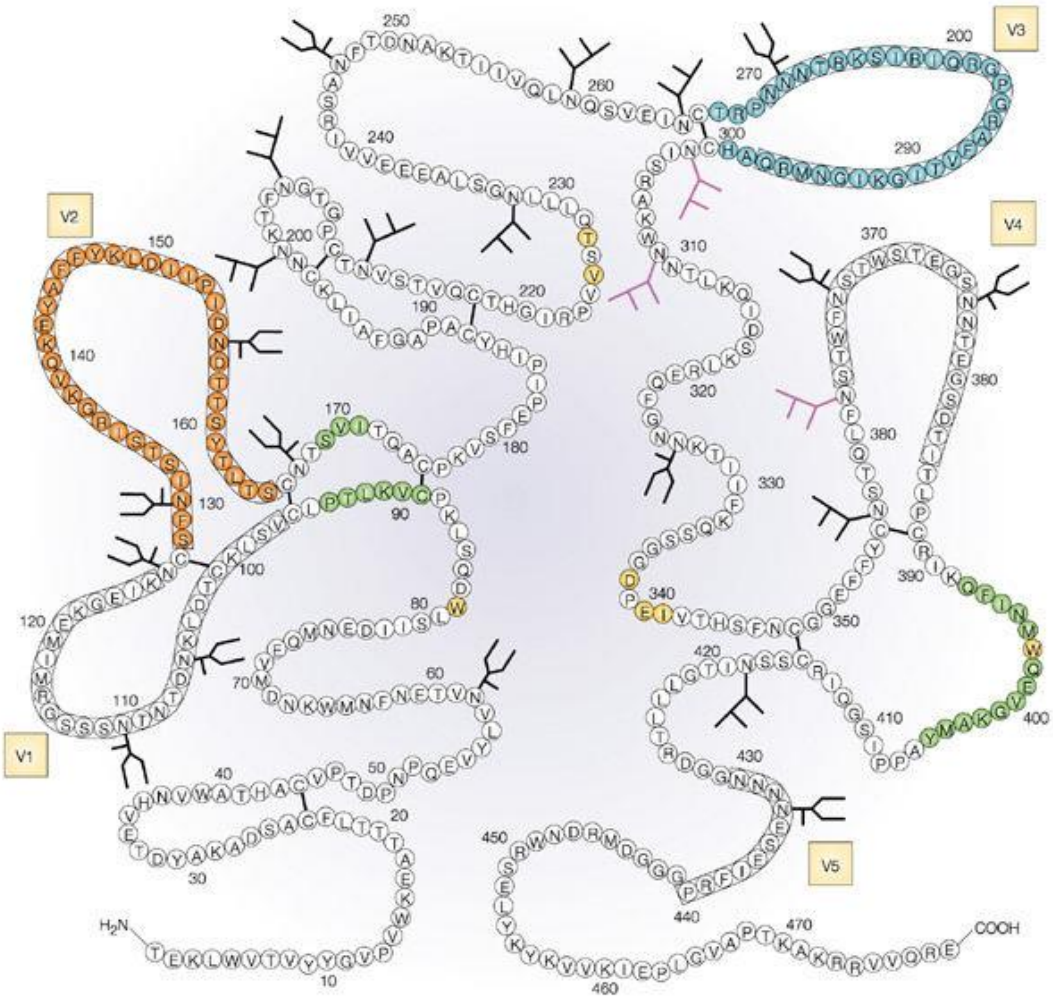

Figure 1-6. The primary structure of HIV-1 gp120. The linear amino acid sequence of gp120 is constrained by 9 disulfide bonds. White boxes indicate positions of the five variable loops (V1-V5). Locations of oligomannose glycans are indicated by black branched structures, hybrid glycans by purple branched structures, and complex-type glycans by U-shaped structures. Reproduced with permission from Zolla-Pazner[122].

In addition to CD4 and the co-receptors CCR5 and CXCR4, HIV envelopes interact with a variety of other cellular receptors. None of these interactions are required for infectivity of $CD4^+$ T cells, but may play roles in other aspects of virus biology *in vivo*. Through variations in the sequence of the V3 loop, Env has been shown to utilize additional chemokine co-receptors, including CCR1, CCR3, CCR8, and CXCR6[123-125]. These co-receptors may play a role in

infection of additional cell types, including macrophages, monocytes, myeloid dendritic cells, microglia, and astrocytes[126-129]. Several cellular receptors act as attachment factors and capture HIV on the cell surface without allowing virus internalization. These cell-captured viruses are then transferred to T cells through a process called *trans*-infection. The main receptor mediating *trans*-infection is dendritic cell-specific intercellular adhesion molecule-3 grabbing non-integrin (DC-SIGN), a C-type lectin that binds to oligomannose glycans on Env[130, 131]. Siglec-1, a sialic acid-binding lectin on dendritic cells[132], and CD21, a complement receptor expressed on B cells[133] have also been shown to mediate *trans*-infection. Granulocytes have additionally been reported to capture HIV through cell-surface heparan sulfate proteoglycans and DC-SIGN, and mediate *trans*-infection[134]. In addition to participating in *trans*-infection, cell-associated heparan sulfate proteoglycans have been proposed to play a role in virus internalization on $CD4^+$ T cells[135].

HIV envelope protein also interacts with several extracellular matrix proteins, including fibronectin, laminin, and heparan sulfate proteoglycans[136, 137]. The nature of HIV interactions with these proteins, and their potential biological significance has not been extensively studied. Recombinant gp120 and gp160 proteins have been shown to attach to a heparin binding site within fibronectin, and one early report indicated that fibronectin functions as an innate antiviral protein and inhibits HIV-1 infection[136]. However, later studies found that matrix-associated fibronectin captures HIV and facilitates infection of T cells, in a mechanism analogous to *trans*-infection[138, 139]. No studies are reported in the literature on the potential role of matrix-associated laminins or proteoglycans on infection.

Integrins and the immune system

Integrins are a superfamily of receptors that mediate cell adhesion to the extracellular matrix, cell-to-cell adhesion, and signaling. Structurally, integrins are heterodimers formed by the association of two chains, designated α and β chains. Each integrin chain is a single-pass membrane protein with a short cytoplasmic tail and multiple extracellular domains, and αβ dimerization occurs through non-covalent interactions between the extracellular domains. 18 α chains and 8 β chains have been described in humans, and these combine to generate 24 distinct heterodimers[140] (Figure 1-7).

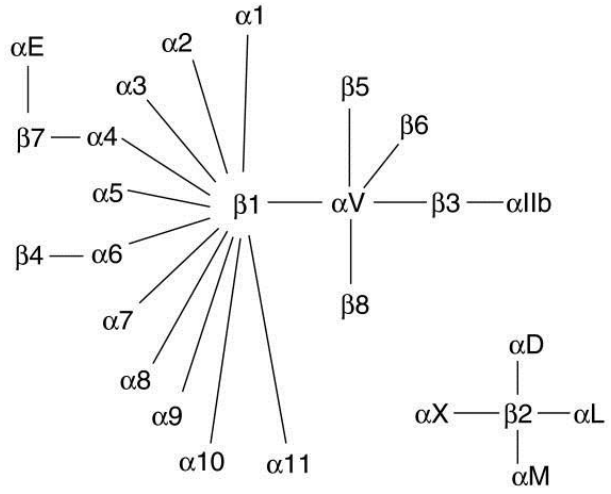

Figure 1-7. The human integrin superfamily. In humans 18 α chains and 8 β chains combine as indicated to generate 24 distinct αβ integrin heterodimers. Reproduced with permission from Takada et al.[140].

While each integrin binds to a unique set of ligands, all integrins function in the same way. In their unliganded state, integrins oscillate rapidly between closed and extended conformations. In the closed conformation, the extracellular domains fold into a compact globular structure and the cytoplasmic tails associate with each other. In the extended conformation, the extracellular domains stretch away from the cell and the chains move apart to

separate the cytoplasmic tails[141] (Figure 1-8). The extended conformation exposes binding sites for both extracellular and intracellular ligands, and binding to these ligands stabilizes the extended conformation. Because of this property, integrins mediate bi-directional signaling referred to as either inside-out or outside-in signaling[142]. With inside-out signaling, intracellular binding to the cytoskeleton stabilizes the extended conformation and increases receptor affinity for extracellular ligands. With outside-in signaling, attachment to extracellular ligands induces the cytoplasmic tails to bind components of the cytoskeleton, including talin and actin. This induces a rearrangement of the cytoskeleton, resulting in clustering of integrins and the formation of a focal adhesion[143]. The cytoplasmic tails of activated integrins also recruit and activate a variety of kinases, including focal adhesion kinase (FAK), integrin-linked kinase (ILK), and Src-family protein tyrosine kinases.

Integrins play a major role in leukocyte homing to specific tissues. These homing interactions are important for normal immune cell migration, as well as recruitment of leukocytes to sites of injury or inflammation[144]. The $\alpha_4\beta_7$ integrin is expressed on subsets of T cells and mediates trafficking to GALT through binding to mucosal vascular addressin cell adhesion molecule 1 (MAdCAM-1), which is expressed almost exclusively within GALT[145, 146]. The chemokine receptor CCR9 also plays a role in cell homing to GALT and is co-expressed with $\alpha_4\beta_7$[147]. T cell expression of both $\alpha_4\beta_7$ and CCR9 is imprinted by exposure to all-trans retinoic acid, which is synthesized by gut-resident dendritic cells. Two additional leukocyte integrins are related to $\alpha_4\beta_7$: $\alpha_4\beta_1$, which is the only other integrin to utilize the α_4 chain; and $\alpha_E\beta_7$, which is the only other integrin to utilize the β_7 chain (see Figure 1-7). $\alpha_E\beta_7$ is an additional gut-homing receptor, and mediates cell homing to mucosal epithelia by binding to E-cadherin[148]. $\alpha_E\beta_7$ plays a major role in dendritic cell homing to the gut, and is also found on intraepithelial T

lymphocytes. $\alpha_4\beta_1$ (also called very late antigen 4, VLA-4) binds to vascular cell adhesion molecule 1 (VCAM-1) and fibronectin, and plays roles in hematopoiesis and immune cell infiltration to inflamed tissue[149]. Similar to VLA-4, $\alpha_4\beta_7$ also binds to VCAM-1 and fibronectin. Through the α_4 chain, both $\alpha_4\beta_7$ and $\alpha_4\beta_1$ recognize unique motifs within their ligands, including LDV (leucine-aspartic acid-valine) in fibronectin[150], LDT (leucine-aspartic acid-threonine) in MAdCAM-1[151], or IDS (isoleucine-aspartic acid-serine) in VCAM-1[152]. Every other type of integrin recognizes a canonical RGD (arginine-glycine-aspartic acid) motif[153].

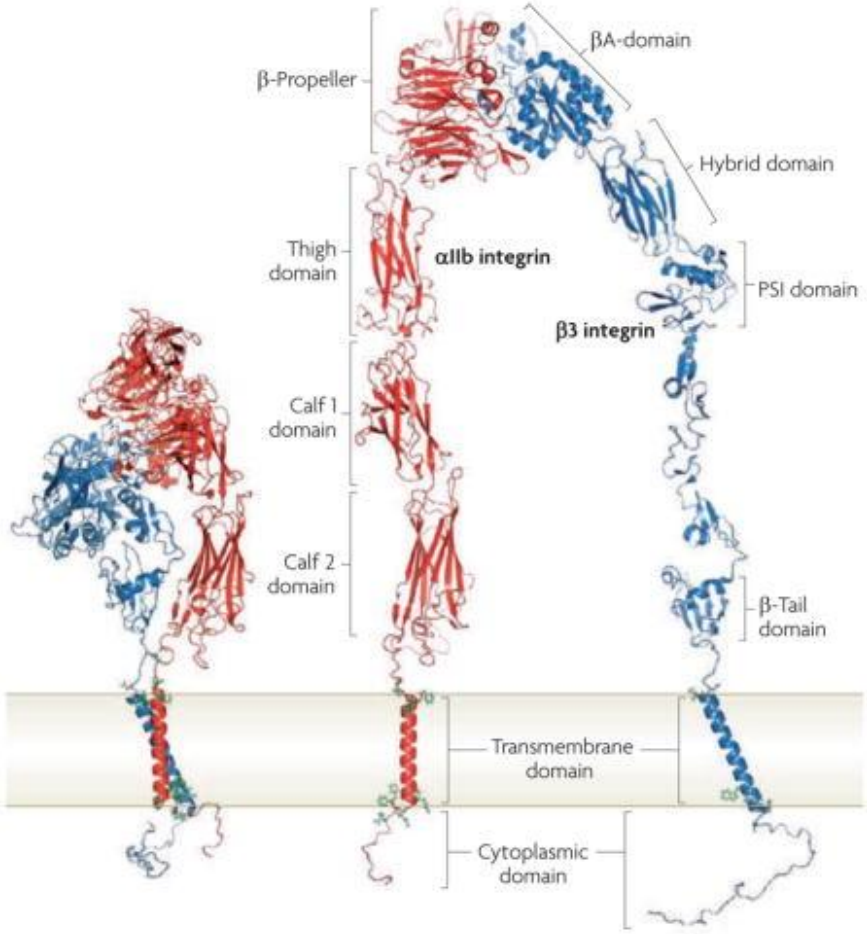

Figure 1-8. Integrin structural dynamics. The $\alpha_{IIb}\beta_3$ integrin is depicted, with α_{IIb} chain in red and β_3 chain in blue. Left: the closed conformation, right: the extended open conformation. Reproduced with permission from Shattil et al.[154].

The role of $\alpha_4\beta_7$ integrin in HIV-1 pathogenesis

$CD4^+$ T lymphocytes that also express $\alpha_4\beta_7$ ($CD4^+\alpha_4\beta_7^+$ T cells) have been shown to be preferential targets for HIV-1 infection both *in vivo* and *in vitro*. $CD4^+\alpha_4\beta_7^+$ T cells are reported to be selectively depleted in HIV-infected patients relative to other $CD4^+$ T cell subsets, and fail to repopulate with cART[155]. Selective loss of $\alpha_4\beta_7^+$ cells from peripheral and intestinal sites has also been observed in SIV infection of rhesus macaques[156-158]. A study by Cicala et al. demonstrated that $\alpha_4\beta_7^+$ T cells are preferentially infected *in vitro*, and that $\alpha_4\beta_7^+$ cells support 15-fold greater levels of virus replication than $\alpha_4\beta_7^-$ cells[159]. This same study also showed that $\alpha_4\beta_7$ expression correlates with cell activation and proliferation, and identified these as factors contributing to high-level replication in $\alpha_4\beta_7^+$ cells.

Because of their gut-homing properties, infected $\alpha_4\beta_7^+$ T cells are hypothesized play a role in HIV spread from mucosal portals of entry to GALT. In support of this, correlations have been observed between HIV-1 sexual transmission rates and levels of $\alpha_4\beta_7^+$ T cells in cervical[160] and foreskin[161] tissues. Within GALT, $\alpha_4\beta_7^+$ T cells may play a role in the rapid spread of HIV and depletion of intestinal T cells. In humans, up to 70% of intestinal T cells express $\alpha_4\beta_7$[162]. Interestingly, similar levels are found in rhesus and pigtail macaques, while only approximately 47% of sooty mangabey intestinal T cells express $\alpha_4\beta_7$[163]. These differences in $\alpha_4\beta_7^+$ T cell frequencies correlate with SIV/HIV pathogenicity observed in these species. In total, several lines of evidence implicate $\alpha_4\beta_7^+$ T cells in the ability of HIV to access GALT and replicate there efficiently, and suggest $\alpha_4\beta_7^+$ cells play a key role in mucosal T cell depletion.

In 2008, a pivotal study published by Arthos et al. described a binding interaction between HIV envelope protein and $\alpha_4\beta_7$, and proposed this as a mechanism mediating preferential infection of $\alpha_4\beta_7^+$ T cells[164]. Envelope binding to $\alpha_4\beta_7$ was demonstrated using recombinant gp120 in an *in vitro* cell binding assay, with cells that express $\alpha_4\beta_7$ but not CD4. With this assay gp120 from multiple HIV isolates was shown to bind to these cells, and binding was inhibited by $\alpha_4\beta_7$–directed antibodies and peptides[164]. This same work proposed the tripeptide motif LDV/I (leucine-aspartic acid-valine/isoleucine) in the V2 loop as an $\alpha_4\beta_7$ binding site within Env. LDV/I is thought to be a structural mimic of $\alpha_4\beta_7$ binding sites in fibronectin, MAdCAM-1, and VCAM-1. This type of integrin mimicry has been observed in envelope and capsid proteins from other virus families[165]. Interestingly, capsid proteins of Rotavirus, another gut-tropic virus, have been shown to bind to both $\alpha_4\beta_7$ and $\alpha_4\beta_1$ through LDV/I motifs[166]. Furthermore, the LDV/I motif is conserved in the vast majority of HIV envelopes despite being located in a hypervariable loop[167], and is positioned at the apex of the Env trimer where it is hypothesized to be accessible for binding. The role of V2 in $\alpha_4\beta_7$ binding was supported by later studies that showed V2 peptides bind to $\alpha_4\beta_7$[168, 169]. Additionally, it was shown that structural modifications to V2 modulate gp120 reactivity with $\alpha_4\beta_7$[170]; specifically, that shortened V2 loops and the removal of N-linked glycans within V2 resulted in up to 10-fold enhancement of gp120-$\alpha_4\beta_7$ binding. These structural features are commonly found in T/F viruses, and this therefore led to the hypothesis that $\alpha_4\beta_7$ reactivity is an important feature of the T/F phenotype.

Env-$\alpha_4\beta_7$ engagement has been hypothesized to enhance infection either by enhancing virus attachment or through $\alpha_4\beta_7$–mediated signaling. Env-$\alpha_4\beta_7$ binding *in vitro* has been shown to mediate outside-in signaling through $\alpha_4\beta_7$, leading to rapid activation of LFA-1[164]. This

mechanism is hypothesized to predispose $\alpha_4\beta_7^+$ cells to efficient cell to cell virus transmission (see Figure 1-4). Separately, $\alpha_4\beta_7$ and CD4 have been shown through Förster resonance energy transfer (FRET) and immunoprecipitation experiments to form a complex, and based on this a model of sequential $\alpha_4\beta_7$ and CD4 binding has been proposed. Subsequent studies have found that $\alpha_4\beta_7$–blocking antibodies and peptides do not inhibit virus attachment to cells[171-173], and based on this the hypothesis of enhanced infection through $\alpha_4\beta_7$–mediated signaling is preferred.

Despite the body of literature supporting gp120-$\alpha_4\beta_7$ binding, this interaction has become a subject of controversy. A 2014 study by Perez et al. failed to detect $\alpha_4\beta_7$ reactivity in a panel of 20 HIV envelope proteins, and concluded that $\alpha_4\beta_7$ binding may be an isolate-specific phenomenon[172]. Another study found that $\alpha_4\beta_7$–blocking antibodies did not inhibit HIV-1 infection *in vitro*, and called into question the biological significance of recombinant gp120 interactions with $\alpha_4\beta_7$[173]. Another study found that LDV stabilizes the global conformation of gp120, which suggests that LDV/I may be highly conserved for this reason and not because of its proposed role in $\alpha_4\beta_7$ binding[174]. Finally, several studies reported that T/F viruses do not replicate more efficiently in $\alpha_4\beta_7^+$ cells than $\alpha_4\beta_7^-$ cells, which casts doubt on the importance of $\alpha_4\beta_7$ reactivity in the T/F phenotype[175, 176]. In total, the preferential infection of $\alpha_4\beta_7^+$ cells is reasonably well-established, but the role of Env-$\alpha_4\beta_7$ interaction in mediating this preferential infection is not clear.

Vaccine and treatment strategies targeting HIV-$\alpha_4\beta_7$ interaction

Since 1987, over 50 candidate HIV vaccines have been studied in more than 100 clinical trials, and of these five large-scale clinical efficacy trials have been conducted. Two paired

AIDSVAX trials from 1998-2003 used gp120 protein as an immunogen to generate anti-HIV humoral responses[177]. Later in the 2005-2007 STEP trial, a recombinant adenovirus immunogen was used to generate cell-mediated immune responses[178]. Unfortunately, all of these trials failed to show any efficacy. The RV144 trial, conducted in Thailand from 2003-2006, combined AIDSVAX with the recombinant canarypox immunogen ALVAC together in a prime-boost regimen, and resulted in a modest 31% reduction in risk of infection[179]. To date, RV144 remains the only HIV vaccine trial that has shown any efficacy. The other remaining large-scale trial, the HVTN505 trial conducted from 2009-2013, tested a regimen consisting of a DNA prime and recombinant adenovirus vector boost, but was halted early due to lack of efficacy[180].

Following the RV144 trial, extensive efforts have been made to analyze the immune responses of trial participants and identify correlates of protection. A large multi-center study published in 2012 found that the only variable significantly correlated with protection was IgG antibodies to the V1/V2 region of HIV envelope[181]. A sieve analysis of breakthrough infections also identified a correlation between lack of vaccine efficacy and mutations in the V2 loop, implying that V2-specific antibodies exerted selective pressure on the virus[182]. However, because the V2 antibodies correlated with protection in RV144 were non-neutralizing, it was unclear how they mediated protection. One hypothesis put forth was that V2 antibodies mediate protection by inhibiting gp120-$\alpha_4\beta_7$ interactions. This hypothesis was supported by studies that mapped RV144 V2 antibodies to epitopes proximal to LDV/I or epitopes that contained LDV/I[183-185]. One other study additionally showed that V2 antibodies obtained from immunized mice blocked gp120-$\alpha_4\beta_7$ binding[186]. Based on these findings and the

proposed role of $\alpha_4\beta_7^+$ cells in mucosal HIV transmission, vaccine strategies aimed at blocking gp120-$\alpha_4\beta_7$ interaction through V2 antibodies are currently being investigated.

Separately, $\alpha_4\beta_7$ antagonists have been investigated for their potential use in HIV therapy. The antibody Act-1[187], which binds specifically to the $\alpha_4\beta_7$ heterodimer, has been extensively studied in SIV infection of rhesus macaques. Act-1 monotherapy has been demonstrated to reduce plasma and gastrointestinal viral loads and improve $CD4^+$ T cell numbers in SIV-infected animals[188, 189]. Additionally, pre-treatment of macaques with Act-1 has been shown to partially inhibit vaginal SIV transmission[190]. More recently, Act-1 was shown to synergize with cART and mediate significant therapeutic effects leading to a state of drug-free virologic control[191]. In this study, Act-1/cART combination therapy resulted in a significant recovery of $CD4^+$ T cells in peripheral and mucosal compartments, as well a reduction in markers of systemic inflammation. Furthermore, after therapy was discontinued plasma virus levels remained suppressed and $CD4^+$ T cell levels were maintained (Figure 1-9). Based on these results, the humanized version of Act-1 (Vedolizumab) is being studied in clinical trials in combination with cART (http://www.clinicaltrials.gov; identifier NCT02788175). However, the therapeutic mechanism of action of Act-1 is not presently known.

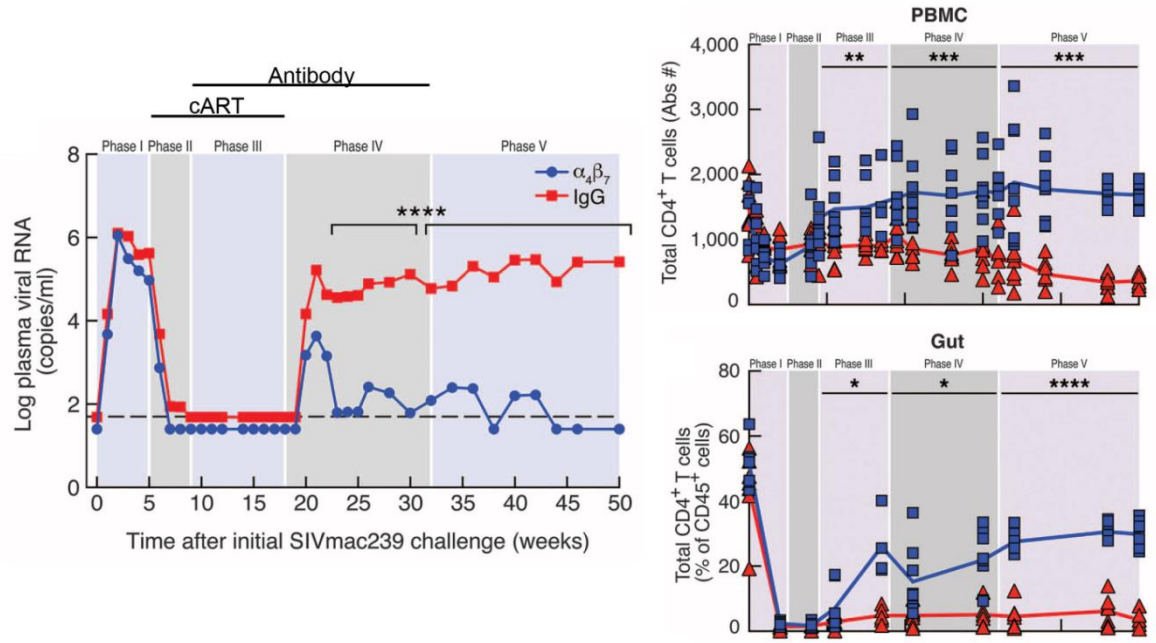

Figure 1-9. Combination cART and $\alpha_4\beta_7$ antagonist therapy in rhesus macaques. This study consisted of five phases of overlapping cART and antibody treatment, indicated by grey shaded regions. Phase I: intravenous infection; phase II: cART initiated; phase III: antibody initiated; phase IV: cART discontinued; phase V: antibody discontinued. Regimens included either control IgG (red) or $\alpha_4\beta_7$–blocking antibody (blue). Left: plasma viral RNA. Top-right: peripheral $CD4^+$ T cells. Bottom-right: intestinal $CD4^+$ T cells. Reproduced with permission from Byrareddy et al.[191].

Goals of this dissertation

The original goal of this project was to develop vaccine immunogens targeting the $\alpha_4\beta_7$-gp120 interaction, by modifying N-linked glycans within the V2 loop of gp120. However, throughout this work I discovered that purified gp120 proteins produced in our laboratory did not bind to $\alpha_4\beta_7$. Because others had observed a lack of gp120-$\alpha_4\beta_7$ reactivity, the first aim of this project was to define the factors that determine $\alpha_4\beta_7$ reactivity of gp120. I made the discovery that in mammalian cell expression systems, $\alpha_4\beta_7$-reactive cellular proteins were co-purified with gp120. I showed that these cellular proteins accounted for all observed $\alpha_4\beta_7$ binding, and that purified gp120 with these cellular proteins removed did not bind to $\alpha_4\beta_7$. Significantly, I also

discovered that these cellular proteins complexed with gp120, and thereby mediated indirect gp120-$\alpha_4\beta_7$ interaction. The second aim of this project was to identify which cellular proteins were responsible for this phenomenon. I showed that $\alpha_4\beta_7$–reactive isoforms of fibronectin, called CS1 fibronectins, bound to both gp120 and $\alpha_4\beta_7$ and mediated indirect gp120-$\alpha_4\beta_7$ interaction. These studies are presented in the second and fourth chapters of this dissertation. Finally, based on the critical role of CS1 fibronectins in gp120-$\alpha_4\beta_7$ binding, I hypothesized that CS1 fibronectins in the extracellular matrix facilitate HIV-1 infection of $\alpha_4\beta_7^+$ T cells. The third aim of this project was to test this hypothesis, and I provided *in vitro* evidence that CS1 fibronectins do play a role in HIV infection. The results of these studies are presented in the third chapter of this dissertation. Collectively, the work presented in this dissertation has changed the current understanding of HIV-$\alpha_4\beta_7$ interactions by challenging the hypothesis of direct gp120-$\alpha_4\beta_7$ binding, and by identifying a previously unknown role of CS1 fibronectins in HIV infection of $\alpha_4\beta_7^+$ T cells.

Chapter 2

Extracellular Matrix Proteins Mediate HIV-1 gp120 Interactions with $\alpha_4\beta_7$

The work presented in this chapter was published:

Journal of Virology. 2017.

DOI: 10.1128/jvi.01005-17

David Plotnik[1], Wenjin Guo[1], Brad Cleveland[1], Priska von Haller[2], Jimmy K. Eng[2], Miklos Guttman[3], Kelly K. Lee[3], James Arthos[4], Shiu-Lok Hu[1,5#]

Department of Pharmaceutics, University of Washington, Seattle, Washington, USA[1];
Department of Genome Sciences, University of Washington, Seattle, Washington, USA[2];
Department of Medicinal Chemistry, University of Washington, Seattle, Washington, USA[3];
Laboratory of Immunoregulation, NIAID, NIH, Bethesda, Maryland, USA[4];
Washington National Primate Research Center, University of Washington, Seattle, Washington, USA[5]

Submitted: 16 June 2017. Accepted: 9 August 2017

Citation: Plotnik D, Guo W, Cleveland B, von Haller P, Eng JK, Guttman M, Lee KK, Arthos J, Hu S-L. 2017. Extracellular matrix proteins mediate HIV-1 gp120 interactions with α4β7. J Virol 91:e01005-17. http://doi.org/10.1128/JVI.01005-17.

Abstract

Gut-homing $\alpha_4\beta_7^{high}$ $CD4^+$ T lymphocytes have been shown to be preferentially targeted by Human Immunodeficiency Virus type 1 (HIV-1) and are implicated in HIV-1 pathogenesis. Previous studies demonstrated that HIV-1 envelope protein gp120 binds and signals through $\alpha_4\beta_7$ and that this likely contributes to the infection of $\alpha_4\beta_7^{high}$ T cells and promotes cell-to-cell virus transmission. Structures within the second variable loop (V2) of gp120, including the tripeptide motif LDV/I, are thought to mediate gp120-$\alpha_4\beta_7$ binding. However, lack of $\alpha_4\beta_7$ binding has been reported in gp120 proteins containing LDV/I, and the precise determinants of gp120-$\alpha_4\beta_7$ binding are not fully defined. In this work, we report the novel finding that fibronectins mediate indirect gp120-$\alpha_4\beta_7$ interactions. We show that Chinese hamster ovary (CHO) cells used to express recombinant gp120 produced fibronectins and other extracellular matrix proteins that co-purified with gp120. CHO cell fibronectins were able to mediate the binding of a diverse panel of gp120 proteins to $\alpha_4\beta_7$ in an *in vitro* cell binding assay. The V2 loop was not required for fibronectin-mediated binding of gp120 to $\alpha_4\beta_7$, nor did V2-specific antibodies block this interaction. Removal of fibronectin through anion exchange chromatography abrogated V2-independent gp120-$\alpha_4\beta_7$ binding. Additionally, we showed a recombinant human fibronectin fragment mediated gp120-$\alpha_4\beta_7$ interactions similarly to CHO cell fibronectin. These findings provide an explanation for the apparentlycontradictory observations regarding the gp120-$\alpha_4\beta_7$ interaction and offer new insights into the potential role of fibronectin and other extracellular matrix proteins in HIV-1 biology.

Importance

Immune tissues within the gut are severely damaged by HIV-1, and this plays an important role in the development of AIDS. Integrin $\alpha_4\beta_7$ plays a major role in the trafficking of lymphocytes, including $CD4^+$ T cells, into gut lymphoid tissues. Previous reports indicate that some HIV-1 gp120 envelope proteins bind to and signal through $\alpha_4\beta_7$, which may help explain the preferential infection of gut $CD4^+$ T cells. In this study, we demonstrate that extracellular matrix proteins can mediate interactions between gp120 and $\alpha_4\beta_7$. This suggests that the extracellular matrix may be an important mediator of HIV-1 interaction with $\alpha_4\beta_7$–expressing cells. These findings provide new insight into the nature of HIV-$\alpha_4\beta_7$ interactions and how these interactions may represent targets for therapeutic intervention.

Introduction

Gut-associated lymphoid tissues (GALT) are preferentially targeted by human immunodeficiency virus type 1 (HIV)[43, 192]. Soon after invading GALT, HIV-1 depletes the majority of intestinal $CD4^+$ T lymphocytes and damages surrounding tissues through bystander effects[44]. This is believed to contribute substantially to immune dysregulation, chronic inflammation, and the development of AIDS[193]. $CD4^+$ T cells expressing the $\alpha_4\beta_7$ integrin have been proposed to play a role in HIV-1's apparent tropism for GALT. First, $\alpha_4\beta_7^{high}$ cells traffic between peripheral mucosal sites and GALT, largely due to an interaction between $\alpha_4\beta_7$ and mucosal vascular addressin cell adhesion molecule 1 (MAdCAM-1) expressed on gut vasculature[145, 146]. For this reason, $\alpha_4\beta_7^{high}$ cells may facilitate viral spread from mucosal portals of entry to intestinal sites. Consistent with this, the frequency of $\alpha_4\beta_7^{high}$ lymphocytes within genital tissues correlates with infection risk *in vivo*[160, 161]. Second, it has been

demonstrated that the $\alpha_4\beta_7^{high}$ memory $CD4^+$ T cell subset is more susceptible to HIV-1 infection than $\alpha_4\beta_7^-$ cells *in vitro*[159]. This is also supported by studies that demonstrate preferential infection of $\alpha_4\beta_7^{high}$ cells *in vivo*[155, 163, 194]. Because these cells are present at high density in the gut[162] and are highly susceptible to HIV-1 infection, they may facilitate HIV-1 propagation throughout GALT.

Binding between $\alpha_4\beta_7$ and the gp120 subunit of HIV-1 envelope protein has been described[164, 168, 169, 186, 195-197]. This interaction has been proposed to enhance HIV-1 infection either by facilitating virus attachment to cells or by activating $\alpha_4\beta_7$ –mediated signaling. Notably, the monoclonal antibodies (MAbs) Act-1 and natalizumab, which block $\alpha_4\beta_7$ and the α_4 integrin chain, respectively, did not significantly inhibit HIV-1 infectivity *in vitro*[159, 173, 198]. In contrast, targeting $\alpha_4\beta_7$ with Act-1 in macaques infected with simian immunodeficiency virus (SIV) resulted in lower virus titers and significant improvements in $CD4^+$ T cell numbers, as well as prevention of mucosal virus transmission[188-190]. These different effects of $\alpha_4\beta_7$ inhibition *in vitro* and *in vivo* argue against $\alpha_4\beta_7$ functioning as a virus attachment factor. Furthermore, a recent study reported that a small-molecule inhibitor of $\alpha_4\beta_7$ failed to inhibit infection *in vivo*, similarly to Act-1[199]. While both Act-1 and this small molecule blocked ligand binding to $\alpha_4\beta_7$, the small molecule initiated $\alpha_4\beta_7$-mediated signaling whereas Act-1 blocked this signaling. This finding suggests that $\alpha_4\beta_7$–mediated signaling may play an important role during infection *in vivo* and further argues against a role for $\alpha_4\beta_7$ as a virus attachment factor. In support of this *in vivo* finding, gp120 has been demonstrated to initiate $\alpha_4\beta_7$ signal transduction, leading to LFA-1 activation *in vitro*. This mechanism has been proposed to contribute to cell-to-cell transmission of HIV-1 and the preferential infection of $\alpha_4\beta_7^{high}$ memory $CD4^+$ T cells[164].

At present, the precise determinants of gp120-$\alpha_4\beta_7$ interactions are not fully understood. The interaction is thought to be mediated by structures within the second variable loop (V2) of gp120, including the conserved tripeptide sequence LDV/I[164]. However, the reactivity of gp120 to $\alpha_4\beta_7$ is reported to vary considerably among gp120 proteins from different strains, and many gp120 molecules containing LDV/I have no measurable $\alpha_4\beta_7$ binding[164, 172]. It is thought that $\alpha_4\beta_7$ reactivity may be strain-specific and modulated by factors including the length of the V2 loop, the presence or absence of N-linked glycans (in variable regions 1, 2, and 4 and conserved region 3 of gp120), and the specific glycoforms present on gp120[170]. These factors are hypothesized to affect $\alpha_4\beta_7$ binding by altering the conformation and exposure of LDV/I. More recently, additional determinants in both the V2 and V3 loops have been proposed to participate in $\alpha_4\beta_7$ binding[168, 169]. Although the nature of the interaction between gp120 and $\alpha_4\beta_7$ is not fully understood, it is clear that any such interaction depends on more than the simple presence or absence of the LDV/I sequence.

In the present work, we sought to understand the nature of gp120-$\alpha_4\beta_7$ binding in greater detail. We determined that CHO cells used to produce recombinant gp120 also produced cellular proteins with high $\alpha_4\beta_7$ binding reactivity, and these proteins copurified with gp120 by lectin chromatography. Importantly, we discovered that these CHO cellular proteins were capable of mediating indirect interactions between $\alpha_4\beta_7$ and HIV-1 envelope proteins. The proteins responsible for this indirect interaction included an $\alpha_4\beta_7$-reactive isoform of fibronectin and other extracellular matrix components. These findings provide evidence that extracellular matrix proteins may mediate interactions between HIV-1 envelope proteins and $\alpha_4\beta_7$ and offer new insight into the potential role of $\alpha_4\beta_7$ in HIV-1 pathogenesis.

Results

The $\alpha_4\beta_7$ binding properties of 93MW959 gp120 depend on protein purification conditions.

Lack of gp120-$\alpha_4\beta_7$ reactivity has been reported in studies that used recombinant gp120 purified by DEAE anion-exchange chromatography[172]. In contrast, earlier reports of gp120-$\alpha_4\beta_7$ reactivity utilized envelope proteins that were purified without the DEAE anion-exchange step[164, 170]. Here, we examined the effects of DEAE chromatography in detail, using gp120 from the 93MW959 isolate (referred to below as MW959), which is reported to have strong $\alpha_4\beta_7$ binding properties[170].

MW959 gp120 was produced by transient transfection of CHO cells and prepared with a three-step purification scheme. First, gp120-containing supernatant was purified on a *Galanthus nivalis* lectin affinity column (GNA). Second, DEAE chromatography was used to divide the GNA eluate into two fractions: DEAE flow-through (material that did not bind to DEAE) and DEAE eluate (material that bound and was subsequently eluted from DEAE). Third, size exclusion chromatography (SEC) was used to analyze material recovered at each of these purification steps.

GNA eluate yielded 3 distinct peaks when analyzed by SEC (Figure 2-1A, blue chromatogram), and these were numbered 1 to 3 in ascending order of their apparent sizes. DEAE chromatography separated peak 3 materials from peaks 1 and 2. DEAE flow-through yielded two peaks which corresponded to peaks 1 and 2 of GNA eluate (Figure 2-1A, green chromatogram). DEAE eluate yielded a single peak on SEC which corresponded to peak 3 of the GNA eluate (Figure 2-1A, red chromatogram).

The products of SEC purification were analyzed with polyacrylamide gel electrophoresis (PAGE) and western blotting. The results from these analyses confirmed that peak 1 contained

gp120 monomers and peak 2 contained gp120 dimers. Western blot analysis showed the majority of recombinant gp120 was present in peaks 1 and 2, whether or not DEAE was used (Figure 2-1B). Native PAGE confirmed that peak 1 primarily contained gp120 monomers and peak 2 primarily contained gp120 dimers, whereas peak 3 contained a diffuse smear of high molecular weight material (Figure 2-1C). Reduced and denatured samples analyzed by SDS-PAGE showed that peak 1 and peak 2 both contained a major band of 120 kDa, which was presumed to be gp120 (Figure 2-1D). The same analysis revealed that peaks 1 and 2 prepared without DEAE contained additional contaminant bands that were not observed in material prepared with DEAE.

Material from each of these peaks was biotinylated and tested for $\alpha_4\beta_7$ binding activity in a flow cytometry-based cell binding assay, using the $\alpha_4\beta_7$–expressing cell line RPMI8866. Soluble MAdCAM-1-Fc fusion protein was used as a positive control for $\alpha_4\beta_7$ binding. Specificity of binding was determined either by pre-blocking cells with the α_4 integrin-blocking antibody 2B4 or by inhibiting integrins through removal of divalent cations with EDTA-containing buffer. All 3 peaks purified without DEAE exhibited $\alpha_4\beta_7$ binding activity (Figure 2-1E). Binding was highest in peak 3, lower in peak 2, and lowest in peak 1. In contrast, DEAE-purified gp120 monomers and dimers exhibited no $\alpha_4\beta_7$ binding activity, but DEAE eluate exhibited high $\alpha_4\beta_7$ reactivity (Figure 2-1F). These results demonstrated that MW959 gp120 prepared without DEAE appeared to react with $\alpha_4\beta_7$, whereas gp120 prepared with DEAE did not.

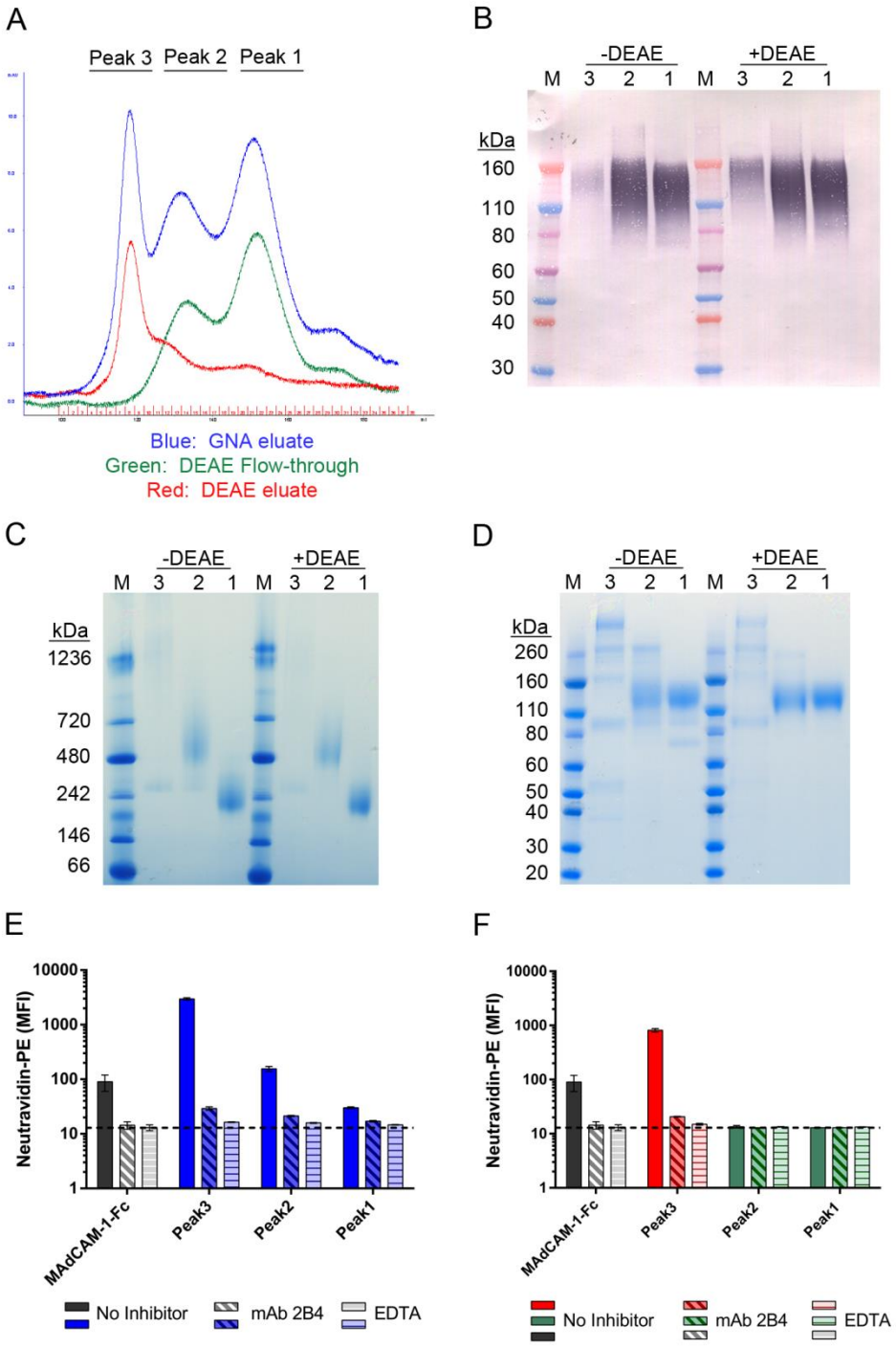

Figure 2-1. Effect of DEAE purification on $\alpha_4\beta_7$ reactivity of MW959 gp120. MW959 gp120 produced in CHO cells was analyzed at different stages of purification. (A) Overlay of UV chromatograms from size-exclusion chromatography. (B to D) Peaks 1 to 3 were collected as indicated for panel A and analyzed by western blotting (B), native-PAGE (C), and SDS-PAGE (D). Protein was loaded at 1µg/lane for western blotting and 5µg/lane for native-PAGE and SDS-PAGE. Lanes: 1 to 3, peaks 1 to 3 from GNA eluate (-DEAE) or DEAE fractionation (+DEAE); M, molecular mass markers. Peak 3 +DEAE is the material recovered from DEAE

eluate, and peaks 1 to 2 +DEAE are materials recovered from DEAE flow-through. The western blot was probed with HIV-1^+ serum and detected with a chromogenic alkaline phosphatase substrate. (E and F) Materials collected for panel A were biotinylated and tested by a flow cytometry assay for binding to the $\alpha_4\beta_7$–expressing cell line RPMI8866. (E) Cell binding of material in peaks 1 to 3 from GNA eluate. (F) Cell binding of material in peaks 1 to 3 from DEAE fractionation. Binding was measured without inhibitors (No Inhibitor), with $\alpha_4\beta_7$–blocking antibody 2B4 (Mab 2B4), or with EDTA (EDTA). The dashed line indicates the background signal from cells stained with neutravidin-PE in the absence of biotinylated proteins. MAdCAM-1-Fc binding was included as a positive control for $\alpha_4\beta_7$ binding. The cell binding results are the means and standard deviations of 3 replicate measures from a single representative experiment.

CHO produces $\alpha_4\beta_7$ –reactive cellular proteins.

The above-mentioned results suggested to us that CHO cells may produce $\alpha_4\beta_7$-reactive substances that are copurified with gp120. To test this, we prepared CHO-conditioned culture medium by growing non-transfected cells under conditions identical to those used for gp120 purification and then processed the resulting medium with GNA affinity chromatography, followed by SEC. The resulting CHO proteins yielded a major peak on SEC at the same elution time as peak 3 in MW959 purification. CHO proteins were collected in 3 separate fractions corresponding to the elution times of peaks 1 to 3 in the MW959 gp120 purification (Figure 2-2A). These fractions were biotinylated and tested for $\alpha_4\beta_7$–binding activity on RPMI8866 cells. All the fractions exhibited $\alpha_4\beta_7$ binding, with the highest activity in fraction 3, lower activity in fraction 2, and the lowest activity in fraction 1 (Figure 2-2B).

These results demonstrated that CHO cells produce $\alpha_4\beta_7$-reactive substances that are enriched by GNA and co-migrate with gp120 monomers and dimers on SEC. Because $\alpha_4\beta_7$ reactivity was not observed in DEAE-purified MW959 gp120, we tested the ability of DEAE to capture and remove these $\alpha_4\beta_7$–reactive substances. Similar to gp120 purification, CHO-conditioned media was processed by GNA and DEAE, followed by SEC. Minimal amounts of protein were recovered in the DEAE flow-through (Figure 2-2C, blue chromatogram), while the

majority of proteins were bound by DEAE and could be recovered in the eluate (Figure 2-2C, green chromatogram). CHO proteins recovered in the DEAE eluate had a SEC elution profile similar to that of CHO proteins captured by GNA (Figure 2-2C, purple chromatogram). These fractions were assayed for $\alpha_4\beta_7$ binding activity as described above. The DEAE flow-through had no detectable $\alpha_4\beta_7$ binding, whereas the DEAE eluate exhibited high $\alpha_4\beta_7$ binding (Figure 2-2D), and this indicated that DEAE is capable of capturing $\alpha_4\beta_7$–reactive CHO proteins. The three CHO protein fractions, collected as shown in Fig 2-2A, were analyzed by SDS-PAGE. Each fraction contained multiple protein bands (Figure 2-2E), and they were similar to the contaminant bands observed in MW959 gp120 purified without DEAE (compare Figure 2-1D). Overall, these results suggested that $\alpha_4\beta_7$ reactivity of MW959 gp120 in our assays depended on the presence of $\alpha_4\beta_7$–reactive CHO proteins.

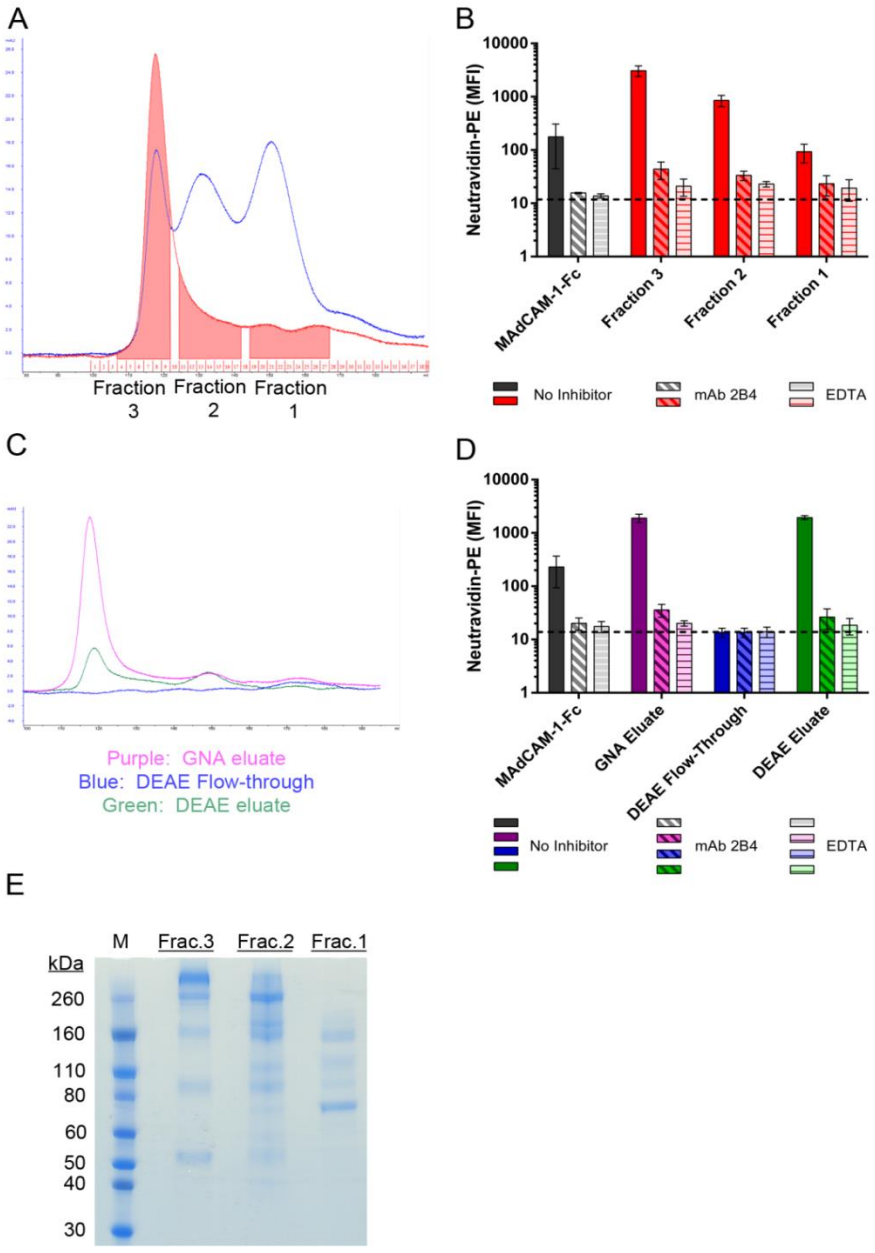

Figure 2-2. CHO cells produce $\alpha_4\beta_7$–reactive cellular proteins. Culture medium was conditioned by CHO cells and processed by GNA. (A) Comparison of GNA eluates from MW959 gp120 (blue) and CHO-conditioned medium (red), analyzed by size exclusion chromatography. CHO cell proteins were collected in 3 fractions, indicated by shaded areas in the red chromatogram. (B) Binding of protein fractions collected for panel A to RPMI8866 cells. The results are the means and standard deviations of 2 separate experiments. (C) CHO cell proteins were fractionated by DEAE and analyzed by size exclusion chromatography. (D) Binding of proteins collected for panel C to RPMI8866 cells. The results are the means and standard deviations of 3 separate experiments. (E) SDS-PAGE analysis of fractions collected for panel A.

It has been reported that gp120 derived from human embryonic kidney 293 (HEK293) cells does not bind to $\alpha_4\beta_7$, and we speculated that this may be due to a lack of $\alpha_4\beta_7$ –reactive proteins produced by 293 cells[170]. Thus, we examined whether human embryonic kidney 293 cells produce $\alpha_4\beta_7$–reactive cellular proteins. 293 cell culture medium was prepared and analyzed as described above. Surprisingly, $\alpha_4\beta_7$ binding activity was again detected (Figure 2-3). However, we also observed that 293 cells secreted fewer cellular proteins overall than CHO cells (91 ± 14µg/liter for 293 versus 546 ± 210µg/liter for CHO cells). Additionally, in separate experiments, we observed that recombinant gp120 yields were higher in 293 cells than in CHO cells (MW959 gp120 production, 1,024µg/liter for 293 cells versus 444.6 ± 148.3µg/liter for CHO cells). From this, we concluded that $\alpha_4\beta_7$ reactivity may not be readily observed in 293 cell-derived gp120 because of a low relative abundance of cellular proteins, even without DEAE purification.

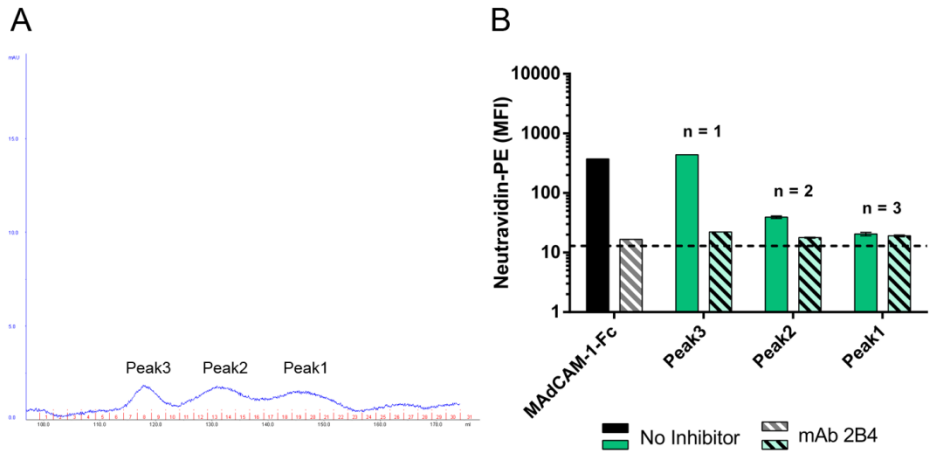

Figure 2-3. HEK293 cells produce $\alpha_4\beta_7$–reactive cellular proteins. HEK293 cell-conditioned medium was processed by GNA and then analyzed by size exclusion chromatography. (A) UV chromatogram showing 3 peaks of 293 cellular proteins collected by size exclusion. (B) Binding of the proteins collected for panel A to RPMI8866 cells. The results presented are means and standard deviations; the number of replicates for each sample is indicated.

Inhibitors of α_4 integrins block binding of CHO cellular proteins.

Several inhibitors have been used to demonstrate the specificity of gp120-$\alpha_4\beta_7$ binding, and we asked if these agents inhibit CHO cell protein binding, as well. First, we tested the effects of the cyclic peptide CWLDVC. It is a competitive inhibitor of the LDV recognition site of α_4 integrins and has been used to demonstrate LDV-dependent $\alpha_4\beta_7$ binding of gp120[164, 200]. CWLDVC completely inhibited MAdCAM-1-Fc binding to RPMI8866 cells and inhibited the majority of CHO protein binding, as well (Figure 2-4A). The scrambled control peptide CDLVWC had no effect on either protein. These results indicate that binding in our assays required the LDV recognition site of an α_4 integrin. EDTA was found in previous assays to inhibit CHO cell protein binding (Figure 2-2B), and it was included in these experiments as a control.

Next, we examined the effects of integrin-blocking antibodies. In previous assays, we established that CHO cell protein binding could be blocked by MAb 2B4, which inhibits the α_4 integrin chain (Figure 2-2B). We confirmed this result and also tested the effects of MAb Act-1, which is specific for the $\alpha_4\beta_7$ heterodimer[187, 201]. Surprisingly, Act-1 was found to inhibit only about half of the CHO cell protein binding signal but completely inhibited MAdCAM-1-Fc binding (Figure 2-4B). The high degree of inhibition observed with MAb 2B4 and CWLDVC peptide, contrasted with the partial inhibition of MAb Act-1, suggested that CHO cell proteins may bind through both $\alpha_4\beta_7$ and the related integrin $\alpha_4\beta_1$. We tested this with MAb P5D2, which blocks the β_1 integrin chain. As expected, P5D2 had no effect on MAdCAM-1-Fc binding. P5D2 did, however, inhibit about half of the CHO cell protein binding (Figure 2-4B). When Act-1 and P5D2 were combined, the effects were additive, and CHO cell protein binding was inhibited to the same level as observed with MAb 2B4 (Figure 2-4b).

These results suggest that CHO cell proteins are capable of binding to both $\alpha_4\beta_7$ and $\alpha_4\beta_1$ This is in contrast to other findings in which gp120-$\alpha_4\beta_7$ binding is primarily through $\alpha_4\beta_7$ and is significantly inhibited by Act-1[164]. One important caveat to these comparisons is that the present study used the RPMI8866 cell line, while prior studies used primary human peripheral blood mononuclear cells (PBMCs). Because receptor expression or binding properties may differ between these cell types, direct comparisons cannot be made. In total, our experiments demonstrated that CHO cell protein binding was blocked by inhibitors of α_4 integrins and that copurified CHO proteins can account for gp120-$\alpha_4\beta_7$ binding signals under certain conditions.

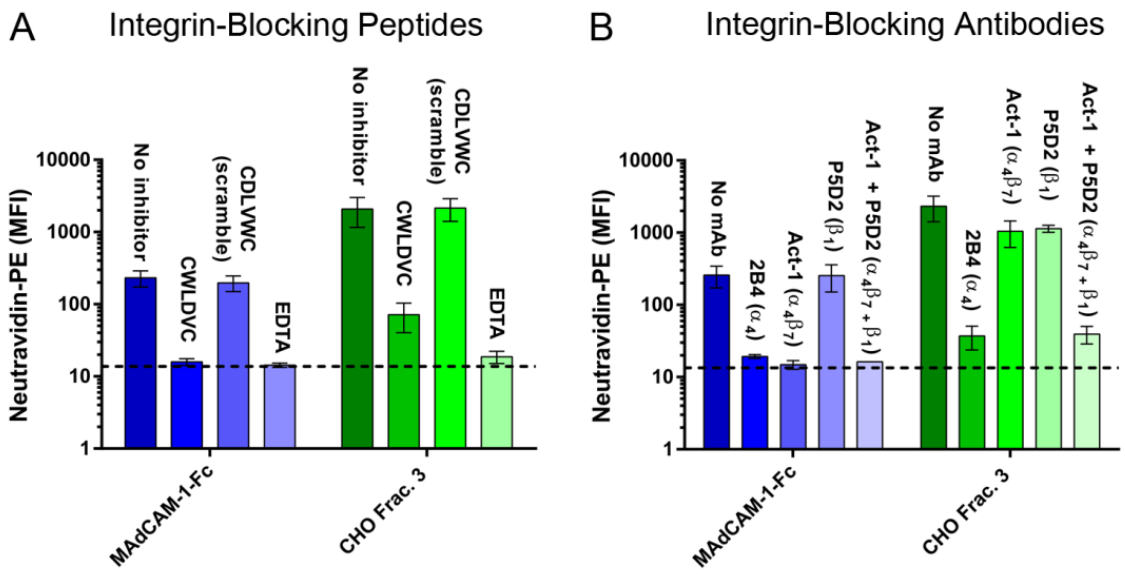

Figure 2-4. Inhibition of CHO cellular protein binding by α_4 integrin inhibitors. (A) Binding of MAdCAM-1-Fc (blue) or CHO cell proteins (green) to RPMI8866 cells in the presence of the cyclic peptide CWLDVC, scrambled control peptide CDLVWC, or buffer containing EDTA. (B) Binding in the presence of antibody 2B4 (α_4 integrin), Act-1 ($\alpha_4\beta_7$ integrin), P5D2 (β_1 integrin), or combination of Act-1 and P5D2. The results are the means and standard deviations of 3 separate experiments.

CHO cellular proteins mediate indirect gp120-$\alpha_4\beta_7$ binding.

Mixing experiments were carried out to better understand the reasons for lack of $\alpha_4\beta_7$ reactivity in DEAE-purified MW959 gp120. In these experiments, labeled (biotinylated) and unlabeled (nonbiotinylated) components were mixed and tested for changes in binding activity of the labeled component in the presence of the unlabeled component. Because cell staining was carried out with neutravidin-R-phycoerythrin (PE), only biotinylated proteins in these mixtures were expected to produce a signal.

First, we ruled out the possibility that DEAE purification introduced $\alpha_4\beta_7$-inhibitory substances. To test this, unlabeled DEAE-purified MW959 gp120 monomers were mixed with either labeled MAdCAM-1-Fc or labeled MW959 gp120 purified without DEAE. In both cases, DEAE-purified material did not inhibit the binding signals (Figure 2-5A), which indicated that DEAE purification did not introduce $\alpha_4\beta_7$-inhibitory activity.

We next asked if CHO cell proteins could modify the binding behavior of DEAE-purified gp120. First, we verified that CHO cell fraction 3, which binds strongly to $\alpha_4\beta_7$, produced no signal when not biotinylated (Figure 2-5Bb). Labeled DEAE-purified MW959 gp120, with no measurable $\alpha_4\beta_7$ binding, was then mixed with unlabeled CHO cell fraction 3. Surprisingly, we discovered a modest $\alpha_4\beta_7$ binding signal when these proteins were incubated for 2 hours prior to being added to cells (Figure 2-5B). The same effect was not seen when the proteins were mixed directly on cells without preincubation (Figure 2-5B). Our interpretation of these results was that CHO cell proteins mediated indirect gp120-$\alpha_4\beta_7$ binding. Because an effect was seen only with 2 hours of incubation, we concluded that the interaction between gp120 and CHO cell proteins was slow under these experimental conditions.

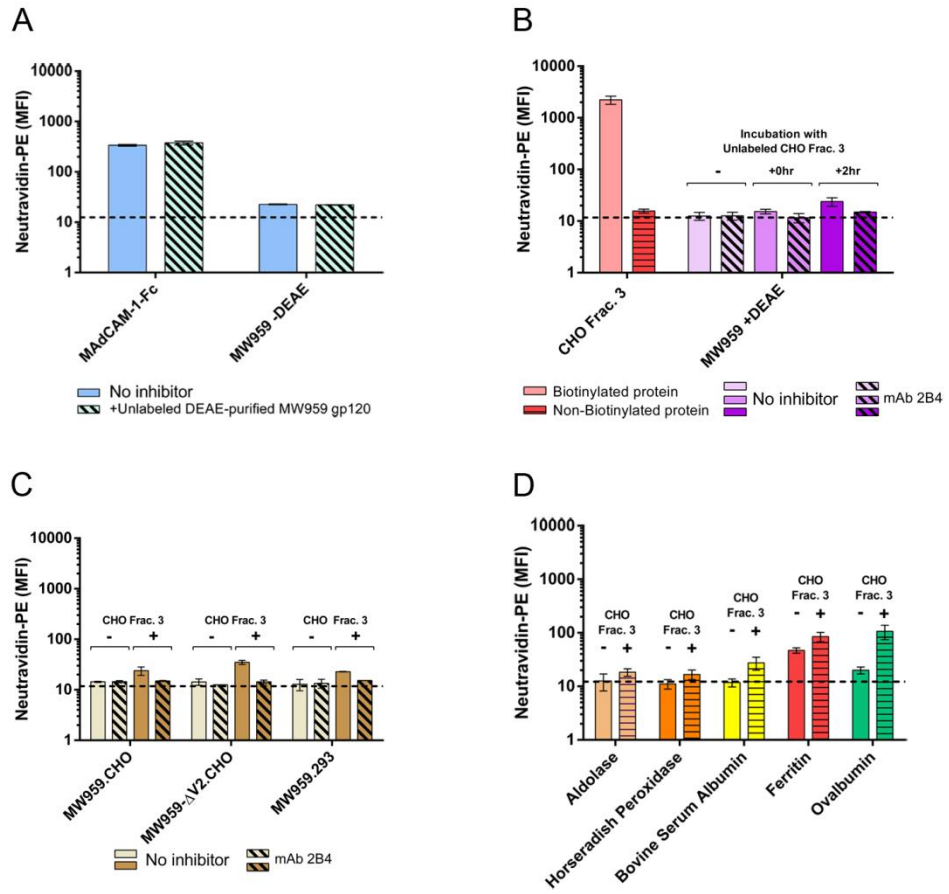

Figure 2-5. CHO cell proteins mediate indirect $\alpha_4\beta_7$ binding. Biotinylated (labeled) and non-biotinylated (unlabeled) proteins were mixed, and binding of the labeled component was measured on RPMI8866 cells by neutravidin-PE staining. (A) DEAE-purified MW959 gp120 was tested for $\alpha_4\beta_7$–inhibitory activity. Binding of labeled MAdCAM-1-Fc or MW959 gp120 prepared without DEAE was measured in the absence (solid bars) or presence (hatched bars) of 10µg unlabeled DEAE-purified gp120. (B) CHO cell proteins were tested for enhancement of $\alpha_4\beta_7$ binding signals. Labeled CHO cell proteins produced binding signals (pink bar), but unlabeled proteins did not (red bar). Binding of DEAE-purified MW959 gp120 was measured without CHO cell proteins, or with unlabeled CHO cell proteins combined with gp120 for 0hr or 2hr. (C) Wild-type MW959 gp120 was produced in CHO and 293 cells, and MW959-ΔV2 with a deleted V2 loop was produced in CHO cells. Binding of these proteins was measured with and without 2hr pre-incubation with unlabeled CHO cell proteins. (D) Binding of five non-HIV-1 proteins with and without 2hr preincubation with unlabeled CHO cell proteins. All the results are the means and standard deviations of 3 replicate measurements.

Because the V2 loop is implicated in gp120-$\alpha_4\beta_7$ binding, we speculated that CHO cell proteins may modulate activity of the V2 loop in a way that enhanced $\alpha_4\beta_7$ reactivity. If this were the case, we reasoned that gp120 without a V2 loop should not produce an $\alpha_4\beta_7$ binding

signal in these mixing experiments. We examined this by creating an MW959 gp120 mutant in which the majority of the V2 loop (amino acid residues 161 to 185) was deleted. This mutant was designated MW959-ΔV2 and was produced in CHO cells and purified with DEAE as described above. MW959-ΔV2 gp120 exhibited no $\alpha_4\beta_7$ binding activity by itself but did produce an $\alpha_4\beta_7$ binding signal in mixing experiments with CHO cell fraction 3 (Figure 2-5C). From this, we concluded that the binding signal seen in mixtures of gp120 and CHO cell proteins did not require the V2 loop.

Next, we examined whether gp120 produced in 293 cells interacted with CHO cell proteins. We speculated that 293 cell-derived gp120 may interact poorly with $\alpha_4\beta_7$–reactive cellular proteins, and this could contribute to lack of $\alpha_4\beta_7$ binding signals. MW959 gp120 was produced in 293 cells and tested in mixing experiments with CHO cell proteins, as described above, and was found to react similarly to CHO cell-derived gp120 (Figure 2-5C). This indicated that interaction between gp120 and cellular proteins was not dependent on specific glycosylation patterns or other posttranslational modifications that might vary between expression systems. It also further supported the hypothesis that low abundance of $\alpha_4\beta_7$–reactive cellular proteins was the likely reason for lack of binding observed in 293 cell-derived gp120.

After determining that CHO cell proteins interact with these MW959 gp120 preparations, we tested the specificity of this interaction with five non-HIV-1 proteins (aldolase, horseradish peroxidase [HRP], bovine serum albumin, ferritin, and ovalbumin). These proteins were biotinylated and tested in mixing experiments as described above. CHO cell proteins did not significantly increase the binding of aldolase or horseradish peroxidase but did increase the binding of bovine serum albumin, ferritin, and ovalbumin (Figure 2-5D). These results indicated

that CHO cell proteins can interact with a variety of proteins, resulting in apparent $\alpha_4\beta_7$ binding, and this interaction was not specific to gp120.

Collectively, these experiments showed that CHO cell proteins are not only capable of producing $\alpha_4\beta_7$ binding signals by themselves, but also produce signals by mediating indirect interactions between $\alpha_4\beta_7$ and gp120. The indirect gp120-$\alpha_4\beta_7$ binding observed in the presence of CHO cell proteins seemed to be due to protein-protein interactions that did not require the V2 loop or CHO cell-specific posttranslational events, such as glycosylation.

CHO cell proteins mediate indirect gp120-$\alpha_4\beta_7$ binding in a panel of diverse HIV-1 envelopes.

The above-described findings were based on gp120 from the MW959 isolate and assays that used the RPMI8866 cell line. We next asked whether these findings would extend to a variety of envelope proteins assayed with primary $CD4^+\alpha_4\beta_7^+$ T cells. Human PBMCs were acquired from two separate donors, and $CD4^+$ cells were isolated from them. Primary $CD4^+$ T cells were activated with anti-CD3 antibody, and cultured in the presence of interleukin-2 and retinoic acid. The expression levels of relevant receptors were then measured by flow cytometry. Cells from both donors expressed high levels of CD4, $\alpha_4\beta_7$, and the marker of cell activation CD45RO (Figure 2-6A). CCR5 was not detected on cells from donor number 1, but was detected on approximately half of the cells from donor number 2 (Figure 2-6A). MAdCAM-1-Fc bound to cells from both donors at similar levels. As expected, MAdCAM binding was not inhibited by the CD4-blocking antibody leu3a but was inhibited by a combination of leu3a and 2B4 antibodies (Figure 2-6B).

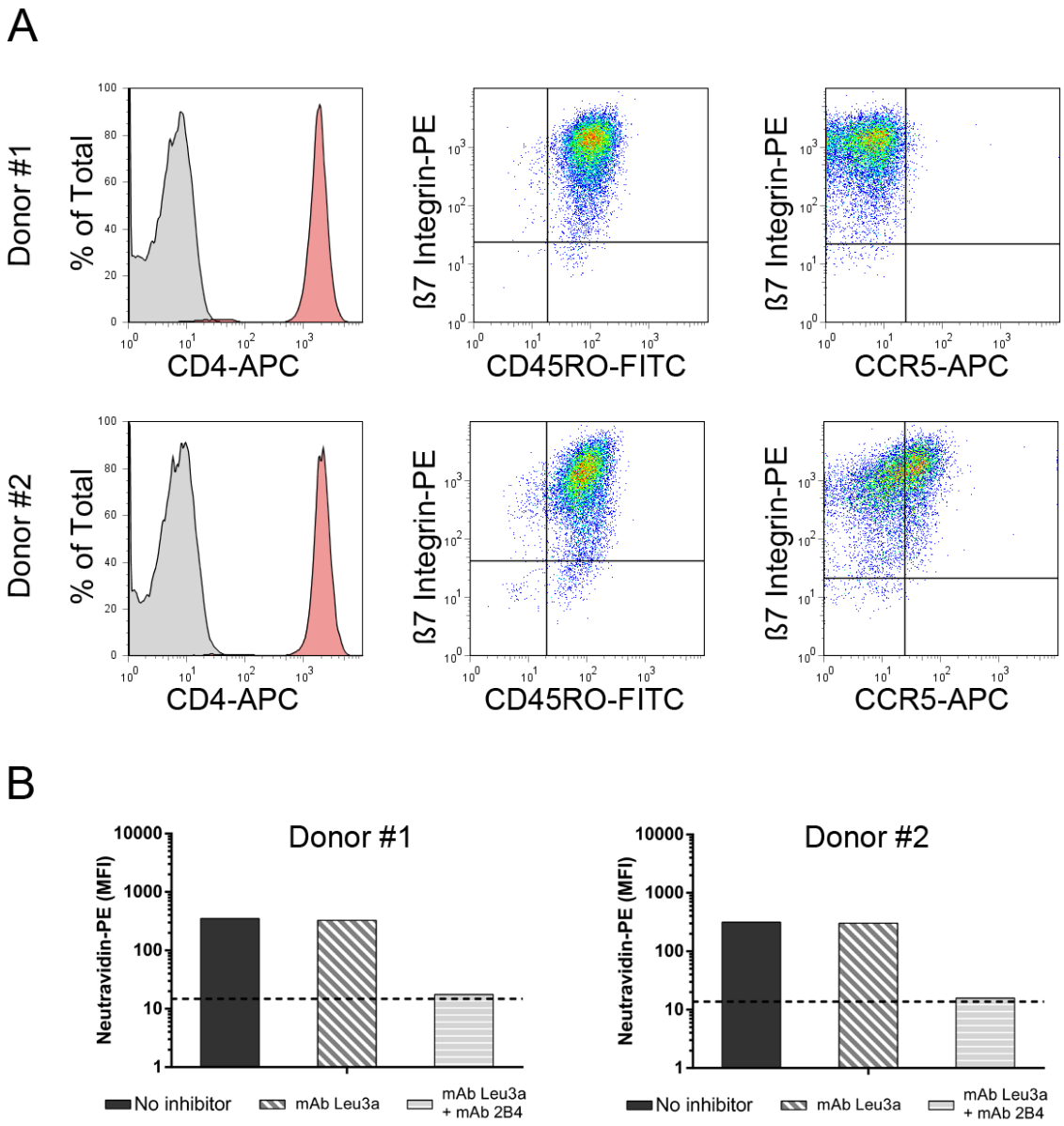

Figure 2-6. Characterization of primary $CD4^+\alpha_4\beta_7^+$ T cells. Human $CD4^+$ cells were enriched from PBMCs of two separate donors and cultured in retinoic acid for 9 days prior to analysis. (A) Expression of CD4, β_7 integrin, CD45RO, and CCR5 measured by flow cytometry. (B) Binding of MAdCAM-1-Fc to cells from both donors. Binding was measured without inhibitors , with the CD4-blocking antibody leu3a, or with a combination of leu3a and 2B4 antibodies.

A panel of DEAE-purified envelope proteins was assembled and included representatives from HIV-1 subtypes A, B, and C. It also included two fully synthetic envelopes: the ancestral subtype B envelope AN1[202], and an envelope based on a consensus of group M sequences

(M.CON-S.d11)[203]. We primarily included gp120 monomers, but also included the BG505.T332N.664 SOSIP trimer and corresponding BG505.T332N.664 SOSIP gp140 monomer[204]. SF162 and 1086 gp120 proteins contained a deletion of the first 7 N-terminal amino acids of the mature protein (d7 mutation), and M.CON-S.d11 contained a deletion of the first 11 N-terminal amino acids[205]. Additionally, the panel contained proteins produced in CHO and 293 cells, as well as one SF162 envelope produced in 293S GnT1$^{-/-}$ cells. All the proteins used in these experiments were prepared with a DEAE purification step.

All of these envelope proteins displayed similar binding profiles on CD4$^{+}\alpha_4\beta_7^{+}$ cells (Figure 2-7). In the absence of CHO cell proteins, all the envelopes produced a binding signal that was completely inhibited by CD4 antagonism with leu3a. In the presence of CHO cell proteins, the binding signal was mostly inhibited by leu3a but displayed residual CD4-independent binding that was inhibited with the addition of $\alpha_4\beta_7$-blocking antibody. CHO cell proteins increased the total binding signal for all the envelopes studied. For most envelopes, binding was increased by 4 to 10%; for 1086.d7 binding was increased by 18%; and for MW959-ΔV2 binding was increased 45%. Increases in binding were statistically significant for SF162.d7.293, SF162.d7.GnT1$^{-/-}$, MW959-ΔV2, 1086.d7.CHO, and M.CON-S.d11.CHO (unpaired t-test, $p < 0.05$). These experiments showed that the majority of gp120 binding was through CD4 but that overall binding could be enhanced by CHO cell protein-mediated interactions with $\alpha_4\beta_7$. In our assays, gp120-$\alpha_4\beta_7$ binding required CHO cell proteins, and was not apparently influenced by other envelope-specific factors (HIV-1 subtype, monomeric or trimeric envelope, and producer cell type).

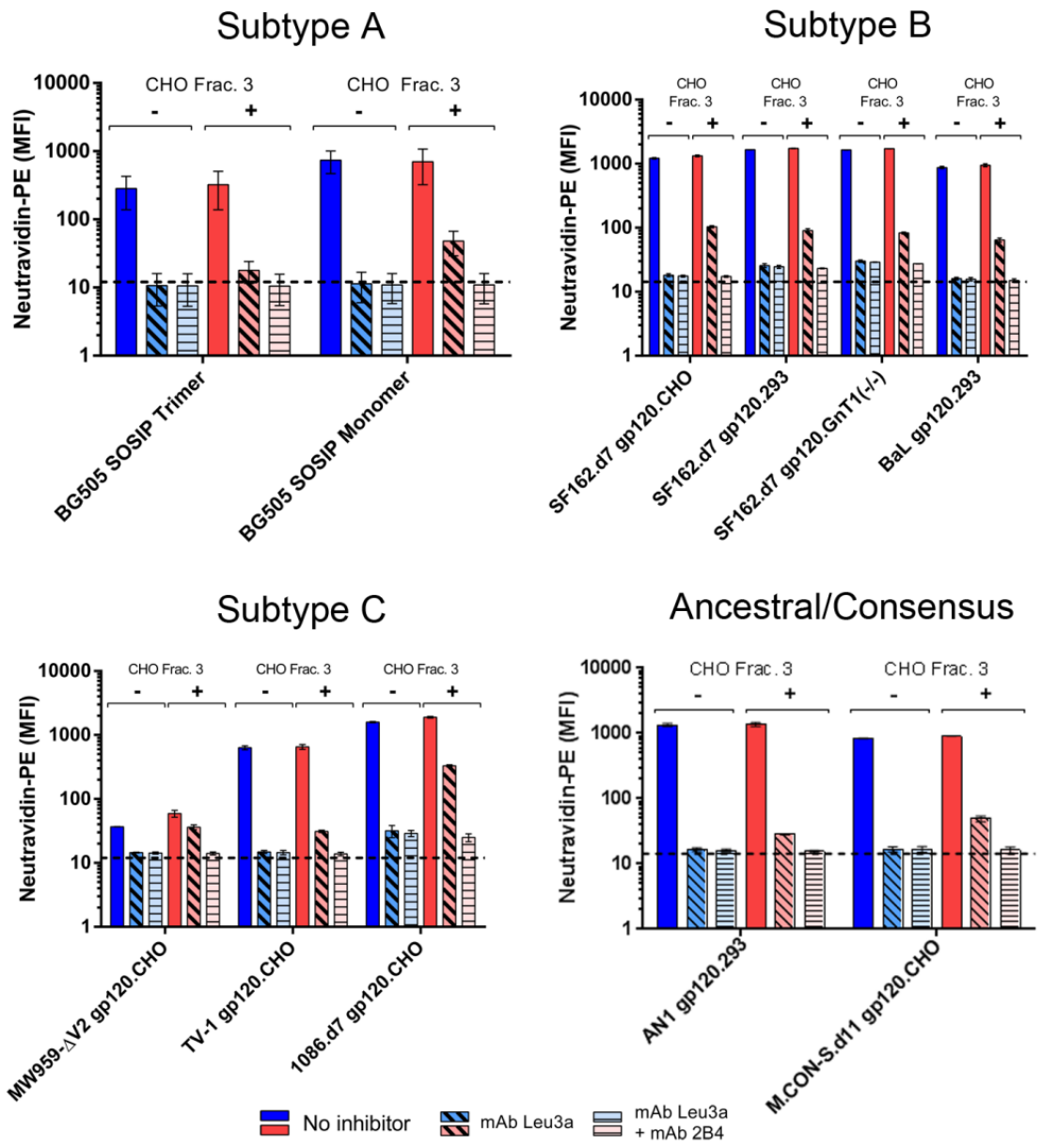

Figure 2-7. CHO cell proteins mediate $\alpha_4\beta_7$ binding signals in a diverse panel of HIV-1 envelopes. Shown is binding of 11 different DEAE-purified envelope proteins to primary $CD4^+\alpha_4\beta_7^+$ T cells. The means and standard deviations of single measures made on cells from both donors are presented. Binding was measured in the absence (blue bars) or presence (red bars) of unlabeled CHO cell proteins. For both of these conditions, binding was measured without inhibitors, with leu3a antibody, or with a combination of leu3a and 2B4 antibodies.

DEAE-purified envelopes display intact V2 epitopes.

Because the gp120-$\alpha_4\beta_7$ interaction is hypothesized to involve LDV/I and possibly other structures within V2, we conducted experiments to verify that DEAE-purified envelopes display intact V2 epitopes. Additionally, several distinct conformations of the V2 loop have been described, and exposure of LDV/I may depend on these conformations[183, 184, 206]. We therefore also asked if DEAE purification selects for any particular V2 conformation and if this could explain the lack of $\alpha_4\beta_7$ reactivity in DEAE-purified envelopes.

A biolayer interferometry assay was used to measure the binding of several envelope proteins to a panel of V2 antibodies. We included representatives from 3 antibody classes that are able to distinguish V2 conformations: PG9 and PG16, which bind V2q quaternary epitopes; CH58, which binds a V2p linear epitope; and 2158, which binds a V2i conformational epitope that includes LDV/I[185]. The antibody FI6v3 to influenza virus hemagglutinin (HA) protein was included as a negative control, and CD4-IgG_2 fusion protein was included as a positive control[207]. No difference was observed in the reactivity of biotinylated versus non-biotinylated envelopes to any of these antibodies, and aliquots of the same biotinylated envelopes used for cell binding assays were used for biolayer interferometry. The results of these experiments are summarized in Table 2-1.

All the envelopes bound to CD4 and were recognized by V2-specific antibodies, which indicated that they were correctly folded. Strain-specific binding to V2 antibodies was observed. Among the envelopes tested, there were representatives that bound to each of the V2 antibodies. As expected, none of the envelopes bound to PG9 and PG16, except for BG505 SOSIP trimer and BG505 gp120 monomer. PG9 and PG16 typically do not react with monomeric gp120 but have been reported previously to react with BG505 gp120 monomers[208].

These experiments confirmed that the DEAE-purified envelopes used in our assays displayed intact and accessible V2 epitopes. With the exception of BG505 gp120, all of them were the same envelope proteins used in our cell binding assays (Figure 2-7). From this, we concluded that lack of $\alpha_4\beta_7$ binding could not be attributed to a gross defect in the V2 loop or disruption of any particular V2 epitope by the additional DEAE purification step. However, the V2 domain can adopt multiple conformations, and we cannot exclude the possibility that specific V2 conformations required for $\alpha_4\beta_7$ reactivity were underrepresented in our protein preparations.

Table 2-1. Envelope protein binding to conformation-dependent V2 antibodies.

Protein (Cell Type)	MAb FI6v3 (negative control)	CD4-IgG_2 (positive control)	MAb 2158 (V2i)	MAb CH58 (V2p)	MAb PG9 (V2q)	MAb PG16 (V2q)
MW959 gp120 (CHO)	NB	100.90 ± 2.69	475.80 ± 8.62	287.10 ± 5.74	NB	NB
SF162.d7 gp120 (CHO)	NB	14.24 ± 0.33	3.25 ± 0.65	NB	NB	NB
1086.d7 gp120 (CHO)	NB	10.36 ± 0.33	23.79 ± 0.29	7.93± 0.14	NB	NB
BG505 gp120 (293)	NB	5.62 ± 0.21	NB	90.97 ± 0.78	25.35 ± 0.74	190.8 ± 2.52
BG505 SOSIP trimer (293)	NB	27.42 ± 0.56	NB	NB	66.98± 0.82	73.31± 1.15

Binding affinity constants (K_D) and associated measurement errors are provided for gp120-antibody pairs in which binding was observed. NB, no binding detected at 1µM concentration of envelope protein (shaded).

Monoclonal antibodies to V2 do not inhibit $\alpha_4\beta_7$ binding signals.

V2 monoclonal antibodies, including mAb 2158, are reported to inhibit gp120-$\alpha_4\beta_7$ binding *in vitro*[169, 186]. Based on this, we asked whether V2 antibodies inhibit $\alpha_4\beta_7$ binding signals seen in our assays with CHO cell proteins, perhaps by disrupting interactions between gp120 and CHO cell proteins. The two V2-directed antibodies CH58 and 2158 were tested in combination with gp120 in which antibody-gp120 interactions had been confirmed by biolayer interferometry. Antibodies and gp120 were incubated for 1 hour prior to incubation with unlabeled CHO cell proteins, and then the mixtures were assayed for $\alpha_4\beta_7$ binding on RPMI8866 cells. With all of the envelopes tested, the binding signal was increased by the addition of CHO cell proteins, but this was not inhibited with the addition of V2 antibodies (Figure 2-8). The V2 antibodies were additionally tested against MAdCAM-1-Fc in a similar manner and did not inhibit MAdCAM binding (Figure 2-8).

Although these experiments were limited in scope, they indicated that under the conditions we employed, V2 antibodies do not inhibit *in vitro* gp120-$\alpha_4\beta_7$ binding, as previously reported. Because the antibodies did not inhibit MAdCAM binding, we also concluded they do not have general $\alpha_4\beta_7$–inhibitory activity. While we were unable to explain previous observations concerning V2 antibodies, these experiments indicate that the indirect binding mediated by CHO cell proteins does not involve the V2 loop and is not blocked by V2 antibodies.

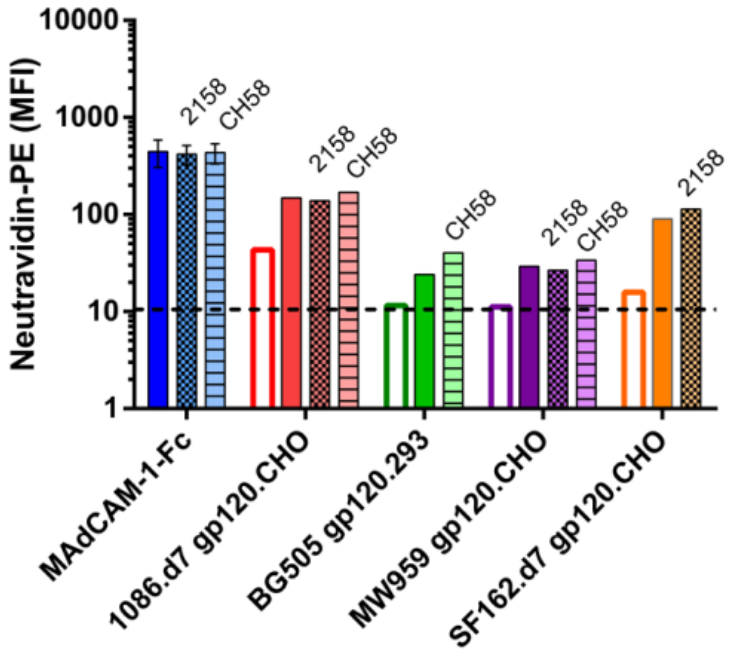

Figure 2-8. V2-directed antibodies do not inhibit $\alpha_4\beta_7$ binding signals. Binding of gp120 without CHO cell proteins (open bars) was compared to binding with 2hr preincubation of gp120 and CHO cell proteins (solid and patterned bars). One hour prior to adding CHO cell proteins, 4µg of gp120 was mixed with either 2µg of MAb 2158 (cross-hatched bars), 2µg MAb CH58 (hatched bars), or a matched volume of buffer without antibody (solid bars). MAdCAM-1-Fc was similarly pre-incubated with MAbs 2158 and CH58. The binding results are single measurements, except MAdCAM-1-Fc, which is the mean and standard deviation of 2 measurements.

CHO cells produce an $\alpha_4\beta_7$–reactive isoform of fibronectin.

Because CHO cellular proteins were the main predictor of gp120-$\alpha_4\beta_7$ binding in our assays, we sought to identify which proteins were responsible for the $\alpha_4\beta_7$ -binding activity. We began by generating lists of proteins present in CHO cell samples using a mass spectrometry (MS) shotgun sequencing approach. Proteins in CHO cell fraction 3, which were largely separated from gp120 monomers by SEC, were analyzed from a CHO cell-conditioned medium sample. We additionally analyzed the CHO cell proteins that were coeluted with MW959 gp120 monomers that could be removed by DEAE. For this, the order of purification steps was

changed: GNA eluate was first separated by SEC, the resulting gp120 monomer fraction was passed through DEAE, and CHO cell proteins retained by DEAE were eluted and analyzed.

The results of these experiments are summarized in Table 2-2, and the complete data set is deposited to the ProteomeXchange Consortium via the PRIDE partner repository with the dataset identifiers PXD006060 (CHO peak3) and PXD006061 (proteins co-eluted with gp120)[209]. For the sake of brevity, Table 2-2 lists only proteins that were identified by 30 or more independent spectra. Additionally, even though keratin was detected, it was presumed to be a contaminant of sample preparation and was excluded. Major components of CHO cell fraction 3 appeared to be extracellular matrix proteins, including the primary components of basement membrane (proteoglycans, fibronectin, collagen, laminin, and nidogen). CHO cell proteins coeluted with gp120 also contained many of these components, including very large proteins (proteoglycans, fibronectin, and laminin). This indicated there was likely a "trailing effect" with SEC, and not all of the high-molecular-weight components were fully excluded from the position where gp120 monomers elute.

Table 2-2. Characterization of CHO proteins by mass spectrometry.

	CHO Fraction 3		Proteins Co-eluted with gp120			
Protein Name	**Number of Independent Spectra**	**% Sequence Coverage**	**Number of Independent Spectra**	**% Sequence Coverage**	**Predicted Molecular Mass (Da)**	**Predicted Isoelectric Point**
Extracellular Matrix Proteins						
Basement membrane-specific heparan sulfate proteoglycan core protein	1246	77.2	212	50.0	333,928	6.41
Fibronectin	463	64.5	137	43.3	273,332	5.46
Chondroitin sulfate proteoglycan 4	192	43.7	113	40.0	251,857	5.40
Laminin subunit alpha-5	172	38.3	90	18.2	405,634	6.49
Laminin subunit beta-1	88	39.6	61	27.7	178,018	4.76
Laminin subunit gamma-1	107	50.0	51	30.8	172,011	4.96
Collagen alpha-1(XII) chain (Fragment)	70	31.5	<30	---	268,332	5.18
Nidogen-1	161	66.4	101	58.0	78,989	4.75
Tubulo-interstitial nephritis antigen-like	113	75.1	<30	---	52,486	6.70
EMILIN-1	129	51.3	34	31.0	107,249	5.24
Thrombospondin-1	48	57.2	31	36.8	60,036	4.25
Matrix metalloproteinase-19	31	43.2	<30	---	58,905	7.71
Matrix metalloproteinase-9	30	36.1	152	60.8	78,844	5.60
Biglycan	37	45.5	<30	---	41,608	6.86
Agrin	67	37.6	<30	---	216,975	5.50
Latent-transforming growth factor beta-binding protein 1	57	30.9	43	28.7	129,962	4.99
Enzymes						
Peroxidasin-like	179	62.4	57	38.1	165,260	6.63
Beta-hexosaminidase	<30	---	33	40.5	60,620	6.05

Carboxypeptidase D	<30	---	39	27.8	123,366	5.79
Fatty acid synthase	93	36.9	<30	---	271,687	5.95
Protein-glutamine gamma-glutamyltransferase 2	63	62.4	33	49.7	77,161	5.11
Lipoprotein lipase	33	56.2	<30	---	50,490	7.95
Alpha-mannosidase	<30	---	68	41.8	111,289	7.01
Neutral alpha-glucosidase AB	<30	---	58	47.2	106,910	5.64
UDP-glucose: glycoprotein glucosyltransferase 1	<30	---	54	39.0	151,425	5.45
Glyceraldehyde-3-phosphate dehydrogenase	46	57.6	<30	---	36,866	8.70
Pyruvate kinase	45	61.4	31	46.4	51,527	7.58
Beta-glucuronidase	<30	---	296	73.1	74,756	6.28
CAD protein	55	30.3	<30	---	242,877	6.06
Lysyl oxidase-like 3	60	42.9	<30	---	87,990	6.80
Lysyl oxidase-like 4	45	45.2	<30	---	84,736	8.32
Lysosomal alpha-glucosidase	<30	---	47	39.3	105,780	5.65
Chaperone and Cellular Stress-Response Proteins						
FK506-binding protein 10	<30	---	44	44.9	64,677	5.43
Endoplasmin	32	36.7	74	52.8	92,565	4.74
Heat shock protein HSP 90-beta	36	46.8	<30	---	47,777	5.33
Clusterin	<30	---	35	42.1	51,724	5.52
Hypoxia up-regulated protein 1	62	43.9	156	63.3	111,395	5.11
78 kDa glucose-regulated protein	<30	---	79	56.3	72,334	5.07
Cytoskeletal Proteins						
Actin, cytoplasmic 1	66	61.9	39	61.6	41,710	5.29
Tubulin alpha chain	35	65.0	37	59.4	50,090	4.94
Tubulin beta chain	35	67.3	42	70.0	49,639	4.78
Cytoplasmic dynein 1 heavy chain 1 (Fragment)	40	11.2	<30	---	526,453	6.13

Cell-Surface Membrane Proteins						
Neogenin	<30	---	41	22.8	154,381	6.17
Desmoplakin	<30	---	44	17.2	328,215	6.53
Protocadherin Fat 1	62	15.0	<30	---	506,399	4.82
CD109 antigen	<30	---	122	50.9	161,764	5.84
Prolow-density lipoprotein receptor-related protein 1	38	19.1	<30	---	245,831	5.10
Other Intracellular Proteins						
Calreticulin	<30	---	50	58.3	48,212	4.34
Cation-independent mannose-6-phosphate receptor	<30	---	92	38.5	186,544	5.25
Elongation factor 2	46	45.2	<30	---	96,581	6.41
Other Secreted Proteins						
Galectin-3-binding protein	244	54.4	69	53.0	63,761	5.06
Inter-alpha-trypsin inhibitor heavy chain H5	101	50.9	45	39.4	101,988	8.73
Serine protease HTRA1	44	48.1	<30	---	28,700	6.54
Olfactomedin-like protein 2B	35	40.7	<30	---	83,491	4.82

Red shading denotes proteins detected by 30 or fewer spectra.

Out of the proteins identified, fibronectin was the only protein with known $\alpha_4\beta_7$ interactions. Cells produce several variants of fibronectin by alternative RNA splicing, and only some of them bind to $\alpha_4\beta_7$[210, 211]. We therefore examined fibronectin in further detail and asked whether CHO cells produced $\alpha_4\beta_7$-reactive fibronectins. Fibronectin-$\alpha_4\beta_7$ binding occurs through the inclusion of the alternatively spliced type III connecting segment (IIICS). Within IIICS is a sequence designated the CS1 peptide that contains an LDV site required for $\alpha_4\beta_7$ binding[212]. We examined spectra from CHO cell fraction 3, and found 11 independent and high-quality spectra containing the complete fibronectin CS1 sequence (available via

ProteomeXchange with identifier PXD006060). These results confirmed that CHO cells produce an $\alpha_4\beta_7$–reactive isoform of fibronectin. The experimentally determined amino acid sequence of CHO cell fibronectin CS1 was DELPQLVTLPHPNLHGPEILDVPST. Notably, this is 100% identical to the human fibronectin CS1 sequence (UniProtKB/Swiss-Prot accession no. P02751.4). Therefore, we concluded it was highly plausible that the CHO cell fibronectins in our samples reacted with human $\alpha_4\beta_7$.

We next attempted to verify this with biochemical assays. First, CHO cell proteins were fractionated by DEAE using stepwise elution with 100mM, 200mM, 300mM, and 400mM sodium chloride. The 200mM fraction was found to retain the relevant binding activity and was used for subsequent assays. Proteins were radiolabeled with ^{125}I (Figure 2-9A) and tested to ensure they retained $\alpha_4\beta_7$ binding activity (Figure 2-9B). Next, RPMI8866 cells were used to selectively capture the $\alpha_4\beta_7$ binding components. For this, cells were incubated with ^{125}I-labeled CHO cell proteins and washed, and then the cell-bound material was dissociated with buffer containing EDTA and CWLDVC peptide. The dissociated material was then separated by SDS-PAGE and visualized by autoradiography. The major component enriched on RPMI8866 cells appeared to be a 260-kDa band (Figure 2-9C). Additionally, a band of approximately 55-kDa also appeared to be retained on RPMI8866 cells (Figure 2-9C). A separate (nonradioactive) sample was separated by SDS-PAGE, and the 260-kDa and 55-kDa bands were excised, digested, and analyzed by liquid chromatography-mass spectrometry (LC-MS). While these experiments were not carried out in a way that allowed quantitative analysis, they did identify components that appeared to be enriched relative to the unfractionated protein mixture. The two major components enriched in the 260-kDa band appeared to be fibronectin (664 peptides) and chondroitin sulfate proteoglycan (867 peptides) (available via ProteomeXchange with identifier

PXD006063). The major components enriched in the 55-kDa band appeared to be tubulointerstitial nephritis antigen-like protein (276 peptides) and calreticulin (186 peptides) (available via ProteomeXchange with identifier PXD006062). Collectively, these findings were consistent with the identification of fibronectin as the CHO cell protein responsible for $\alpha_4\beta_7$ reactivity.

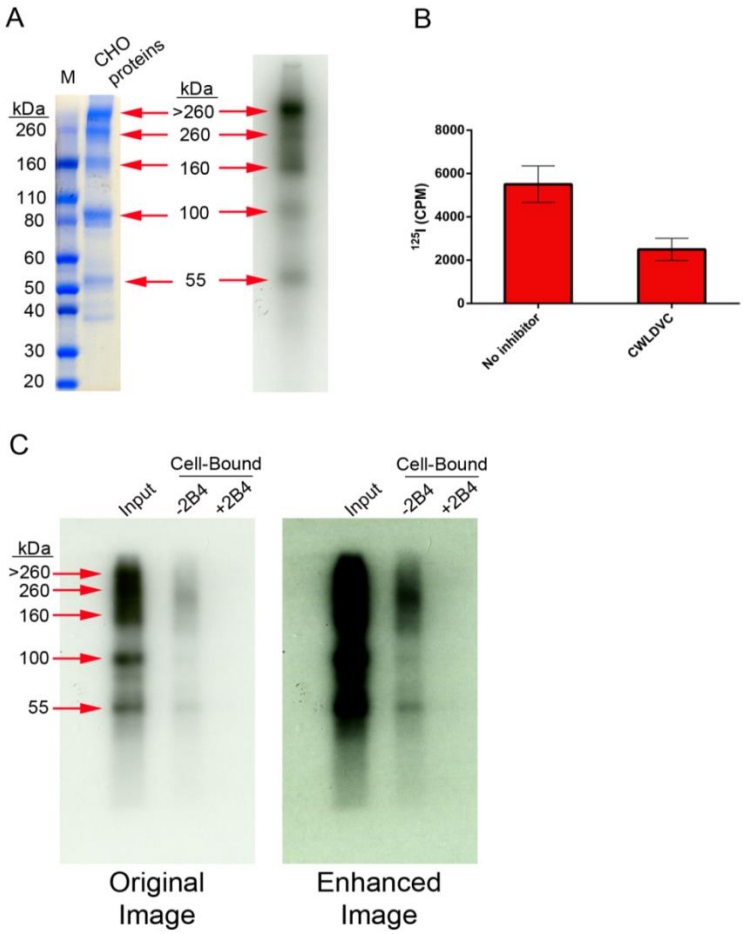

Figure 2-9. Identification of fibronectin as an $\alpha_4\beta_7$ binding component of CHO cell proteins. The CHO cell proteins were labeled with ^{125}I. (A) Comparison of proteins detected by autoradiography to 25µg of proteins stained with Coomassie blue. Five major bands present in the Coomassie-stained gel were also identified by autoradiography, as indicated. (B) Proteins displayed $\alpha_4\beta_7$–dependent binding to RPMI88666 cells after radiolabeling. (C) RPMI8866 cells were used to capture and identify $\alpha_4\beta_7$ binding components. ^{125}I-labeled protein was captured on cells in the presence or absence of MAb 2B4, and then cell-bound material was dissociated and analyzed. Input protein was compared to cell-bound material by SDS-PAGE and autoradiography. Shown are the original autoradiograph and a contrast-enhanced image. The cells retained a major band of approximately 260kDa and a minor band of 55kDa.

Heparin sulfate inhibits fibronectin-mediated gp120-$\alpha_4\beta_7$ binding.

Previous reports indicate that gp120 binds to the C-terminal heparin binding domain of fibronectin and that this can be inhibited with heparin sulfate[136]. Based on this, we tested the ability of heparin to inhibit gp120-$\alpha_4\beta_7$ interactions mediated by CHO cell fibronectin. Mixtures of 1086.d7 gp120 and CHO cell proteins were incubated for 2 hours, and then various concentrations of heparin sulfate were added and binding to RPMI8866 cells was measured. Chondroitin sulfate, a glycosaminoglycan related to heparin, was used as a control in these experiments.

Heparin sulfate was able to inhibit fibronectin-mediated gp120-$\alpha_4\beta_7$ binding in a concentration-dependent manner (Figure 2-10). The half-maximal inhibitory concentration (IC_{50}) of heparin was calculated as 0.25µg/mL (95% confidence interval, 0.11 to 0.59µg/mL). In contrast, chondroitin sulfate did not have a measurable inhibitory effect at the concentrations tested. These experiments supported the hypothesis that gp120 interacted with the heparin binding domain of CHO cell fibronectin.

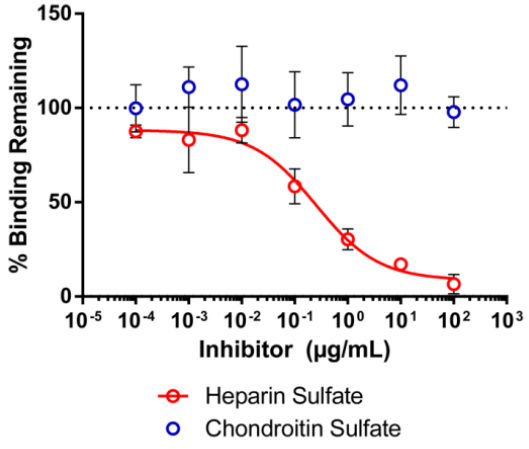

Figure 2-10. Heparin inhibits fibronectin-mediated gp120-$\alpha_4\beta_7$ binding. 1086.d7 gp120 was incubated for 2 hours with CHO cell proteins. Heparin sulfate or chondroitin sulfate was added at the indicated concentrations 10 minutes prior to incubation with RPMI8866 cells. The results are the means and standard deviations of three replicates; the red line is a best-fit curve of the heparin inhibition data.

A recombinant human fibronectin fragment reproduces CHO cell protein binding behavior

Last, we asked if purified human fibronectin proteins could reproduce the binding phenomena observed with CHO cell proteins. Three fibronectin proteins were chosen for study. First was human plasma fibronectin, which was not expected to react with $\alpha_4\beta_7$. Second was cellular fibronectins isolated from cultured human foreskin fibroblasts. These fibronectins were expected to be a heterogeneous mixture and potentially to contain $\alpha_4\beta_7$–reactive isoforms. Last was RetroNectin, a chimeric recombinant human fibronectin fragment produced in *Escherichia coli* containing the cell binding domain, C-terminal heparin binding domain, and CS1 peptide of human fibronectin (TaKaRa)[213].

These three proteins were biotinylated and tested for $\alpha_4\beta_7$ binding activity. As expected, plasma fibronectin did not bind to RPMI8866 cells. Cellular fibronectin produced a weak $\alpha_4\beta_7$ binding signal, and RetroNectin produced a robust signal (Figure 2-11A). The proteins were then tested for the presence of the CS1 peptide by western blotting. All the proteins reacted with polyclonal anti-fibronectin antisera, but only RetroNectin reacted with monoclonal antibody to CS1 (Figure 2-11B). Because RetroNectin bound strongly to $\alpha_4\beta_7$ and was verified to contain CS1, it was used in subsequent assays. In mixing experiments, similar to those performed with CHO cell proteins, cell binding was observed in mixtures of unlabeled RetroNectin and labeled MW959 gp120 or MW959-ΔV2 gp120 (Fig 2.11C). These results confirmed that human fibronectins can mediate indirect gp120-$\alpha_4\beta_7$ interactions similarly to CHO cell proteins.

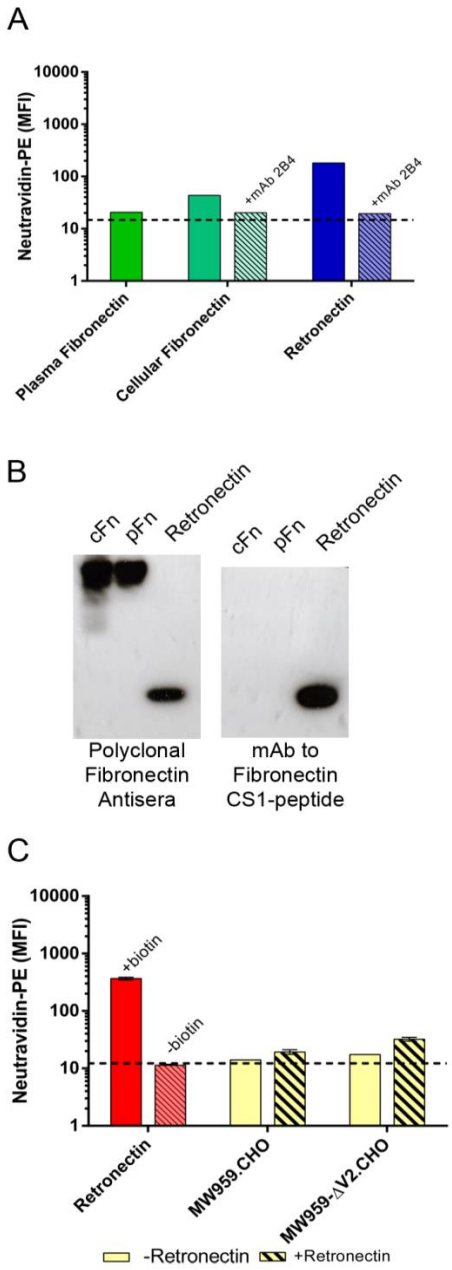

Figure 2-11. The recombinant human fibronectin fragment RetroNectin mediates gp120-$\alpha_4\beta_7$ binding. (A) Plasma fibronectin, cellular fibronectin, and RetroNectin were biotinylated and tested for binding to RPMI8866 cells. The results of a single representative experiment are shown. (B) Western blot analysis of plasma fibronectin (pFn), cellular fibronectin (cFn), and RetroNectin. Shown are two parallel blots developed with either polyclonal fibronectin antiserum or monoclonal antibody to the fibronectin CS1 peptide; 1µg of protein was loaded per lane. (C) RetroNectin mediates gp120 binding to RPMI8866 cells. Biotinylated RetroNectin (+biotin) produces a binding signal, and nonbiotinylated RetroNectin (-biotin) does not. Binding of wild-type MW959 and MW959 with the V2 loop deleted was measured with (hatched bars) and without (solid bars) 2hr preincubation with RetroNectin. The results are the means and standard deviations of 3 replicate measures.

Discussion

In this work, we provide evidence that extracellular matrix proteins, including fibronectin, can mediate indirect interactions between gp120 and $\alpha_4\beta_7$. We initially observed that CHO cellular fibronectins, which copurified with gp120, could facilitate binding of gp120 to $\alpha_4\beta_7$. We then extended this observation and verified that a recombinant human fibronectin fragment could also mediate gp120-$\alpha_4\beta_7$ binding. These observations help reconcile conflicting reports concerning gp120-$\alpha_4\beta_7$ interactions[164, 172], and at the same time raise the interesting possibility that the extracellular matrix may play a role in mediating HIV-1-$\alpha_4\beta_7$ contact *in vivo*. This may have important implications with respect to $\alpha_4\beta_7$ as a potential target for antiretroviral therapy and vaccines.

It has been reported that the LDV/I amino acid sequence within the V2 loop facilitates gp120-$\alpha_4\beta_7$ interactions[164, 168-170]. LDV/I is a well-conserved feature of V2 and has been hypothesized to be a structural mimic of the integrin binding motifs in MAdCAM-1 (LDT), VCAM-1 (IDS), and fibronectin (LDV)[164]. In MAdCAM-1 and VCAM-1, these sites coordinate magnesium cations that bind to the α_4 integrin metal ion-dependent adhesion site, while adjacent amino acid residues provide specificity that is critical for receptor binding[214, 215]. Mimicry of integrin binding motifs has been reported in several distantly related virus families and may be a common strategy used to control host tropism[165]; however, it is not known whether viruses use these motifs as integrin contact sites or as sites that accommodate divalent cations. Within HIV-1 envelopes, LDV/I has been proposed to coordinate divalent cations. However, similar to $\alpha_4\beta_7$ binding with its native ligands, structures adjacent to the LDV/I site are likely required for receptor binding. In support of this, it has recently been reported that structures adjacent to LDV/I within short and cyclic V2 peptides promote binding

to $\alpha_4\beta_7$[168, 169]. Additionally, the conformation of the V2 loop may impact $\alpha_4\beta_7$ reactivity. Our group (KKL & SLH) has previously demonstrated that the V2 loop in gp120 is highly dynamic and flexible[216]. Cocrystallization studies with V2 MAbs have revealed both helical and β-strand conformations[217]. These findings underscore the structural heterogeneity of the V2 loop. Presently, it is not known which conformations of V2 may mediate $\alpha_4\beta_7$ binding. Among the recombinant envelope proteins employed in this study, all contained an LDV/I site. Additionally, these envelope proteins presented a diverse set of V2 conformations, as defined by their reactivity with a panel of conformation-dependent V2 antibodies. Despite this, we did not detect $\alpha_4\beta_7$ reactivity in any of these proteins. This implies that LDV/I and other V2 structures within these envelope proteins were not presented in a way that was accessible to $\alpha_4\beta_7$. Further studies are required to clarify if any specific V2 conformations may be required for $\alpha_4\beta_7$ binding. Ideally, such studies would compare the $\alpha_4\beta_7$ binding properties of DEAE-purified gp120 and V2 peptides matched to those proteins.

Vaccine-elicited V2-specific antibodies have been correlated with reduced risk of HIV-1 acquisition in the RV144 trial, but the underlying mechanism for this observation remains unclear[181]. One possibility is that V2-directed antibodies may disrupt HIV-1 engagement with $\alpha_4\beta_7$ and thus contribute to protection. In support of this, a small number of studies show gp120-$\alpha_4\beta_7$ binding *in vitro* can be inhibited by V2-specific antibodies. Specifically, it has been reported that MAb 697D and MAb 2158 both inhibit binding of a Clade A gp120[169], and several mouse V2 MAbs inhibit binding of MN gp120[186]. In contrast to these findings, we failed to detect any inhibitory effect of V2 MAbs on fibronectin-mediated gp120 binding to $\alpha_4\beta_7$. Thus, it remains unclear whether any vaccine-induced V2-specific antibody may offer protection through inhibiting HIV-1-$\alpha_4\beta_7$ interaction. In this context, we note that an alternative role for

V2-directed antibodies mediating antibody-dependent cellular cytotoxicity has also been proposed as a mechanism for protection in RV144[218].

In this report, we identified an indirect interaction between gp120 and $\alpha_4\beta_7$ that is mediated by the extracellular matrix. Specifically, we identified fibronectin as a protein that could mediate this interaction. Fibronectins are large glycoproteins of the extracellular matrix with functional roles in regulating cell migration, embryonic development, and wound healing[219]. They have also been shown to interact with gp120 and enhance the infectivity of HIV-1[139]. Twenty fibronectin splice variants have been described in humans, and those containing the alternatively spliced IIICS support $\alpha_4\beta_7$ binding through an LDV site[211, 212]. In contrast, all fibronectin isoforms bind gp120 through the invariant C-terminal heparin binding domain[136]. In our work, we observed that CHO cells produce a fibronectin variant containing the CS1 peptide within IIICS that supports $\alpha_4\beta_7$ binding. CHO cell proteins including fibronectin, and the recombinant human fibronectin fragment RetroNectin, mediated indirect gp120-$\alpha_4\beta_7$ binding. Based on these observations, we speculate that $\alpha_4\beta_7$–reactive matrix fibronectins may colocalize with HIV-1 and $\alpha_4\beta_7^+$ cells *in vivo* and thus lead to the preferential infection of these cells. However, because our work is based on *in vitro* gp120 protein interactions, further studies are required to determine whether fibronectin plays any role in HIV-1 infection of $\alpha_4\beta_7^+$ cells.

Prior studies have demonstrated that fibronectin-gp120 contact occurs through the heparin binding domain of fibronectin [136]. In agreement with this, we showed that fibronectin-mediated gp120-$\alpha_4\beta_7$ binding in our assays could be inhibited by heparin sulfate. However, it is less clear which structures within gp120 are involved in this binding. The V3 loop and CD4 binding site have both been implicated in gp120-fibronectin interactions; however,

neither has been definitively demonstrated to be sufficient or necessary for binding[136, 138]. It is possible that specific structures within gp120 may engage fibronectin. Alternatively, the interaction may be less specific, involving interactions with glycans or charged amino acid residues. In studies reported here, we found the V2 loop is not likely to be involved in gp120-fibronectin interactions. However, more studies are needed to determine the nature of gp120-fibronectin interactions and whether these interactions may be inhibited by anti-HIV-1 antibodies.

At present, $\alpha_4\beta_7$ antagonists are being investigated for use in HIV-1 treatment. In particular, the $\alpha_4\beta_7$–blocking monoclonal antibody Act-1 has been extensively studied. A primatized version of Act-1 has been developed, and treatment with this antibody resulted in lower viral loads and higher $CD4^+$ cell numbers in SIV-infected macaques[188-190]. Additionally, treatment prior to vaginal challenge reduced the efficiency of SIV transmission[190]. More recently, a combination regimen of antiretroviral drugs and Act-1 was shown to reconstitute gut $CD4^+$ cells and induce a state of drug-free virological control in SIV-infected macaques[191]. Currently, early-phase clinical trials are under way to test whether the humanized version of Act-1 (vedolizumab) can achieve similar results in humans (http://www.clinicaltrials.gov; identifier NCT02788175). Our studies raise an interesting scenario in which indirect HIV-1-$\alpha_4\beta_7$ interactions, mediated by fibronectin, may be inhibited by Act-1. Further studies are needed to explore this as a possible mechanism of action for any therapeutic effect against HIV-1 attributable to Act-1.

In summary, our work demonstrates that an indirect gp120-$\alpha_4\beta_7$ interaction can be mediated by extracellular matrix proteins, such as fibronectin. Our findings further suggest that studies of the *in vivo* effects of $\alpha_4\beta_7$ antagonists may need to take into consideration the role of

extracellular matrix proteins, such as fibronectin, in mediating indirect interactions between HIV-1 and $\alpha_4\beta_7$. Further studies are needed to clarify whether and how the extracellular matrix in relevant species and tissues may play a role in HIV-1 infection of gut-homing cells.

Materials and Methods

Reagents and cell lines

The following fluorophores were used in flow cytometry analysis: allophycocyanin (APC), phycoerythrin (PE), and fluorescein isothiocyanate (FITC). Fluorescent antibodies to CD4 (clone RPA-T4, APC), CCR5 (clone 2D7, APC), and β_7 integrin (clone FIB504, PE) were from Becton Dickinson. Fluorescent antibody to CD45RO (clone UCHL1, FITC) was from Biolegend. Neutravidin conjugated to PE was from ThermoFisher Scientific. CD4-blocking antibody Leu3a (clone SK3) was from Becton Dickinson. Integrin-blocking antibodies 2B4 and P5D2 were from R&D systems. Human V2 monoclonal antibody 2158 was a gift from Susan Zolla-Pazner. Human V2 monoclonal antibodies PG9 and PG16 were from the International AIDS Vaccine Initiative. FI6v3 influenza virus HA monoclonal antibody was produced in house from a stable HEK293F cell line and purified from culture supernatants by protein A affinity chromatography. The following reagents were obtained through the NIH AIDS Reagent Program, Division of AIDS (DAIDS), NIAID, NIH: CD4-IgG_2 fusion protein from Progenics Pharmaceuticals, Human V2 monoclonal antibody CH58 from Barton F. Haynes and Hua-Xin Liao, and anti-human $\alpha_4\beta_7$ integrin antibody Act-1 from A. A. Ansari. The CWLDVC and CLDVWC peptides were purchased from GenScript. These peptides were cyclized by disulfide bonds, and purity was 98% or greater as assessed by high-pressure liquid chromatography and mass spectrometry. The MAdCAM-1-Fc fusion protein was from R&D Systems. Biotinylated

HRP was from Pierce. Aldolase, Ovalbumin, and Ferritin were from GE Life Sciences. Bovine serum albumin (BSA), plasma fibronectin, cellular fibronectin, heparin sulfate derived from porcine intestinal mucosa (189U/mg), and chondroitin sulfate B derived from porcine intestinal mucosa were from Sigma-Aldrich. RetroNectin was from TaKaRa. RPMI8866 cells were from Sigma-Aldrich and were maintained at $0.2x10^6$ to $1.0x10^6$ cells/mL at 37°C and 5% CO_2 in RPMI-1640 medium supplemented with 10% fetal bovine serum, 2mM L-glutamine, 100U/mL penicillin, and 100µg/mL streptomycin. Freestyle CHO-S and Freestyle 293-F cells used to produce recombinant proteins were purchased from ThermoFisher Scientific and cultured in serum-free and antibiotic-free media according to the manufacturer's instructions in spinner cultures maintained at 37°C and 8% CO_2.

Human $CD4^+$ $\alpha_4\beta_7^+$ cells

Used leukocyte filters from healthy donors were purchased from Bloodworks Northwest (Seattle, Washington) and used to isolate human PBMCs. Cells were recovered from the filters by back flushing with 200mL of phosphate-buffered saline (PBS) containing 0.2g/liter EDTA and 10,000U/liter heparin. PBMCs were separated by Ficoll Paque, and magnetic cell separation was used to enrich $CD4^+$ cells by negative selection (Miltenyi Biotec). The cells were activated for 2 days with 250ng/mL OKT3 antibody (Biolegend) and cultured continuously with 20U/mL interleukin-2 (Roche) and 10nM all-trans retinoic acid (Sigma-Aldrich). The culture medium was RPMI-1640 supplemented with fetal bovine serum, glutamine, and antibiotics as described above. The cells were used for binding studies 9 days after establishing cultures.

Source of HIV-1 gp120 expression plasmids and proteins

An expression plasmid for MW959 gp120 was produced by Genewiz. The nucleotide sequence for 93MW959.18 gp120 (GenBank accession no. U08453.1) was codon optimized for expression in CHO cells, synthesized *de novo,* and inserted by topoisomerase cloning into the pcDNA3.1/V5-His TOPO vector (Invitrogen). The first 30 amino acids of the native 93MW959.18 sequence were replaced with the human tissue plasminogen activator leader peptide (amino acid sequence MDAMKRGLCCVLLLCGAVFVSAS). This plasmid was used to generate the MW959-ΔV2 gp120 mutant by site-directed mutagenesis (QuikChange lightning kit; Agilent) using a primer with the following sequence: ATGAAGAACTGCTCCTTCAACGAGAAGGACAACAGC. Expression plasmids for BG505.T332N.664 SOSIP and furin were gifts from John Moore[204]. The expression plasmid for BG505 gp120 was generated from the BG505.T332N.664 SOSIP plasmid by introducing a stop codon. The expression plasmid for AN1 gp120 was from James Arthos, as previously described[164].

The following proteins were prepared in the laboratory of Dr. Shiu-Lok Hu at the University of Washington: MW959 produced in CHO and 293 cells, MW959-ΔV2 produced in CHO cells, BG505 SOSIP produced in 293 cells, BG505 gp120 produced in 293 cells, and AN1 gp120 produced in 293 cells. The following proteins were produced at the Duke Human Vaccine Institute, Duke University Medical Center, and provided as a gift by David Montefiori: SF162.d7 gp120 produced in CHO, 293, and 293S GnT1$^{-/-}$ cells and 1086.d7 gp120 produced in CHO cells. TV-1 gp120 was produced in CHO cells by Novartis and provided as a gift by David Montefiori. The following reagents were obtained through the NIH AIDS Reagent Program, Division of AIDS, NIAID, NIH: BaL gp120 produced in 293 cells from DAIDS, NIAID, and

M.CON-S.d11 gp120 produced in 293 cells from the Duke Human Vaccine Institute, Duke University Medical Center. Unless otherwise specified, purification of all these proteins included DEAE chromatography.

Production and purification of recombinant HIV-1 envelopes

HIV-1 envelope expression plasmids were prepared with an endotoxin-free plasmid megaprep kit (Qiagen). The transfection procedure was the same for CHO-S and 293-F cells; $1.0x10^9$ cells were suspended in 50mL of medium containing 1mg of plasmid and 2mg of polyethelyeneimine (Polysciences, Inc.). Cultures were incubated for 4 hours and then diluted to 1 liter and maintained for 3 days. The culture supernatants were clarified by centrifugation and passed through a 0.2µm filter, and protease inhibitors (aprotinin, leupeptin, and pepstatin A, all from Sigma-Aldrich) were added. For BG505 SOSIP production, cells were cotransfected with 750µg BG505 SOSIP expression vector and 250µg furin expression vector to ensure complete furin-mediated cleavage of the SOSIP trimer. For cell-conditioned media without recombinant protein expression, $1.0x10^9$ cells were diluted to 1 liter and maintained for 3 days before harvesting as described above.

Purification was carried out with an ÄKTA 10/100 purifier (GE Life Sciences) maintained at 4°C. A 10mL GNA column (*G. nivalis* lectin conjugated to agarose; Vector Laboratories) was prepared and pre-equilibrated with binding buffer (150mM NaCl, 20mM Tris-HCl, pH 7.5). Culture supernatant was loaded onto GNA at 1 mL/min. The column was then washed with 10 column volumes (CV) of high-salt wash buffer (500mM NaCl, 20mM Tris-HCl, pH 7.5), followed by 10 CV of binding buffer, and bound protein was eluted with binding buffer containing 1M methyl-α-D-mannopyranoside (Sigma-Aldrich). Peak fractions were pooled and

exchanged into DEAE binding buffer (100mM NaCl, 20mM Tris-HCl, pH 8.0) by diafiltration with Centricon centrifugal concentrators (Millipore) using 1,500 or greater diavolumes. The sample was then loaded at 1 mL/min onto a prepacked 5mL DEAE sepharose column (GE Life Sciences). Column flowthrough was collected, and the column was washed with 2 CV DEAE binding buffer. Material bound to DEAE was eluted by applying a gradient of 0-100% DEAE elution buffer (1M NaCl, 20mM Tris-HCl, pH 8.0) over 5 CV. Samples were concentrated with Amicon centrifugal concentrators (Millipore), and then purified by SEC on a 320mL HighLoad 26/600 Superdex 200 column (GE Life Sciences). SEC was carried out at 1.2 mL/min with PBS (10mM sodium phosphate, 150mM NaCl, pH 7.4). Peak fractions were pooled and concentrated with Amicon centrifugal concentrators, and protein concentrations were determined by a bicinchoninic acid assay (Pierce).

Polyacrylamide gel electrophoresis and western blot analyses

Reagents used for protein gels were obtained from ThermoFisher Scientific. For SDS-PAGE, protein samples were reduced and denatured in NuPage lithium dodecyl sulfate buffer containing dithiothreitol (DTT) at 70°C for 10min. Proteins were then separated by electrophoresis on a 4 to 12% Bis-Tris gel using Novex Sharp prestained protein standards as molecular weight markers. SimplyBlue Coomassie G-250 stain was used to visualize proteins according to the manufacturer's instructions. For Native PAGE, nondenatured proteins were loaded on a 3 to 12% Bis-Tris native gel using NativeMark unstained protein standards as molecular weight markers. The gel was run and stained according to manufacturer's instructions.

For western blotting, proteins separated by SDS-PAGE were transferred to polyvinylidene difluoride (PVDF) membranes with an iBlot device (Invitrogen). The membranes were incubated for 1 hour in blocking buffer (PBS containing 5% nonfat milk and 0.05% Tween-20), and then incubated overnight at 4°C with primary antibodies diluted in blocking buffer. For gp120 detection, pooled plasma from 131 Zambian women infected with Clade C HIV-1 (a gift from Charles Wood) was diluted 1:2,000. For fibronectin detection, rabbit polyclonal anti-fibronectin (Abcam) was diluted 1:1,000. For fibronectin CS1 detection, mouse monoclonal IgM against human fibronectin CS1 peptide (Santa Cruz Biotechnology; clone P1F11) was diluted 1:200. The membranes were washed three times in PBS containing 0.05% Tween-20 and then incubated for 1 hour with secondary antibodies diluted in blocking buffer. For gp120 detection, alkaline phosphatase-conjugated goat anti-human IgG (Sigma-Aldrich) was diluted 1:10,000. For fibronectin detection, HRP-conjugated goat anti-rabbit IgG (Calbiochem) was diluted 1:10,000. For fibronectin CS1 detection, HRP-conjugated goat anti-mouse IgM (Santa Cruz Biotechnology) was diluted 1:2,000. The membranes were washed extensively with PBS containing 0.05% Tween-20 and then incubated with BCIP (5-bromo-4-chloro-3-indolylphosphate)-nitroblue tetrazolium (NBT) substrate (Sigma-Aldrich) for alkaline phosphatase detection or chemiluminescence substrate (Pierce) for HRP detection. HRP signals were captured on film (Amersham Hyperfilm ECL; GE Life Sciences).

Protein biotinylation

Proteins were biotinylated with EZ-Link N-hydroxysuccinimide (NHS) biotin reagent (Pierce). The proteins were combined with NHS biotin in a 1:20 molar ratio and incubated for 30min at room temperature. Samples from cell-conditioned media were labeled with the same biotin/protein ratio as was used for gp120 labeling. Reactions were quenched by adding Tris-

HCl, pH 8.0, and then samples were dialyzed overnight against HEPES-buffered saline (150mM NaCl, 10mM HEPES, pH 7.4) at 4°C, followed by an additional 3 hours in fresh buffer. The concentration of biotinylated proteins was measured by a bicinchoninic acid assay (Pierce) or by absorbance at 280nm on a NanoDrop 1000 spectrophotometer (ThermoFisher Scientific). Proteins were put into single-use aliquots and stored at -80°C until they were used in cell binding assays.

Flow cytometry-based $\alpha_4\beta_7$ binding assay

Binding assays were performed as previously described[164]. All binding and washing steps were carried out at 4°C in either manganese-containing buffer (150mM NaCl, 10mM HEPES, pH 7.4, 1mM $MnCl_2$, 100µM $CaCl_2$, 0.5% BSA, 0.09% sodium azide) or EDTA-containing buffer without divalent cations (150mM NaCl, 10mM HEPES pH 7.4, 5mM EDTA, 0.5% BSA, 0.09% sodium azide). The cells were either RPMI8866, which expresses $\alpha_4\beta_7$ but not CD4, or primary $CD4^+\alpha_4\beta_7^+$ T cells. The cells were washed with binding buffer and plated on 96-well plates at $1.0x10^6$ cells/mL, 200µL per well. Fc receptors were blocked with 15µg/mL normal mouse IgG and 5µg/mL normal human IgG. Some wells received 2µg of the following: integrin-blocking antibody 2B4, P5D2, or Act-1 or CD4-blocking antibody leu3a. In wells in which multiple antibodies were combined, 2µg of each antibody was used. Other wells received 5µg of integrin-blocking peptides CWLDVC or the scrambled control CDLVWC. Cells were incubated for 10min with inhibitors, and then biotinylated proteins were added and the cells were incubated for an additional 20min at 4°C; 4µg of biotinylated protein was added to each well, except for MAdCAM-1-Fc, which was added at 100ng per well. For mixing experiments, 4µg of unlabeled proteins were combined with 4µg of biotinylated proteins at 4°C for 0 or 2 hours prior

to adding to cells. For experiments with V2 monoclonal antibodies, 4µg of biotinylated gp120 was combined with 2µg of antibody and incubated for 1 hour at room temperature, and then 4µg of unlabeled proteins (or matched volume of buffer without protein) was added, and the mixtures were incubated at 4°C for an additional 2 hours prior to adding them to cells. For heparin sulfate and chondroitin sulfate competition experiments, 4µg of biotinylated gp120 was incubated for 2 hours with 4µg of unlabeled proteins, followed by 10 min incubation with 100µg/mL to 100pg/mL inhibitor prior to adding it to cells. Following protein binding, the cells were washed twice and stained for 20min at 4°C in binding buffer containing fluorescent probes. RPMI8866 cells were stained with 2.5µg/mL neutravidin-PE, and primary cells were stained with a mixture of neutravidin-PE and 1:100 dilutions of CD45RO-FITC and CCR5-APC antibodies. Aliquots of cells without biotinylated proteins were carried through the preceding wash/bind steps and stained with 1:100 dilutions of CD4-APC and integrin β_7-PE antibodies. The cells were washed twice, and then fixed in PBS containing 1% formaldehyde prior to analysis. Data were acquired on a BD FACSCalibur instrument with CellQuest Pro software (Becton Dickinson; version 6.0). A total of 20,000 events were recorded for each sample. The data were analyzed with FlowJo software (Treestar; version 7.2.2). The neutravidin-PE binding signal was reported in units of median fluorescence intensity (MFI).

V2 antibody binding by biolayer interferometry

An Octet RED96 instrument (Fortebio) was used to perform biolayer interferometry. The assay buffer was PBS with 1% BSA, 0.03% Tween-20, and 0.02% sodium azide. Antibodies were diluted in assay buffer to 10µg/mL, and serial dilutions of envelope proteins were prepared in assay buffer (1000nM, 500nM, 250nM, 125nM, and 62.5nM). The regeneration buffer was

0.1M glycine, pH 1.5; 200µL of each solution per well was used in a low-binding 96-well plate. All assay steps were carried out at 32°C with constant mixing at 1,000RPM. Anti-human IgG Fc biosensors (Fortebio) were pre-equilibrated in assay buffer and then transferred to antibody-containing wells for 300s. After antibody capture, the sensors were washed in assay buffer and baseline signals were recorded for 60s. Antibody-coated tips were transferred to wells containing envelope proteins, and association curves were recorded for 180s. The tips were then transferred to wells containing assay buffer and dissociation curves were recorded for 300s. The tips were regenerated by cycling 3 times between regeneration and assay buffers for 5s in each buffer, and the tips were reused up to 3 times. A baseline signal was measured in every assay from an antibody-coated tip carried through association and dissociation steps in wells containing assay buffer without envelope proteins. Data were analyzed with ForteBio data analysis software (version 7.1). Data processing was as follows: baseline signals were subtracted, baselines were aligned to Y-axis, and interstep correction and Savitzky-Golay filtering were applied. Response curves were fit to processed data with a 1:1 global fit model and were used to compute association (K_a), dissociation (K_d), and binding affinity (K_D) constants.

Mass spectrometry protein identification

For in-solution digestion, 1µg samples of proteins were vacuum dried in siliconized tubes with a Savant SpeedVac concentrator (ThermoFisher). The proteins were reconstituted in denaturation buffer (7M urea, 100mM ammonium bicarbonate, 5mM DTT) and incubated at 56°C for 45min. Cysteines were alkylated with 14mM iodoacetamide for 30min at room temperature. The iodoacetamide was quenched with additional 5mM DTT, and the solution was diluted 1:4 with 100mM ammonium bicarbonate. Calcium chloride and sequencing-grade

trypsin (Promega) were added to 1mM and 4ng/µL, respectively, and samples were incubated overnight at 37°C. Trypsin digestion was stopped with 0.4% (vol/vol) trifluoroacetic acid. Samples were centrifuged to remove precipitates, and acidified supernatants were vacuum concentrated to 20µL. Tryptic peptides were desalted with C_{18} ZipTips (Millipore) according to the manufacturer's instructions.

For in-gel digestion, proteins were separated by SDS-PAGE and visualized with Coomassie blue as described above. Individual protein bands were excised and dehydrated by 3 washes with acetonitrile. Gel pieces were rehydrated in buffer containing 25mM ammonium bicarbonate and 5mM DTT, and incubated for 45min at 56°C. Cysteines were alkylated in 25mM ammonium bicarbonate and 80mM iodoacetamide for 30min. Gel slices were rinsed with water, dehydrated in acetonitrile, and then rehydrated in 50mM ammonium bicarbonate containing 12.5ng/uL trypsin and incubated overnight at 37°C. Tryptic peptides were extracted by one wash with water and three washes with 50% acetonitrile containing 5% formic acid, and were vacuum concentrated to 10µL.

Samples were analyzed on an Orbitrap Fusion Lumos mass spectrometer (ThermoFisher Scientific) equipped with a nano-Acquity ultraperformance liquid chromatography (UPLC) system (Waters) and in-house-developed nanospray ionization source. 30cm columns were prepared in-house from fused silica capillary tubing (75µm inner diameter x 360µm outer diameter; Kinesis Scientific) with laser-pulled tips and packed with 5µm C_{18} resin with 120 Å pore size (Reprosil-Pur C18-AQ; ESI Source Solutions). The mobile phases were 0.1% formic acid in water (A) and 0.1% formic acid in acetonitrile (B). 5µL of sample was loaded onto the column from the autosampler and desalted for 40min with 2% mobile phase B at 300nL/min. Peptides were separated using a linear gradient from 5-30% mobile phase B over 80min and a

flow rate of 300nL/min. The column was then washed with 80% mobile phase B for 10min, followed by equilibration with 2% mobile phase B for 20min prior to subsequent injections. Eluted peptides were detected using a data-dependent acquisition method. Survey scans of peptide precursors were performed in the Orbitrap mass analyzer from 375 to 1575 m/z at 120k resolution (at 200 m/z) with a 7×10^5 ion count target and a maximum injection time of 50ms. After survey scans, tandem MS (MS/MS) was performed on the most abundant precursors exhibiting a charge state of 2 to 4 and greater than 1×10^4 intensity by isolating them in the quadrupole with an isolation width of 1.6 m/z. High-energy collisional dissociation fragmentation was applied with normalized collision energy of 30%, and resulting fragments were detected using the rapid scan rate in the ion trap. The ion count target for MS/MS was set to 1×10^4, and the maximum injection time limited to 100ms. Dynamic exclusion was set to 30s with 10ppm mass tolerance around the precursor and its isotopes.

Thermo .raw files were converted to the mzXML format using ReAdW (version 2016.1.0) converter. The mzXML files were searched against a *Cricetulus griseus* protein sequence database downloaded from UniProt appended with common contaminant sequences (24,000 total sequence entries). A database search was performed using Comet (version 2016.01 rev. 2) with the following search parameters: 20 ppm precursor tolerance, concatenated target-decoy search, tryptic digest allowing 2 missed cleavages, oxidized methionine variable modification, and carboxyamidomethylation static modification on cysteine. The Comet search results were then processed with PeptideProphet and ProteinProphet tools from the Trans-Proteomic Pipeline software suite (version 5.0.0; Typhoon).

Protein radiolabeling, cell binding, and autoradiography studies

CHO cell proteins captured on DEAE and eluted with 200mM NaCl were used for radiolabeling. Iodine-125 (44.4 MBq; Perkin Elmer; catalog number NEZ033010MC) was diluted in 70µL of PBS. One iodobead (Pierce) was rinsed with PBS and added to the ^{125}I solution for 5min at room temperature. The, 70µg of protein diluted to 230µL in PBS was added to the ^{125}I-iodobead solution and incubated for 5min at room temperature. The reaction was stopped by rapidly transferring protein to a clean tube. Unreacted ^{125}I was removed by passing the sample through a disposable PD-10 desalting column (GE Life Sciences) with PBS and manually collecting 500µL fractions. Protein-containing fractions were pooled and concentrated to 100µL with Amicon centrifugal concentrators (Millipore). Aliquots of the sample were counted in a Packard Cobra II gamma counter, and the ratio of radiolabeled protein to unreacted ^{125}I was assessed by instant thin-layer chromatography (iTLC). For this, 1µL of sample was dried onto an iTLC strip (Agilent), and the strip was developed for 10min in PBS with 20% methanol and then dried. ^{125}I-labeled protein remained at the bottom of the strip, and unreacted ^{125}I migrated to the top. The strip was cut in half, and the radioactivity in both halves was measured by gamma counting. The total activity of the final product was 46.6KBq/µL, and 97.9% of it was protein-associated. 5µL of radiolabeled protein was reduced, denatured, and separated by SDS-PAGE as described above, and the gel was exposed for 30min to film (Amersham Hyperfilm MP, GE Life Sciences) at room temperature for autoradiography.

The procedure for cell binding studies with ^{125}I-labeled protein was similar to the flow cytometry binding assays described above. RPMI8866 cells were washed with manganese-containing binding buffer, put into 200µL aliquots in 1.5mL tubes at $1.0x10^6$ cells/mL, and incubated with or without 5µg of CWLDVC peptide. Radiolabeled protein (46KBq [$2.76x10^6$

DPM]) was added to each tube and incubated for 20min at 4°C, and then cells were washed twice and counted in a Packard Cobra II gamma counter. Tubes without cells were carried through the preceding wash/binding steps, and counts from them were subtracted from the cell counts to determine cell-associated radioactivity.

The binding procedure was modified to enrich and identify $\alpha_4\beta_7$–reactive proteins using RPMI8866 cells. The cells were washed in manganese-containing buffer and separated into two 500µL aliquots at $2.0x10^6$ cells/mL. 10µg of 2B4 antibody was added to one tube, and samples were incubated for 10min; 168KBq ($1.0x10^7$ DPM) of radiolabeled protein was added, and the cells were incubated for 30min at 4°C. The cells were washed 3 times in 1mL of manganese-containing buffer without added BSA and transferred to a clean tube at each wash. The cells were then incubated for 30min at 37°C in 300µL of dissociation buffer (150mM NaCl, 10mM HEPES pH 7.4, 5mM EDTA, and 250µg/mL CWLDVC peptide). The dissociation buffer was collected; concentrated to 30µL with Amicon centrifugal concentrators (Millipore); and then reduced, denatured, and separated by SDS-PAGE as described above. Input sample (140Bq [8,400 DPM]) was included on the gel to compare the protein compositions of input and cell-dissociated samples. Autoradiography was performed by exposing the gel to film, as described above, with a BioMax HE intensifying screen (Kodak) at -80°C for 11 days.

Statistical Analysis

Graphpad Prism software (version 6.03) was used for all graphing and statistical analyses. Binding of gp120 in the presence or absence of CHO cell proteins was compared using an unpaired t test, with a significance level (α) of 0.05. Nonlinear regression was used to fit heparin inhibition data and to calculate the IC_{50}.

Acknowledgements

We thank Scott Wilbur and Don Hamlin of the Department of Radiation Oncology, University of Washington, for assistance with radiolabeling experiments. We also thank David Montefiori, Susan Zolla-Pazner, and Charles Wood for generously sharing reagents that were used in our experiments. Finally, we thank James Williams for producing and purifying the FI6v3 antibody used in this work.

This work is supported by the Bill and Melinda Gates Foundation Collaboration for AIDS Vaccine Discovery OPP1033102 (WG, BC, MG, KKL, SLH), National Institutes of Health grant P51 OD010425 (SLH), and University of Washington Proteomics Resource grant UWPR95794 (PVH, JKE). DP was supported by a Pharmaceutical Sciences Training Grant (T32 GM007750) from the National Institute of General Medical Sciences, National Institutes of Health. The funders had no role in study design, data collection and analysis, decision to publish, or preparation of the manuscript.

Chapter 3

CS1 Fibronectins Facilitate HIV-1 Infection of $\alpha_4\beta_7^+$ T Lymphocytes

The work presented in this chapter will be submitted for publication to:

The Journal of Virology

Abstract

$CD4^+$ T lymphocytes expressing the $\alpha_4\beta_7$ integrin receptor have been proposed to play important roles in Human Immunodeficiency Virus-1 (HIV) pathogenesis. It has been shown that $\alpha_4\beta_7^+$ cells are preferentially targeted by HIV, and contribute to pathology in gut-associated lymphoid tissues, which is a hallmark of HIV pathogenesis. However, the basis for preferential infection of $\alpha_4\beta_7^+$ T cells is not fully understood. We recently reported that fibronectin splice variants containing the CS1 motif are mediators of HIV envelope-$\alpha_4\beta_7$ interactions. Based on this, we hypothesized that CS1 fibronectins mediate preferential infection of $\alpha_4\beta_7^+$ T cells. We tested this *in vitro* using a recombinant CS1 fibronectin fragment (RetroNectin™). Immobilized RetroNectin was used to capture HIV, and virus binding was measured by p24 ELISA. Viruses bound to RetroNectin in a specific and saturable manner. Infectivity of captured viruses was assessed by co-culturing with $CD4^+\alpha_4\beta_7^+$ T cells and monitoring p24 production. RetroNectin-mediated infection resulted in peak p24 output of 133.3pg/mL, more than twofold higher than that observed with infection by unbound viruses. RetroNectin-mediated infection was attenuated by α_4 integrin antibodies Act-1 and 2B4, but was resistant to neutralizing antibodies VRC01, PG16, and 2G12. Cell-to-cell virus transmission between autologous T cells was three times more efficient in the presence of RetroNectin as compared to BSA. Preliminary findings indicated that CS1 fibronectins are expressed in the intestinal tissues of infected pigtail

macaques. Together, these studies demonstrate a potential role for CS1 fibronectins in the infection of $\alpha_4\beta_7^+$ T cells and the pathogenesis of HIV/AIDS.

Importance

It has been known for decades that HIV primarily infects $CD4^+$ T cells. More recently, $CD4^+$ T cells that also display the $\alpha_4\beta_7$ receptor have been identified as preferred targets for HIV. These $\alpha_4\beta_7^+$ cells reside in gut lymphoid tissues in large numbers, and are thought to play key roles in HIV disease by allowing the virus to invade and replicate in the gut. Based on this, $\alpha_4\beta_7$–directed antibodies are being investigated for HIV treatment, and have shown promise in animal models. However, the mechanism HIV uses to target $\alpha_4\beta_7^+$ T cells is not fully understood. In this study, we show that the extracellular matrix protein CS1 fibronectin facilitates infection of $\alpha_4\beta_7^+$ cells by binding to both HIV and $\alpha_4\beta_7$. The identification of this novel virus-host interaction provides additional insight into how HIV may target $\alpha_4\beta_7^+$ cells *in vivo*, and has important implications for HIV therapy.

Introduction

The gastrointestinal system plays a key role in Human Immunodeficiency Virus-1 (HIV) pathogenesis. Gut-associated lymphoid tissues (GALT) contain large numbers of activated effector memory $CD4^+CCR5^+$ T cells, and thus provide an ideal environment for high-level virus replication [43]. During the acute phase of infection, GALT are invaded and intestinal $CD4^+$ T cells are rapidly and profoundly depleted. In contrast to peripheral T cells, intestinal T cells cannot be restored to pre-infection levels with antiretroviral therapy [44, 89]. The loss of gut T cells is closely associated with intestinal inflammation and immune dysregulation, which are

major drivers of $CD4^+$ cell decline and the development of Acquired Immune Deficiency Syndrome (AIDS) [193].

T lymphocytes expressing the gut-homing integrin $\alpha_4\beta_7$ are implicated in the ability of HIV to invade and replicate within GALT. These cells are preferential targets for HIV infection *in vitro* [159], and are rapidly depleted from both peripheral and intestinal sites *in vivo* [44, 155]. Similar phenomena have been observed in non-human primates infected with Simian Immunodeficiency Virus (SIV) [61, 163, 220], indicating that $\alpha_4\beta_7^+$ cells likely play roles in the pathogenesis of multiple primate lentiviruses. Consistent with this, a series of studies in Rhesus macaques (*Macaca mulatta*) demonstrated that treatment with the $\alpha_4\beta_7$–inhibitory antibody Act-1 inhibited SIV replication and mucosal transmission, and contributed to the reconstitution of intestinal T cells when combined with standard antiretroviral therapy [188-191]. These studies highlight the importance of $\alpha_4\beta_7^+$ T cells in HIV/SIV pathogenesis *in vivo*, as well as the potential utility of $\alpha_4\beta_7$–targeted therapeutics for antiviral treatment.

Despite the evidence implicating $\alpha_4\beta_7^+$ cells in pathogenesis, exactly how these cells are targeted by HIV remains an open question. Early studies indicated that the gp120 subunit of HIV envelope protein binds to $\alpha_4\beta_7$, and that this interaction contributes to preferential infection [164]; however, it was subsequently reported that many gp120 proteins do not bind to $\alpha_4\beta_7$ [172]. Furthermore, despite the fact that Act-1 mediates antiviral activities *in vivo*, Act-1 and other α_4 integrin antibodies do not inhibit infection *in vitro* [159, 173, 198]. These discrepancies indicate that direct gp120-$\alpha_4\beta_7$ interactions are not likely to explain the preferential infection of $\alpha_4\beta_7^+$ T cells. In this context, we recently reported that the extracellular matrix protein fibronectin is an important mediator of gp120-$\alpha_4\beta_7$ engagement [221]. Specifically, we showed that fibronectin splice variants containing the $\alpha_4\beta_7$–binding CS1 motif ("CS1 fibronectins") bound to both HIV

envelope protein and $\alpha_4\beta_7$, and thus mediated indirect gp120-$\alpha_4\beta_7$ engagement. Previous studies showed that surfaces coated with plasma fibronectin (a non-CS1 fibronectin variant) capture HIV, stabilize extracellular viruses, and mediate enhanced infection of T cells *in vitro* [138, 139]. However, these studies did not specifically investigate either CS1 fibronectins or the effects of fibronectins on HIV infection of $\alpha_4\beta_7^+$ T cells. In this work, we built upon what is known about HIV-fibronectin interactions and hypothesized that CS1 fibronectins mediate interactions between HIV and $\alpha_4\beta_7^+$ T cells, and thereby facilitate the preferential infection of $\alpha_4\beta_7^+$ cells.

In this study we used RetroNectin™ (TaKaRa), a recombinant C-terminal fibronectin fragment, as a model CS1 fibronectin. Fibronectin splice variants and the structure of RetroNectin have been described [213, 222, 223], and are illustrated in Figure 3-1. RetroNectin contains the two fibronectin binding motifs critical for HIV-$\alpha_4\beta_7$ interaction: the C-terminal heparin binding domain which binds to HIV envelope protein [136], and CS1 which binds to $\alpha_4\beta_7$. We show that RetroNectin binds to HIV and mediates enhanced infection of $CD4^+\alpha_4\beta_7^+$ T cells *in vitro*. Furthermore, we show that the α_4 integrin antibodies Act-1 and 2B4 inhibit RetroNectin-mediated infection. We additionally show that CS1 fibronectin isoforms are present in infected tissues from pigtail macaques *in vivo*. Based on these findings, we propose a model in which CS1 fibronectins provide a substrate for the co-localization of HIV and $\alpha_4\beta_7^+$ T cells, and thus facilitate the infection of those cells.

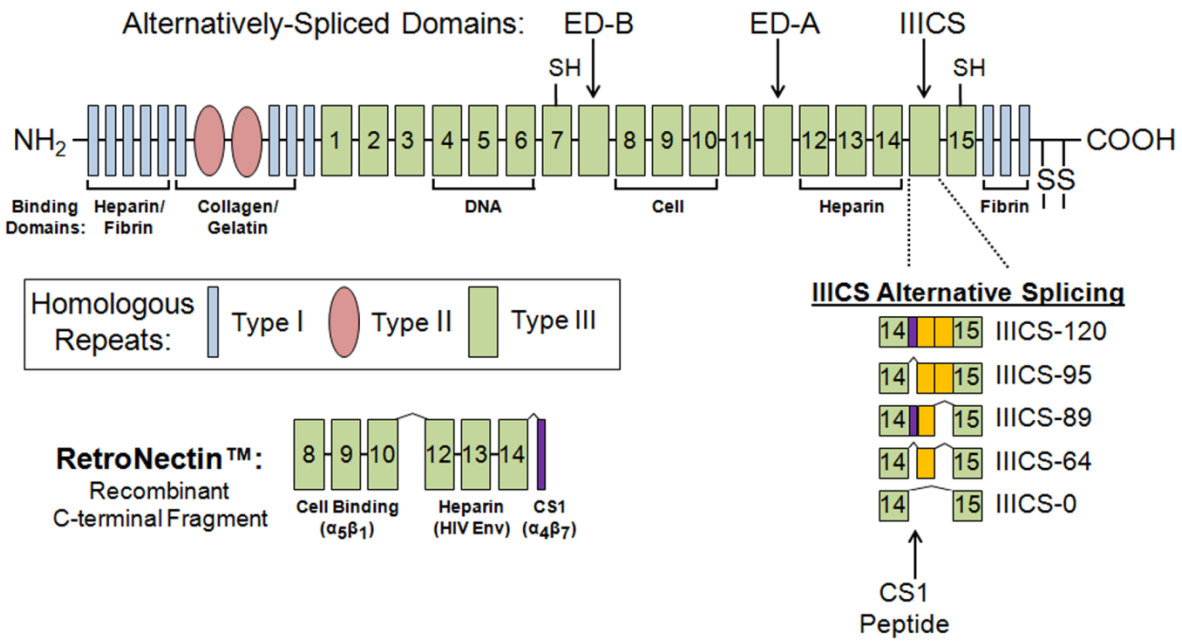

Figure 3-1. The Structure of Fibronectin and RetroNectin. The fibronectin gene is composed of three repeating homologous units, designated types I, II, and III. Additional type III units (ED-A, ED-B, and IIICS) may be included in certain isoforms through alternative splicing. IIICS is further spliced in five different combinations, as indicated. The CS1 motif within IIICS (purple block) binds to $\alpha_4\beta_7$ and $\alpha_4\beta_1$ through a LDV sequence. "CS1 fibronectins" are those isoforms that contain CS1. RetroNectin is a recombinant CS1 fibronectin fragment, containing C-terminal binding domains important for interactions with both cells and HIV. In addition to CS1, RetroNectin contains the C-terminal heparin binding domain which interacts with HIV envelope protein, and the "cell binding" domain which binds to $\alpha_5\beta_1$ through a RGD sequence.

Results

RetroNectin captures HIV and mediates infection of human T cells

We first developed an *in vitro* assay to study the impact of CS1 fibronectins on HIV infection. The assay is illustrated in Figure 3-2A, and was based on similar experiments described by Tellier et al.[138]. RetroNectin was chosen as a model CS1 fibronectin fragment, and was immobilized on 96-well polystyrene plates. Nonspecific binding was blocked with bovine serum albumin (BSA), and then HIV-1 BaL was captured and unbound viruses were removed by washing. In some experiments, bound viruses were lysed and quantified by p24

ELISA. In separate experiments, primary human $CD4^+\alpha_4\beta_7^+$ T cells were plated over captured viruses to assess their infectivity.

RetroNectin captured HIV-1 BaL in a concentration-dependent and saturable manner. To optimize RetroNectin coating, wells were incubated with a range of RetroNectin concentrations and then used to capture 2ng of p24 (Figure 3-2B). Under these conditions, maximum virus binding was approximately 127pg of p24 per well (95% CI: 115-139pg). Since RetroNectin captured only 6% of the input virus, we reasoned that virus binding was either limited by the surface area of the wells, or that specific forms of the virus bound to RetroNectin. To differentiate between these possibilities, we incubated varying amounts of p24 (2.0-0.25ng) on wells coated with 10µg/mL RetroNectin (Figure 3-2C). In these experiments we found a linear relationship between virus input and the amount of virus captured (r^2: 0.9714), and only 6-7% of virus was captured for each input concentration. This indicated that RetroNectin selectively captured a subset of viruses under our incubation and washing conditions, and that total binding was not necessarily restricted by surface area of the wells.

Next, we tested whether captured viruses retained infectivity on primary human $CD4^+\alpha_4\beta_7^+$ T cells. Cells were plated on wells in which viruses were captured with increasing concentrations of RetroNectin, and we examined the relationship between the level of virus captured and kinetics of infection (Figure 3-2D). Wells coated with RetroNectin concentrations of 3.12-50µg/mL captured between 45-114pg of p24, and mediated robust infection. In these samples, p24 was detected after 3 days of culture, and at this time-point was proportional to the amount of virus captured. After 5 days of culture p24 output was similar between samples, presumably because of multiple rounds of virus replication and spread. After 7 days, p24 output declined in inverse proportion to the RetroNectin concentration. Wells coated with RetroNectin

concentrations of 1.56μg/mL or less captured small or undetectable amounts of p24, and mediated a significantly weaker infection that was not detectable until 5 days of culture.

Based on these results, we selected a RetroNectin coating concentration of 10μg/mL for subsequent experiments. To assess the specificity of virus capture by RetroNectin, we examined whether additional extracellular matrix proteins capture HIV (Figure 3-2E). Plates were coated with plasma fibronectin, laminin, collagen, nidogen, and BSA, all at concentrations of 10μg/mL. The amount of HIV captured by these proteins was below the limit of detection of our assay (data not shown). To determine whether low levels of HIV were captured, cells were plated over wells to allow for amplification of captured viruses. Using this method, we found that plasma fibronectin and laminin both captured small amounts of viruses which retained infectivity. This was consistent with reports by others that plasma fibronectin and laminin bind to HIV[136, 138]. In contrast, collagen, nidogen, and BSA did not capture a significant amount of virus. In total, these experiments showed that RetroNectin captured HIV by specific binding interactions, and that captured viruses retained infectivity.

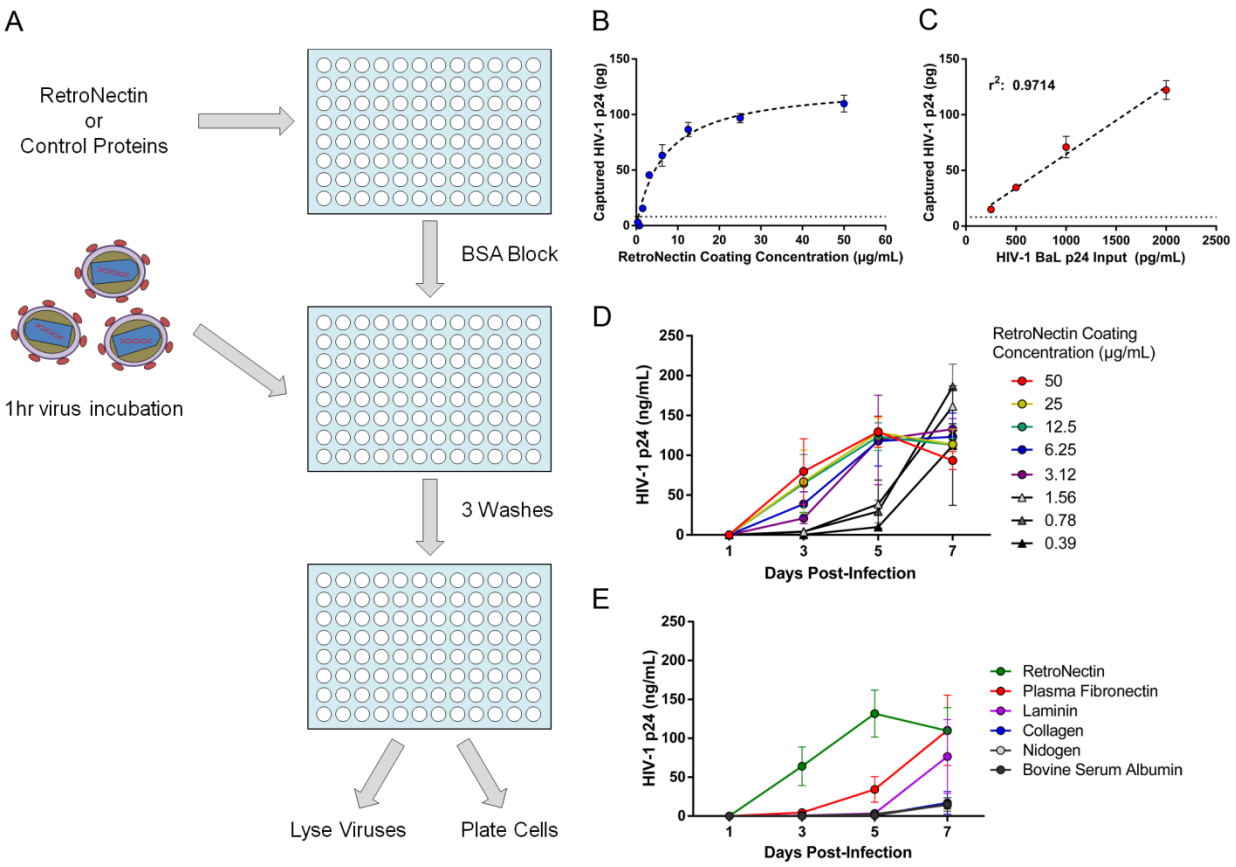

Figure 3-2. RetroNectin Binds to HIV and Mediates T Cell Infection. A) Illustration of HIV binding experiments. B) Capture of HIV-1 BaL on wells coated with a range of RetroNectin concentrations. C) Capture of BaL at different virus input concentrations on wells coated with 10µg/mL RetroNectin. The horizontal dotted line in B and C represents the lower limit of detection. D) The relationship between virus capture over a range of RetroNectin concentrations and the kinetics of infection of $CD4^{+}\alpha_4\beta_7^{+}$ T cells. E) Comparison of infection resulting from BaL viruses captured by RetroNectin versus control proteins. All data shown are the mean and standard deviation of triplicate measurements.

HIV envelope and virus-associated integrins mediate virus attachment to RetroNectin

We next used a panel of inhibitors to determine the nature of HIV binding to RetroNectin. RetroNectin contains three fibronectin adhesion domains: 1) the central cell binding domain, which is a ligand of $\alpha_5\beta_1$ integrin; 2) the heparin binding domain, which binds to HIV envelope protein as well as cell-surface proteoglycans; and 3) CS1, which is a ligand of both $\alpha_4\beta_7$ and $\alpha_4\beta_1$ integrins [213, 222, 223]. Heparin sulfate was used to inhibit HIV envelope

interactions with the heparin binding domain, and chondroitin sulfate was included as a specificity control. The antibody P5D2, which blocks β_1 integrin, was used to test for interactions with the cell binding domain. Interactions with the CS1 motif were tested with the antibody 2B4 which inhibits $\alpha_4\beta_1$ and $\alpha_4\beta_7$ integrins, as well as Act-1 which is specific for $\alpha_4\beta_7$.

These inhibitors were first tested for their ability to block recombinant BaL gp120 envelope protein binding to RetroNectin (Figure 3-3A). As anticipated, only heparin sulfate significantly inhibited gp120 binding. Next, we tested the effects of these inhibitors on HIV-1 BaL virus binding to RetroNectin (Figure 3-3B). We expected similar results to the gp120 protein binding, but instead found that virus binding was weakly inhibited by heparin and significantly inhibited by the α_4 integrin antibodies. This suggested that, under our experimental conditions, virus-associated α_4 integrins may have been present and played significant roles in mediating HIV attachment to RetroNectin.

The results of this screen were expanded by constructing dose-response curves for the inhibitors that showed activity. First, the effects of heparin sulfate on gp120 and virus binding were compared (Figure 3-3C). The inhibition data for gp120 binding fit a standard sigmoidal inhibition curve, and heparin inhibited 60% of total binding with an IC_{50} of 0.54µg/mL (95% CI: 0.23-1.29µg/mL). In contrast, the inhibition data for virus binding fit a biphasic curve. The first portion of the curve, corresponding to heparin concentrations of 0.005–25.0µg/mL, resulted in inhibition of 35% of total binding with an IC_{50} of 0.18µg/mL (95% CI: 0.09-0.36µg/mL). This IC_{50} was not significantly different from that obtained for gp120 binding, which suggested that this portion of the curve reflected virus binding mediated by envelope protein. The remainder of the curve, corresponding to heparin concentrations above 25µg/mL, resulted in inhibition of 20% of total binding with an IC_{50} of 2037µg/mL (95% CI: 232-17,850µg/mL). This phenomenon

was not observed in the gp120 inhibition curve, indicating that there was a binding interaction between viruses and RetroNectin distinct from the interaction mediated by envelope protein.

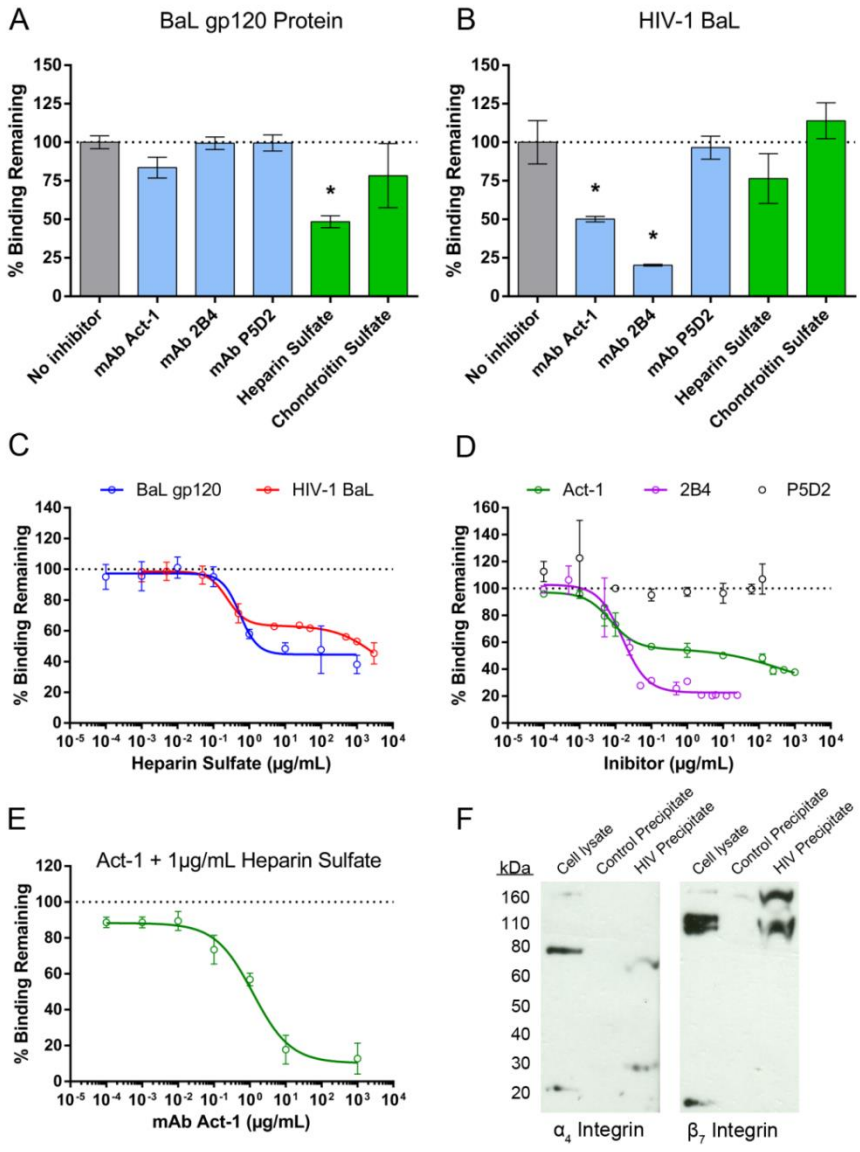

Figure 3-3. Analysis of HIV Binding to RetroNectin. A panel of inhibitors was screened for activity against RetroNectin binding to A) BaL gp120 protein or B) BaL viruses. Asterisks indicate statistically significant inhibition (T-test, $p < 0.05$). C) Inhibition profiles of BaL gp120 and viruses against a range of heparin sulfate concentrations. D) Inhibition profile of BaL viruses against a range of integrin-directed antibodies Act-1, 2B4, and P5D2. E) Inhibition of virus binding over a range of Act-1 concentrations supplemented with 1µg/mL heparin sulfate. All inhibition data are the mean and standard deviation of triplicate measurements. F) Western blot of $\alpha_4\beta_7^+$ T cell lysates, lysates of BaL virus precipitate, or lysates of virus-free control precipitate. Parallel blots were probed for α_4 and β_7 integrins as indicated. Results are representative of two independent experiments.

Additional dose-response curves were constructed to assess the effects of antibodies P5D2, 2B4, and Act-1 on virus binding (Figure 3-3D). P5D2 did not show any inhibitory effect over the range of concentrations used, indicating that integrin $\alpha_5\beta_1$ was not involved. In contrast, both α_4 integrin antibodies showed concentration-dependent binding inhibition. 2B4 inhibition fit a standard sigmoidal curve and inhibited 80% of the total binding with an IC_{50} of 0.016µg/mL (95% CI: 0.011-0.023µg/mL). The data for Act-1 inhibition fit a biphasic curve. The first portion of the curve, corresponding to Act-1 concentrations of 0.0001-1.0µg/mL, resulted in inhibition of 50% of total binding with an IC_{50} of 0.008µg/mL (95% CI: 0.005-0.013µg/mL). This IC_{50} was not significantly different from that obtained for 2B4 inhibition. However, because 2B4 inhibited a greater portion of the binding than Act-1, and also interacts with both α_4 integrins, we concluded that virus binding was likely mediated by both $\alpha_4\beta_7$ and $\alpha_4\beta_1$ integrins. In support of this, others have reported that HIV incorporates both of these integrins [224, 225]. The final portion of the Act-1 inhibition curve, corresponding to Act-1 concentrations above 1µg/mL, resulted in inhibition of 10% of total binding with an IC_{50} of 174µg/mL (95% CI: 34-887µg/mL). We did not characterize this additional inhibition, but speculated that it may be due low-affinity interactions between Act-1 and $\alpha_4\beta_1$ or another undefined target.

Next, we tested combinations of Act-1 and heparin to confirm that both $\alpha_4\beta_7$ and HIV envelope protein interactions contributed to binding. A range of Act-1 concentrations were combined with 1µg/mL heparin sulfate (Figure 3-3E). The addition of heparin shifted the Act-1 inhibition curve so that it was no longer biphasic, and the combination of these agents inhibited 90-95% of the total binding. The IC_{50} for Act-1 under these conditions was 1.23µg/mL (95% CI: 0.68-2.20µg/mL). This synergistic inhibition confirmed that HIV binding to RetroNectin was likely mediated by interactions with both envelope protein and virus-associated α_4 integrins.

Last, we confirmed that α_4 and β_7 integrins were both present in our virus stocks. HIV BaL was precipitated from virus-containing supernatant using polyethylene glycol, and then lysed. An equivalent volume of culture supernatant from uninfected PBMCs was treated in the same manner as a negative control. As a positive control, lysates were prepared from primary $\alpha_4\beta_7^+$ T cells. The precipitates and cell lysates were separated by sodium-dodecyl sulfate polyacrylamide gel electrophoresis (SDS-PAGE), and then analyzed by western blot. Both α_4 and β_7 integrins were detected in the cell lysates and virus precipitates (Figure 3-3F). Cell-associated α_4 integrin was detected as a band of approximately 70kDa, and a similar band was detected in the virus precipitate. Cell-associated β_7 integrin was detected as a doublet of bands at approximately 100-110kDa, and similar bands were detected in the virus precipitate, in addition to a higher-molecular weight species of about 160kDa. In combination with the inhibitor studies, these experiments provided evidence that $\alpha_4\beta_7$ integrin was present on the viruses used in our study, and played a role in virus attachment to RetroNectin.

α_4 integrin antibodies attenuate RetroNectin-mediated HIV infection

Next, we examined the effects of these inhibitors on infection of primary human $CD4^+$ $\alpha_4\beta_7^+$ T cells. Cell infection was performed as described, either by plating cells over RetroNectin-captured viruses, or by infecting cells for 24hr with free viruses. Cells were cultured continuously in inhibitors, with a complete media change and replenishment of inhibitors every 2 days. Antibodies were tested at 10µg/mL, and both heparin and chondroitin sulfate were tested at 1µg/mL.

In the absence of inhibitors, RetroNectin-associated viruses produced infection that was 2-3 times more robust than infection by free viruses (Figure 3-4A). Other groups have similarly

reported that HIV captured by adhesion molecules displays increased infectivity relative to free virus [138, 224, 225]. It is noteworthy that in our experiments virus input was normalized: 2ng of p24 was added per well for infection with free viruses, and an input of 2ng was used for RetroNectin-mediated virus capture. We hypothesized that the enhanced infection observed with RetroNectin was due to co-localization of viruses and cells on the RetroNectin substrate, which enhanced infection efficiency.

Based on this, we reasoned that inhibitors which blocked virus or cell binding to RetroNectin would inhibit infection. Consistent with this, treatment of cultures with either Act-1 or 2B4 significantly attenuated infection by RetroNectin-associated viruses (Figure 3-4B). P5D2, which did not impact virus binding, also did not inhibit infection. Importantly, 2B4 and Act-1 did not inhibit infection by free viruses. This is in agreement with previously-reported observations [159, 173, 198], and suggests that neither of these antibodies block virus attachment or entry to target cells. Because Act-1 and heparin synergistically inhibited virus binding to RetroNectin, we tested whether these agents synergistically inhibited infection. The combination of Act-1 and heparin did attenuate infection to a greater extent than Act-1 alone. Furthermore, the kinetics of infection in the presence of Act-1 and heparin resembled that of infection by free viruses, which suggested that this combination of inhibitors completely reversed RetroNectin-mediated enhancement of infection.

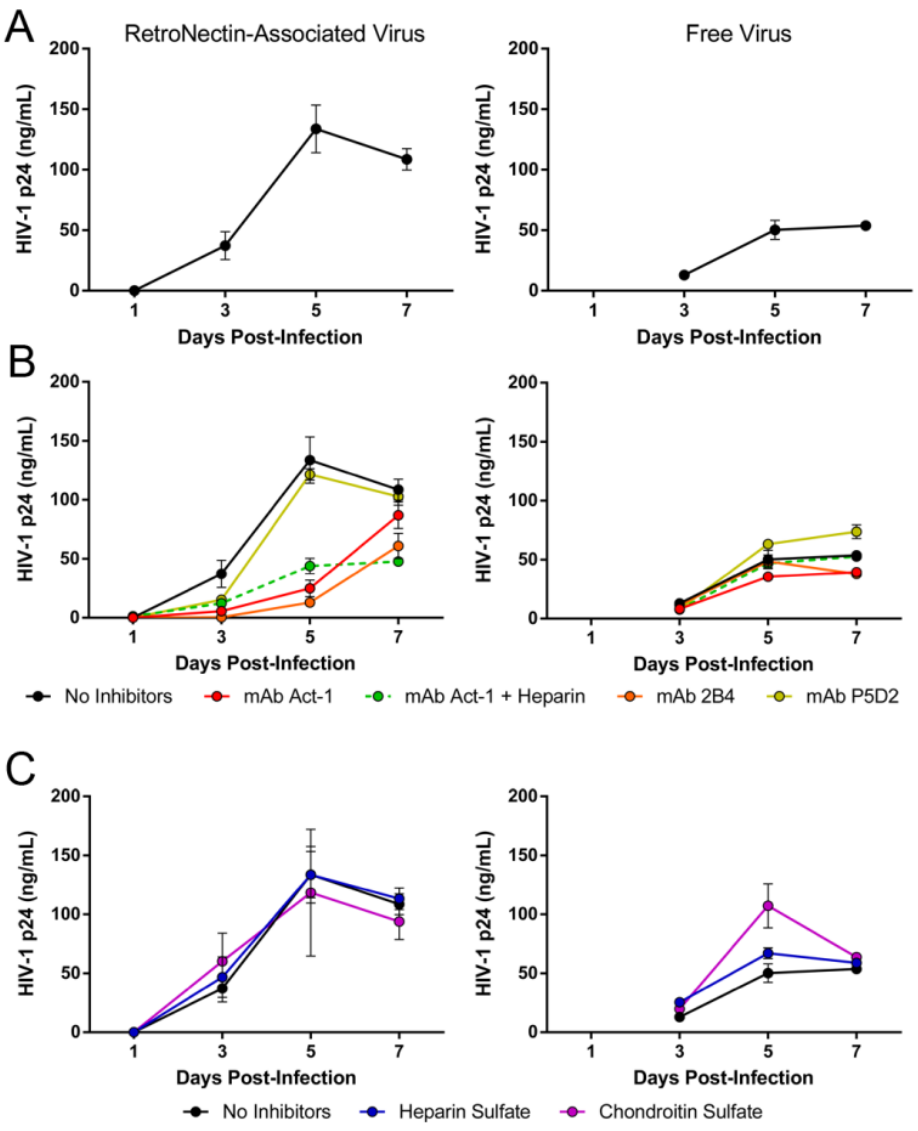

Figure 3-4. Comparison of Infection by RetroNectin-Associated and Free Viruses. A-C) Kinetics of infection resulting from plating $CD4^{+}\alpha_4\beta_7^{+}$ T cells over RetroNectin-captured viruses (left) or from infection with unbound viruses (right). Presented are the kinetics of infection in A) the absence of inhibitors, B) the presence of integrin antibodies, and C) the presence of heparin or chondroitin sulfate. Data are the mean and standard deviation of triplicate measurements.

While heparin by itself was able to partially inhibit virus binding to RetroNectin, it failed to inhibit infection by RetroNectin-associated viruses (Figure 3-4C). Interestingly, heparin and chondroitin sulfate both enhanced infection by free viruses. This was unexpected, as others have reported that these and other polyanions, including dextran sulfate, inhibit HIV entry and binding

[226, 227]. The conflict between our findings and previous reports may be due to the cell types used; we used primary T cells while these other studies used cell lines.

Because all of the preceding studies were conducted using HIV- BaL, we tested whether RetroNectin mediated infection by additional HIV strains. Three strains were compared to BaL: KNH1207 (subtype A), SF162 (subtype B), and 93MW959 (subtype C). The titers of these virus stocks were all approximately three times lower than that of the BaL stock. Therefore, virus input on RetroNectin-coated wells was normalized by infectivity (150 $TCID_{50}$ per well) rather than p24. All of the viruses tested were captured and remained infectious on $CD4^+$ $\alpha_4\beta_7^+$ T cells (Figure 3-5). Furthermore, Act-1 attenuated the infectivity of each of these viruses. These experiments indicated that the observations made with BaL were generalizable to additional HIV strains.

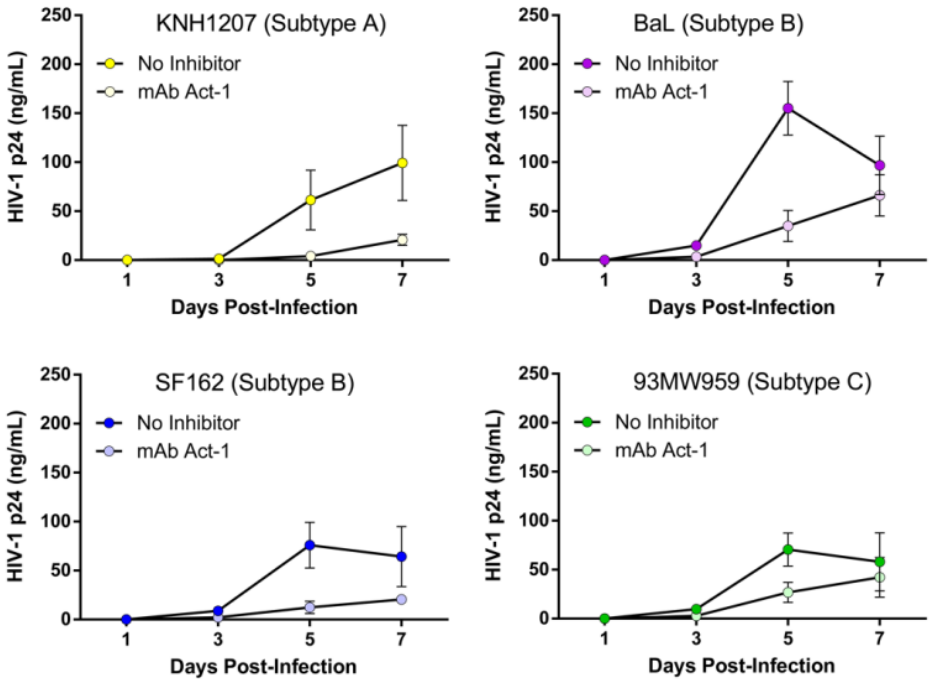

Figure 3-5. RetroNectin Mediates Infection by Different HIV Strains. RetroNectin was used to capture four different HIV viruses, as indicated. The kinetics of infection in the presence and absence of Act-1 are presented. Results are the mean and standard deviation of triplicate measurements.

RetroNectin-associated HIV is resistant to neutralizing antibodies

We next conducted experiments to determine the activity of neutralizing antibodies on RetroNectin-mediated infection. We originally hypothesized that some HIV-directed antibodies may inhibit RetroNectin-HIV binding, and thus attenuate infection. Therefore, we tested the ability of several antibodies to inhibit either BaL gp120 protein or BaL virus binding to RetroNectin. Because previous reports indicate that HIV binding to fibronectin occurs via the CD4 binding site or third variable loop (V3) of gp120 [136, 138], we tested the following antibodies targeting these epitopes: VRC01 (CD4 binding site) [228], PGT121 (V3) [229], and 2G12 (glycan-dependent V3) [230-233]. PG16 was used to test for interactions with quaternary V2 epitopes, which are present on virus-associated envelopes but not on purified gp120 [234]. A32 was used as a control, because this antibody is non-neutralizing and binds to soluble gp120 but not virion-associated trimeric envelope protein [235, 236]. Surprisingly, we found that none of these antibodies significantly inhibited gp120 binding (Figure 3-6A) or virus binding (Figure 3-6B), which indicated that no particular envelope-RetroNectin interaction that we tested was critical for virus binding. This result further implied that envelope-RetroNectin interactions may not be mediated by any single HIV epitope, but may be mediated by multiple epitopes or interactions with glycans.

Next, in order to verify that the anti-HIV antibodies were functional, we tested their ability to neutralize infection. $CD4^{+}\alpha_4\beta_7^{+}$ T cells were infected by free viruses, and cultured continuously in the antibodies at 10μg/mL. As anticipated, infection was potently inhibited by VRC01, PG16, PGT121, and 2G12, but not by A32 (Figure 3-6C), which indicated the antibodies were functional. We additionally tested for neutralizing activity against RetroNectin-associated viruses. Surprisingly, we found that BaL was resistant to most of the antibodies and

able to replicate in their presence (Figure 3-6D). Notably, PG16 and 2G12 had no inhibitory effect, and VRC01 showed only modest inhibition that was overcome after 7 days of culture. PGT121 was the exception to these, and completely inhibited infection by RetroNectin-associated viruses. Our interpretation of these results was that RetroNectin-mediated infection occurred through a mechanism that contributed to neutralization resistance.

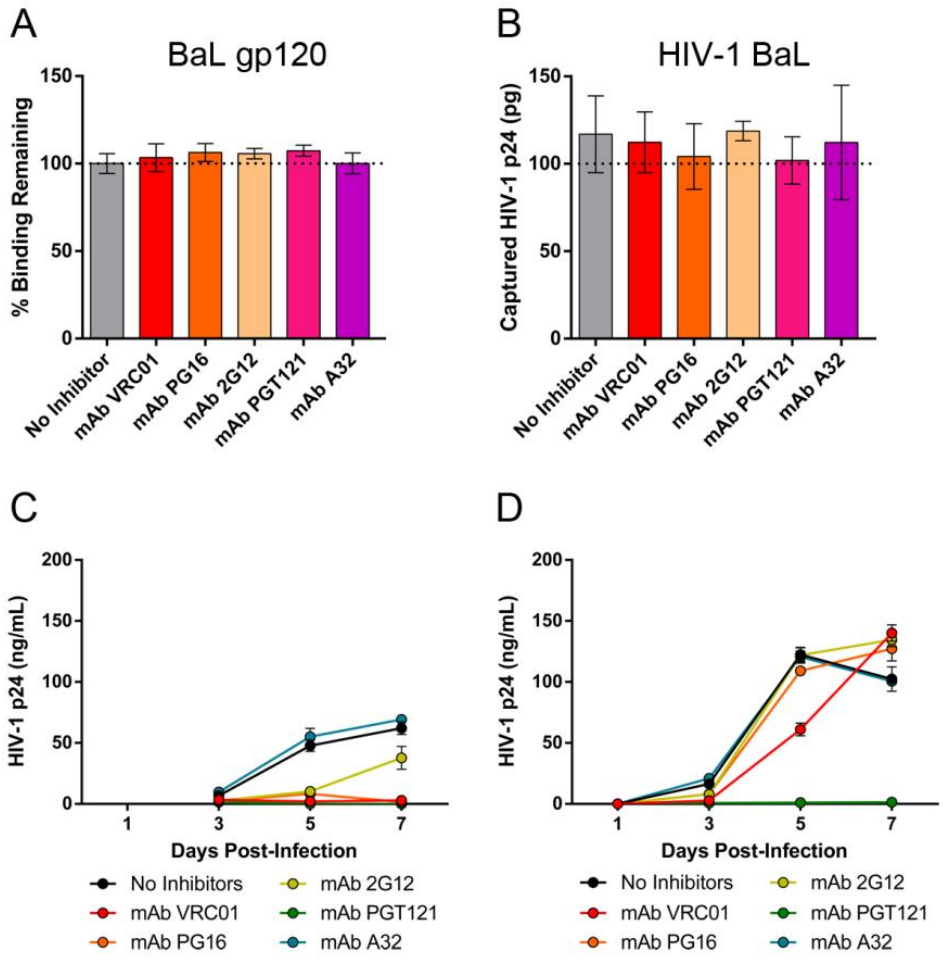

Figure 3-6. Effect of Neutralizing Antibodies on RetroNectin-Mediated Infection. The neutralizing antibodies tested did not inhibit RetroNectin binding to A) BaL gp120 or B) BaL viruses. Kinetics of infection by C) free viruses or D) RetroNectin-associated viruses was measured in the presence of the indicated antibodies. Antibodies were all used at 10µg/mL. Results are the mean and standard deviation of triplicate measurements.

Cell-to-cell virus transmission is enhanced on RetroNectin

Others have reported resistance to neutralizing antibodies including VRC01 and 2G12 in the context of cell-to-cell virus transmission between T cells [82, 83]. Based on this, we hypothesized that RetroNectin enhanced cell-to-cell virus spread, and thus contributed to neutralization resistance. To test this, we used a cell-to-cell virus transmission assay, similar to that described by Malbec et al. [83]. In this assay, uninfected target $CD4^{+}\alpha_4\beta_7^{+}$ T cells were labeled with a fluorescent dye and mixed with autologous HIV-infected cells. Cells were then stained one or two days later for intracellular p24, and the percentage of infected target cells was measured by flow cytometry.

We found that cell-to-cell transmission was approximately three times greater when cells were cultured on RetroNectin versus BSA. After 48 hours of culture on BSA, approximately 18% of target cells were $p24^{+}$; however 58% of target cells were $p24^{+}$ when cultured on RetroNectin. Representative results of this assay are illustrated in Figure 3-7A and a time-course of cell-to-cell transmission on BSA and RetroNectin is presented in Figure 3-7B. As an additional control to verify that we measured cell-to-cell transmission and not cell-free infection, supernatants were collected from infected cells and used to infect target cells for 48 hours (described in Methods). From this, we estimated that cell-free viruses accounted for infection of 5% of the cells (Figure 3-7B, dotted line), and the remainder of the p24 signal could be attributed to cell-to-cell transmission.

In parallel experiments, 2B4, Act-1, and neutralizing antibodies were added to cells cultured on RetroNectin. After 48 hours, Act-1, 2B4, VRC01, and PGT121 all significantly inhibited cell-to-cell transmission, whereas PG16, 2G12, and A32 had no effect (Figure 3-7C). These were similar to the results observed in the context of infection by RetroNectin-captured

viruses (compare to Figure 3-4B and Figure 3-6D), which suggested that cell-to-cell transmission likely contributed to the enhanced infection observed by RetroNectin-associated viruses.

In cultures treated with Act-1 or 2B4, we observed significant cell clumping and a reduction in cell adhesion to the wells. Others have reported similar homotypic cell clustering in cells treated with these and other α_4 and β_7 integrin antibodies [173, 237]. Interestingly, it has been observed that cell clustering induced by Act-1 and 2B4 enhances cell-to-cell virus spread *in vitro* [173]. Therefore, the effects of these antibodies in our assays may have been complex; they may have inhibited cell-to-cell contacts mediated by RetroNectin, but also facilitated different cell-to-cell contacts by cell clumping.

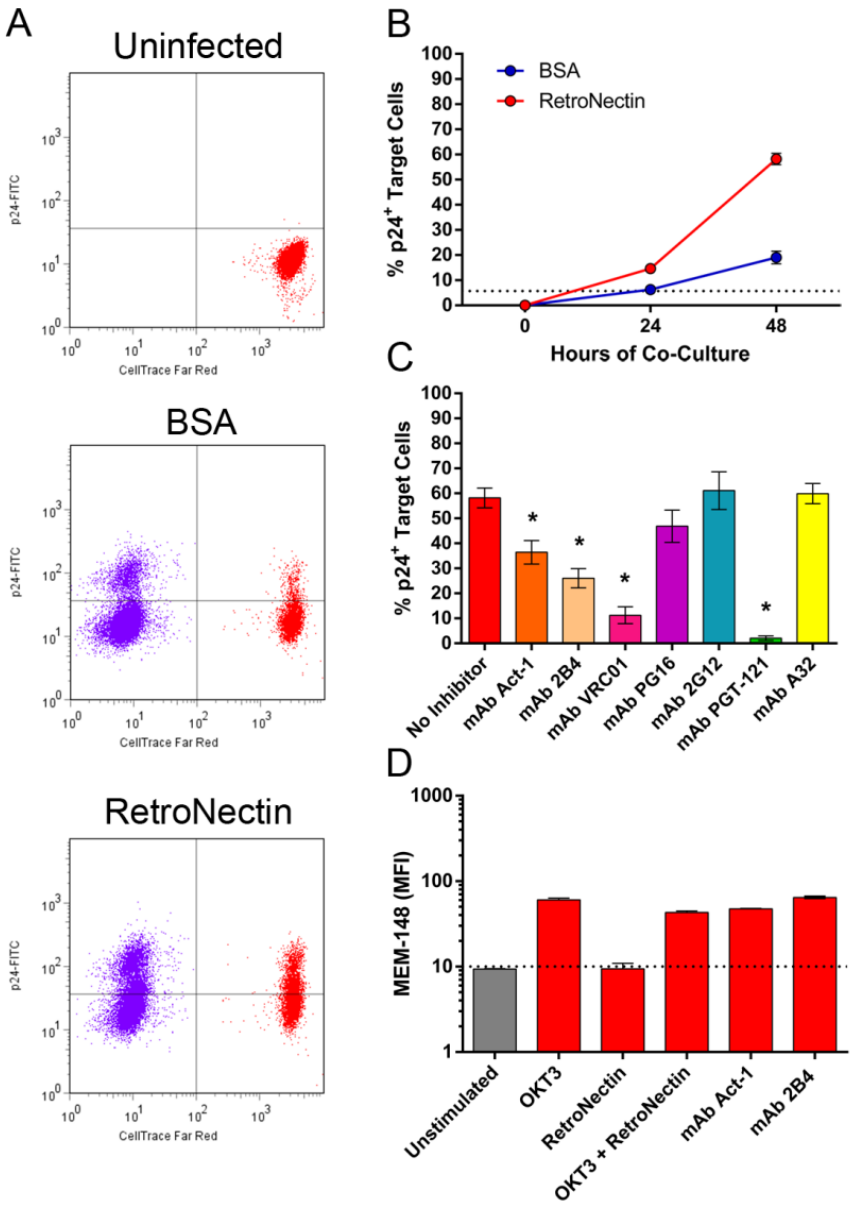

Figure 3-7. RetroNectin Enhances Cell-to-Cell Virus Transmission. A) Representative results of the assay. Donor cells infected with BaL are shown in purple and autologous uninfected target cells labeled with CellTrace Far Red dye are in red. Results are after 48hr of culture on wells coated with either BSA or RetroNectin. B) Time-course of cell-to-cell transmission on BSA or RetroNectin. The horizontal dotted line represents the level of infection attributed to cell-free viruses. C) The effects of integrin and HIV-directed antibodies on cell-to-cell transmission after 48hr of culture on RetroNectin. Asterisks indicate statistically significant inhibition (T-test, $p < 0.05$). D) Expression of activated LFA-1, measured by staining with the MEM-148 antibody. Expression was measured in unstimulated $CD4^{+}\alpha_4\beta_7^{+}$ T cells cultured on plates coated with anti-CD3 antibody (OKT3), RetroNectin, or a combination of both with and without the addition of Act-1 or 2B4. All results are the mean and standard deviation of triplicate measurements.

In the case of VRC01, cell-to-cell transmission was significantly but not totally inhibited. Low levels of virus transmission that persisted in the presence of VRC01 may explain why this antibody slowed but did not completely stop RetroNectin-mediated infection (Figure 3-6B). In contrast, PGT121 potently inhibited both RetroNectin-mediated infection and cell-to-cell transmission. This effect may be specific to the BaL isolate used in this study, however it is noteworthy that PGT121 has been observed to potently inhibit cell-to-cell transmission of other viruses [83].

A key receptor involved in the formation of virological synapses and cell-to-cell transmission is LFA-1 (lymphocyte function associated antigen-1) [238, 239]. LFA-1 becomes activated and mediates cell-cell adhesion when T cells are stimulated with anti-CD3 antibodies [240, 241], and is also reported to be induced by $\alpha_4\beta_7$-mediated signaling [164]. Because of this, we speculated that cell binding to RetroNectin via $\alpha_4\beta_7$ may enhance LFA-1 activation, and thus contribute to cell-to-cell transmission. To test this, unstimulated $CD4^+\alpha_4\beta_7^+$ T cells were cultured on plates coated with either the CD3 antibody OKT3, RetroNectin, or a combination of both. Cells were then stained with the antibody MEM-148, which specifically detects activated LFA-1 [242]. Treatment of cells with OKT3 induced LFA-1 activation, but RetroNectin by itself did not (Figure 3-7D). Furthermore, the combination of RetroNectin and OKT3 did not activate LFA-1 more than OKT3 alone, and LFA-1 activation was not inhibited by Act-1 or 2B4. Collectively, these results indicated that RetroNectin did not modulate LFA-1 activity in our assays, and that this mechanism did not explain the enhanced cell-to-cell transmission observed on RetroNectin.

RetroNectin provides costimulatory signals leading to T cell proliferation

Fibronectin has been reported to transmit costimulatory signals to $CD4^+$ T cells through $\alpha_5\beta_1$ and $\alpha_4\beta_1$ integrins [243]. Based on this, we hypothesized that RetroNectin similarly activated T cells by binding to these integrins, and thus contributed to enhanced infection. Unstimulated $CD4^+\alpha_4\beta_7{}^+$ T cells were cultured in the presence of OKT3, IL-2, or RetroNectin in various combinations, as indicated. Three days later, cell proliferation was measured by incorporation of the thymidine analog EdU (described in the methods). Using this assay, we found proliferation was not induced by any individual stimulus, but was induced by combinations of OKT3 with either IL-2 or RetroNectin (Figure 3-8A). This demonstrated that IL-2 and RetroNectin both delivered costimulatory signals that lead to cell proliferation.

We next used inhibitors to determine which interactions between cells and RetroNectin provided costimulation. 2B4 and P5D2 both partially inhibited proliferation, and the combination of these antibodies completely inhibited proliferation (Figure 3-8B). In contrast, no effect was observed when cells were incubated with Act-1, heparin, or chondroitin sulfate. These results indicated that costimulatory signals were mediated by RetroNectin binding to both $\alpha_5\beta_1$ and $\alpha_4\beta_1$, but not by binding to $\alpha_4\beta_7$ or cell-associated proteoglycans. These findings were in agreement with previous reports regarding fibronectin-mediated costimulation. At the same time, these results did not support the hypothesis that increased cell activation accounted for the enhanced infection observed with RetroNectin. P5D2 and Act-1 had opposing effects on proliferation and infection: P5D2 inhibited proliferation but not infection, while Act-1 inhibited infection but not proliferation. While fibronectin-mediated cell activation may not have played a role in our particular assays, it may have relevance to infection *in vivo*. It is possible that sub-optimally activated $\alpha_4\beta_7{}^+$ cells may become activated upon binding to CS1 fibronectins, and

thereby become more readily infected by HIV. In this context, others have recently reported that RetroNectin facilitates HIV infection of sub-optimally active $CD34^+$ hematopoietic stem cell populations [244].

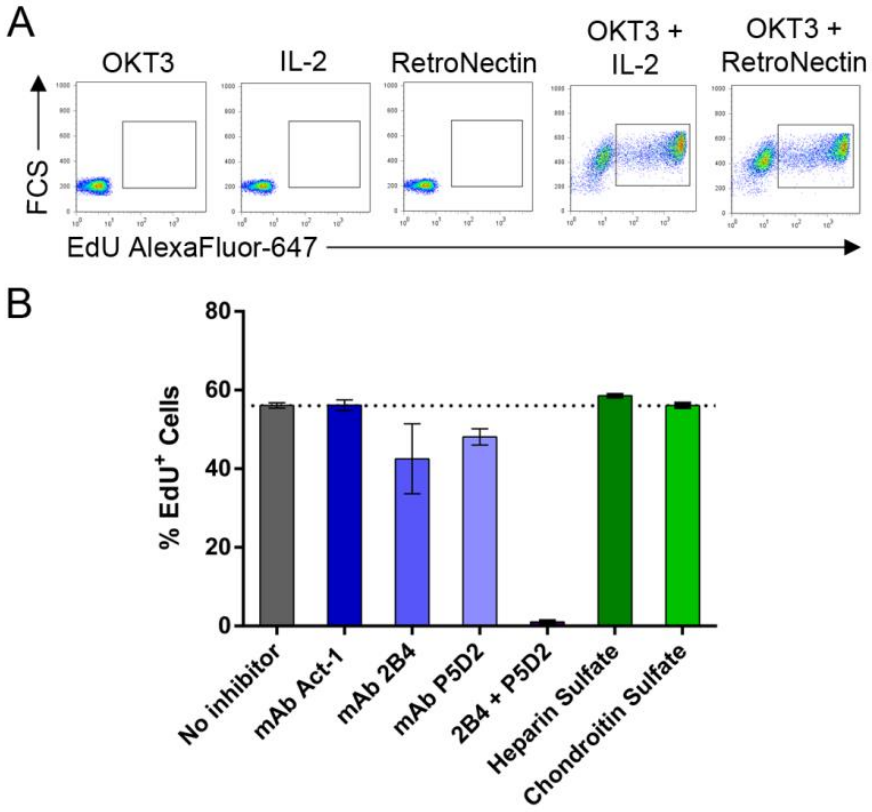

Figure 3-8. RetroNectin-Mediated T Cell Activation. Cell proliferation was assessed by measuring incorporation of the thymidine analog EdU. A) Representative results after culturing unstimulated $CD4^+\alpha_4\beta_7^+$ T cells for 3 days with the indicated stimuli. B) EdU incorporation measured on cells stimulated for 3 days on OKT3 and RetroNectin, with the addition of the indicated inhibitors. Results are the mean and standard deviation of triplicate measurements.

CS1 fibronectin expression in pigtail macaque tissues

To establish the biological significance of our findings, we used immunohistochemistry to verify the presence of CS1 fibronectins. Intestinal tissues were chosen because they are the principal site of infection and inflammation, and also contain a high density of $\alpha_4\beta_7^+$ cells[162].

Thus, we hypothesized that CS1 fibronectins are present and contribute to the infection of $\alpha_4\beta_7^+$ cells in intestinal sites. For our studies, we utilized jejunum biopsies from pigtail macaques (*Macaca nemestrina*) infected with SIV-HIV chimeric viruses (SHIV-1157ipd3N4). The specific animals under study are described by Ho et al.[245]. Tissues were collected at necropsy approximately one year after infection, and then formalin-fixed and paraffinized for archival storage.

Robust expression of CS1 fibronectin was observed in the tissues studied (Figure 3-9). Expression was strongest in aggregates of immune cells and the lamina propria, weaker in the muscularis mucosa, and absent in the epithelium. These results indicated that in the context of SHIV-infected pigtail macaques, CS1 fibronectins were expressed in the gut-associated lymphoid tissues and may play roles in infection and intestinal pathology. By extension, pigtail macaques may serve as a good model for studying the role of CS1 fibronectins *in vivo.* These studies also lay the groundwork for further experiments to investigate CS1 fibronectin expression in additional species including humans and rhesus macaques, as well as studies to examine CS1 fibronectin expression in additional tissues and stages of infection.

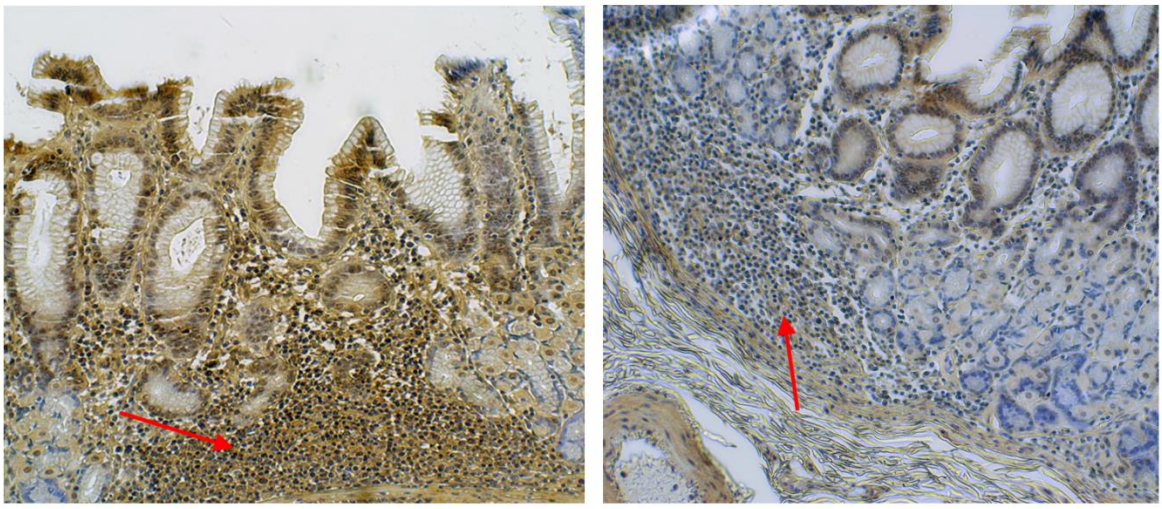

Figure 3-9. CS1 Fibronectin Expression in Pigtail Macaque Tissue. Representative results of CS1 fibronectin staining in jejunum biopsies from SHIV-infected pigtail macaques. Shown are results from animal# K03135, described in detail by Ho et al.[245]. Red arrows indicate immune cell aggregates.

Discussion

In this study we provide *in vitro* evidence that CS1 fibronectins facilitate the infection of $CD4^{+}\alpha_4\beta_7^{+}$ T cells. We show that the CS1 fibronectin fragment RetroNectin provides a substrate for the attachment and co-localization of HIV and $\alpha_4\beta_7^{+}$ T cells *in vitro*, and mediates robust infection that is correlated with increased cell-to-cell virus transmission, cell activation, and resistance to neutralizing antibodies. In support of a biological role for CS1 fibronectins, we show that these proteins are present in the extracellular matrix of infected intestinal tissues from macaques. We additionally show that $\alpha_4\beta_7$-directed antibodies significantly attenuate infection mediated by RetroNectin, and propose that this mechanism may contribute to the antiviral activity of these antibodies *in vivo*.

In this work, we found that HIV bound to RetroNectin through two distinct interactions. The first was through HIV envelope protein binding to the fibronectin C-terminal heparin binding domain, which has been previously described [136]. The second was through

interactions between virion-associated $\alpha_4\beta_7$ and $\alpha_4\beta_1$ integrins and the CS1 motif. Others have described these integrin-mediated interactions as well; Liao et al. reported that virion-associated $\alpha_4\beta_1$ mediates attachment to VCAM-1 (vascular cell adhesion molecule-1) [224], and Guzzo et al. reported that virion-associated $\alpha_4\beta_7$ mediates attachment to MAdCAM-1 (mucosal vascular addressin cell adhesion molecule-1) [225]. Our experiments corroborate these observations, and identify CS1 fibronectin as an additional ligand that interacts with virus-associated integrins. Between the two virus-RetroNectin interactions we identified, the interaction with envelope protein was relatively weaker than the interaction with integrins. However, this may not necessarily be the case with full-length fibronectin molecules. Additional interactions between HIV envelope and the N-terminal III_1-C fibronectin fragment have been described [138]. Therefore, HIV envelope may play a more significant role in virus adhesion to full-length fibronectins than to RetroNectin. It is also worth noting that additional extracellular matrix molecules, including laminin, reportedly to bind to HIV envelope protein [136]. Thus, HIV adhesion to the extracellular matrix via envelope protein *in vivo* may be stronger than what is predicted through our studies with RetroNectin. However, the significance of RetroNectin – and by extension CS1 fibronectins – is that these molecules lend specificity that may lead to co-localization of HIV-1 with $\alpha_4\beta_7^+$ cells.

CS1 fibronectins are not normal components of healthy adult tissues, but are oncofetal variants expressed in pathological conditions. Expression of CS1 fibronectins has been observed in inflammatory conditions including allergic contact dermatitis [246], rheumatoid arthritis [247], dupuytren's contracture [248], as well as oral cancer [249]. The cytokine TGFβ-1 (transforming growth factor β-1) has been implicated in the *in vivo* upregulation of CS1 fibronectin [248], and also has been shown through *in vitro* experiments to increase the

production of CS1 splice variants [250, 251]. Separately, it has been reported that HIV-infected lymphocytes secrete TGFβ-1, and thereby increase fibronectin production in infected tissues [252]. Together, these findings suggest the interesting possibility that HIV-infected lymphocytes may stimulate expression of CS1 fibronectins in local tissue environments via TGFβ-1. In our studies, we provide evidence that CS1 fibronectins are expressed in pigtail macaque intestinal tissues in the context of SHIV infection. These findings raise the interesting possibility that CS1 fibronectin expression may be upregulated in the context of infection and that TGFβ-1 may play a role in this. Further studies are needed to examine this possibility, and examine the relationship between CS1 fibronectins, TGFβ-1, $\alpha_4\beta_7^+$ cells, and viruses in tissues.

The results of our studies have particular relevance in the context of $\alpha_4\beta_7$–directed antiviral therapy. The antibody Act-1 has been shown to mediate important antiviral effects in Rhesus macaques infected with SIV [188-191]. However, it has also been demonstrated that Act-1 does not mediate antiviral effects *in vitro* [173]. Through our studies we have identified *in vitro* conditions in which Act-1 exhibits significant anti-HIV activity; namely, that Act-1 attenuated RetroNectin-mediated infection. We attributed this effect to the ability of Act-1 to block both virus and cell binding to RetroNectin, and thus to prevent co-localization of viruses and cells. Based on this, we propose that one mechanism of antiviral activity of Act-1 *in vivo* may be the inhibition of virus and $\alpha_4\beta_7^+$ cell co-localization on CS1 fibronectins. Other possible mechanisms of action may include downregulation of inflammatory responses and inhibition of cell-to-cell transmission by Act-1. In addition to these findings, we found that the antibody 2B4 and combinations of Act-1 with heparin more potently inhibited infection than Act-1 alone. Significantly, the concentration of heparin used in these experiments (1µg/mL or 189U/L) was the same concentration used clinically for anticoagulation therapy. Based on these results, we

propose further studies on the *in vivo* antiviral properties of Natalizumab, which has a similar specificity to 2B4, as well as combinations of Vedolizumab (Act-1) with heparin sulfate.

Through these studies we have identified a novel potential role for CS1 fibronectins in facilitating HIV-1 infection of $\alpha_4\beta_7^+$ cells. We provide *in vitro* evidence that CS1 fibronectins enhance HIV infection by promoting cell-to-cell transmission and resistance to neutralizing antibodies. These studies clarify the mechanism by which HIV targets $\alpha_4\beta_7^+$ cells for infection, and have important implications for understanding the effects of intergrin antagonists and neutralizing antibodies in HIV therapy.

Materials and Methods

Reagents

The following anti-HIV-1 gp120 monoclonal antibodies were obtained through the NIH AIDS Reagent Program, Division of AIDS, NIAID, NIH: VRC01 (cat#12033), from Dr. John Mascola; PGT121 (cat#12343); 2G12 (cat#1476) from Polymun Scientific; and A32 (cat#11438) from Dr. James E. Robinson. The Human anti-HIV-1 V2 monoclonal antibody PG16 was from the International AIDS Vaccine Initiative. The anti-human $\alpha_4\beta_7$ integrin antibody Act-1 (cat#11718)[187] was obtained through the NIH AIDS Reagent Program, Division of AIDS, NIAID, NIH from Dr. A. A. Ansari. Integrin-blocking monoclonal antibodies 2B4 and P5D2 were from R&D Systems. Heparin sulfate (189 U/mg) and chondroitin sulfate B, both isolated from porcine intestinal mucosa, were from Sigma-Aldrich. RetroNectin was from TaKaRa. Bovine serum albumin, human plasma fibronectin, type 4 collagen from human placenta, and laminin from cultured human fibroblasts were all from Sigma-Aldrich. Recombinant human nidogen was from R&D systems. All cell culture reagents were from ThermoFisher.

Source of human PBMCs and CD4$^+$ $\alpha_4\beta_7^+$ T cells

Used leukocyte filters from healthy donors were purchased from BloodWorks Northwest (Seattle, Washington), and PBMCs were obtained by back-flushing filters as previously described [221]. For propagation of HIV stocks, PBMCs were separated by ficoll-paque, and then activated for 2 days with 250ng/mL OKT3 antibody (Biolegend), and 100U/mL interleukin-2 (IL-2, from Chiron Corp.). Purified CD4$^+$ T cells were obtained from ficoll-purified PBMCs by using a magnetic negative selection kit (Miltenyi Biotec). 95% or more of the cells obtained by this method were CD4$^+$, as assessed by staining with allophycocyanin-conjugated antibody to CD4 (Beckton Dickinson, clone RPA-T4). For proliferation experiments, T cells were maintained without the addition of mitogens. For all other experiments, cells were activated for 2 days with 250ng/mL OKT3, and incubated continuously with 100U/mL IL-2 as well as 10nM all-trans retinoic acid (Sigma-Aldrich) to induce $\alpha_4\beta_7$ expression. Cells were used for infection studies 9 days after establishing cultures. Culture media was RPMI-1640 supplemented with 10% fetal bovine serum (FBS), 2mM glutamine, 100U/mL penicillin, and 100µg/mL streptomycin.

HIV-1 p24 ELISA

An in-house enzyme-linked immunosorbent assay (ELISA) was used to quantify HIV-1 p24 protein in culture supernatants and viral lysates. Antibodies for p24 capture and detection and a p24 protein standard were obtained from the AIDS and Cancer Virus Program, Leidos Biomedical Research Inc., Frederick National Laboratory for Cancer Research, National Cancer Institute, Frederick, MD. Mouse monoclonal IgG p24 capture antibody was diluted 1:2,000 in PBS per the supplier's instructions, and immobilized overnight on 96-well high-binding

polystyrene plates. Non-specific binding sites were then blocked by 1hr incubation with 1% BSA at room temperature. Blocking solution was removed, and samples and standards were added and incubated overnight at 37°. For subsequent wash steps, wash buffer was PBS containing 0.05% Tween-20, and each well was washed 5 times with 350µL of buffer. Wells were washed and then incubated at 37°C for 1hr with rabbit anti-p24 detector antibody diluted 1:200 into RPMI1640 media containing 10% FBS and 2% mouse serum. Wells were washed again, and then incubated at 37°C for 1hr with peroxidase-conjugated goat-anti-rabbit IgG (SeraCare, Milford, MA) diluted 1:20,000 into RPMI1640 media containing 2% mouse serum, 5% goat serum, and 0.01% Tween-20. Wells were washed once more, and 3,3',5,5'-Tetramethylbenzidine (SeraCare) was added and incubated for 30min at room temperature. Color development was stopped with the addition of 1N HCl, and absorbance was read at 450nm in an iMark plate reader (Bio-Rad). Each sample was assayed at 4 separate dilutions, and values within the linear range of the assay were used for determination of p24 concentrations. The limit of detection of this assay was approximately 400pg/mL p24. For detection of lower levels of p24 in certain samples, a commercial p24 ELISA kit (Zeptometrix) with a limit of detection of 8pg/mL was used according to the manufacturer's instructions.

HIV-1 virus production and characterization

The following HIV-1 virus stocks were obtained from the NIH AIDS Reagent Program, Division of AIDS, NIAID, NIH: KNH1207 (cat#11247, subtype A) from Dr. Victoria Polonis [253]; Ba-L (Cat#510, subtype B, referred to herein as "BaL") from Dr. Suzanne Gartner, Dr. Mikulas Popovic and Dr. Robert Gallo [254]; SF162 (cat#276, subtype B) from Dr. Jay Levy [255]; and 93MW959 (cat#2915, subtype C) from Dr. Paolo Miotti. Fresh virus stocks were

produced in cultures of human PBMCs stimulated with OKT3 and IL-2 and maintained at $5.0x10^6$ cells/mL. Cell were infected with 2.5ng of p24 per million cells for 24hr, and then exchanged into fresh media containing 100U/mL IL-2. Cultures were maintained for 14 days post-infection, with a complete media change every 2-3 days. At each media change culture supernatants were passed through a 0.4µm syringe filter, and stored in 1mL aliquots at -80°C. Supernatants were lysed by adding Triton X-100 to 1%, and p24 content was measured by ELISA. Samples collected at the days of peak p24 output were used for subsequent experiments.

A standard titration assay was used to determine half-maximal tissue-culture infective doses ($TCID_{50}$). Virus stocks were serially diluted, and then incubated with aliquots of $5.0x10^5$ stimulated PBMCs in a volume of 200µL in round-bottom 96-well plates. 4 replicate wells were infected for each virus dilution. The inoculum was removed after 24 hours and media was changed on days 5, 9, and 11 post-infection. Culture supernatants from day 11 were lysed and used to measure p24 concentrations by ELISA. Wells with 200pg/mL p24 or greater were considered positive, and the method of Reed and Muench was used to compute $TCID_{50}$ values [256].

Detection of virus-associated integrins by western blot

Viruses were precipitated from 4mL of HIV-1 BaL stock, corresponding to approximately 800ng p24, using the polyethylene glycol-based PEG-it virus precipitation solution (System Biosciences) per the manufacturer's instructions. As a negative control, 4mL of culture supernatant from uninfected PBMCs was prepared in an identical manner. Precipitates were lysed in 100µL of RIPA buffer (Pierce) containing protease inhibitors. As a positive control, $5.0x10^6$ $CD4^+\alpha_4\beta_7^+$ T cells were lysed in 100µL of RIPA buffer. Lysates were reduced

and denatured, separated by SDS-PAGE, and transferred to PVDF membranes as previously described [221]. Membranes were blocked for 1hr in PBS containing 5% nonfat milk and 0.05% Tween-20, and then incubated overnight at 4°C with antibodies diluted in this same blocking buffer. Detection of α_4 integrin was performed with rabbit polyclonal ITGA4 antibody (ThermoFisher, cat#PA5-20599) at 1µg/mL, and detection of β_7 integrin was performed with rabbit monoclonal antibody clone EP5948 (abcam) at 1µg/mL in blocking buffer. Membranes were washed three times in PBS containing 0.05% Tween-20, and then incubated for 1hr in peroxidase-conjugated goat-anti-rabbit IgG (SeraCare) at 100ng/mL in blocking buffer. Membranes were washed extensively, and then incubated in chemiluminescence substrate (Pierce) before capturing signals on film (Amersham hyperfilm ECL, GE Life Sciences).

HIV-1 gp120 protein and virus binding to RetroNectin

RetroNectin was diluted to 50-0.39µg/mL in PBS as indicated, plated at 100µL/well on 96-well flat-bottom polystyrene plates, and incubated overnight at 4°C. RetroNectin solutions were discarded and wells were blocked with 200µL of 1% BSA in PBS for 30min at 37°C. For gp120 binding, biotinylated HIV-1 BaL gp120 was utilized. HIV-1 BaL gp120 recombinant protein was obtained from DAIDS, NIAID through the NIH AIDS Reagent Program, Division of AIDS, NIAID, NIH (cat#4961), and was biotinylated as previously described [221]. 5µg of biotinylated gp120 was diluted in PBS and added to each well in a volume of 100µL, and incubated for 30min at 37°C. For inhibitor studies, gp120 and inhibitors were combined in a total volume of 100µL for 10min prior to incubating on the wells. Following incubation, gp120 solutions were discarded and wells were washed three times with 200µL of PBS. Peroxidase-conjugated streptavidin (Zeptometrix, provided with p24 ELISA kit) was prepared according to

the manufacturer's instructions and added at 100µL/well for 30min at 37°C. Wells were washed five times with 350µL of PBS containing 0.05% Tween-20, and then developed with 3,3',5,5'-Tetramethylbenzidine for 30min, stopped with 1N HCl, and read at 450nm as described above for p24 ELISA.

For virus binding studies, HIV-1 BaL viruses were diluted in cell culture media (RPMI1640 containing 10% FBS, glutamine, and antibiotics), added to each well in a volume of 100µL, and incubated for 1hr at 37°C. Virus input was normalized by p24, and between 2.0-0.03ng of p24 was added per well, as indicated. For inhibitor studies with heparin and integrin-blocking antibodies, the viruses and inhibitors were combined in a volume of 100µL for 10min prior to incubating on wells. For studies with HIV envelope-directed antibodies, viruses and antibodies were combined in a volume of 100µL and incubated for 1hr at 37°C prior to incubating on wells. Virus solutions were discarded and wells were washed three times with 200µL of warm cell culture media. Bound viruses were then lysed with 200µL of 1% Triton X-100 in PBS, and lysates were assayed by p24 ELISA.

In vitro HIV-1 infection assays

For infection with RetroNectin-associated viruses, viruses were captured on RetroNectin-coated plates as described above. After washing to remove unbound virus, $2.5x10^5$ activated $CD4^+\alpha_4\beta_7^+$ T cells were added in a volume of 150µL/well. Culture media was completely changed at days 1, 3, 5, and 7 after initiating cultures, and p24 content in supernatants was determined by ELISA. Culture media contained 100U/mL IL-2 and 10nM retinoic acid. For inhibitor studies, inhibitors were added at the indicated concentrations and replenished with each media change.

For infection with free viruses, 96-well plates were blocked with 1% BSA for 30min at 37°C. Aliquots of $2.5x10^5$ $CD4^+\alpha_4\beta_7^+$ T cells were combined with 2ng of HIV-1 BaL in a volume of 150µL and incubated for 24hr on these plates. The inoculum was removed and cells were exchanged into fresh media, and media was subsequently changed on days 3, 5, and 7 post-infection. Culture supernatants from days 3, 5, and 7 were assayed for p24 content by ELISA.

Cell-to-cell virus transmission assays

Cell-to-cell HIV transmission between autologous $CD4^+\alpha_4\beta_7^+$ T cells was measured in a similar manner as described [83]. Donor $CD4^+\alpha_4\beta_7^+$ T cells were infected with HIV-1 BaL and maintained for 5 days to allow for virus spread. Uninfected target $CD4^+\alpha_4\beta_7^+$ T cells from the same donor were fluorescently labeled with CellTrace Far Red cell proliferation kit (ThermoFisher) according to the manufacturer's instructions. Donor cells were washed twice with media to remove unbound viruses, and were combined with target cells in a 2:1 donor:target ratio. Cell mixtures were incubated on plates coated with RetroNectin or BSA, in a volume of 200µL containing $2.5x10^5$ total cells. Inhibitors were added at the initiation of cultures. At 24hr and 48hr, cells were removed and stained for intracellular p24 content. To estimate the level of infection attributable to free viruses released into the media, aliquots of infected cells were maintained in parallel for 48hr and supernatants were collected. Uninfected cells were then incubated in these virus-containing supernatants for 48hr and stained for intracellular p24.

For p24 staining, cells were washed twice with PBS containing 1% BSA, and fixed for 10min in 1% formalin. Fixed cells were washed in 1% BSA and once more in PBS containing 0.05% saponin and 1% BSA. Cells were incubated in fluorescein isothiocyanate-conjugated p24 antibody (clone KC57, Beckman Coulter) diluted 1:40 in saponin buffer for 30min at room

temperature. Excess antibody was removed with two washes in saponin buffer, and cells were fixed in 2% formalin and analyzed by flow cytometry. Data were acquired on a BD FACSCalibur cytometer with CellQuest Pro software (Beckton Dickinson, version 6.0) and analyzed with FlowJo software (Treestar, version 7.2.2). 20,000 events were recorded for each sample.

In separate experiments, levels of LFA-1 were measured in $CD4^{+}\alpha_4\beta_7^{+}$ T cells in response to mitogens or inhibitors. $2.5x10^5$ unstimulated cells were incubated for three days on wells coated with 100ng OKT3, 1µg RetroNectin, or both. Samples incubated on OKT3/RetroNectin-coated wells were additionally incubated with or without inhibitors, as indicated. For staining, cells were washed in 1% BSA, incubated for 20min at 37°C in phycoerythrin-conjugated MEM-148 antibody (abcam) diluted 1:20 in 1% BSA, washed twice in 1% BSA, and then fixed in 1% formalin. Cells were analyzed by flow cytometry as described above.

T cell proliferation assay

T Cell proliferation in response to OKT3, OKT3 and IL-2, or OKT3 and RetroNectin was measured with a Click-iT EdU AlexaFluor-647 cell proliferation kit (ThermoFisher). This method relies on incorporation of the thymidine analog EdU (5-ethynyl-2'-deoxyuridine) into proliferating cells, and subsequent detection by reaction of fluorescent azide derivatives to EdU. 96-well plates were coated overnight with 100ng of OKT3, 1µg RetroNectin, or both. Aliquots of $2.5x10^5$ unstimulated T cells were plated on these wells. In some wells coated with OKT3, 100U/mL IL-2 was added to the media to provide co-stimulation. In some wells coated with OKT3 and RetroNectin, inhibitors were added at the initiation of the culture as indicated. Cells were maintained for 3 days in the presence of mitogens and inhibitors, and EdU was added at

100μM and cells were incubated for an additional 2hr. Staining for EdU was then performed according to the manufacturer's instructions.

Detection of CS1 fibronectin by immunohistochemistry

Tissues utilized in this study were archived formalin-fixed paraffin-embedded tissues from SHIV-infected pigtail macaques obtained through the Washington National Primate Research Center. 4μm sections were cut onto slides, dewaxed with xylene, and rehydrated to PBS through graded alcohols. Antigen retrieval was carried out by 10min incubation in citrate buffer, pH 6.0, at 95°C (Sigma-Aldrich). Slides were cooled in PBS, endogenous peroxidases were blocked for 5min in 3% hydrogen peroxide, and nonspecific protein binding was blocked for 20min in 10% goat serum. Samples were incubated overnight at 4°C with either the CS1-specific mouse monoclonal IgM antibody P1F11 (Santa Cruz Biotechnology) or an isotype control mouse IgM (clone PRF-03, ThermoFisher), both diluted to 10μg/mL in 10% goat serum. Slides were washed three times with PBS, and then incubated for 1hr in peroxidase-conjugated goat-anti-mouse IgM (abcam) diluted to 2μg/mL in 10% goat serum. Slides were washed extensively, incubated in immPACT DAB peroxidase substrate (Vector Laboratories) according to the manufacturer's instructions, and counterstained for 30s in hematoxylin (Vector Laboratories).

Curve fitting and statistical analysis

GraphPad Prism software (version 6.03) was used for graphing, linear and non-linear regression, and statistical analysis. Virus binding data were fit to a standard one-site hyperbolic binding curve. Inhibition data were fit to either a standard sigmoidal four-parameter logistic

curve or a biphasic dose-response curve. The appropriate model was determined by visual inspection of residual plots, and R^2 values for all fits were 0.91 or higher. Maximum binding (B_{max}) for binding curves, IC_{50} values for inhibition curves, and associated confidence intervals were computed by GraphPad Prism software. Comparisons of mean binding or infection values were performed by a student's T-test with a significance threshold (α) of 0.05.

Acknowledgements

We thank Lynn Schnapp for sharing her experiences and discussing assay design with us. We thank Rodman Smith of Leidos Biomedical Research, Inc. for providing p24 ELISA reagents. Finally, we thank Brian Johnson and Megan Larmore at the University of Washington Histology and Imaging Core for assistance with immunohistochemistry experiments.

Chapter 4

Recombinant Vaccinia Virus-Expressed HIV-1 gp120 Does Not Bind to $\alpha_4\beta_7$

*Glycan analysis data presented in Figure 4-8 was provided by Miklos Guttman

Abstract

The only vaccine trial to date that demonstrated efficacy against Human Immunodeficiency Virus (HIV) was the RV144 trial. This trial used poxvirus-based immunogens and elicited antibodies directed to the second variable loop (V2) of HIV envelope protein subunit gp120. These V2 antibodies were correlated with protection in RV144; however the mechanism for this protection is not understood. It has been proposed that gp120 binds to the integrin receptor $\alpha_4\beta_7$ through V2, and V2-directed antibodies may inhibit this binding. We recently demonstrated that purified gp120 produced from Chinese hamster ovary (CHO) and human embryonic kidney 293 (HEK293) cells does not bind to $\alpha_4\beta_7$ through the V2 loop, which puts this hypothesis in doubt. However, we did not study the binding properties of poxvirus-expressed gp120, which may have important structural and antigenic differences compared to gp120 from these expression systems. In the present study, we extended our previous observations and studied the binding properties of gp120 produced by recombinant vaccinia viruses (rVV). Recombinant gp120 from 8 HIV strains was produced by rVV infection of CHO and BSC-40 cells and purified to apparent homogeneity. A flow cytometry assay was used to measure protein binding to primary human $CD4^+\alpha_4\beta_7^+$ T cells, and binding specificity was differentiated by blocking receptors with antibodies. Of the 8 gp120 proteins tested, all bound to CD4 but not to $\alpha_4\beta_7$. Both kifunensine treatment and removal

of N-linked glycans from the V2 loop increased CD4 binding, but did not modulate $\alpha_4\beta_7$ reactivity. In total, we found no evidence that rVV-expressed gp120 binds directly to $\alpha_4\beta_7$. Further studies are needed to understand the role of V2 antibodies in vaccine-mediated protection against HIV.

Introduction

The envelope glycoprotein (Env) of Human immunodeficiency virus type 1 (HIV-1) is a primary vaccine target. In preclinical studies, both passively-administered[257-261] and vaccine-elicited[108, 262] antibodies targeting Env have been demonstrated to protect macaques against challenge with Simian immunodeficiency viruses (SIV) or SIV/HIV chimeric viruses (SHIV). Env-specific antibodies have also been identified as a significant correlate of protection in the RV144 vaccine trial, the only trial conducted to date that demonstrated any protective efficacy in humans[179, 181]. During HIV-1 infection, Env is expressed as a single polypeptide chain (gp160) and is further processed by cellular proteases into the soluble gp120 and membrane-bound gp41 subunits[100]. Env proteins expressed on the surfaces of viruses and infected cells are presented as trimers of non-covalently associated gp120-gp41 heterodimers[263]. In RV144, vaccinees were administered two different Env immunogens in a prime-boost regimen. The recombinant canarypox product ALVAC-HIV (vCP1521; Sanofi Pasteur) was used for priming doses. ALVAC-HIV encodes the HIV-1 structural genes *gag* and *pol* as well as gp160, and likely mediated expression of membrane-bound trimeric Env *in situ*. Boosting doses consisted of purified recombinant gp120 subunit protein (AIDSVAX B/E; VaxGen). Importantly, in the AIDSVAX trials that preceded RV144, immunization with gp120

protein alone did not achieve protection[177]. Thus, in RV144 the combination of poxvirus-expressed Env followed by purified gp120 likely played a role in eliciting protective antibodies.

In an extensive analysis of RV144 vaccinees, the only variable significantly correlated with protection was serum IgG specific to the first and second variable loops (V1V2) of gp120[181]. Interestingly, these V1V2 antibodies were non-neutralizing, and it is not yet clear how they may have mediated protection. The V2 loop of Env has been reported to engage the integrin receptor $\alpha_4\beta_7$, and through this interaction may facilitate infection of gut-homing $\alpha_4\beta_7^+$ T cells and enhance mucosal transmission of HIV-1[164, 170]. Based on these observations, it has been postulated that V1V2 antibodies in RV144 may have mediated protection by inhibiting Env-$\alpha_4\beta_7$ interaction[183-185, 264]. However, we recently reported that highly purified gp120 produced in Chinese hamster ovary (CHO) and human embryonic kidney 293 (HEK293) cells does not bind directly to $\alpha_4\beta_7$ through the V2 loop[221]. Instead, we discovered that fibronectin mediated Env-$\alpha_4\beta_7$ interactions indirectly, and these interactions did not require the V2 loop and were not inhibited by V2-specific antibodies. However, we did not study the potential $\alpha_4\beta_7$ binding properties of poxvirus-expressed Env proteins. It remains unknown if poxvirus-produced gp120 presents different V2 epitopes than gp120 produced in other expression systems, or how these factors may impact immune responses elicited by poxvirus priming *in vivo*.

Post-translational modifications to Env, including glycosylation patterns, have been proposed to impact Env-$\alpha_4\beta_7$ binding by modulating the conformation or exposure of the V2 loop. Specifically, enhanced $\alpha_4\beta_7$ reactivity has been associated with minimally-processed oligomannose glycans[170, 265]. Therefore, it remains possible that Env produced by poxviruses may engage $\alpha_4\beta_7$, while Env produced by CHO or HEK293 does not. This is of particular relevance in the context of understanding antibody responses to immunization with

Env-expressing recombinant poxviruses. In this study we produced gp120 by infecting cells *in vitro* with recombinant vaccinia viruses (rVV), and investigated the $\alpha_4\beta_7$–binding properties of these gp120 molecules. We found that rVV-expressed gp120 was highly pure and primarily displayed oligomannose glycans, but did not bind to $\alpha_4\beta_7$. We additionally found that fibronectin mediated binding of rVV-expressed gp120 to $\alpha_4\beta_7$. Results from this study support the hypothesis that Env does not bind to $\alpha_4\beta_7$ directly through the V2 loop, and suggests that V1V2 antibodies in RV144 were unlikely to have inhibited HIV interactions with $\alpha_4\beta_7$.

Results

Characterization of $CD4^+\alpha_4\beta_7^+$ T cells

In this study gp120 binding to CD4 and $\alpha_4\beta_7$ was measured with a cell binding assay, using primary human T cells from three separate donors. $CD4^+$ T cells were purified from peripheral blood mononuclear cells (PBMCs) by magnet-activated cell separation (MACS), and then cultured with all-trans retinoic acid to stimulate $\alpha_4\beta_7$ expression as previously described[164, 221]. Expression of CD4 and β_7 integrin was measured by flow cytometry; 98.4% ±0.8% of cells expressed CD4, and 92.4% ± 8.9% expressed β_7 integrin. MAdCAM-1-Fc was used as a positive control for $\alpha_4\beta_7$ binding and to validate the following inhibitors: mAb Leu3a (CD4-blocking antibody), mAb 2B4 (α_4 integrin-blocking antibody), and EDTA (nonspecific inhibitor of all integrins). MAdCAM-1-Fc bound at similar levels to cells from all three donors. As expected, MAdCAM-1-Fc binding was inhibited by mAb 2B4 and EDTA but not by mAb Leu3a. Cell phenotyping and MAdCAM-1-Fc binding controls are presented in Figure 4-1.

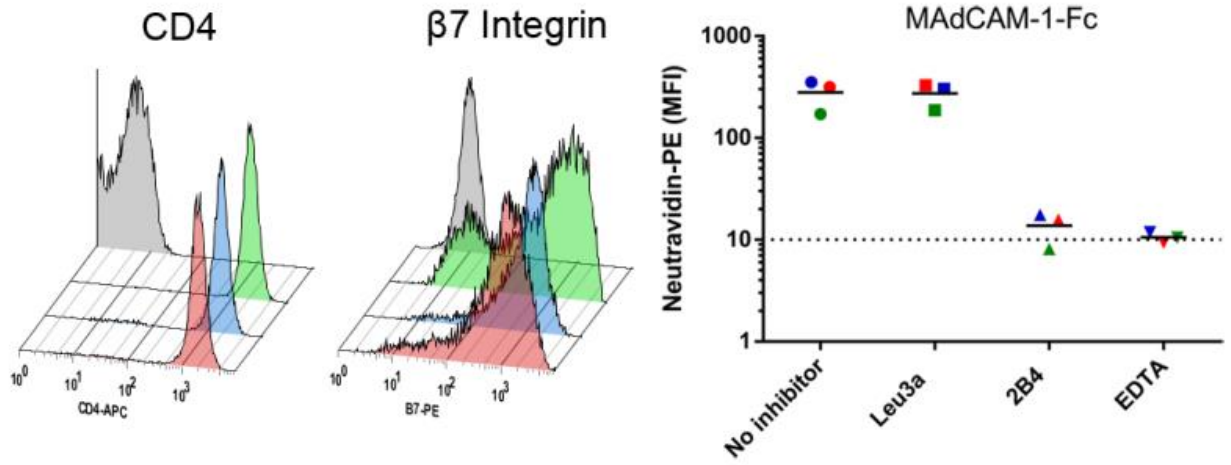

Figure 4-1. Characterization of $CD4^+\alpha_4\beta_7^+$ T cells. Expression of CD4 (left) and β_7 integrin (middle) measured by flow cytometry. Grey curves are unstained background signals; red, blue, and green curves are measurements from each of the three donors. MAdCAM-1-Fc binding to cells from all three donors (right); binding value for each individual donor is shown in red, blue, and green symbols, black bars represent mean binding values. The dotted line indicates background signal from cells stained without MAdCAM-1-Fc.

MW959 gp120 expressed by recombinant vaccinia viruses does not bind to $\alpha_4\beta_7$

In previous studies we extensively characterized gp120 from the MW959 isolate produced in both CHO and HEK293 cells[221]. In these expression systems we found that DEAE anion exchange chromatography removed $\alpha_4\beta_7$–reactive cellular proteins, and that gp120 purified with DEAE did not bind to $\alpha_4\beta_7$. In the present study, we extended these observations and studied the $\alpha_4\beta_7$ binding properties of MW959 gp120 expressed by recombinant vaccinia viruses (rVV). We first expressed gp120 by infecting the African green monkey kidney cell line BSC-40 with rVV, and purified the protein as previously described[266]. Notably, this purification method includes a DEAE anion exchange step. MW959 gp120 prepared by this method was purified to apparent homogeneity as assessed by sodium dodecyl sulfate polyacrylamide gel electrophoresis (SDS-PAGE), and was immunoreactive with pooled plasma

from HIV-infected patients (Figure 4-2A). This MW959 gp120 preparation bound to primary $CD4^{+}\alpha_4\beta_7^{+}$ T cells in a concentration-dependent manner, and binding was inhibited by Leu3a but not by EDTA or 2B4 (Figure 4-2A). These results indicated that this MW959 gp120 preparation bound to CD4 but not to $\alpha_4\beta_7$.

We next expressed MW959 gp120 in rVV-infected CHO cells, to assess whether producer cell substrate affected binding activity. Because CHO cells are not permissive to vaccinia viruses[267], we expressed gp120 using an adaptation of the method described by Ramsey-Ewing and Moss[268]. CHO cells were co-infected with rVV expressing MW959 gp120, and a second rVV expressing a cowpox host range protein which permits vaccinia virus replication in CHO. MW959 gp120 produced by this method was purified and analyzed as described above. In terms of purity and immunoreactivity, no significant differences were observed between this preparation and gp120 prepared in BSC-40 cells (Figure 4-2B). MW959 gp120 produced in CHO cells also bound to CD4 but not $\alpha_4\beta_7$, however overall binding was approximately 20% greater in the CHO-derived material. The overall yield of gp120 from CHO cells was significantly lower than that obtained from BSC-40 (0.34mg/liter from CHO, 3.67mg/liter from BSC-40). In total, we found no evidence that MW959 gp120 purified from rVV-infected CHO or BSC-40 cells bound to $\alpha_4\beta_7$.

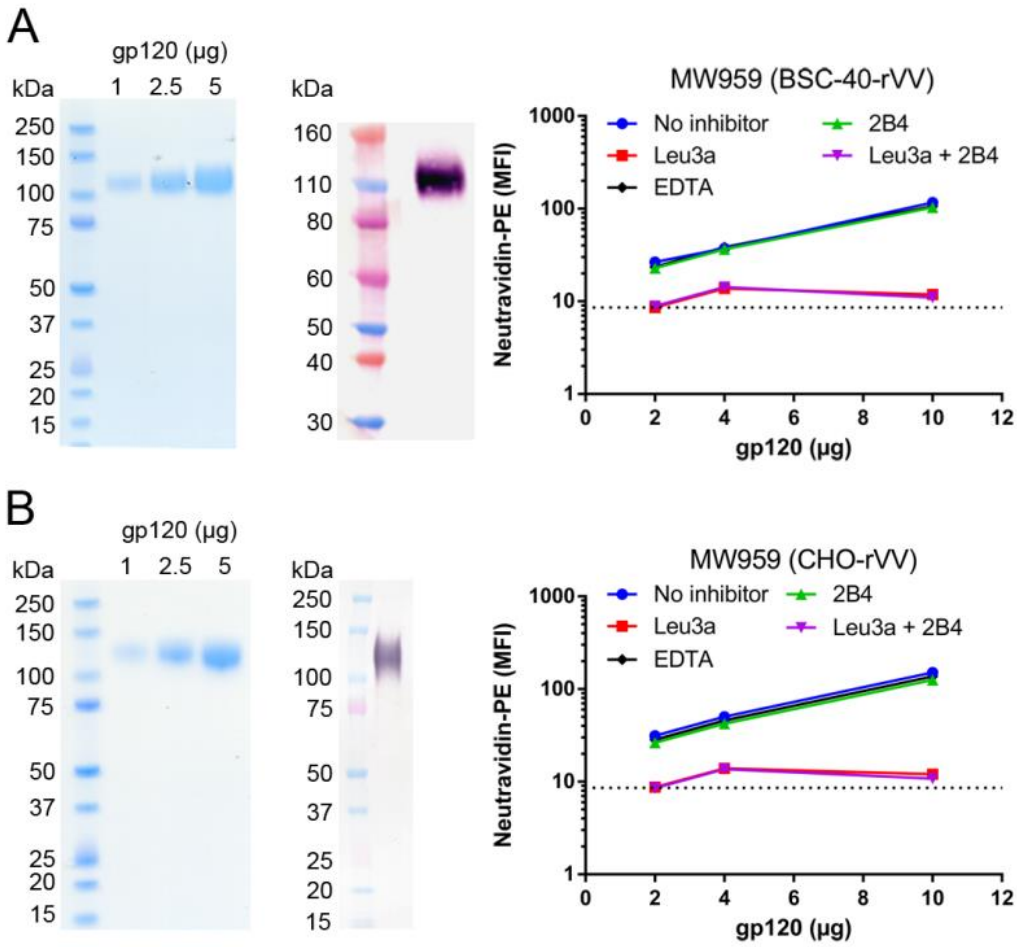

Figure 4-2. Analysis of MW959 gp120 produced by rVV infection. MW959 gp120 was produced by rVV infection of BSC-40 (A) and CHO (B). Purified gp120 was analyzed by SDS-PAGE with coomassie blue staining (left), and by western blot probed with pooled serum from HIV-infected patients (center). Protein was loaded at the indicated amounts for SDS-PAGE, and was loaded at 1µg/lane for western blot. Protein binding to $CD4^{+}\alpha_4\beta_7^{+}$ T cells was measured over a range of gp120 concentrations in the presence of the indicated inhibitors (right). The dotted line in cell binding graphs indicates background signal from cells stained without gp120.

Removal of N-linked glycans in V2 enhances gp120 binding to CD4

Removal of N-linked glycans in the V2 loop of MW959 has been reported to increase gp120 binding to $\alpha_4\beta_7$[170]. These glycan modifications are hypothesized to increase binding by

exposing or stabilizing the putative $\alpha_4\beta_7$ binding site LDV/I within V2. Based on this, we tested whether removal of N-linked glycans would result in $\alpha_4\beta_7$ reactivity of MW959 gp120 produced by our rVV expression system. Two MW959 mutants were generated in which the glycans at amino acid residues 139 and 184 were removed (N139Q and N184Q, respectively). Previous reports indicated that the N139Q mutation increased $\alpha_4\beta_7$ binding approximately 2-fold, and the N184Q mutation increased binding 3.5-fold[170]. Glycan mutant gp120 proteins were produced by rVV infection of BSC-40 and purified as described above, and then gp120 binding was measured on $CD4^+\alpha_4\beta_7^+$ T cells (Figure 4-3). The overall binding of the N139Q mutant was 3.5 times higher than wild-type gp120, and binding of the N184Q mutant was 4.5 times higher. However, binding of all three proteins was fully inhibited by Leu3a and not significantly inhibited by 2B4 or EDTA. Thus, while we reproduced the observation that these glycan modifications increased gp120 binding, we concluded that this was due to enhanced CD4 reactivity and found no evidence for $\alpha_4\beta_7$ binding in these gp120 preparations.

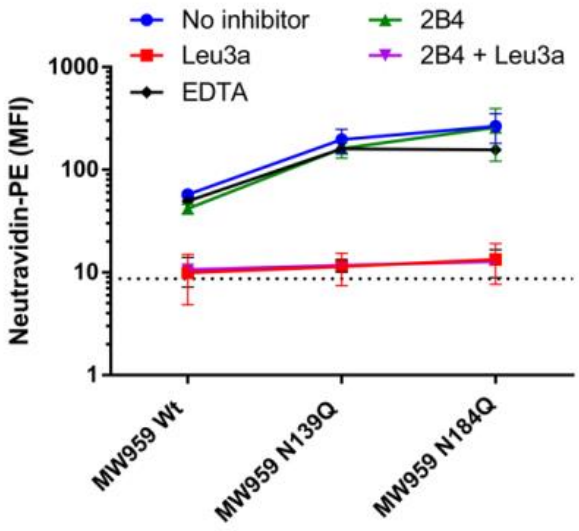

Figure 4-3. Cell binding of MW959 glycan mutants. Binding activity of wild-type MW959 and the glycan mutants N139Q and N184Q on $CD4^+\alpha_4\beta_7^+$ T cells. Results are means and standard deviations of triplicate measurements. The dotted line indicates background signal from cells stained without gp120.

gp120-$\alpha_4\beta_7$ binding is not affected by lectin affinity purification conditions.

In previous studies of gp120-$\alpha_4\beta_7$ binding, two methods have been used for eluting gp120 from *Galanthus nivalis* lectin affinity columns. In the first method, gp120 was eluted by competition with methyl-α-D-mannopyranoside (MMP) in a neutral pH buffer (20mM Tris-HCl, pH 7.5)[164]. In the second method, gp120 was eluted by MMP in a low pH buffer (20mM glycine, pH 2.5)[170, 269]. The rationale proposed for using low pH buffer was that a subpopulation of gp120 may bind tightly to the column and require harsher conditions to be eluted. Furthermore, this subpopulation of tight-binding gp120 was hypothesized to display glycans that enhanced $\alpha_4\beta_7$ reactivity. Based on this hypothesis, we tested whether the failure of rVV-expressed gp120 to bind $\alpha_4\beta_7$ could be attributed to lectin affinity purification conditions. A 1-liter supernatant of MW959 gp120 was produced by infecting BSC-40 cells with rVV, and then the supernatant was divided in half and purified with each of the methods described above. After elution from the lectin column, the remaining purification procedure was the same for each sample and included a DEAE purification step. The gp120 yield was approximately 3 times greater with the neutral pH method (neutral pH: 1.83mg, low pH: 0.62mg). The overall cell binding of gp120 produced by the neutral-pH method was approximately 10% greater than binding of material produced by the low-pH method. MW959 gp120 produced by both methods bound to CD4 but not to $\alpha_4\beta_7$ (Figure 4-4). It should be noted that the data in Figure 4-4 were acquired on a different cytometer than was used for other experiments, and because of this the binding and baseline values are approximately 10-fold higher than what is reported in other Figures. From these experiments, we found no evidence that lectin elution method affected the $\alpha_4\beta_7$ binding properties of gp120, and we additionally found that the neutral pH method resulted in better yields of gp120.

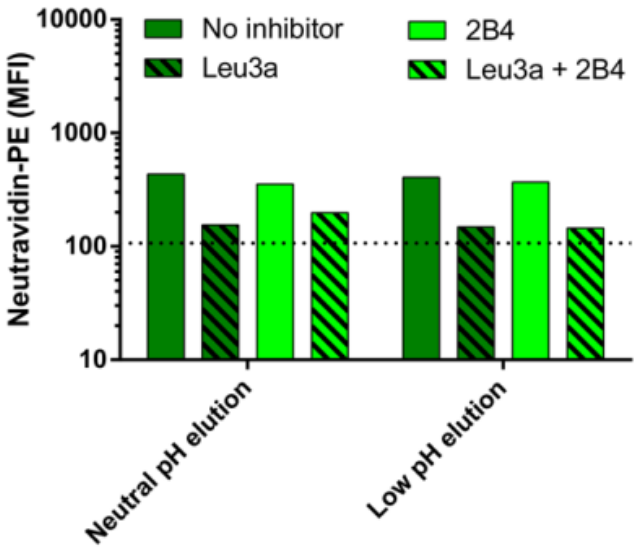

Figure 4-4. Comparison of lectin affinity elution methods. MW959 gp120 produced in rVV-infected BSC-40 cells was captured on a *Galanthus nivalis* lectin column and then eluted with neutral pH or low pH conditions. Cell binding of the resulting gp120 was measured on $CD4^+\alpha_4\beta_7^+$ T cells using a LSRII cytometer (Becton Dickinson). The dotted line indicates background signal from cells stained without gp120.

Kifunensine treatment does not enhance $\alpha_4\beta_7$-reactivity of gp120

A previous study by Nawaz et al. reported that AN1 gp120 (a synthetic ancestral clade B gp120) bound strongly to $\alpha_4\beta_7$ when it was expressed in CHO lec1 cells[170]. These cells are deficient in N-acetylglucosamine glycosyl transferase activity[270], and produce proteins with only minimally-processed oligomannose glycans. Thus, it was hypothesized that oligomannose glycans enhance the $\alpha_4\beta_7$ reactivity of HIV-1 envelope proteins. However, in the same study no significant $\alpha_4\beta_7$ binding was observed in AN1 gp120 produced in HEK293 cells treated with kifunensine, a mannosidase I inhibitor that restricts glycan processing and also produces proteins with oligomannose glycans[271]. Therefore, the role of oligomannose glycans in modulating $\alpha_4\beta_7$ reactivity is not clear, and needs to be examined further.

To address this, we produced MW959 gp120 with kifunensine in rVV-infected BSC-40 cells, in order to enrich gp120 with high-mannose glycan content. As an additional control we repeated the experiments described by Nawaz et al., and produced AN1 gp120 by transient transfection of HEK293 cells with and without kifunensine. Both MW959 and AN1 gp120 preparations were purified with a DEAE chromatography step. SDS-PAGE analysis indicated both gp120 preparations were purified to apparent homogeneity, and the apparent mass of kifunensine-treated gp120 was smaller than the mass of gp120 produced without kifunensine (Figure 4-5). Additionally, analysis of size exclusion chromatograms confirmed that the apparent molecular size of kifunensine-treated material was smaller than untreated material. The smaller size of kifunensine-treated gp120 provided indirect confirmation that the kifunensine treatment was likely effective in restricting glycan processing. In cell binding assays, the overall binding of MW959 gp120 produced with kifunensine was approximately 3 times higher than gp120 produced without kifunensine. However, binding of both preparations was completely inhibited by Leu3a and not affected by 2B4 (Figure 4-5A). Cell binding of AN1 gp120 produced with kifunensine was approximately 15% higher than gp120 produced without kifunensine. Similar to MW959, both AN1 gp120 preparations were fully inhibited by Leu3a and not inhibited by 2B4 (Figure 4-5B). In total, kifunensine treatment in our experiments produced gp120 that likely displayed oligomannose glycans, but this was not associated with any measurable $\alpha_4\beta_7$ binding.

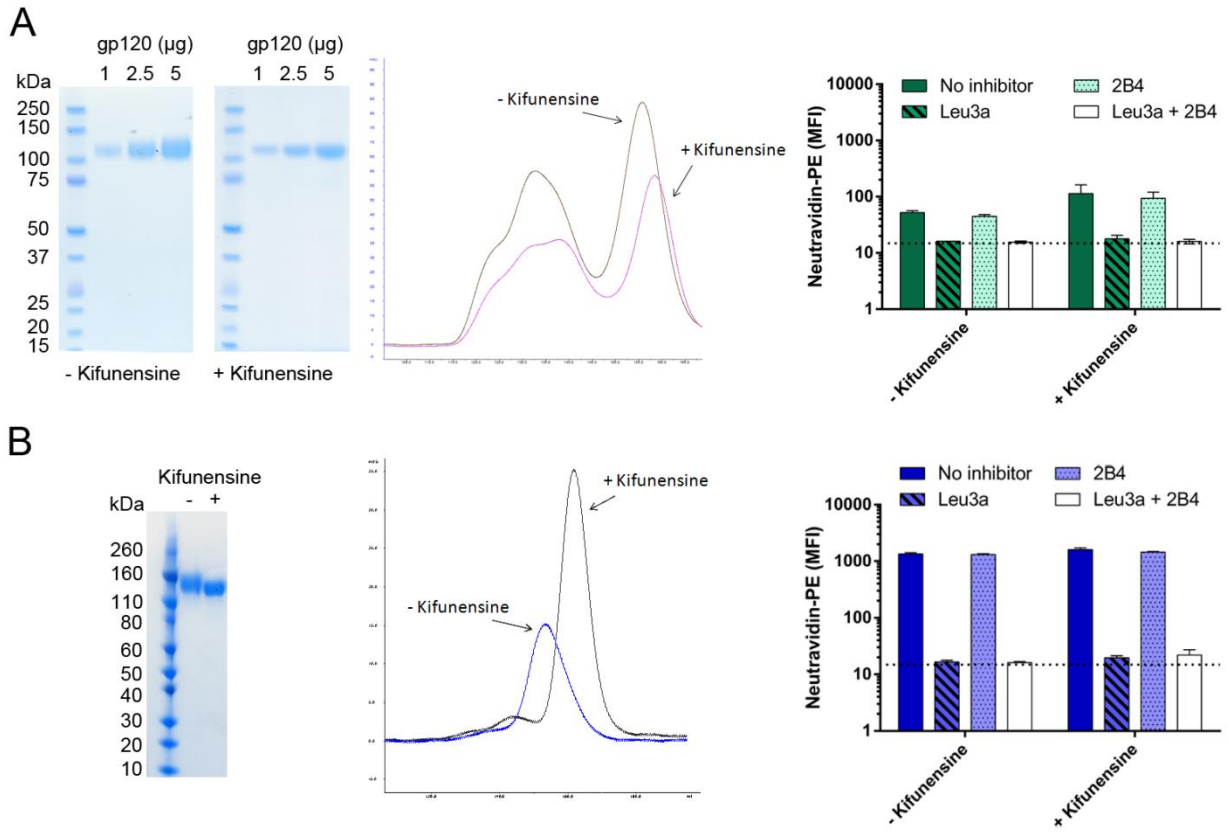

Figure 4-5. The effect of kifunensine treatment on gp120 binding. (A) MW959 gp120 produced in rVV-infected BSC-40; (B) AN1 gp120 produced by transfection of HEK293 cells. Purified proteins were analyzed by SDS-PAGE (left) and size exclusion chromatography (center). MW959 gp120 was analyzed on two separate gels; the gel showing gp120 without kifunensine treatment is the same as pictured in Figure 4-2A. Binding activity of the resulting preparations was measured on $CD4^{+}\alpha_4\beta_7^{+}$ T cells (right). Cell binding measurements are means and standard deviations of duplicate measurements. The dotted lines in cell binding graphs indicate background signal from cells stained without gp120.

Cellular proteins mediate $\alpha_4\beta_7$ binding of rVV-expressed gp120

We next extended our observations with the MW959 gp120 isolate, and measured the CD4 and $\alpha_4\beta_7$ binding properties of 7 additional gp120 proteins produced by rVV infection of BSC-40. Additionally, in our previous work we reported that $\alpha_4\beta_7$–reactive cellular proteins produced by CHO mediated indirect gp120-$\alpha_4\beta_7$ binding. Based on this, we tested whether $\alpha_4\beta_7$–

reactive cellular proteins also mediated binding of rVV-expressed gp120. We originally intended to test whether BSC-40 cells produced $\alpha_4\beta_7$–reactive cellular proteins. However, our BSC-40 expression system uses cell culture medium containing fetal bovine serum, and we were unable to purify BSC-40 cellular proteins without significant serum contamination. Therefore, we performed these experiments with CHO cellular proteins, which we have extensively characterized[221].

All 8 gp120 proteins tested displayed the same binding behavior on $CD4^+\alpha_4\beta_7^+$ T cells (Figure 4-6). While different levels of binding were observed, Leu3a fully inhibited the binding of all proteins. When gp120 was incubated with $\alpha_4\beta_7$–reactive CHO proteins for 2 hours, Leu3a did not fully inhibit binding while a combination of Leu3a and 2B4 did. In total, the rVV-produced gp120 proteins we tested did not bind to $\alpha_4\beta_7$ by themselves, but did bind to $\alpha_4\beta_7$ indirectly through interactions mediated by CHO cellular proteins.

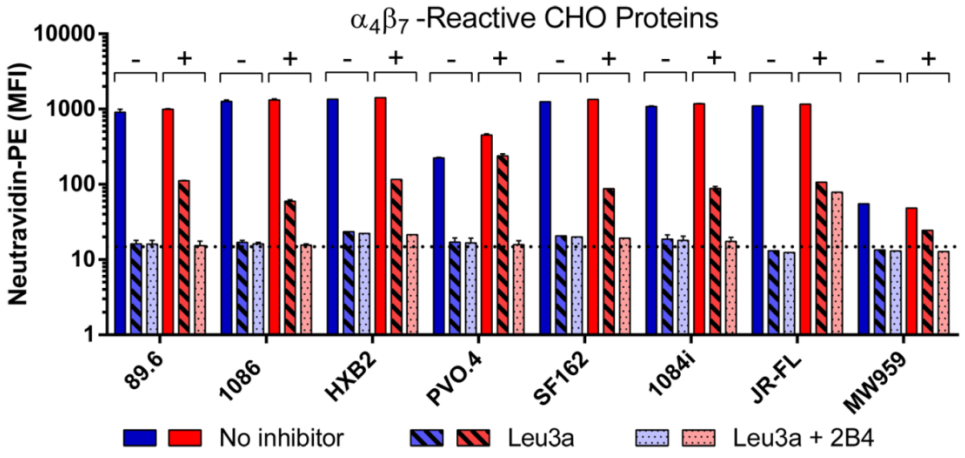

Figure 4-6. Cellular proteins mediate $\alpha_4\beta_7$ binding of rVV-expressed gp120. Binding of 8 different gp120 isolates to $CD4^+\alpha_4\beta_7^+$ T cells. All gp120 proteins were produced in rVV infected BSC-40. Binding was tested without cellular proteins (blue) or with 2hr pre-incubation with $\alpha_4\beta_7$–reactive CHO cellular proteins (red), in the presence of the indicated inhibitors. The dotted line indicates background signal from cells stained without gp120.

RetroNectin mediates $\alpha_4\beta_7$ binding of rVV-expressed JR-FL gp120

In our previous work, we found that the extracellular matrix protein CS1 fibronectin was responsible for mediating indirect gp120-$\alpha_4\beta_7$ binding[221]. Based on this, we tested whether CS1 fibronectins also mediated indirect $\alpha_4\beta_7$ binding of rVV-expressed gp120. For this experiment we used the recombinant CS1 fibronectin fragment RetroNectin (TaKaRa), which contains binding sites for $\alpha_4\beta_7$ and $\alpha_5\beta_1$ integrins as well as a heparin binding site that interacts with Env[136, 213]. JR-FL gp120 produced in rVV infected BSC-40 was incubated for 2 hours with varying concentrations of RetroNectin, and then tested in a cell binding assay with the $\alpha_4\beta_7$–expressing cell line RPMI8866. RetroNectin increased gp120 binding in a concentration-dependent manner, and this was inhibited by competition with 2B4 (Figure 4-7). A small portion of RetroNectin-mediated binding could not be inhibited by 2B4. We speculated that this may be due to RetroNectin-gp120 complexes binding to $\alpha_5\beta_1$ integrin, however we did not test this. Similar to our previous observations, this experiment demonstrated that interactions between $\alpha_4\beta_7$ and rVV-expressed gp120 were mediated by CS1 fibronectins.

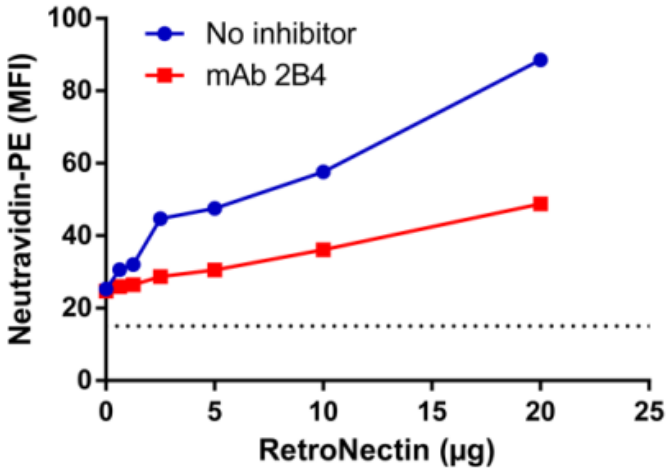

Figure 4-7. RetroNectin mediates JR-FL gp120 binding to $\alpha_4\beta_7$. JR-FL gp120 produced by rVV was incubated for 2hr with varying concentrations of RetroNectin, and tested for cell binding activity on the $\alpha_4\beta_7$ expressing cell line RPMI8866. The dotted line indicates background signal from cells stained without gp120.

Analysis of gp120 glycans by capillary electrophoresis

The glycosylation pattern of Env varies depending on producer cell type[272], and glycosylation patterns have also been proposed to modulate $\alpha_4\beta_7$ reactivity[170, 265]. Based on this, we analyzed the glycosylation pattern of gp120 produced in rVV-infected BSC-40 cells, to gain insight into the nature of N-linked glycans on gp120 and their relationship to $\alpha_4\beta_7$ reactivity. For this analysis we used the SF162 isolate, and compared glycosylation patterns of gp120 produced by rVV infection of BSC-40 to glycosylation patterns of gp120 produced by transient transfection of either CHO or HEK293. N-linked glycans were released from gp120 with PNGase F, fluorescently labeled with APTS, and analyzed by capillary electrophoresis (CE). Large qualitative differences were observed between these three samples (Figure 4-8). rVV-produced gp120 displayed the highest proportion of high-mannose glycans, while CHO-

produced gp120 displayed a high proportion of complex glycans. The complex glycan content of HEK293-produced gp120 was in between that of rVV and CHO-produced material. While these experiments were only conducted with the SF162 isolate, it is reasonable to assume that gp120 from other isolates produced by rVV infection of BSC-40 may also predominately display oligomannose glycans. In the present study we found no evidence for $\alpha_4\beta_7$ reactivity of rVV-produced gp120, and in our previous work we found no evidence for $\alpha_4\beta_7$ reactivity of gp120 produced by CHO or HEK293[221]. Therefore, based on our data we are unable to substantiate the observation that $\alpha_4\beta_7$ binding correlates with high mannose glycoforms, or that any particular glycosylation pattern modulates $\alpha_4\beta_7$ reactivity of gp120.

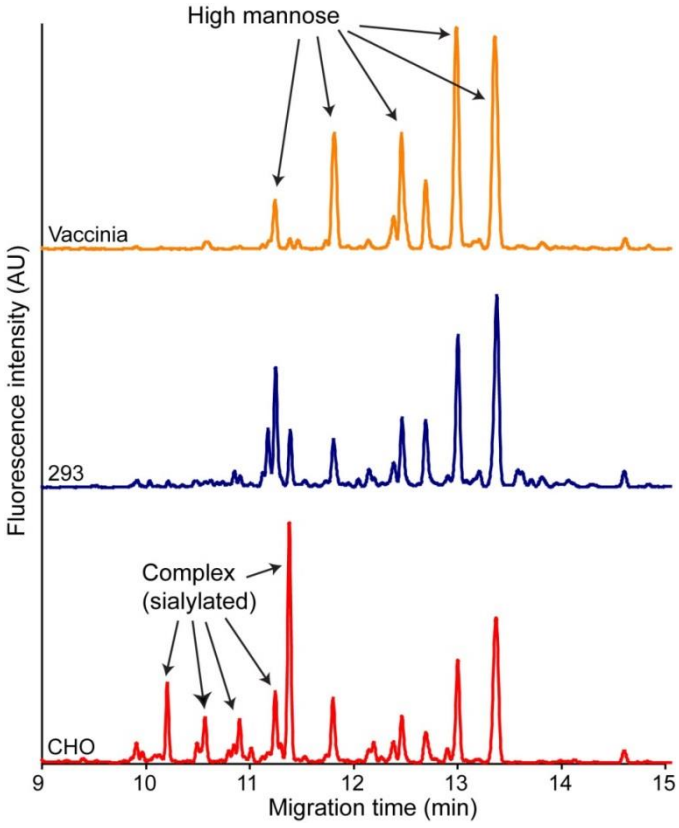

Figure 4-8. Comparison of N-linked glycans on recombinant gp120 from three expression systems. N-linked glycans were analyzed by CE from SF162 gp120 produced by rVV infection of BSC-40 (top), or transient transfection of HEK293 (middle) and CHO (bottom). Major peaks corresponding to either high-mannose or complex glycans are indicated.

Discussion

In this study we examined the CD4 and $\alpha_4\beta_7$ binding properties of gp120 produced by African green monkey or Chinese hamster ovary cells infected with rVV *in vitro*. These proteins were purified to apparent homogeneity using a method that included DEAE anion exchange chromatography. We showed that gp120 produced and purified by this method primarily displayed oligomannose glycans and bound strongly to CD4, but showed no detectable $\alpha_4\beta_7$ reactivity. We additionally tested factors proposed to modulate $\alpha_4\beta_7$ reactivity, including removal of N-linked glycans in V2, modification of oligomannose glycan content with kifunensine, and different lectin affinity purification methods; however none of these factors produced gp120 that bound to $\alpha_4\beta_7$. Finally, we demonstrated that $\alpha_4\beta_7$–reactive cellular proteins mediated indirect gp120-$\alpha_4\beta_7$ binding in a panel of rVV-expressed gp120 proteins. These findings from these studies support the conclusion that poxvirus-expressed gp120 does not bind to $\alpha_4\beta_7$ through the V2 loop.

Recombinant poxviruses have been used for decades as HIV vaccine immunogens. Following the successful use of vaccinia viruses to eradicate smallpox, the concept of using recombinant vaccinia viruses to immunize against other diseases was proposed. In the early 1980's, a method was established for incorporating foreign genes into the thymidine kinase (TK) locus of vaccinia viruses through homologous recombination[273], and this was later adapted to generate rVV expressing HIV transgenes[274, 275]. These rVV were shown in Phase I clinical trials to elicit transient cellular responses[276], and later were demonstrated to elicit robust integrated cellular and humoral responses when used in a prime-boost regimen with purified Env protein[277, 278]. The canarypox vector ALVAC, which is unable to replicate in mammalian cells, was similarly modified to express HIV-1 transgenes and also successfully elicited cellular

and humoral responses to HIV-1 in a prime-boost regimen[279]. Based on the safety and antigenicity of prime-boost immunization with ALVAC-HIV in Phase I and II trials[280], this regimen was later tested in the RV144 Phase III trial[179]. While ALVAC and rVV are different poxvirus vectors, they have been shown in head-to-head comparisons to elicit similar immune responses[281, 282], and they performed similarly in preclinical and Phase I trials. Therefore, insights into the antigenic and structural properties of rVV-expressed Env proteins are likely applicable to Env derived from other poxvirus systems including ALVAC, and are relevant to understanding the immune responses observed in RV144.

It would be exceedingly challenging to characterize the structural properties of Env produced *in vivo* by vaccination with recombinant poxviruses, and to our knowledge no studies of this kind have been performed. However, Env produced by rVV infection *in vitro* is a reasonable surrogate for understanding the properties of poxvirus-generated Env proteins *in vivo*. In this study, we identified three important structural features of poxvirus-expressed Env. First, we demonstrated that rVV-expressed gp120 presented an intact CD4 binding site, and was therefore likely to be properly folded. We showed here that rVV-expressed gp120 bound to cell-surface CD4, and in previous studies our group showed that rVV-expressed gp120 bound to soluble CD4 and to CD4 binding site-directed antibodies[109, 266]. Second, we demonstrated that rVV-expressed gp120 primarily displayed oligomannose glycans, in contrast to CHO and HEK293-expressed gp120 which displayed more hybrid and complex glycans. Native Env on the surface of HIV-1 viruses has been reported to primarily display oligomannose glycans[105, 106]. Additionally, several neutralizing antibodies including PG9 and PG16[110], 2G12[111], and PGT128[283] recognize epitopes that include oligomannose glycans. For these reasons, the oligomannose glycan content of rVV-expressed Env may be desirable, and provide an advantage

for poxvirus-based immunization platforms and protein expression systems. Third, we demonstrate that rVV-expressed gp120 does not engage $\alpha_4\beta_7$ directly through the V2 loop. We did not perform detailed structural analyses of V1V2 epitopes presented by poxvirus-expressed Env, and are unable to say which V1V2 conformations may have been present in the proteins studied. However, we found no evidence of $\alpha_4\beta_7$ reactivity in rVV-expressed gp120, and observed no correlation between oligomannose glycan content and $\alpha_4\beta_7$ reactivity. In agreement with our previous studies using gp120 expressed in CHO and HEK293 cells, we found that $\alpha_4\beta_7$-reactive cellular proteins and RetroNectin mediated indirect binding between $\alpha_4\beta_7$ and poxvirus-expressed gp120. These findings support the hypothesis that gp120 does not bind to $\alpha_4\beta_7$ directly through the V2 loop, but indirect gp120-$\alpha_4\beta_7$ binding mediated by fibronectin is a property shared by diverse Env proteins with different glycosylation profiles.

In total, poxvirus-expressed gp120 produced and purified by the methods described in this study is highly pure, primarily displays oligomannose glycans, and binds well to CD4 but does not bind to $\alpha_4\beta_7$. These studies provide additional evidence supporting the hypothesis that gp120 does not bind to $\alpha_4\beta_7$ through the V2 loop, and suggests that protection in the RV144 trial was not likely to have been mediated by V1V2 antibodies that inhibited HIV interactions with $\alpha_4\beta_7$.

Materials and Methods

Reagents and cell lines

Fluorescent antibodies to CD4 (clone RPA-T4, conjugated to allophycocyanin) and β_7 integrin (clone FIB504, conjugated to phycoerythrin) were from Becton-Dickinson. CD4-

blocking antibody Leu3a (clone SK3) was from Becton-Dickinson. Integrin-blocking antibody 2B4 and the MAdCAM-1-Fc fusion protein were from R&D systems. RetroNectin was from TaKaRa. RPMI8866 cells were from Sigma-Aldrich and were grown in RPMI1640 medium supplemented with 10% fetal bovine serum and penicillin/streptomycin. BSC-40 cells were from the American Type Culture Collection (ATCC) and were grown in DMEM medium supplemented with 10% fetal bovine serum and penicillin/streptomycin. Freestyle CHO-S and Freestyle 293-F cells used to produce recombinant proteins were from ThermoFisher Scientific and were cultured in serum-free and antibiotic-free media according to the manufacturer's instructions in spinner cultures maintained at 37°C and 8% CO_2. $\alpha_4\beta_7$–reactive cellular proteins from CHO were prepared as previously described[221].

Construction of recombinant vaccinia viruses

The GenBank accession numbers for HIV *env* genes used in this study were as follows: MW959 (U08453.1); 89.6 (AF038398); 1086c (KC894079); HXB2 (K03455); PVO.4 (AAW64259); SF162 (P19550); 1084i (AAV80387); JR-FL (U63632). HIV-1 *env* genes were cloned into an expression vector under the control of an early/late vaccinia virus promoter, and flanked by sequences from the vaccinia virus TK gene as previously described[284]. In some constructs the gp160 gene was used and modified by introducing a stop codon at the gp120-gp41 cleavage site. Recombinant vaccinia viruses were generated by transfecting BSC-40 cells with these constructs and infecting cells with vaccinia virus (New York City Board of Health strain). Recombinant vaccinia viruses were propagated and purified as previously described[285].

In vitro expression of recombinant gp120

Confluent monolayers of BSC-40 cells were infected with rVV at a multiplicity of infection (MOI) of 3. 48hr after infection, cell supernatants were harvested and clarified by centrifugation. For gp120 expression by rVV in CHO cells, $1.0x10^9$ cells were incubated for 2hr in 100mL of inoculum containing both Env-expressing rVV and the cowpox host range protein-expressing virus vT7CP[268], each at a MOI of 3. The culture was then diluted to 1L and cultured for 48hr prior to collection. Empigen BB (Sigma-Aldrich) was added to all rVV-containing supernatants to a final concentration of 0.25%. AN1 gp120 was expressed by transient transfection of HEK293 cells as previously described[221], and culture supernatants were collected 72hr after transfection. In the indicated samples, 20μM kifunensine (Sigma-Aldrich) was added immediately after infection with rVV or transfection with plasmid DNA.

Purification of gp120

Purification was carried out using an ÄKTA 10/100 purifier (GE Life Sciences) as previously described[221, 266]. Briefly, supernatants were loaded at 1mL/min onto columns of *Galanthus nivalis*-conjugated agarose in tris-buffered saline containing 0.25% Empigen BB. After washing, gp120 was eluted with tris-buffered saline containing 1M MMP. In the indicated experiment, gp120 was alternatively eluted with 500mM MMP in glycine, pH 2.5, into collection tubes containing 1M Tris-HCl, pH 8.0. Peak fractions were pooled and dialyzed extensively against low-salt Tris-buffered saline (100mM NaCl), and then passed through a DEAE sepharose column (GE Healthcare). The DEAE flowthrough material was concentrated and purified by size exclusion chromatography on a 320mL HighLoad 26/600 Superdex 200 column (GE Life

Sciences) with phosphate-buffered saline. Centrifugal concentrators (Millipore EMD) were used to concentrate monomeric gp120, and protein quantity was assayed with a bicinchoninic acid assay (Pierce).

Protein gels and western blot

Purified gp120 proteins were reduced and denatured, and then separated by SDS-PAGE as previously described, using either the Novex prestained sharp (ThermoFisher) or PrecisionPlus Dual Color (Bio-Rad) molecular mass standards[221, 266]. Coomassie blue staining was performed with SimplyBlue Coomassie G-250 (ThermoFisher) according to the manufacturer's instructions. For western blot, proteins were transferred to polyvinylidene difluoride (PVDF) membranes. Membranes were blocked with 5% nonfat milk, incubated overnight with pooled plasma from 131 Zambian women infected with Clade C HIV-1 (a gift from Charles Wood) diluted 1:2,000, and then incubated for 1hr in alkaline phosphatase-conjugated goat anti-human IgG (Sigma-Aldrich) diluted 1:10,000 as previously described[221]. Alkaline phosphatase detection was carried out with BCIP (5-bromo-4-chloro-3-indolylphosphate)-nitroblue tetrazolium (NBT) substrate (Sigma-Aldrich).

gp120 glycan release, derivatization, and analysis by capillary electrophoresis

N-linked glycans were released from purified gp120 monomers with PNGase F, fluorescently labeled with 9-Aminopyrene-1,4,6-trisulfonic acid (APTS), and analyzed by capillary electrophoresis (CE) as previously described[286]. Briefly, 20µg of gp120 was

incubated overnight with DTT and PNGase F (Prozyme) at 37°C. Released glycans were passed through 10 kDa molecular weight cut-off spin filters (Sigma-Aldrich), and then dried in a vacuum concentrator. Dried glycans were labeled with APTS overnight at 37°C, and then separated from unreacted dye by washing with acetonitrile on normal phase microcolumns (PhyNexus, San Jose, CA, USA). A P/ACE MDQ automated capillary electrophoresis instrument (Beckman Coulter) equipped with an Argon-ion laser fluorescent detector (excitation: 488nm, emission: 520nm) was used to analyze APTS-labeled glycans. 50cm effective length N-CHO coated 50μm inner diameter capillary columns (Beckman Coulter) were used for all analyses, filled with N-CHO Carbohydrate Separation Gel Buffer (Beckman Coulter). 500 V/cm was applied in reversed polarity mode (cathode at the injection side and the anode at the detection side). Samples were pressure injected by 1 psi (6.89 kPa) for 5 sec. The Karat 32 version 7.0 software package (Beckman Coulter) was used for data acquisition and analysis. An APTS-Dextran ladder was also sampled and used to calculate glucose unit (GU) for each of the major peaks. Glycans were identified based on GUs in Glycobase version 3.0 (NIBRT, Dublin, Ireland)[287].

Primary human $CD4^+\alpha_4\beta_7^+$ T cells

PBMCs were obtained by back-flushing used leukocyte filters purchased from BloodWorks Northwest (Seattle, Washington, USA). $CD4^+$ T cells were purified from PBMCs using a negative selection kit (Miltenyi Biotec). $CD4^+$ T cells were then activated in anti-CD3 antibody OKT3 (Biolegend) for 2 days, and cultured continuously in 20U/mL interleukin-2

(Roche) and 10nM all-trans retinoic acid (Sigma-Aldrich). Cells were used for binding studies after 9 or more days of culture.

Cell binding assay

Protein biotinylation and cell binding were all performed as previously described[221]. Briefly, proteins used for cell binding assays were biotinylated with the EZ-Link N-hydroxysuccinimide (NHS) biotin reagent (Pierce). RPMI8866 cells or primary $CD4^{+}\alpha_4\beta_7^{+}$ cells were washed in buffer and aliquots of $2.0x10^5$ cells were used for staining. Buffer was either HEPES-buffered saline containing manganese, or HEPES-buffered saline containing EDTA. Cells were pre-incubated for 10min with 2µg of Leu3a or 2B4 as indicated, and then incubated for 20min with either 4µg of biotinylated gp120 or 100ng of biotinylated MAdCAM-1-Fc. In some experiments, 4µg aliquots of gp120 were pre-incubated for 2hr with 4µg of $\alpha_4\beta_7$–reactive CHO cellular proteins or the indicated amounts of RetroNectin prior to cell binding. Cells were washed twice and then stained for 20min in 2.5µg/mL neutravidin conjugated to Phycoerythrin (ThermoFisher). Cells were washed twice more, and then fixed in 1% formalin and analyzed by flow cytometry. In most experiments, analysis was performed with a BD FACSCalibur instrument using CellQuest Pro software (Becton Dickinson; version 6.0). In the indicated experiment, analysis was performed with a BD LSRII instrument using FACSDIVA software (Becton Dickinson; version 8.0.1).

Acknowledgements

We thank members of the Virology Core of the Washington National Primate Research Center for producing rVV-infected supernatants for gp120 purification. We thank Yun Li for producing the HXB2 rVV, Lifei Yang for producing the 89.6 and 1086c rVV, and Samantha Townsley for producing the PVO.4 and JR-FL rVV. We thank Bernard Moss for generously providing the vT7CP virus used in this work. We additionally thank Hannah Kalinowski for her assistance with rVV infection of CHO cells. CE data for SF162 glycans was generously provided by Csaba Váradi and András Guttman.

This work was supported by the Bill and Melinda Gates Foundation Collaboration for AIDS Vaccine Discovery OPP1033102 and National Institutes of Health grant P51 OD010425. DP was supported by a Pharmaceutical Sciences Training Grant from the National Institute of General Medical Sciences, National Institutes of Health. The funders had no role in study design, data collection and analysis, decision to publish, or preparation of the manuscript.

Chapter 5

Summary and General Conclusions

Summary of key findings

In 2008 Arthos et al. published the seminal work which described gp120-$\alpha_4\beta_7$ binding mediated by the LDV/I motif in the V2 loop of Envelope protein[164]. Throughout the following decade, the potential role of Envelope-$\alpha_4\beta_7$ interaction in HIV transmission, pathogenesis, treatment, and prevention developed into a major research theme. Over 100 papers have cited gp120-$\alpha_4\beta_7$ binding as a mechanism mediating preferential infection of $\alpha_4\beta_7^+$ T cells, and the primary focus of 68 papers has been on some aspect of the HIV-$\alpha_4\beta_7$ interaction. An analysis and summary of these 68 papers is presented in Table 5-1 and Figure 5-1 below.

Table 5-1. Summary of the HIV-$\alpha_4\beta_7$ Literature from 2008 to 2018.

Primary Focus of Study	Literature Reference	Number of Papers
Biochemistry of gp120-$\alpha_4\beta_7$ Binding	[164, 168-170, 172, 221, 288]	7
Virion Interactions with $\alpha_4\beta_7$ *in vitro*	[134, 159, 173, 176, 195-197, 225, 265, 269, 289, 290]	12
Frequency of the LDV/I Motif and its Role in Pathogenesis	[167, 175, 291-293]	5
LDV/I Structure, V2 Antibodies, and Vaccine Applications	[184-186, 294-299]	9
Antiviral Activity of $\alpha_4\beta_7$ Antagonists	[188-191, 198, 199, 300, 301]	8
$\alpha_4\beta_7^+$ Cells in HIV/SIV Pathogenesis *in vivo*	[156-158, 160, 161, 163, 171, 194, 302-309]	16
Reviews and Methodology Papers	[264, 310-319]	11

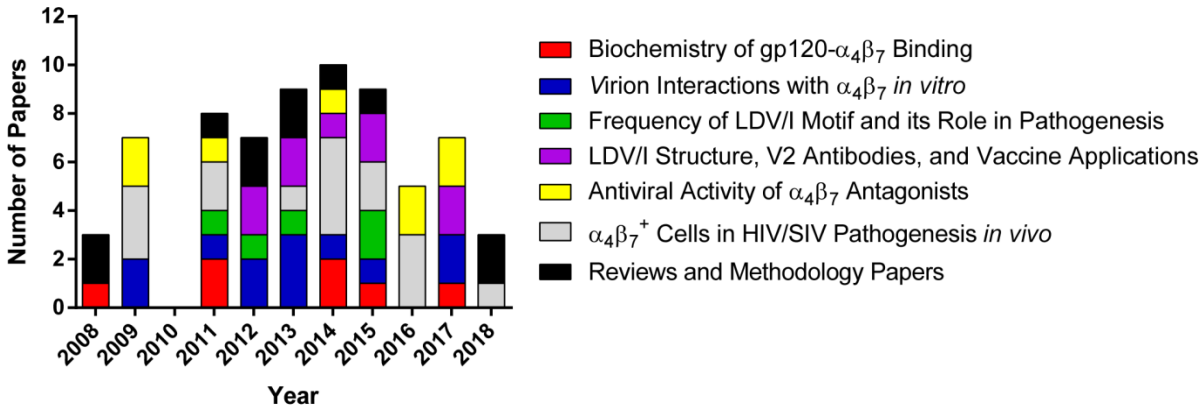

Figure 5-1. Analysis of the HIV-$\alpha_4\beta_7$ Literature from 2008 to 2018.

The work presented in this dissertation challenges the prevailing model of gp120-$\alpha_4\beta_7$ binding mediated by the V2 loop, and fundamentally changes the interpretation of existing HIV-$\alpha_4\beta_7$ literature. I presented discoveries that demonstrated CS1 fibronectin is a critical mediator of gp120-$\alpha_4\beta_7$ binding, and that purified gp120 does not bind to $\alpha_4\beta_7$ by itself. First, I showed that the mammalian cell lines used to produce recombinant gp120 also produced $\alpha_4\beta_7$–reactive cellular proteins. Second, I showed that these cellular proteins co-purified with gp120 but could be removed by DEAE anion exchange chromatography, and that DEAE-purified gp120 did not bind to $\alpha_4\beta_7$. Third, I discovered that cellular proteins not only bound to $\alpha_4\beta_7$, but also complexed with gp120 and mediated indirect gp120-$\alpha_4\beta_7$ binding. Fourth, through mutagenesis and antibody inhibition experiments I showed that the V2 loop was not required for this mode of gp120-$\alpha_4\beta_7$ interaction. Fifth, I identified CS1 fibronectin as the protein responsible for mediating gp120-$\alpha_4\beta_7$ interaction through mass spectrometry and other biochemical experiments. Collectively, these findings changed the current understanding of the biochemical basis for gp120-$\alpha_4\beta_7$ interaction, and identified CS1 fibronectin as a key player in this interaction.

Based on the potential biological significance of this finding, I then investigated the role that CS1 fibronectins may play in HIV-1 infection. Through *in vitro* experiments, I provided proof-of-concept that immobilized CS1 fibronectins bound to HIV virions and co-localized them with $\alpha_4\beta_7^+$ T cells, and thus mediated preferential infection of $\alpha_4\beta_7^+$ T cells. I additionally showed that CS1 fibronectins contributed to virus replication and spread by facilitating cell-to-cell virus transmission and cellular activation. These findings provided a novel mechanistic explanation for the preferential infection of $\alpha_4\beta_7^+$ T cells, and identified CS1 fibronectins in the extracellular matrix as potentially important mediators of virus replication and immune activation *in vivo*.

Implications for HIV transmission and pathogenesis

Based on the work presented in this dissertation, I propose a new model describing the role of CS1 fibronectins in facilitating HIV-1 infection of $\alpha_4\beta_7^+$ T cells *in vivo* (Figure 5-2). This model is composed of three parts which are linked together in a positive feedback cycle. First, CS1 fibronectins in the extracellular matrix bind to HIV virions and co-localize them preferentially to $\alpha_4\beta_7^+$ T cells. HIV binding to fibronectin is mediated either by envelope protein interactions with the fibronectin heparin binding domain or through virus-associated α_4–integrins (Figure 3-3), while cell binding is primarily mediated by $\alpha_4\beta_7$ binding to CS1[210]. Second, following this initial infection event, additional $\alpha_4\beta_7^+$ T cells bind to the extracellular matrix via CS1 fibronectins and develop into a focus of infection. CS1 fibronectins co-localize T cells, which facilitates efficient cell-to-cell virus transmission (Figure 3-7). Cell-to-cell transmission results in rapid virus propagation and may also contribute to T cell killing through

pyroptosis[85]. Additionally, cell-to-cell transmission promotes resistance to neutralizing antibodies, and thus contributes to immune evasion (Figure 3-6). Importantly, cell binding to fibronectin also activates T cells via integrin-mediated signaling (Figure 3-8). This may contribute to the activation, infection, and killing of quiescent T cell subsets such as central memory T cells, and thus degrade the regenerative capacity of the immune system. Third, CS1 fibronectin synthesis is induced at foci of infection. This occurs through the release of TGFβ-1 by HIV-infected cells which activates fibronectin synthesis in fibroblasts[252] and biases splicing to favor CS1 isoforms[250]. Finally, the increased expression of CS1 fibronectin in the extracellular matrix captures additional viruses and cells, and perpetuates the cycle.

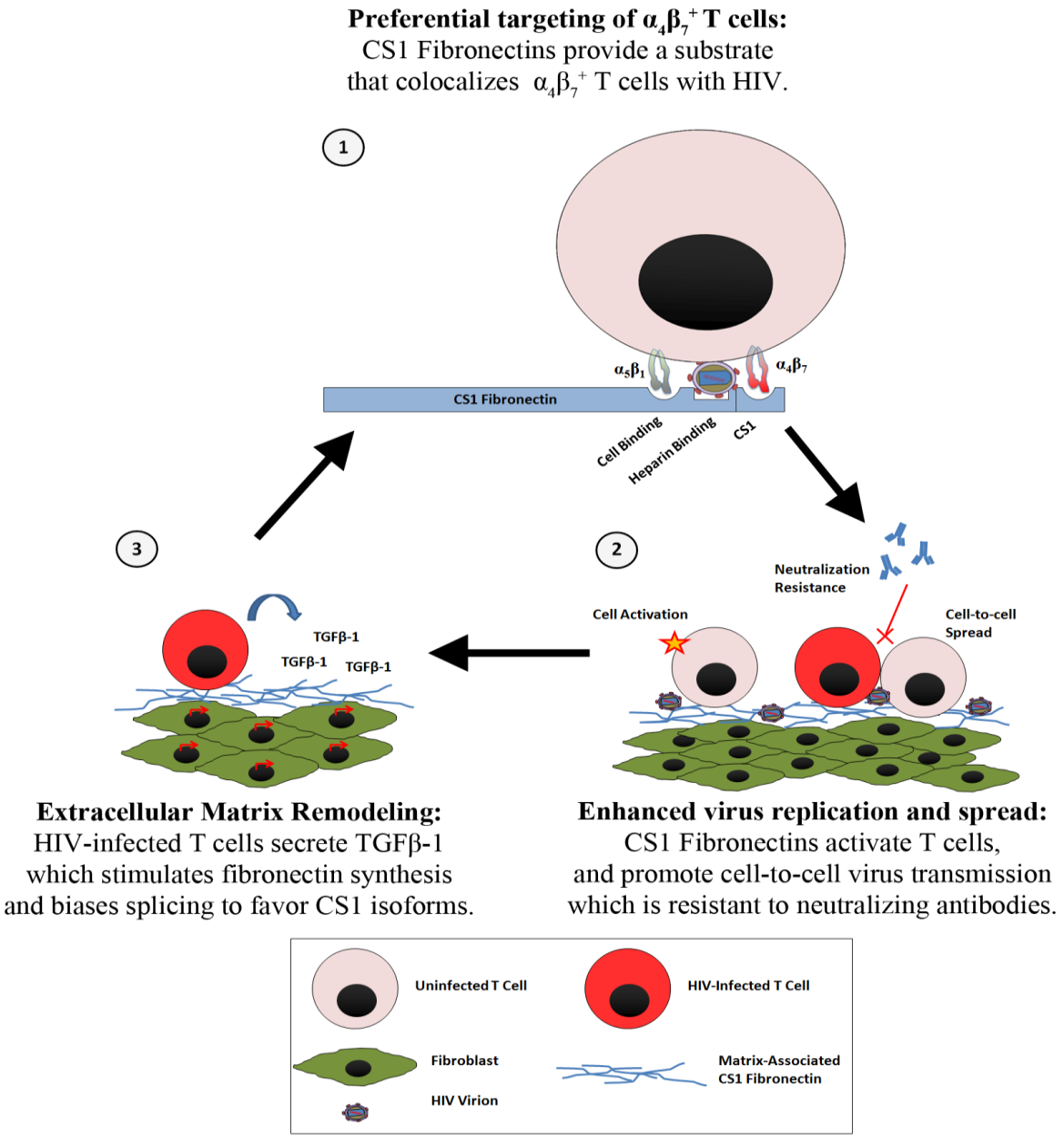

Figure 5-2. Proposed Model of CS1 Fibronectin-Mediated HIV Infection of $\alpha_4\beta_7^+$ T Cells.

These events may play important roles during mucosal HIV transmission. $\alpha_4\beta_7^+$ T cells have been hypothesized to promote HIV dissemination to GALT through becoming infected in the periphery and then migrating to the intestines. In support of this, it has been shown that higher frequencies of $\alpha_4\beta_7^+$ T cells in genital tissues correlates with increased risk of HIV

transmission[160, 161]. It is possible $\alpha_4\beta_7^+$ T cells become infected at mucosal sites by chance, or it is possible that they are specifically targeted. During the first several days following transmission, viruses are contained within portals of entry and replicate slowly in localized foci of infection[32]. It is possible that CS1 fibronectin expression is induced within these foci, which then recruits circulating $\alpha_4\beta_7^+$ T cells and mediates their infection. After becoming infected, these $\alpha_4\beta_7^+$ T cells may then migrate to the intestines and disseminate the virus to GALT.

Once HIV reaches the GALT, it replicates rapidly and destroys the majority of intestinal $CD4^+$ T cells. In contrast to peripheral $CD4^+$ T cells, intestinal T cells are severely exhausted and unable to replenish even with antiretroviral treatment[89]. The mechanisms described above may partially account for the high rate of virus replication, cytotoxicity, and degradation of T cell regenerative capacity at mucosal sites. During the acute infection fibronectin-mediated cell-to-cell spread between $\alpha_4\beta_7^+$ T cells in GALT may underpin both robust virus replication and high levels of cell killing through pyroptosis. CS1 fibronectin expression in GALT may be induced during acute infection and then persist into the chronic phase, contributing to persistent cell activation, viral immune evasion, and virus replication. These combined effects could play important roles in the activation-mediated killing of central memory T cells, and the loss of T cell regenerative capacity.

Implications for HIV vaccine design

Based on the potential role of $\alpha_4\beta_7^+$ T cells in promoting HIV transmission, the HIV-$\alpha_4\beta_7$ interaction has been proposed as a vaccine target. Specifically, it has been proposed that antibodies targeting the LDV/I motif in the V2 loop may disrupt gp120-$\alpha_4\beta_7$ engagement and thus inhibit the infection of $\alpha_4\beta_7^+$ T cells in mucosal sites[264]. This hypothesis relies on four lines of evidence. First are the original studies which demonstrated gp120-$\alpha_4\beta_7$ binding, and subsequent studies which showed that T/F envelopes display increased $\alpha_4\beta_7$ reactivity through structural modifications to the V2 loop[164, 170]. Second are studies which demonstrated that the LDV/I signature in viral envelopes is correlated with transmission fitness[167, 175, 291-293]. Third is the immune correlates analysis of the RV144 trial, which indicated that non-neutralizing V2 antibodies are correlated with protection from HIV acquisition[181]. Fourth are a group of studies which showed that certain V2 antibodies isolated from RV144 vaccinees bind at or near the LDV/I site in the V2 loop[294, 295]. Out of these factors, the immune correlates analysis from RV144 may have played the most significant role in generating interest in this vaccine concept; following the publication of this work in 2012, the role of the LDV/I motif in transmission and the potential protective effect of LDV/I-directed antibodies became recurring themes in the literature (Figure 5-1, green and purple symbols).

In this dissertation, I showed that highly-purified HIV envelope proteins do not bind to $\alpha_4\beta_7$, and that all instances of gp120-$\alpha_4\beta_7$ binding reported in the literature may be attributed to the effects of co-purified CS1 fibronectins. I additionally showed that the V2 loop does not participate in gp120 interactions with fibronectin and that V2-directed antibodies do not inhibit gp120-$\alpha_4\beta_7$ interaction mediated by CS1 fibronectin (Figures 2-5 and 2-8). Based on these findings, there is currently no definitive evidence that the V2 loop participates in HIV-$\alpha_4\beta_7$

contact, either through direct gp120-$\alpha_4\beta_7$ binding or through binding mediated by CS1 fibronectins. It should be noted that several studies have demonstrated that V2 peptides can bind to $\alpha_4\beta_7$, and these results are not in doubt because such peptides are chemically-defined[168, 169]. However, until it is demonstrated that rigorously-purified gp120 binds to $\alpha_4\beta_7$, the significance of these peptide studies remains uncertain. Overall, the results presented in this dissertation show that V2 antibodies are unlikely to inhibit HIV-$\alpha_4\beta_7$ interactions, and highlight the need for further studies to account for the potential protective role of V2-specific antibodies.

Implications for $\alpha_4\beta_7$ antagonists in HIV therapy

The antiviral effects of $\alpha_4\beta_7$–directed monoclonal antibodies have been studied extensively, and show strikingly different effects *in vitro* versus *in vivo*. Both the $\alpha_4\beta_7$–specific antibody Act-1 (Vedolizumab) and the $\alpha_4\beta_7/\alpha_4\beta_1$-binding antibody Natalizumab failed to inhibit HIV infection of $CD4^+\alpha_4\beta_7^+$ T cells *in vitro*[173, 198]. In contrast, Act-1 mediated significant therapeutic effects *in vivo* in studies of SIV-infected rhesus macaques. In two studies, Act-1 monotherapy decreased plasma and gastrointestinal viral loads and was associated with higher $CD4^+$ cell numbers[188, 189]. In a separate study Act-1 combined with cART was shown to be associated with apparent reconstitution of the immune system, including regeneration of mucosal $CD4^+$ T cells, decreased systemic inflammation, and drug-free virological suppression[191]. At present, the hypothesis of direct gp120-$\alpha_4\beta_7$ binding is unable to account for these contradictory effects of $\alpha_4\beta_7$ inhibition.

The studies presented in this dissertation provide a basis for reconciling these findings, and identify a potential mechanism for the therapeutic effects of Act-1 *in vivo*. I showed that in

the context of infection mediated by CS1 fibronectins *in vitro*, $\alpha_4\beta_7$ –blocking antibodies significantly attenuated infection (Figure 3-4). These antibodies blocked both cell and virus adhesion to CS1 fibronectin, and thus inhibited infection and cell-to-cell transmission (Figure 3-7). These mechanisms may play a similar role *in vivo* and break up foci of infection within GALT. By doing so this could break the cycle outlined in Figure 5-2, leading to decreases in TGFβ-1 and downregulation of CS1 fibronectins. These effects may then contribute to the resolution of intestinal inflammation, and decrease activation-mediated T cell killing. Such effects would not be present in 'classical' *in vitro* infection assays, which measures cell infection by free viruses.

In my studies, I found that the $\alpha_4\beta_7/\alpha_4\beta_1$ –blocking antibody 2B4 more potently inhibited HIV binding to CS1 fibronectin than Act-1 (Figure 3-3). 2B4 also inhibited fibronectin-mediated infection to a greater degree than Act-1 (Figures 3-4 and 3-7). These findings indicate that T cells likely bind to the CS1 domain through both of these integrins, and suggest that 2B4 or Natalizumab may have greater potency than Act-1 *in vivo*. However, one drawback of Natalizumab is that it inhibits $\alpha_4\beta_1$–mediated T cell homing, and this has been associated with an increased risk of progressive multifocal leukoencephalopathy[320]. Because progressive multifocal leukoencephalopathy is also a complication of HIV disease, Natalizumab treatment may be contraindicated in HIV patients. Further studies are indicated to assess the potential risks and benefits of treating HIV with Natalizumab versus Vedolizumab.

Potential use of heparins and TGFβ-1 antagonists in HIV therapy

The model of infection resulting from this dissertation not only clarifies the potential role of $\alpha_4\beta_7$ antagonists in HIV therapy, but also raises the possibility that heparins and TGFβ-1 receptor antagonists may provide therapeutic benefit. Both of these agents may inhibit the infection cycle illustrated in Figure 5-2 in different ways; heparins by blocking HIV binding to fibronectin, and TGFβ-1 antagonists by inhibiting CS1 fibronectin expression.

In this dissertation I showed that HIV binding to fibronectin was inhibited by heparin sulfate, and that Act-1 and heparin worked synergistically to potently inhibit virus binding (Figure 3-3). I additionally showed that a combination of heparin and Act-1 attenuated HIV infection more potently than Act-1 alone (Figure 3-4). Notably, the concentration of heparin used in these studies was approximately 180 U/liter, which is slightly less than the concentration used clinically for anticoagulation therapy. Unfractionated heparin itself is probably not well-suited for use in HIV therapy because of the risk of bleeding complications. However, it has been demonstrated by others that low molecular-weight heparins including Enoxaparin inhibit HIV replication *in vitro* and can be safely administered to patients long-term without such risks[321]. Based on these results, *in vivo* studies of therapeutic effects of Act-1/Enoxaparin combinations are indicated.

Several small molecule TGFβ-1 receptor antagonists have been discovered, and investigated for use in cancer and fibrotic diseases[322-324], and therapeutic anti-TGFβ monoclonal antibodies including Fresolimumab have also been developed[325]. Any of these agents may be used to inhibit TGFβ-1 signaling in HIV infection, and thereby decrease HIV-mediated fibrosis. TGFβ-1 is also known to mediate a variety of non-fibrotic

immunosuppressive effects in HIV infection[326], and TGFβ-1 inhibitors may provide additional benefit by blocking these pathways. In total, the model of infection presented in this dissertation predicts that TGFβ-1 antagonists would provide therapeutic benefit, and suggests that these agents should be studied further *in vivo*.

General conclusions

Through this dissertation I have made several significant contributions to the field of HIV research. First, I clarified the nature of the biochemical interaction between HIV envelope protein and the $\alpha_4\beta_7$ receptor. Prior to my work this was the subject of controversy, and the precise determinants of gp120-$\alpha_4\beta_7$ binding were not clear. I provided a clear and evidence-based rationale for resolving this controversy. I simultaneously demonstrated that gp120 does not bind to $\alpha_4\beta_7$, and described a novel mechanism for gp120-$\alpha_4\beta_7$ interaction mediated by CS1 fibronectins. Second, I developed a new model describing the role of CS1 fibronectins in HIV-1 infection. This model explains how $\alpha_4\beta_7^+$ T cells may be preferentially infected by HIV, and identifies a previously unknown role for CS1 fibronectins in facilitating virus replication and immune activation. This model additionally provides a basis for understanding the therapeutic activity of $\alpha_4\beta_7$ antagonists in HIV disease, and identifies additional therapeutic targets which are worthy of future investigation. Based on this work, future studies are indicated to investigate the role of CS1 fibronectins in infection *in vivo*, and to assess the potential clinical value of using TGFβ-1 antagonists and heparins in combination with $\alpha_4\beta_7$ antagonists and cART.

References

1. Hymes KB, Cheung T, Greene JB, Prose NS, Marcus A, Ballard H, et al. Kaposi's sarcoma in homosexual men-a report of eight cases. Lancet (London, England). 1981;2(8247):598-600. Epub 1981/09/19. PubMed PMID: 6116083.
2. Kaposi's sarcoma and Pneumocystis pneumonia among homosexual men--New York City and California. MMWR Morbidity and mortality weekly report. 1981;30(25):305-8. Epub 1981/07/03. PubMed PMID: 6789108.
3. https://www.aids.gov/hiv-aids-basics/hiv-aids-101/aids-timeline/.
4. Barre-Sinoussi F, Chermann JC, Rey F, Nugeyre MT, Chamaret S, Gruest J, et al. Isolation of a T-lymphotropic retrovirus from a patient at risk for acquired immune deficiency syndrome (AIDS). Science. 1983;220(4599):868-71. Epub 1983/05/20. PubMed PMID: 6189183.
5. Gallo RC, Sarin PS, Gelmann EP, Robert-Guroff M, Richardson E, Kalyanaraman VS, et al. Isolation of human T-cell leukemia virus in acquired immune deficiency syndrome (AIDS). Science. 1983;220(4599):865-7. Epub 1983/05/20. PubMed PMID: 6601823.
6. Marx JL. Strong new candidate for AIDS agent. Science. 1984;224(4648):475-7. Epub 1984/05/04. PubMed PMID: 6324344.
7. Faria NR, Rambaut A, Suchard MA, Baele G, Bedford T, Ward MJ, et al. HIV epidemiology. The early spread and epidemic ignition of HIV-1 in human populations. Science. 2014;346(6205):56-61. Epub 2014/10/04. doi: 10.1126/science.1256739. PubMed PMID: 25278604; PubMed Central PMCID: PMCPMC4254776.
8. Hemelaar J. The origin and diversity of the HIV-1 pandemic. Trends in molecular medicine. 2012;18(3):182-92. Epub 2012/01/14. doi: 10.1016/j.molmed.2011.12.001. PubMed PMID: 22240486.
9. Thomson MM, Perez-Alvarez L, Najera R. Molecular epidemiology of HIV-1 genetic forms and its significance for vaccine development and therapy. The Lancet Infectious diseases. 2002;2(8):461-71. Epub 2002/08/02. PubMed PMID: 12150845.
10. Gao F, Bailes E, Robertson DL, Chen Y, Rodenburg CM, Michael SF, et al. Origin of HIV-1 in the chimpanzee Pan troglodytes troglodytes. Nature. 1999;397(6718):436-41. Epub 1999/02/16. doi: 10.1038/17130. PubMed PMID: 9989410.
11. D'Arc M, Ayouba A, Esteban A, Learn GH, Boue V, Liegeois F, et al. Origin of the HIV-1 group O epidemic in western lowland gorillas. Proc Natl Acad Sci U S A. 2015;112(11):E1343-52. Epub 2015/03/04. doi: 10.1073/pnas.1502022112. PubMed PMID: 25733890; PubMed Central PMCID: PMCPMC4371950.
12. Vallari A, Holzmayer V, Harris B, Yamaguchi J, Ngansop C, Makamche F, et al. Confirmation of putative HIV-1 group P in Cameroon. J Virol. 2011;85(3):1403-7. Epub 2010/11/19. doi: 10.1128/jvi.02005-10. PubMed PMID: 21084486; PubMed Central PMCID: PMCPMC3020498.
13. Marx PA, Li Y, Lerche NW, Sutjipto S, Gettie A, Yee JA, et al. Isolation of a simian immunodeficiency virus related to human immunodeficiency virus type 2 from a west African pet sooty mangabey. J Virol. 1991;65(8):4480-5. Epub 1991/08/01. PubMed PMID: 1840620; PubMed Central PMCID: PMCPMC248889.
14. Jochelson K, Mothibeli M, Leger JP. Human immunodeficiency virus and migrant labor in South Africa. International journal of health services : planning, administration, evaluation. 1991;21(1):157-73. Epub 1991/01/01. doi: 10.2190/11ue-l88j-46hn-hr0k. PubMed PMID: 2004869.

15. Garry RF, Witte MH, Gottlieb AA, Elvin-Lewis M, Gottlieb MS, Witte CL, et al. Documentation of an AIDS virus infection in the United States in 1968. Jama. 1988;260(14):2085-7. Epub 1988/10/14. PubMed PMID: 3418874.

16. Hemelaar J, Gouws E, Ghys PD, Osmanov S. Global and regional distribution of HIV-1 genetic subtypes and recombinants in 2004. Aids. 2006;20(16):W13-23. Epub 2006/10/21. doi: 10.1097/01.aids.0000247564.73009.bc. PubMed PMID: 17053344.

17. Shen C, Craigo J, Ding M, Chen Y, Gupta P. Origin and Dynamics of HIV-1 Subtype C Infection in India. PLoS ONE. 2011;6(10):e25956. doi: 10.1371/journal.pone.0025956. PubMed PMID: PMC3189977.

18. Wilkinson E, Engelbrecht S, de Oliveira T. History and origin of the HIV-1 subtype C epidemic in South Africa and the greater southern African region. Scientific Reports. 2015;5:16897. doi: 10.1038/srep16897. PubMed PMID: PMC4648088.

19. Cabello M, Romero H, Bello G. Multiple introductions and onward transmission of non-pandemic HIV-1 subtype B strains in North America and Europe. Scientific Reports. 2016;6:33971. doi: 10.1038/srep33971. PubMed PMID: PMC5032033.

20. Hemelaar J, Gouws E, Ghys PD, Osmanov S. Global trends in molecular epidemiology of HIV-1 during 2000-2007. Aids. 2011;25(5):679-89. Epub 2011/02/08. doi: 10.1097/QAD.0b013e328342ff93. PubMed PMID: 21297424; PubMed Central PMCID: PMCPMC3755761.

21. Ye J, Xin R, Yu S, Bai L, Wang W, Wu T, et al. Phylogenetic and Temporal Dynamics of Human Immunodeficiency Virus Type 1 CRF01_AE in China. PLoS ONE. 2013;8(1):e54238. doi: 10.1371/journal.pone.0054238. PubMed PMID: PMC3554705.

22. http://www.unaids.org/en/resources/fact-sheet.

23. Hladik F, McElrath MJ. Setting the stage: host invasion by HIV. Nat Rev Immunol. 2008;8(6):447-57. Epub 2008/05/13. doi: 10.1038/nri2302. PubMed PMID: 18469831; PubMed Central PMCID: PMCPMC2587276.

24. Fox J, Fidler S. Sexual transmission of HIV-1. Antiviral research. 2010;85(1):276-85. Epub 2009/10/31. doi: 10.1016/j.antiviral.2009.10.012. PubMed PMID: 19874852.

25. Lehman DA, Farquhar C. Biological mechanisms of vertical human immunodeficiency virus (HIV-1) transmission. Reviews in medical virology. 2007;17(6):381-403. Epub 2007/06/02. doi: 10.1002/rmv.543. PubMed PMID: 17542053.

26. John-Stewart G, Mbori-Ngacha D, Ekpini R, Janoff EN, Nkengasong J, Read JS, et al. Breast-feeding and Transmission of HIV-1. Journal of acquired immune deficiency syndromes (1999). 2004;35(2):196-202. Epub 2004/01/15. PubMed PMID: 14722454; PubMed Central PMCID: PMCPmc3382106.

27. Des Jarlais DC, Kerr T, Carrieri P, Feelemyer J, Arasteh K. HIV infection among persons who inject drugs: ending old epidemics and addressing new outbreaks. Aids. 2016;30(6):815-26. Epub 2016/02/03. doi: 10.1097/qad.0000000000001039. PubMed PMID: 26836787; PubMed Central PMCID: PMCPMC4785082.

28. Galel SA, Lifson JD, Engleman EG. Prevention of AIDS transmission through screening of the blood supply. Annual review of immunology. 1995;13:201-27. Epub 1995/01/01. doi: 10.1146/annurev.iy.13.040195.001221. PubMed PMID: 7612221.

29. Keele BF, Giorgi EE, Salazar-Gonzalez JF, Decker JM, Pham KT, Salazar MG, et al. Identification and characterization of transmitted and early founder virus envelopes in primary HIV-1 infection. Proc Natl Acad Sci U S A. 2008;105(21):7552-7. Epub 2008/05/21. doi: 10.1073/pnas.0802203105. PubMed PMID: 18490657; PubMed Central PMCID: PMCPMC2387184.

30. Baggaley RF, White RG, Boily MC. HIV transmission risk through anal intercourse: systematic review, meta-analysis and implications for HIV prevention. Int J Epidemiol. 2010;39(4):1048-63. doi: 10.1093/ije/dyq057. PubMed PMID: 20406794; PubMed Central PMCID: PMCPMC2929353.

31. Boily M-C, Baggaley RF, Wang L, Masse B, White RG, Hayes R, et al. Heterosexual risk of HIV-1 infection per sexual act: a systematic review and meta-analysis of observational studies. The Lancet Infectious diseases. 2009;9(2):118-29. doi: 10.1016/S1473-3099(09)70021-0. PubMed PMID: PMC4467783.

32. Miller CJ, Li Q, Abel K, Kim EY, Ma ZM, Wietgrefe S, et al. Propagation and dissemination of infection after vaginal transmission of simian immunodeficiency virus. J Virol. 2005;79(14):9217-27. doi: 10.1128/JVI.79.14.9217-9227.2005. PubMed PMID: 15994816; PubMed Central PMCID: PMCPMC1168785.

33. Chohan B, Lang D, Sagar M, Korber B, Lavreys L, Richardson B, et al. Selection for human immunodeficiency virus type 1 envelope glycosylation variants with shorter V1-V2 loop sequences occurs during transmission of certain genetic subtypes and may impact viral RNA levels. J Virol. 2005;79(10):6528-31. Epub 2005/04/29. doi: 10.1128/jvi.79.10.6528-6531.2005. PubMed PMID: 15858037; PubMed Central PMCID: PMCPMC1091724.

34. Sagar M, Wu X, Lee S, Overbaugh J. Human immunodeficiency virus type 1 V1-V2 envelope loop sequences expand and add glycosylation sites over the course of infection, and these modifications affect antibody neutralization sensitivity. J Virol. 2006;80(19):9586-98. Epub 2006/09/16. doi: 10.1128/jvi.00141-06. PubMed PMID: 16973562; PubMed Central PMCID: PMCPMC1617272.

35. Derdeyn CA, Decker JM, Bibollet-Ruche F, Mokili JL, Muldoon M, Denham SA, et al. Envelope-constrained neutralization-sensitive HIV-1 after heterosexual transmission. Science. 2004;303(5666):2019-22. Epub 2004/03/27. doi: 10.1126/science.1093137. PubMed PMID: 15044802.

36. Parker ZF, Iyer SS, Wilen CB, Parrish NF, Chikere KC, Lee FH, et al. Transmitted/founder and chronic HIV-1 envelope proteins are distinguished by differential utilization of CCR5. J Virol. 2013;87(5):2401-11. Epub 2012/12/28. doi: 10.1128/jvi.02964-12. PubMed PMID: 23269796; PubMed Central PMCID: PMCPMC3571396.

37. Salazar-Gonzalez JF, Salazar MG, Keele BF, Learn GH, Giorgi EE, Li H, et al. Genetic identity, biological phenotype, and evolutionary pathways of transmitted/founder viruses in acute and early HIV-1 infection. J Exp Med. 2009;206(6):1273-89. Epub 2009/06/03. doi: 10.1084/jem.20090378. PubMed PMID: 19487424; PubMed Central PMCID: PMCPMC2715054.

38. Parrish NF, Gao F, Li H, Giorgi EE, Barbian HJ, Parrish EH, et al. Phenotypic properties of transmitted founder HIV-1. Proc Natl Acad Sci U S A. 2013;110(17):6626-33. Epub 2013/04/02. doi: 10.1073/pnas.1304288110. PubMed PMID: 23542380; PubMed Central PMCID: PMCPMC3637789.

39. McMichael AJ, Borrow P, Tomaras GD, Goonetilleke N, Haynes BF. The immune response during acute HIV-1 infection: clues for vaccine development. Nat Rev Immunol. 2010;10(1):11-23. doi: 10.1038/nri2674. PubMed PMID: 20010788; PubMed Central PMCID: PMCPMC3119211.

40. Eberl G, Lochner M. The development of intestinal lymphoid tissues at the interface of self and microbiota. Mucosal Immunol. 2009;2(6):478-85. Epub 2009/09/11. doi: 10.1038/mi.2009.114. PubMed PMID: 19741595.

41. Koboziev I, Karlsson F, Grisham MB. Gut-associated lymphoid tissue, T cell trafficking, and chronic intestinal inflammation. Annals of the New York Academy of Sciences. 2010;1207 Suppl 1:E86-93. Epub 2010/10/27. doi: 10.1111/j.1749-6632.2010.05711.x. PubMed PMID: 20961311; PubMed Central PMCID: PMCPMC3075575.

42. Reboldi A, Cyster JG. Peyer's patches: organizing B-cell responses at the intestinal frontier. Immunol Rev. 2016;271(1):230-45. Epub 2016/04/19. doi: 10.1111/imr.12400. PubMed PMID: 27088918; PubMed Central PMCID: PMCPMC4835804.
43. Brenchley JM, Douek DC. HIV infection and the gastrointestinal immune system. Mucosal Immunol. 2008;1(1):23-30. doi: 10.1038/mi.2007.1. PubMed PMID: 19079157; PubMed Central PMCID: PMCPMC2777614.
44. Guadalupe M, Reay E, Sankaran S, Prindiville T, Flamm J, McNeil A, et al. Severe CD4+ T-cell depletion in gut lymphoid tissue during primary human immunodeficiency virus type 1 infection and substantial delay in restoration following highly active antiretroviral therapy. J Virol. 2003;77(21):11708-17. Epub 2003/10/15. PubMed PMID: 14557656; PubMed Central PMCID: PMCPMC229357.
45. Marchetti G, Tincati C, Silvestri G. Microbial translocation in the pathogenesis of HIV infection and AIDS. Clinical microbiology reviews. 2013;26(1):2-18. Epub 2013/01/09. doi: 10.1128/cmr.00050-12. PubMed PMID: 23297256; PubMed Central PMCID: PMCPMC3553668.
46. Fiebig EW, Wright DJ, Rawal BD, Garrett PE, Schumacher RT, Peddada L, et al. Dynamics of HIV viremia and antibody seroconversion in plasma donors: implications for diagnosis and staging of primary HIV infection. AIDS. 2003;17(13):1871-9. doi: 10.1097/01.aids.0000076308.76477.b8. PubMed PMID: 12960819.
47. Grossman Z, Meier-Schellersheim M, Paul WE, Picker LJ. Pathogenesis of HIV infection: what the virus spares is as important as what it destroys. Nat Med. 2006;12(3):289-95. Epub 2006/03/08. doi: 10.1038/nm1380. PubMed PMID: 16520776.
48. Cohen MS, Shaw GM, McMichael AJ, Haynes BF. Acute HIV-1 Infection. N Engl J Med. 2011;364(20):1943-54. Epub 2011/05/20. doi: 10.1056/NEJMra1011874. PubMed PMID: 21591946; PubMed Central PMCID: PMCPMC3771113.
49. Weber J. The pathogenesis of HIV-1 infection. British medical bulletin. 2001;58:61-72. Epub 2001/11/21. PubMed PMID: 11714624.
50. Rodriguez B, Sethi AK, Cheruvu VK, Mackay W, Bosch RJ, Kitahata M, et al. Predictive value of plasma HIV RNA level on rate of CD4 T-cell decline in untreated HIV infection. Jama. 2006;296(12):1498-506. Epub 2006/09/28. doi: 10.1001/jama.296.12.1498. PubMed PMID: 17003398.
51. Paiardini M, Muller-Trutwin M. HIV-associated chronic immune activation. Immunol Rev. 2013;254(1):78-101. Epub 2013/06/19. doi: 10.1111/imr.12079. PubMed PMID: 23772616; PubMed Central PMCID: PMCPMC3729961.
52. Holmes CB, Losina E, Walensky RP, Yazdanpanah Y, Freedberg KA. Review of human immunodeficiency virus type 1-related opportunistic infections in sub-Saharan Africa. Clin Infect Dis. 2003;36(5):652-62. Epub 2003/02/21. doi: 10.1086/367655. PubMed PMID: 12594648.
53. Gupta S, Havens PL, Southern JF, Firat SY, Jogal SS. Epstein-Barr virus-associated intracranial leiomyosarcoma in an HIV-positive adolescent. Journal of pediatric hematology/oncology. 2010;32(4):e144-7. Epub 2010/03/13. doi: 10.1097/MPH.0b013e3181c80bf3. PubMed PMID: 20224440.
54. Ensoli B, Cafaro A. HIV-1 and Kaposi's sarcoma. European journal of cancer prevention : the official journal of the European Cancer Prevention Organisation (ECP). 1996;5(5):410-2. Epub 1996/10/01. PubMed PMID: 8972281.
55. Aboulafia DM, Mitsuyasu RT. Hematologic abnormalities in AIDS. Hematology/oncology clinics of North America. 1991;5(2):195-214. Epub 1991/04/01. PubMed PMID: 2022589.
56. Baker JV. Chronic HIV disease and activation of the coagulation system. Thrombosis research. 2013;132(5):495-9. Epub 2013/09/17. doi: 10.1016/j.thromres.2013.08.016. PubMed PMID: 24034985; PubMed Central PMCID: PMCPMC4197841.

57. Reiter GS. The HIV wasting syndrome. AIDS clinical care. 1996;8(11):89-91, 3, 6. Epub 1996/11/01. PubMed PMID: 11363990.
58. Bosinger SE, Sodora DL, Silvestri G. Generalized immune activation and innate immune responses in simian immunodeficiency virus infection. Curr Opin HIV AIDS. 2011;6(5):411-8. Epub 2011/07/12. doi: 10.1097/COH.0b013e3283499cf6. PubMed PMID: 21743324; PubMed Central PMCID: PMCPMC3261611.
59. Pandrea I, Apetrei C. Where the wild things are: pathogenesis of SIV infection in African nonhuman primate hosts. Current HIV/AIDS reports. 2010;7(1):28-36. Epub 2010/04/29. doi: 10.1007/s11904-009-0034-8. PubMed PMID: 20425055; PubMed Central PMCID: PMCPMC2824118.
60. Chahroudi A, Bosinger SE, Vanderford TH, Paiardini M, Silvestri G. Natural SIV hosts: showing AIDS the door. Science. 2012;335(6073):1188-93. Epub 2012/03/10. doi: 10.1126/science.1217550. PubMed PMID: 22403383; PubMed Central PMCID: PMCPMC3822437.
61. Veazey RS, DeMaria M, Chalifoux LV, Shvetz DE, Pauley DR, Knight HL, et al. Gastrointestinal tract as a major site of CD4+ T cell depletion and viral replication in SIV infection. Science. 1998;280(5362):427-31. Epub 1998/05/09. PubMed PMID: 9545219.
62. Mattapallil JJ, Douek DC, Hill B, Nishimura Y, Martin M, Roederer M. Massive infection and loss of memory CD4+ T cells in multiple tissues during acute SIV infection. Nature. 2005;434(7037):1093-7. Epub 2005/03/29. doi: 10.1038/nature03501. PubMed PMID: 15793563.
63. Li Q, Duan L, Estes JD, Ma ZM, Rourke T, Wang Y, et al. Peak SIV replication in resting memory CD4+ T cells depletes gut lamina propria CD4+ T cells. Nature. 2005;434(7037):1148-52. Epub 2005/03/29. doi: 10.1038/nature03513. PubMed PMID: 15793562.
64. Mehandru S, Dandekar S. Role of the gastrointestinal tract in establishing infection in primates and humans. Curr Opin HIV AIDS. 2008;3(1):22-7. Epub 2008/01/01. doi: 10.1097/COH.0b013e3282f331b0. PubMed PMID: 19372940.
65. Dalgleish AG, Beverley PC, Clapham PR, Crawford DH, Greaves MF, Weiss RA. The CD4 (T4) antigen is an essential component of the receptor for the AIDS retrovirus. Nature. 1984;312(5996):763-7. Epub 1984/12/20. PubMed PMID: 6096719.
66. Maddon PJ, Dalgleish AG, McDougal JS, Clapham PR, Weiss RA, Axel R. The T4 gene encodes the AIDS virus receptor and is expressed in the immune system and the brain. Cell. 1986;47(3):333-48. Epub 1986/11/07. PubMed PMID: 3094962.
67. Dragic T, Litwin V, Allaway GP, Martin SR, Huang Y, Nagashima KA, et al. HIV-1 entry into CD4+ cells is mediated by the chemokine receptor CC-CKR-5. Nature. 1996;381(6584):667-73. Epub 1996/06/20. doi: 10.1038/381667a0. PubMed PMID: 8649512.
68. Alkhatib G, Combadiere C, Broder CC, Feng Y, Kennedy PE, Murphy PM, et al. CC CKR5: a RANTES, MIP-1alpha, MIP-1beta receptor as a fusion cofactor for macrophage-tropic HIV-1. Science. 1996;272(5270):1955-8. Epub 1996/06/28. PubMed PMID: 8658171.
69. Choe H, Farzan M, Sun Y, Sullivan N, Rollins B, Ponath PD, et al. The beta-chemokine receptors CCR3 and CCR5 facilitate infection by primary HIV-1 isolates. Cell. 1996;85(7):1135-48. Epub 1996/06/28. PubMed PMID: 8674119.
70. Berson JF, Long D, Doranz BJ, Rucker J, Jirik FR, Doms RW. A seven-transmembrane domain receptor involved in fusion and entry of T-cell-tropic human immunodeficiency virus type 1 strains. J Virol. 1996;70(9):6288-95. Epub 1996/09/01. PubMed PMID: 8709256; PubMed Central PMCID: PMCPMC190654.
71. Roberts JD, Bebenek K, Kunkel TA. The accuracy of reverse transcriptase from HIV-1. Science. 1988;242(4882):1171-3. Epub 1988/11/25. PubMed PMID: 2460925.

72. Jayappa KD, Ao Z, Yao X. The HIV-1 passage from cytoplasm to nucleus: the process involving a complex exchange between the components of HIV-1 and cellular machinery to access nucleus and successful integration. International journal of biochemistry and molecular biology. 2012;3(1):70-85. Epub 2012/04/18. PubMed PMID: 22509482; PubMed Central PMCID: PMCPMC3325773.

73. Barre-Sinoussi F, Ross AL, Delfraissy JF. Past, present and future: 30 years of HIV research. Nature reviews Microbiology. 2013;11(12):877-83. Epub 2013/10/29. doi: 10.1038/nrmicro3132. PubMed PMID: 24162027.

74. Jolly C, Kashefi K, Hollinshead M, Sattentau QJ. HIV-1 cell to cell transfer across an Env-induced, actin-dependent synapse. J Exp Med. 2004;199(2):283-93. Epub 2004/01/22. doi: 10.1084/jem.20030648. PubMed PMID: 14734528; PubMed Central PMCID: PMCPMC2211771.

75. Piguet V, Sattentau Q. Dangerous liaisons at the virological synapse. J Clin Invest. 2004;114(5):605-10. Epub 2004/09/03. doi: 10.1172/jci22812. PubMed PMID: 15343375; PubMed Central PMCID: PMCPMC514595.

76. Monel B, Beaumont E, Vendrame D, Schwartz O, Brand D, Mammano F. HIV cell-to-cell transmission requires the production of infectious virus particles and does not proceed through env-mediated fusion pores. J Virol. 2012;86(7):3924-33. doi: 10.1128/JVI.06478-11. PubMed PMID: 22258237; PubMed Central PMCID: PMCPMC3302491.

77. Sattentau Q. Avoiding the void: cell-to-cell spread of human viruses. Nature reviews Microbiology. 2008;6(11):815-26. Epub 2008/10/17. doi: 10.1038/nrmicro1972. PubMed PMID: 18923409.

78. Sourisseau M, Sol-Foulon N, Porrot F, Blanchet F, Schwartz O. Inefficient human immunodeficiency virus replication in mobile lymphocytes. J Virol. 2007;81(2):1000-12. Epub 2006/11/03. doi: 10.1128/jvi.01629-06. PubMed PMID: 17079292; PubMed Central PMCID: PMCPMC1797449.

79. Mazurov D, Ilinskaya A, Heidecker G, Lloyd P, Derse D. Quantitative comparison of HTLV-1 and HIV-1 cell-to-cell infection with new replication dependent vectors. PLoS Pathog. 2010;6(2):e1000788. Epub 2010/03/03. doi: 10.1371/journal.ppat.1000788. PubMed PMID: 20195464; PubMed Central PMCID: PMCPMC2829072.

80. Chen P, Hubner W, Spinelli MA, Chen BK. Predominant mode of human immunodeficiency virus transfer between T cells is mediated by sustained Env-dependent neutralization-resistant virological synapses. J Virol. 2007;81(22):12582-95. Epub 2007/08/31. doi: 10.1128/jvi.00381-07. PubMed PMID: 17728240; PubMed Central PMCID: PMCPMC2169007.

81. Sigal A, Kim JT, Balazs AB, Dekel E, Mayo A, Milo R, et al. Cell-to-cell spread of HIV permits ongoing replication despite antiretroviral therapy. Nature. 2011;477(7362):95-8. doi: 10.1038/nature10347. PubMed PMID: 21849975.

82. Abela IA, Berlinger L, Schanz M, Reynell L, Gunthard HF, Rusert P, et al. Cell-cell transmission enables HIV-1 to evade inhibition by potent CD4bs directed antibodies. PLoS Pathog. 2012;8(4):e1002634. doi: 10.1371/journal.ppat.1002634. PubMed PMID: 22496655; PubMed Central PMCID: PMCPMC3320602.

83. Malbec M, Porrot F, Rua R, Horwitz J, Klein F, Halper-Stromberg A, et al. Broadly neutralizing antibodies that inhibit HIV-1 cell to cell transmission. J Exp Med. 2013;210(13):2813-21. doi: 10.1084/jem.20131244. PubMed PMID: 24277152; PubMed Central PMCID: PMCPMC3865481.

84. McCoy LE, Groppelli E, Blanchetot C, de Haard H, Verrips T, Rutten L, et al. Neutralisation of HIV-1 cell-cell spread by human and llama antibodies. Retrovirology. 2014;11:83. Epub 2015/02/24. doi: 10.1186/s12977-014-0083-y. PubMed PMID: 25700025; PubMed Central PMCID: PMCPMC4189184.

85. Galloway NL, Doitsh G, Monroe KM, Yang Z, Munoz-Arias I, Levy DN, et al. Cell-to-Cell Transmission of HIV-1 Is Required to Trigger Pyroptotic Death of Lymphoid-Tissue-Derived CD4 T Cells. Cell reports. 2015;12(10):1555-63. Epub 2015/09/01. doi: 10.1016/j.celrep.2015.08.011. PubMed PMID: 26321639; PubMed Central PMCID: PMCPMC4565731.

86. Lu W, Demers AJ, Ma F, Kang G, Yuan Z, Wan Y, et al. Next-Generation mRNA Sequencing Reveals Pyroptosis-Induced CD4+ T Cell Death in Early Simian Immunodeficiency Virus-Infected Lymphoid Tissues. J Virol. 2016;90(2):1080-7. Epub 2015/11/13. doi: 10.1128/jvi.02297-15. PubMed PMID: 26559826; PubMed Central PMCID: PMCPMC4702687.

87. Doitsh G, Galloway NL, Geng X, Yang Z, Monroe KM, Zepeda O, et al. Cell death by pyroptosis drives CD4 T-cell depletion in HIV-1 infection. Nature. 2014;505(7484):509-14. Epub 2013/12/21. doi: 10.1038/nature12940. PubMed PMID: 24356306; PubMed Central PMCID: PMCPMC4047036.

88. Chun TW, Fauci AS. HIV reservoirs: pathogenesis and obstacles to viral eradication and cure. Aids. 2012;26(10):1261-8. Epub 2012/04/05. doi: 10.1097/QAD.0b013e328353f3f1. PubMed PMID: 22472858.

89. Mehandru S, Poles MA, Tenner-Racz K, Jean-Pierre P, Manuelli V, Lopez P, et al. Lack of mucosal immune reconstitution during prolonged treatment of acute and early HIV-1 infection. PLoS medicine. 2006;3(12):e484. Epub 2006/12/07. doi: 10.1371/journal.pmed.0030484. PubMed PMID: 17147468; PubMed Central PMCID: PMCPMC1762085.

90. Cihlar T, Fordyce M. Current status and prospects of HIV treatment. Current opinion in virology. 2016;18:50-6. Epub 2016/03/30. doi: 10.1016/j.coviro.2016.03.004. PubMed PMID: 27023283.

91. Gallo R, Wong-Staal F, Montagnier L, Haseltine WA, Yoshida M. HIV/HTLV gene nomenclature. Nature. 1988;333(6173):504. Epub 1988/06/09. doi: 10.1038/333504a0. PubMed PMID: 2836736.

92. Fernandes J, Jayaraman B, Frankel A. The HIV-1 Rev response element: an RNA scaffold that directs the cooperative assembly of a homo-oligomeric ribonucleoprotein complex. RNA biology. 2012;9(1):6-11. Epub 2012/01/20. doi: 10.4161/rna.9.1.18178. PubMed PMID: 22258145; PubMed Central PMCID: PMCPMC3342944.

93. Jacks T, Power MD, Masiarz FR, Luciw PA, Barr PJ, Varmus HE. Characterization of ribosomal frameshifting in HIV-1 gag-pol expression. Nature. 1988;331(6153):280-3. Epub 1988/01/21. doi: 10.1038/331280a0. PubMed PMID: 2447506.

94. Garcia JV, Miller AD. Downregulation of cell surface CD4 by nef. Research in virology. 1992;143(1):52-5. Epub 1992/01/01. PubMed PMID: 1565858.

95. Heinzinger NK, Bukrinsky MI, Haggerty SA, Ragland AM, Kewalramani V, Lee MA, et al. The Vpr protein of human immunodeficiency virus type 1 influences nuclear localization of viral nucleic acids in nondividing host cells. Proc Natl Acad Sci U S A. 1994;91(15):7311-5. Epub 1994/07/19. PubMed PMID: 8041786; PubMed Central PMCID: PMCPMC44389.

96. Strebel K. HIV accessory proteins versus host restriction factors. Current opinion in virology. 2013;3(6):692-9. Epub 2013/11/20. doi: 10.1016/j.coviro.2013.08.004. PubMed PMID: 24246762; PubMed Central PMCID: PMCPMC3855913.

97. Laguette N, Rahm N, Sobhian B, Chable-Bessia C, Munch J, Snoeck J, et al. Evolutionary and functional analyses of the interaction between the myeloid restriction factor SAMHD1 and the lentiviral Vpx protein. Cell Host Microbe. 2012;11(2):205-17. Epub 2012/02/07. doi: 10.1016/j.chom.2012.01.007. PubMed PMID: 22305291; PubMed Central PMCID: PMCPMC3595996.

98. http://hivinsite.ucsf.edu/InSite?page=kb-02-01-02.

99. McCune JM, Rabin LB, Feinberg MB, Lieberman M, Kosek JC, Reyes GR, et al. Endoproteolytic cleavage of gp160 is required for the activation of human immunodeficiency virus. Cell. 1988;53(1):55-67. Epub 1988/04/08. PubMed PMID: 2450679.

100. Freed EO, Myers DJ, Risser R. Mutational analysis of the cleavage sequence of the human immunodeficiency virus type 1 envelope glycoprotein precursor gp160. J Virol. 1989;63(11):4670-5. Epub 1989/11/01. PubMed PMID: 2677400; PubMed Central PMCID: PMCPMC251101.

101. Capon DJ, Ward RH. The CD4-gp120 interaction and AIDS pathogenesis. Annual review of immunology. 1991;9:649-78. Epub 1991/01/01. doi: 10.1146/annurev.iy.09.040191.003245. PubMed PMID: 1910691.

102. Breitling J, Aebi M. N-linked protein glycosylation in the endoplasmic reticulum. Cold Spring Harbor perspectives in biology. 2013;5(8):a013359. Epub 2013/06/12. doi: 10.1101/cshperspect.a013359. PubMed PMID: 23751184; PubMed Central PMCID: PMCPMC3721281.

103. Behrens AJ, Crispin M. Structural principles controlling HIV envelope glycosylation. Curr Opin Struct Biol. 2017;44:125-33. Epub 2017/04/01. doi: 10.1016/j.sbi.2017.03.008. PubMed PMID: 28363124; PubMed Central PMCID: PMCPMC5513759.

104. Stanley P. Golgi glycosylation. Cold Spring Harbor perspectives in biology. 2011;3(4). Epub 2011/03/29. doi: 10.1101/cshperspect.a005199. PubMed PMID: 21441588; PubMed Central PMCID: PMCPMC3062213.

105. Doores KJ, Bonomelli C, Harvey DJ, Vasiljevic S, Dwek RA, Burton DR, et al. Envelope glycans of immunodeficiency virions are almost entirely oligomannose antigens. Proc Natl Acad Sci U S A. 2010;107(31):13800-5. Epub 2010/07/21. doi: 10.1073/pnas.1006498107. PubMed PMID: 20643940; PubMed Central PMCID: PMCPMC2922250.

106. Bonomelli C, Doores KJ, Dunlop DC, Thaney V, Dwek RA, Burton DR, et al. The glycan shield of HIV is predominantly oligomannose independently of production system or viral clade. PLoS One. 2011;6(8):e23521. Epub 2011/08/23. doi: 10.1371/journal.pone.0023521. PubMed PMID: 21858152; PubMed Central PMCID: PMCPMC3156772.

107. Binley JM, Ban YE, Crooks ET, Eggink D, Osawa K, Schief WR, et al. Role of complex carbohydrates in human immunodeficiency virus type 1 infection and resistance to antibody neutralization. J Virol. 2010;84(11):5637-55. Epub 2010/03/26. doi: 10.1128/jvi.00105-10. PubMed PMID: 20335257; PubMed Central PMCID: PMCPMC2876609.

108. Li Y, Cleveland B, Klots I, Travis B, Richardson BA, Anderson D, et al. Removal of a single N-linked glycan in human immunodeficiency virus type 1 gp120 results in an enhanced ability to induce neutralizing antibody responses. J Virol. 2008;82(2):638-51. doi: 10.1128/JVI.01691-07. PubMed PMID: 17959660; PubMed Central PMCID: PMCPMC2224603.

109. Townsley S, Li Y, Kozyrev Y, Cleveland B, Hu SL. Conserved Role of an N-Linked Glycan on the Surface Antigen of Human Immunodeficiency Virus Type 1 Modulating Virus Sensitivity to Broadly Neutralizing Antibodies against the Receptor and Coreceptor Binding Sites. J Virol. 2016;90(2):829-41. Epub 2015/10/30. doi: 10.1128/jvi.02321-15. PubMed PMID: 26512079; PubMed Central PMCID: PMCPMC4702696.

110. Doores KJ, Burton DR. Variable loop glycan dependency of the broad and potent HIV-1-neutralizing antibodies PG9 and PG16. J Virol. 2010;84(20):10510-21. doi: 10.1128/JVI.00552-10. PubMed PMID: 20686044; PubMed Central PMCID: PMCPMC2950566.

111. Stanfield RL, De Castro C, Marzaioli AM, Wilson IA, Pantophlet R. Crystal structure of the HIV neutralizing antibody 2G12 in complex with a bacterial oligosaccharide analog of mammalian oligomannose. Glycobiology. 2015;25(4):412-9. Epub 2014/11/09. doi: 10.1093/glycob/cwu123. PubMed PMID: 25380763; PubMed Central PMCID: PMCPMC4339877.

112. Starcich BR, Hahn BH, Shaw GM, McNeely PD, Modrow S, Wolf H, et al. Identification and characterization of conserved and variable regions in the envelope gene of HTLV-III/LAV, the retrovirus of AIDS. Cell. 1986;45(5):637-48. Epub 1986/06/06. PubMed PMID: 2423250.
113. Willey RL, Rutledge RA, Dias S, Folks T, Theodore T, Buckler CE, et al. Identification of conserved and divergent domains within the envelope gene of the acquired immunodeficiency syndrome retrovirus. Proc Natl Acad Sci U S A. 1986;83(14):5038-42. Epub 1986/07/01. PubMed PMID: 3014529; PubMed Central PMCID: PMCPMC323885.
114. Leonard CK, Spellman MW, Riddle L, Harris RJ, Thomas JN, Gregory TJ. Assignment of intrachain disulfide bonds and characterization of potential glycosylation sites of the type 1 recombinant human immunodeficiency virus envelope glycoprotein (gp120) expressed in Chinese hamster ovary cells. J Biol Chem. 1990;265(18):10373-82. Epub 1990/06/25. PubMed PMID: 2355006.
115. Moscoso CG, Xing L, Hui J, Hu J, Kalkhoran MB, Yenigun OM, et al. Trimeric HIV Env provides epitope occlusion mediated by hypervariable loops. Sci Rep. 2014;4:7025. Epub 2014/11/15. doi: 10.1038/srep07025. PubMed PMID: 25395053; PubMed Central PMCID: PMCPMC4231788.
116. Lasky LA, Nakamura G, Smith DH, Fennie C, Shimasaki C, Patzer E, et al. Delineation of a region of the human immunodeficiency virus type 1 gp120 glycoprotein critical for interaction with the CD4 receptor. Cell. 1987;50(6):975-85. Epub 1987/09/11. PubMed PMID: 2441877.
117. Kwong PD, Wyatt R, Robinson J, Sweet RW, Sodroski J, Hendrickson WA. Structure of an HIV gp120 envelope glycoprotein in complex with the CD4 receptor and a neutralizing human antibody. Nature. 1998;393(6686):648-59. Epub 1998/06/26. doi: 10.1038/31405. PubMed PMID: 9641677; PubMed Central PMCID: PMCPMC5629912.
118. Decker JM, Bibollet-Ruche F, Wei X, Wang S, Levy DN, Wang W, et al. Antigenic conservation and immunogenicity of the HIV coreceptor binding site. J Exp Med. 2005;201(9):1407-19. Epub 2005/05/04. doi: 10.1084/jem.20042510. PubMed PMID: 15867093; PubMed Central PMCID: PMCPMC2213183.
119. Pancera M, Zhou T, Druz A, Georgiev IS, Soto C, Gorman J, et al. Structure and immune recognition of trimeric pre-fusion HIV-1 Env. Nature. 2014;514(7523):455-61. Epub 2014/10/09. doi: 10.1038/nature13808. PubMed PMID: 25296255; PubMed Central PMCID: PMCPMC4348022.
120. Gallo SA, Finnegan CM, Viard M, Raviv Y, Dimitrov A, Rawat SS, et al. The HIV Env-mediated fusion reaction. Biochimica et biophysica acta. 2003;1614(1):36-50. Epub 2003/07/23. PubMed PMID: 12873764.
121. Klasse PJ. The molecular basis of HIV entry. Cellular microbiology. 2012;14(8):1183-92. Epub 2012/05/16. doi: 10.1111/j.1462-5822.2012.01812.x. PubMed PMID: 22583677; PubMed Central PMCID: PMCPMC3417324.
122. Zolla-Pazner S. Identifying epitopes of HIV-1 that induce protective antibodies. Nat Rev Immunol. 2004;4(3):199-210. Epub 2004/03/25. doi: 10.1038/nri1307. PubMed PMID: 15039757.
123. Jiang C, Parrish NF, Wilen CB, Li H, Chen Y, Pavlicek JW, et al. Primary infection by a human immunodeficiency virus with atypical coreceptor tropism. J Virol. 2011;85(20):10669-81. Epub 2011/08/13. doi: 10.1128/jvi.05249-11. PubMed PMID: 21835785; PubMed Central PMCID: PMCPMC3187499.
124. Gorry PR, Dunfee RL, Mefford ME, Kunstman K, Morgan T, Moore JP, et al. Changes in the V3 region of gp120 contribute to unusually broad coreceptor usage of an HIV-1 isolate from a CCR5 Delta32 heterozygote. Virology. 2007;362(1):163-78. Epub 2007/01/24. doi: 10.1016/j.virol.2006.11.025. PubMed PMID: 17239419; PubMed Central PMCID: PMCPMC1973138.

125. Shimizu N, Tanaka A, Oue A, Mori T, Ohtsuki T, Apichartpiyakul C, et al. Broad usage spectrum of G protein-coupled receptors as coreceptors by primary isolates of HIV. Aids. 2009;23(7):761-9. Epub 2009/03/25. doi: 10.1097/QAD.0b013e328326cc0d. PubMed PMID: 19307942.
126. Carter CA, Ehrlich LS. Cell biology of HIV-1 infection of macrophages. Annual review of microbiology. 2008;62:425-43. Epub 2008/09/13. doi: 10.1146/annurev.micro.62.081307.162758. PubMed PMID: 18785842.
127. Koppensteiner H, Brack-Werner R, Schindler M. Macrophages and their relevance in Human Immunodeficiency Virus Type I infection. Retrovirology. 2012;9:82. Epub 2012/10/06. doi: 10.1186/1742-4690-9-82. PubMed PMID: 23035819; PubMed Central PMCID: PMCPMC3484033.
128. Coleman CM, Wu L. HIV interactions with monocytes and dendritic cells: viral latency and reservoirs. Retrovirology. 2009;6:51. Epub 2009/06/03. doi: 10.1186/1742-4690-6-51. PubMed PMID: 19486514; PubMed Central PMCID: PMCPMC2697150.
129. Alexaki A, Liu Y, Wigdahl B. Cellular Reservoirs of HIV-1 and their Role in Viral Persistence. Current HIV research. 2008;6(5):388-400. PubMed PMID: PMC2683678.
130. Geijtenbeek TB, van Kooyk Y. DC-SIGN: a novel HIV receptor on DCs that mediates HIV-1 transmission. Current topics in microbiology and immunology. 2003;276:31-54. Epub 2003/06/12. PubMed PMID: 12797442.
131. Cavrois M, Neidleman J, Greene WC. The achilles heel of the trojan horse model of HIV-1 trans-infection. PLoS Pathog. 2008;4(6):e1000051. Epub 2008/06/28. doi: 10.1371/journal.ppat.1000051. PubMed PMID: 18584030; PubMed Central PMCID: PMCPMC2430767.
132. Izquierdo-Useros N, Lorizate M, Puertas MC, Rodriguez-Plata MT, Zangger N, Erikson E, et al. Siglec-1 is a novel dendritic cell receptor that mediates HIV-1 trans-infection through recognition of viral membrane gangliosides. PLoS biology. 2012;10(12):e1001448. Epub 2012/12/29. doi: 10.1371/journal.pbio.1001448. PubMed PMID: 23271952; PubMed Central PMCID: PMCPMC3525531 application based on this work has been filed (EP11382392.6, 2011). The authors declare that no other competing financial interests exist.
133. Moir S, Malaspina A, Li Y, Chun TW, Lowe T, Adelsberger J, et al. B cells of HIV-1-infected patients bind virions through CD21-complement interactions and transmit infectious virus to activated T cells. J Exp Med. 2000;192(5):637-46. Epub 2000/09/07. PubMed PMID: 10974030; PubMed Central PMCID: PMCPMC2193277.
134. Jiang AP, Jiang JF, Guo MG, Jin YM, Li YY, Wang JH. Human Blood-Circulating Basophils Capture HIV-1 and Mediate Viral trans-Infection of CD4+ T Cells. J Virol. 2015;89(15):8050-62. Epub 2015/05/29. doi: 10.1128/jvi.01021-15. PubMed PMID: 26018157; PubMed Central PMCID: PMCPMC4505656.
135. Patel M, Yanagishita M, Roderiquez G, Bou-Habib DC, Oravecz T, Hascall VC, et al. Cell-surface heparan sulfate proteoglycan mediates HIV-1 infection of T-cell lines. AIDS Res Hum Retroviruses. 1993;9(2):167-74. Epub 1993/02/01. doi: 10.1089/aid.1993.9.167. PubMed PMID: 8096145.
136. Bozzini S, Falcone V, Conaldi PG, Visai L, Biancone L, Dolei A, et al. Heparin-binding domain of human fibronectin binds HIV-1 gp120/160 and reduces virus infectivity. J Med Virol. 1998;54(1):44-53. Epub 1998/01/27. PubMed PMID: 9443108.
137. Vives RR, Imberty A, Sattentau QJ, Lortat-Jacob H. Heparan sulfate targets the HIV-1 envelope glycoprotein gp120 coreceptor binding site. J Biol Chem. 2005;280(22):21353-7. Epub 2005/03/31. doi: 10.1074/jbc.M500911200. PubMed PMID: 15797855.

138. Tellier MC, Greco G, Klotman M, Mosoian A, Cara A, Arap W, et al. Superfibronectin, a multimeric form of fibronectin, increases HIV infection of primary CD4+ T lymphocytes. J Immunol. 2000;164(6):3236-45. Epub 2000/03/08. PubMed PMID: 10706716.

139. Greco G, Pal S, Pasqualini R, Schnapp LM. Matrix Fibronectin Increases HIV Stability and Infectivity. The Journal of Immunology. 2002;168(11):5722-9. doi: 10.4049/jimmunol.168.11.5722.

140. Takada Y, Ye X, Simon S. The integrins. Genome Biol. 2007;8(5):215. doi: 10.1186/gb-2007-8-5-215. PubMed PMID: 17543136; PubMed Central PMCID: PMCPMC1929136.

141. Zhu J, Zhu J, Springer TA. Complete integrin headpiece opening in eight steps. J Cell Biol. 2013;201(7):1053-68. doi: 10.1083/jcb.201212037. PubMed PMID: 23798730; PubMed Central PMCID: PMCPMC3691460.

142. Harburger DS, Calderwood DA. Integrin signalling at a glance. Journal of cell science. 2009;122(Pt 2):159-63. Epub 2009/01/02. doi: 10.1242/jcs.018093. PubMed PMID: 19118207; PubMed Central PMCID: PMCPMC2714413.

143. Carragher NO, Frame MC. Focal adhesion and actin dynamics: a place where kinases and proteases meet to promote invasion. Trends in cell biology. 2004;14(5):241-9. Epub 2004/05/08. doi: 10.1016/j.tcb.2004.03.011. PubMed PMID: 15130580.

144. Huttenlocher A, Horwitz AR. Integrins in cell migration. Cold Spring Harbor perspectives in biology. 2011;3(9):a005074. Epub 2011/09/03. doi: 10.1101/cshperspect.a005074. PubMed PMID: 21885598; PubMed Central PMCID: PMCPMC3181029.

145. Gorfu G, Rivera-Nieves J, Ley K. Role of beta7 integrins in intestinal lymphocyte homing and retention. Current molecular medicine. 2009;9(7):836-50. Epub 2009/10/29. PubMed PMID: 19860663; PubMed Central PMCID: PMCPMC2770881.

146. Denucci CC, Mitchell JS, Shimizu Y. Integrin function in T-cell homing to lymphoid and nonlymphoid sites: getting there and staying there. Critical reviews in immunology. 2009;29(2):87-109. Epub 2009/06/06. PubMed PMID: 19496742; PubMed Central PMCID: PMCPMC2744463.

147. De Calisto J, Villablanca EJ, Wang S, Bono MR, Rosemblatt M, Mora JR. T-cell homing to the gut mucosa: general concepts and methodological considerations. Methods in molecular biology (Clifton, NJ). 2012;757:411-34. Epub 2011/09/13. doi: 10.1007/978-1-61779-166-6_24. PubMed PMID: 21909925.

148. del Rio ML, Bernhardt G, Rodriguez-Barbosa JI, Forster R. Development and functional specialization of CD103+ dendritic cells. Immunol Rev. 2010;234(1):268-81. Epub 2010/03/03. doi: 10.1111/j.0105-2896.2009.00874.x. PubMed PMID: 20193025.

149. Bertoni A, Alabiso O, Galetto AS, Baldanzi G. Integrins in T Cell Physiology. International journal of molecular sciences. 2018;19(2). Epub 2018/02/09. doi: 10.3390/ijms19020485. PubMed PMID: 29415483.

150. Komoriya A, Green LJ, Mervic M, Yamada SS, Yamada KM, Humphries MJ. The minimal essential sequence for a major cell type-specific adhesion site (CS1) within the alternatively spliced type III connecting segment domain of fibronectin is leucine-aspartic acid-valine. J Biol Chem. 1991;266(23):15075-9. Epub 1991/08/15. PubMed PMID: 1869542.

151. Viney JL, Jones S, Chiu HH, Lagrimas B, Renz ME, Presta LG, et al. Mucosal addressin cell adhesion molecule-1: a structural and functional analysis demarcates the integrin binding motif. J Immunol. 1996;157(6):2488-97. Epub 1996/09/15. PubMed PMID: 8805649.

152. Newham P, Craig SE, Seddon GN, Schofield NR, Rees A, Edwards RM, et al. Alpha4 integrin binding interfaces on VCAM-1 and MAdCAM-1. Integrin binding footprints identify accessory binding sites that play a role in integrin specificity. J Biol Chem. 1997;272(31):19429-40. Epub 1997/08/01. PubMed PMID: 9235944.

153. Ruoslahti E. RGD and other recognition sequences for integrins. Annual review of cell and developmental biology. 1996;12:697-715. Epub 1996/01/01. doi: 10.1146/annurev.cellbio.12.1.697. PubMed PMID: 8970741.

154. Shattil SJ, Kim C, Ginsberg MH. The final steps of integrin activation: the end game. Nat Rev Mol Cell Biol. 2010;11(4):288-300. Epub 2010/03/24. doi: 10.1038/nrm2871. PubMed PMID: 20308986; PubMed Central PMCID: PMCPMC3929966.

155. Krzysiek R, Rudent A, Bouchet-Delbos L, Foussat A, Boutillon C, Portier A, et al. Preferential and persistent depletion of CCR5+ T-helper lymphocytes with nonlymphoid homing potential despite early treatment of primary HIV infection. Blood. 2001;98(10):3169-71. Epub 2001/11/08. PubMed PMID: 11698309.

156. Wang X, Xu H, Gill AF, Pahar B, Kempf D, Rasmussen T, et al. Monitoring alpha4beta7 integrin expression on circulating CD4+ T cells as a surrogate marker for tracking intestinal CD4+ T-cell loss in SIV infection. Mucosal Immunol. 2009;2(6):518-26. doi: 10.1038/mi.2009.104. PubMed PMID: 19710637; PubMed Central PMCID: PMCPMC3702381.

157. Kader M, Wang X, Piatak M, Lifson J, Roederer M, Veazey R, et al. Alpha4(+)beta7(hi)CD4(+) memory T cells harbor most Th-17 cells and are preferentially infected during acute SIV infection. Mucosal Immunol. 2009;2(5):439-49. doi: 10.1038/mi.2009.90. PubMed PMID: 19571800; PubMed Central PMCID: PMCPMC2763371.

158. Kader M, Bixler S, Roederer M, Veazey R, Mattapallil JJ. CD4 T cell subsets in the mucosa are CD28+Ki-67-HLA-DR-CD69+ but show differential infection based on alpha4beta7 receptor expression during acute SIV infection. Journal of medical primatology. 2009;38 Suppl 1:24-31. Epub 2009/10/30. doi: 10.1111/j.1600-0684.2009.00372.x. PubMed PMID: 19863675; PubMed Central PMCID: PMCPMC2813512.

159. Cicala C, Martinelli E, McNally JP, Goode DJ, Gopaul R, Hiatt J, et al. The integrin alpha4beta7 forms a complex with cell-surface CD4 and defines a T-cell subset that is highly susceptible to infection by HIV-1. Proc Natl Acad Sci U S A. 2009;106(49):20877-82. doi: 10.1073/pnas.0911796106. PubMed PMID: 19933330; PubMed Central PMCID: PMCPMC2780317.

160. McKinnon LR, Nyanga B, Chege D, Izulla P, Kimani M, Huibner S, et al. Characterization of a human cervical CD4+ T cell subset coexpressing multiple markers of HIV susceptibility. J Immunol. 2011;187(11):6032-42. Epub 2011/11/04. doi: 10.4049/jimmunol.1101836. PubMed PMID: 22048765.

161. Liu A, Yang Y, Liu L, Meng Z, Li L, Qiu C, et al. Differential compartmentalization of HIV-targeting immune cells in inner and outer foreskin tissue. PLoS One. 2014;9(1):e85176. Epub 2014/01/24. doi: 10.1371/journal.pone.0085176. PubMed PMID: 24454812; PubMed Central PMCID: PMCPMC3893184.

162. Farstad IN, Halstensen TS, Lien B, Kilshaw PJ, Lazarovits AI, Brandtzaeg P. Distribution of beta 7 integrins in human intestinal mucosa and organized gut-associated lymphoid tissue. Immunology. 1996;89(2):227-37. Epub 1996/10/01. PubMed PMID: 8943719; PubMed Central PMCID: PMCPMC1456483.

163. Byrareddy SN, Sidell N, Arthos J, Cicala C, Zhao C, Little DM, et al. Species-specific differences in the expression and regulation of alpha4beta7 integrin in various nonhuman primates. J Immunol. 2015;194(12):5968-79. doi: 10.4049/jimmunol.1402866. PubMed PMID: 25948815.

164. Arthos J, Cicala C, Martinelli E, Macleod K, Van Ryk D, Wei D, et al. HIV-1 envelope protein binds to and signals through integrin alpha4beta7, the gut mucosal homing receptor for peripheral T cells. Nat Immunol. 2008;9(3):301-9. doi: 10.1038/ni1566. PubMed PMID: 18264102.

165. Triantafilou K, Takada Y, Triantafilou M. Mechanisms of integrin-mediated virus attachment and internalization process. Critical reviews in immunology. 2001;21(4):311-22. Epub 2002/04/02. PubMed PMID: 11922076.

166. Graham KL, Fleming FE, Halasz P, Hewish MJ, Nagesha HS, Holmes IH, et al. Rotaviruses interact with alpha4beta7 and alpha4beta1 integrins by binding the same integrin domains as natural ligands. J Gen Virol. 2005;86(Pt 12):3397-408. doi: 10.1099/vir.0.81102-0. PubMed PMID: 16298987.

167. Hait SH, Soares EA, Sprinz E, Arthos J, Machado ES, Soares MA. Worldwide Genetic Features of HIV-1 Env alpha4beta7 Binding Motif: The Local Dissemination Impact of the LDI Tripeptide. Journal of acquired immune deficiency syndromes (1999). 2015;70(5):463-71. Epub 2015/11/17. doi: 10.1097/qai.0000000000000802. PubMed PMID: 26569174; PubMed Central PMCID: PMCPMC4966603.

168. Peachman KK, Karasavvas N, Chenine AL, McLinden R, Rerks-Ngarm S, Jaranit K, et al. Identification of New Regions in HIV-1 gp120 Variable 2 and 3 Loops that Bind to alpha4beta7 Integrin Receptor. PLoS One. 2015;10(12):e0143895. Epub 2015/12/02. doi: 10.1371/journal.pone.0143895. PubMed PMID: 26625359; PubMed Central PMCID: PMCPMC4666614.

169. Tassaneetrithep B, Tivon D, Swetnam J, Karasavvas N, Michael NL, Kim JH, et al. Cryptic determinant of alpha4beta7 binding in the V2 loop of HIV-1 gp120. PLoS One. 2014;9(9):e108446. doi: 10.1371/journal.pone.0108446. PubMed PMID: 25265384; PubMed Central PMCID: PMCPMC4180765.

170. Nawaz F, Cicala C, Van Ryk D, Block KE, Jelicic K, McNally JP, et al. The genotype of early-transmitting HIV gp120s promotes alpha (4) beta(7)-reactivity, revealing alpha (4) beta(7) +/CD4+ T cells as key targets in mucosal transmission. PLoS Pathog. 2011;7(2):e1001301. doi: 10.1371/journal.ppat.1001301. PubMed PMID: 21383973; PubMed Central PMCID: PMCPMC3044691.

171. Ding J, Tasker C, Lespinasse P, Dai J, Fitzgerald-Bocarsly P, Lu W, et al. Integrin alpha4beta7 Expression Increases HIV Susceptibility in Activated Cervical CD4+ T Cells by an HIV Attachment-Independent Mechanism. Journal of acquired immune deficiency syndromes (1999). 2015;69(5):509-18. Epub 2015/07/15. doi: 10.1097/qai.0000000000000676. PubMed PMID: 26167616; PubMed Central PMCID: PMCPMC4503378.

172. Perez LG, Chen H, Liao HX, Montefiori DC. Envelope glycoprotein binding to the integrin alpha4beta7 is not a general property of most HIV-1 strains. J Virol. 2014;88(18):10767-77. doi: 10.1128/JVI.03296-13. PubMed PMID: 25008916; PubMed Central PMCID: PMCPMC4178844.

173. Parrish NF, Wilen CB, Banks LB, Iyer SS, Pfaff JM, Salazar-Gonzalez JF, et al. Transmitted/founder and chronic subtype C HIV-1 use CD4 and CCR5 receptors with equal efficiency and are not inhibited by blocking the integrin alpha4beta7. PLoS Pathog. 2012;8(5):e1002686. doi: 10.1371/journal.ppat.1002686. PubMed PMID: 22693444; PubMed Central PMCID: PMCPMC3364951.

174. O'Rourke SM, Schweighardt B, Phung P, Fonseca DP, Terry K, Wrin T, et al. Mutation at a single position in the V2 domain of the HIV-1 envelope protein confers neutralization sensitivity to a highly neutralization-resistant virus. J Virol. 2010;84(21):11200-9. doi: 10.1128/JVI.00790-10. PubMed PMID: 20702624; PubMed Central PMCID: PMCPMC2953176.

175. Pena-Cruz V, Etemad B, Chatziandreou N, Nyein PH, Stock S, Reynolds SJ, et al. HIV-1 envelope replication and alpha4beta7 utilization among newly infected subjects and their corresponding heterosexual partners. Retrovirology. 2013;10:162. Epub 2013/12/29. doi: 10.1186/1742-4690-10-162. PubMed PMID: 24369910; PubMed Central PMCID: PMCPMC3883469.

176. Etemad B, Gonzalez OA, McDonough S, Pena-Cruz V, Sagar M. Early infection HIV-1 envelope V1-V2 genotypes do not enhance binding or replication in cells expressing high levels of alpha4beta7 integrin. Journal of acquired immune deficiency syndromes (1999). 2013;64(3):249-53. Epub 2013/06/26. doi: 10.1097/QAI.0b013e3182a06ddd. PubMed PMID: 23797693; PubMed Central PMCID: PMCPMC3800220.

177. Flynn NM, Forthal DN, Harro CD, Judson FN, Mayer KH, Para MF. Placebo-controlled phase 3 trial of a recombinant glycoprotein 120 vaccine to prevent HIV-1 infection. J Infect Dis. 2005;191(5):654-65. Epub 2005/02/03. doi: 10.1086/428404. PubMed PMID: 15688278.

178. Buchbinder SP, Mehrotra DV, Duerr A, Fitzgerald DW, Mogg R, Li D, et al. Efficacy assessment of a cell-mediated immunity HIV-1 vaccine (the Step Study): a double-blind, randomised, placebo-controlled, test-of-concept trial. Lancet (London, England). 2008;372(9653):1881-93. Epub 2008/11/18. doi: 10.1016/s0140-6736(08)61591-3. PubMed PMID: 19012954; PubMed Central PMCID: PMCPMC2721012.

179. Rerks-Ngarm S, Pitisuttithum P, Nitayaphan S, Kaewkungwal J, Chiu J, Paris R, et al. Vaccination with ALVAC and AIDSVAX to prevent HIV-1 infection in Thailand. N Engl J Med. 2009;361(23):2209-20. Epub 2009/10/22. doi: 10.1056/NEJMoa0908492. PubMed PMID: 19843557.

180. Hammer SM, Sobieszczyk ME, Janes H, Karuna ST, Mulligan MJ, Grove D, et al. Efficacy trial of a DNA/rAd5 HIV-1 preventive vaccine. N Engl J Med. 2013;369(22):2083-92. doi: 10.1056/NEJMoa1310566. PubMed PMID: 24099601; PubMed Central PMCID: PMCPMC4030634.

181. Haynes BF, Gilbert PB, McElrath MJ, Zolla-Pazner S, Tomaras GD, Alam SM, et al. Immune-correlates analysis of an HIV-1 vaccine efficacy trial. N Engl J Med. 2012;366(14):1275-86. Epub 2012/04/06. doi: 10.1056/NEJMoa1113425. PubMed PMID: 22475592; PubMed Central PMCID: PMCPMC3371689.

182. Rolland M, Edlefsen PT, Larsen BB, Tovanabutra S, Sanders-Buell E, Hertz T, et al. Increased HIV-1 vaccine efficacy against viruses with genetic signatures in Env V2. Nature. 2012;490(7420):417-20. Epub 2012/09/11. doi: 10.1038/nature11519. PubMed PMID: 22960785; PubMed Central PMCID: PMCPMC3551291.

183. Liao HX, Bonsignori M, Alam SM, McLellan JS, Tomaras GD, Moody MA, et al. Vaccine induction of antibodies against a structurally heterogeneous site of immune pressure within HIV-1 envelope protein variable regions 1 and 2. Immunity. 2013;38(1):176-86. doi: 10.1016/j.immuni.2012.11.011. PubMed PMID: 23313589; PubMed Central PMCID: PMCPMC3569735.

184. Mayr LM, Cohen S, Spurrier B, Kong XP, Zolla-Pazner S. Epitope mapping of conformational V2-specific anti-HIV human monoclonal antibodies reveals an immunodominant site in V2. PLoS One. 2013;8(7):e70859. doi: 10.1371/journal.pone.0070859. PubMed PMID: 23923028; PubMed Central PMCID: PMCPMC3726596.

185. Spurrier B, Sampson J, Gorny MK, Zolla-Pazner S, Kong XP. Functional implications of the binding mode of a human conformation-dependent V2 monoclonal antibody against HIV. J Virol. 2014;88(8):4100-12. doi: 10.1128/JVI.03153-13. PubMed PMID: 24478429; PubMed Central PMCID: PMCPMC3993739.

186. Nakamura GR, Fonseca DP, O'Rourke SM, Vollrath AL, Berman PW. Monoclonal antibodies to the V2 domain of MN-rgp120: fine mapping of epitopes and inhibition of alpha4beta7 binding. PLoS One. 2012;7(6):e39045. doi: 10.1371/journal.pone.0039045. PubMed PMID: 22720026; PubMed Central PMCID: PMCPMC3374778.

187. Lazarovits AI, Moscicki RA, Kurnick JT, Camerini D, Bhan AK, Baird LG, et al. Lymphocyte activation antigens. I. A monoclonal antibody, anti-Act I, defines a new late lymphocyte

activation antigen. J Immunol. 1984;133(4):1857-62. Epub 1984/10/01. PubMed PMID: 6088627.

188. Pereira LE, Onlamoon N, Wang X, Wang R, Li J, Reimann KA, et al. Preliminary in vivo efficacy studies of a recombinant rhesus anti-alpha(4)beta(7) monoclonal antibody. Cellular immunology. 2009;259(2):165-76. Epub 2009/07/21. doi: 10.1016/j.cellimm.2009.06.012. PubMed PMID: 19616201; PubMed Central PMCID: PMCPMC2765715.

189. Ansari AA, Reimann KA, Mayne AE, Takahashi Y, Stephenson ST, Wang R, et al. Blocking of alpha4beta7 gut-homing integrin during acute infection leads to decreased plasma and gastrointestinal tissue viral loads in simian immunodeficiency virus-infected rhesus macaques. J Immunol. 2011;186(2):1044-59. doi: 10.4049/jimmunol.1003052. PubMed PMID: 21149598; PubMed Central PMCID: PMCPMC3691699.

190. Byrareddy SN, Kallam B, Arthos J, Cicala C, Nawaz F, Hiatt J, et al. Targeting alpha4beta7 integrin reduces mucosal transmission of simian immunodeficiency virus and protects gut-associated lymphoid tissue from infection. Nat Med. 2014;20(12):1397-400. doi: 10.1038/nm.3715. PubMed PMID: 25419708; PubMed Central PMCID: PMCPMC4257865.

191. Byrareddy SN, Arthos J, Cicala C, Villinger F, Ortiz KT, Little D, et al. Sustained virologic control in SIV+ macaques after antiretroviral and alpha4beta7 antibody therapy. Science. 2016;354(6309):197-202. Epub 2016/10/16. doi: 10.1126/science.aag1276. PubMed PMID: 27738167.

192. Siewe B, Landay A. Key Concepts in the Early Immunology of HIV-1 Infection. Current infectious disease reports. 2012;14(1):102-9. Epub 2011/12/29. doi: 10.1007/s11908-011-0235-3. PubMed PMID: 22203492.

193. Picker LJ. Immunopathogenesis of acute AIDS virus infection. Current opinion in immunology. 2006;18(4):399-405. Epub 2006/06/07. doi: 10.1016/j.coi.2006.05.001. PubMed PMID: 16753288.

194. Girard A, Vergnon D, Depince-Berger AE, Roblin X, Lutch F, Lambert C, et al. A high rate of beta7+ gut homing lymphocytes in HIV infected Immunogical Non Responders is associated with poor CD4 T cell recovery during suppressive HAART. Journal of acquired immune deficiency syndromes (1999). 2016. Epub 2016/02/09. doi: 10.1097/qai.0000000000000943. PubMed PMID: 26855246.

195. Li H, Pauza CD. HIV envelope-mediated, CCR5/alpha4beta7-dependent killing of CD4-negative gammadelta T cells which are lost during progression to AIDS. Blood. 2011;118(22):5824-31. Epub 2011/09/20. doi: 10.1182/blood-2011-05-356535. PubMed PMID: 21926353; PubMed Central PMCID: PMCPMC3228498.

196. Li H, Pauza CD. The alpha4beta7 integrin binds HIV envelope but does not mediate bystander killing of gammadelta T cells. Blood. 2012;120(3):698-9. doi: 10.1182/blood-2012-03-420117. PubMed PMID: 22822002.

197. Li C, Jin W, Du T, Wu B, Liu Y, Shattock RJ, et al. Binding of HIV-1 virions to alpha4beta 7 expressing cells and impact of antagonizing alpha4beta 7 on HIV-1 infection of primary CD4+ T cells. Virologica Sinica. 2014;29(6):381-92. Epub 2014/12/21. doi: 10.1007/s12250-014-3525-8. PubMed PMID: 25527342.

198. Pauls E, Ballana E, Moncunill G, Bofill M, Clotet B, Ramo-Tello C, et al. Evaluation of the anti-HIV activity of natalizumab, an antibody against integrin alpha4. Aids. 2009;23(2):266-8. Epub 2008/12/31. PubMed PMID: 19112691.

199. Arrode-Bruses G, Goode D, Kleinbeck K, Wilk J, Frank I, Byrareddy S, et al. A Small Molecule, Which Competes with MAdCAM-1, Activates Integrin alpha4beta7 and Fails to Prevent Mucosal Transmission of SHIV-SF162P3. PLoS Pathog. 2016;12(6):e1005720. Epub 2016/06/28. doi:

10.1371/journal.ppat.1005720. PubMed PMID: 27348748; PubMed Central PMCID: PMCPMC4922556.

200. Vanderslice P, Ren K, Revelle JK, Kim DC, Scott D, Bjercke RJ, et al. A cyclic hexapeptide is a potent antagonist of alpha 4 integrins. J Immunol. 1997;158(4):1710-8. Epub 1997/02/15. PubMed PMID: 9029107.

201. Schweighoffer T, Tanaka Y, Tidswell M, Erle DJ, Horgan KJ, Luce GE, et al. Selective expression of integrin alpha 4 beta 7 on a subset of human CD4+ memory T cells with Hallmarks of gut-trophism. J Immunol. 1993;151(2):717-29. Epub 1993/07/15. PubMed PMID: 7687621.

202. Doria-Rose NA, Learn GH, Rodrigo AG, Nickle DC, Li F, Mahalanabis M, et al. Human immunodeficiency virus type 1 subtype B ancestral envelope protein is functional and elicits neutralizing antibodies in rabbits similar to those elicited by a circulating subtype B envelope. J Virol. 2005;79(17):11214-24. doi: 10.1128/JVI.79.17.11214-11224.2005. PubMed PMID: 16103173; PubMed Central PMCID: PMCPMC1193599.

203. Liao HX, Sutherland LL, Xia SM, Brock ME, Scearce RM, Vanleeuwen S, et al. A group M consensus envelope glycoprotein induces antibodies that neutralize subsets of subtype B and C HIV-1 primary viruses. Virology. 2006;353(2):268-82. Epub 2006/10/14. PubMed PMID: 17039602; PubMed Central PMCID: PMCPMC1762135.

204. Sanders RW, Derking R, Cupo A, Julien JP, Yasmeen A, de Val N, et al. A next-generation cleaved, soluble HIV-1 Env trimer, BG505 SOSIP.664 gp140, expresses multiple epitopes for broadly neutralizing but not non-neutralizing antibodies. PLoS Pathog. 2013;9(9):e1003618. doi: 10.1371/journal.ppat.1003618. PubMed PMID: 24068931; PubMed Central PMCID: PMCPMC3777863.

205. Alam SM, Liao HX, Tomaras GD, Bonsignori M, Tsao CY, Hwang KK, et al. Antigenicity and immunogenicity of RV144 vaccine AIDSVAX clade E envelope immunogen is enhanced by a gp120 N-terminal deletion. J Virol. 2013;87(3):1554-68. Epub 2012/11/24. doi: 10.1128/jvi.00718-12. PubMed PMID: 23175357; PubMed Central PMCID: PMCPMC3554162.

206. McLellan JS, Pancera M, Carrico C, Gorman J, Julien JP, Khayat R, et al. Structure of HIV-1 gp120 V1/V2 domain with broadly neutralizing antibody PG9. Nature. 2011;480(7377):336-43. doi: 10.1038/nature10696. PubMed PMID: 22113616; PubMed Central PMCID: PMCPMC3406929.

207. Laursen NS, Wilson IA. Broadly neutralizing antibodies against influenza viruses. Antiviral research. 2013;98(3):476-83. Epub 2013/04/16. doi: 10.1016/j.antiviral.2013.03.021. PubMed PMID: 23583287; PubMed Central PMCID: PMCPMC3987986.

208. Hoffenberg S, Powell R, Carpov A, Wagner D, Wilson A, Kosakovsky Pond S, et al. Identification of an HIV-1 clade A envelope that exhibits broad antigenicity and neutralization sensitivity and elicits antibodies targeting three distinct epitopes. J Virol. 2013;87(10):5372-83. Epub 2013/03/08. doi: 10.1128/jvi.02827-12. PubMed PMID: 23468492; PubMed Central PMCID: PMCPMC3648150.

209. Vizcaino JA, Csordas A, Del-Toro N, Dianes JA, Griss J, Lavidas I, et al. 2016 update of the PRIDE database and its related tools. Nucleic acids research. 2016;44(22):11033. Epub 2016/09/30. doi: 10.1093/nar/gkw880. PubMed PMID: 27683222; PubMed Central PMCID: PMCPMC5159556.

210. Ruegg C, Postigo AA, Sikorski EE, Butcher EC, Pytela R, Erle DJ. Role of integrin alpha 4 beta 7/alpha 4 beta P in lymphocyte adherence to fibronectin and VCAM-1 and in homotypic cell clustering. J Cell Biol. 1992;117(1):179-89. Epub 1992/04/01. PubMed PMID: 1372909; PubMed Central PMCID: PMCPMC2289398.

211. Gutman A, Kornblihtt AR. Identification of a third region of cell-specific alternative splicing in human fibronectin mRNA. Proc Natl Acad Sci U S A. 1987;84(20):7179-82. Epub 1987/10/01. PubMed PMID: 3478690; PubMed Central PMCID: PMCPMC299253.

212. Mould AP, Wheldon LA, Komoriya A, Wayner EA, Yamada KM, Humphries MJ. Affinity chromatographic isolation of the melanoma adhesion receptor for the IIICS region of fibronectin and its identification as the integrin alpha 4 beta 1. J Biol Chem. 1990;265(7):4020-4. Epub 1990/03/05. PubMed PMID: 2137460.

213. Pollok KE, Hanenberg H, Noblitt TW, Schroeder WL, Kato I, Emanuel D, et al. High-efficiency gene transfer into normal and adenosine deaminase-deficient T lymphocytes is mediated by transduction on recombinant fibronectin fragments. J Virol. 1998;72(6):4882-92. Epub 1998/05/30. PubMed PMID: 9573255; PubMed Central PMCID: PMCPMC110042.

214. Green N, Rosebrook J, Cochran N, Tan K, Wang JH, Springer TA, et al. Mutational analysis of MAdCAM-1/alpha4beta7 interactions reveals significant binding determinants in both the first and second immunuglobulin domains. Cell adhesion and communication. 1999;7(3):167-81. Epub 2000/01/08. PubMed PMID: 10626902.

215. Clements JM, Newham P, Shepherd M, Gilbert R, Dudgeon TJ, Needham LA, et al. Identification of a key integrin-binding sequence in VCAM-1 homologous to the LDV active site in fibronectin. Journal of cell science. 1994;107 (Pt 8):2127-35. Epub 1994/08/01. PubMed PMID: 7527054.

216. Liang Y, Guttman M, Davenport TM, Hu SL, Lee KK. Probing the Impact of Local Structural Dynamics of Conformational Epitopes on Antibody Recognition. Biochemistry. 2016;55(15):2197-213. Epub 2016/03/24. doi: 10.1021/acs.biochem.5b01354. PubMed PMID: 27003615.

217. Jiang X, Totrov M, Li W, Sampson JM, Williams C, Lu H, et al. Rationally Designed Immunogens Targeting HIV-1 gp120 V1V2 Induce Distinct Conformation-Specific Antibody Responses in Rabbits. J Virol. 2016;90(24):11007-19. Epub 2016/11/01. doi: 10.1128/jvi.01409-16. PubMed PMID: 27707920; PubMed Central PMCID: PMCPMC5126360.

218. Bonsignori M, Pollara J, Moody MA, Alpert MD, Chen X, Hwang KK, et al. Antibody-dependent cellular cytotoxicity-mediating antibodies from an HIV-1 vaccine efficacy trial target multiple epitopes and preferentially use the VH1 gene family. J Virol. 2012;86(21):11521-32. Epub 2012/08/17. doi: 10.1128/jvi.01023-12. PubMed PMID: 22896626; PubMed Central PMCID: PMCPMC3486290.

219. Pankov R, Yamada KM. Fibronectin at a glance. Journal of cell science. 2002;115(Pt 20):3861-3. Epub 2002/09/24. PubMed PMID: 12244123.

220. Kewenig S, Schneider T, Hohloch K, Lampe-Dreyer K, Ullrich R, Stolte N, et al. Rapid mucosal CD4(+) T-cell depletion and enteropathy in simian immunodeficiency virus-infected rhesus macaques. Gastroenterology. 1999;116(5):1115-23. Epub 1999/04/30. PubMed PMID: 10220503.

221. Plotnik D, Guo W, Cleveland B, von Haller P, Eng JK, Guttman M, et al. Extracellular Matrix Proteins Mediate HIV-1 gp120 Interactions with alpha4beta7. J Virol. 2017. Epub 2017/08/18. doi: 10.1128/jvi.01005-17. PubMed PMID: 28814519.

222. Kimizuka F, Taguchi Y, Ohdate Y, Kawase Y, Shimojo T, Hashino K, et al. Production and characterization of functional domains of human fibronectin expressed in Escherichia coli. Journal of biochemistry. 1991;110(2):284-91. Epub 1991/08/01. PubMed PMID: 1761524.

223. Hanenberg H, Xiao XL, Dilloo D, Hashino K, Kato I, Williams DA. Colocalization of retrovirus and target cells on specific fibronectin fragments increases genetic transduction of mammalian cells. Nat Med. 1996;2(8):876-82. Epub 1996/08/01. PubMed PMID: 8705856.

224. Liao Z, Roos JW, Hildreth JE. Increased infectivity of HIV type 1 particles bound to cell surface and solid-phase ICAM-1 and VCAM-1 through acquired adhesion molecules LFA-1 and VLA-4. AIDS Res Hum Retroviruses. 2000;16(4):355-66. Epub 2000/03/15. doi: 10.1089/088922200309232. PubMed PMID: 10716373.

225. Guzzo C, Ichikawa D, Park C, Phillips D, Liu Q, Zhang P, et al. Virion incorporation of integrin alpha4beta7 facilitates HIV-1 infection and intestinal homing. Science immunology. 2017;2(11). Epub 2017/08/02. doi: 10.1126/sciimmunol.aam7341. PubMed PMID: 28763793.

226. Ito M, Baba M, Sato A, Pauwels R, De Clercq E, Shigeta S. Inhibitory effect of dextran sulfate and heparin on the replication of human immunodeficiency virus (HIV) in vitro. Antiviral research. 1987;7(6):361-7. Epub 1987/07/01. PubMed PMID: 2445284.

227. Baba M, Pauwels R, Balzarini J, Arnout J, Desmyter J, De Clercq E. Mechanism of inhibitory effect of dextran sulfate and heparin on replication of human immunodeficiency virus in vitro. Proc Natl Acad Sci U S A. 1988;85(16):6132-6. Epub 1988/08/01. PubMed PMID: 2457906; PubMed Central PMCID: PMCPMC281919.

228. Wu X, Yang ZY, Li Y, Hogerkorp CM, Schief WR, Seaman MS, et al. Rational design of envelope identifies broadly neutralizing human monoclonal antibodies to HIV-1. Science. 2010;329(5993):856-61. Epub 2010/07/10. doi: 10.1126/science.1187659. PubMed PMID: 20616233; PubMed Central PMCID: PMCPMC2965066.

229. Walker LM, Huber M, Doores KJ, Falkowska E, Pejchal R, Julien JP, et al. Broad neutralization coverage of HIV by multiple highly potent antibodies. Nature. 2011;477(7365):466-70. Epub 2011/08/19. doi: 10.1038/nature10373. PubMed PMID: 21849977; PubMed Central PMCID: PMCPMC3393110.

230. Crawford JM, Earl PL, Moss B, Reimann KA, Wyand MS, Manson KH, et al. Characterization of primary isolate-like variants of simian-human immunodeficiency virus. J Virol. 1999;73(12):10199-207. Epub 1999/11/13. PubMed PMID: 10559336; PubMed Central PMCID: PMCPMC113073.

231. Etemad-Moghadam B, Sun Y, Nicholson EK, Karlsson GB, Schenten D, Sodroski J. Determinants of neutralization resistance in the envelope glycoproteins of a simian-human immunodeficiency virus passaged in vivo. J Virol. 1999;73(10):8873-9. Epub 1999/09/11. PubMed PMID: 10482646; PubMed Central PMCID: PMCPMC112913.

232. Mascola JR, Lewis MG, Stiegler G, Harris D, VanCott TC, Hayes D, et al. Protection of Macaques against pathogenic simian/human immunodeficiency virus 89.6PD by passive transfer of neutralizing antibodies. J Virol. 1999;73(5):4009-18. Epub 1999/04/10. PubMed PMID: 10196297; PubMed Central PMCID: PMCPMC104180.

233. Trkola A, Purtscher M, Muster T, Ballaun C, Buchacher A, Sullivan N, et al. Human monoclonal antibody 2G12 defines a distinctive neutralization epitope on the gp120 glycoprotein of human immunodeficiency virus type 1. J Virol. 1996;70(2):1100-8. Epub 1996/02/01. PubMed PMID: 8551569; PubMed Central PMCID: PMCPMC189917.

234. Walker LM, Phogat SK, Chan-Hui PY, Wagner D, Phung P, Goss JL, et al. Broad and potent neutralizing antibodies from an African donor reveal a new HIV-1 vaccine target. Science. 2009;326(5950):285-9. doi: 10.1126/science.1178746. PubMed PMID: 19729618; PubMed Central PMCID: PMCPMC3335270.

235. Moore JP, Thali M, Jameson BA, Vignaux F, Lewis GK, Poon SW, et al. Immunochemical analysis of the gp120 surface glycoprotein of human immunodeficiency virus type 1: probing the structure of the C4 and V4 domains and the interaction of the C4 domain with the V3 loop. J Virol. 1993;67(8):4785-96. Epub 1993/08/01. PubMed PMID: 7687303; PubMed Central PMCID: PMCPMC237865.

236. Wyatt R, Moore J, Accola M, Desjardin E, Robinson J, Sodroski J. Involvement of the V1/V2 variable loop structure in the exposure of human immunodeficiency virus type 1 gp120 epitopes induced by receptor binding. J Virol. 1995;69(9):5723-33. Epub 1995/09/01. PubMed PMID: 7543586; PubMed Central PMCID: PMCPMC189432.

237. Bednarczyk JL, McIntyre BW. A monoclonal antibody to VLA-4 alpha-chain (CDw49d) induces homotypic lymphocyte aggregation. J Immunol. 1990;144(3):777-84. Epub 1990/02/01. PubMed PMID: 2295817.
238. Jolly C, Mitar I, Sattentau QJ. Adhesion molecule interactions facilitate human immunodeficiency virus type 1-induced virological synapse formation between T cells. J Virol. 2007;81(24):13916-21. Epub 2007/10/05. doi: 10.1128/jvi.01585-07. PubMed PMID: 17913807; PubMed Central PMCID: PMCPMC2168851.
239. Starling S, Jolly C. LFA-1 Engagement Triggers T Cell Polarization at the HIV-1 Virological Synapse. J Virol. 2016;90(21):9841-54. Epub 2016/08/26. doi: 10.1128/jvi.01152-16. PubMed PMID: 27558417; PubMed Central PMCID: PMCPMC5068534.
240. van Kooyk Y, van de Wiel-van Kemenade P, Weder P, Kuijpers TW, Figdor CG. Enhancement of LFA-1-mediated cell adhesion by triggering through CD2 or CD3 on T lymphocytes. Nature. 1989;342(6251):811-3. Epub 1989/12/14. doi: 10.1038/342811a0. PubMed PMID: 2574829.
241. Dustin ML, Springer TA. T-cell receptor cross-linking transiently stimulates adhesiveness through LFA-1. Nature. 1989;341(6243):619-24. Epub 1989/10/19. doi: 10.1038/341619a0. PubMed PMID: 2477710.
242. Drbal K, Angelisova P, Cerny J, Hilgert I, Horejsi V. A novel anti-CD18 mAb recognizes an activation-related epitope and induces a high-affinity conformation in leukocyte integrins. Immunobiology. 2001;203(4):687-98. Epub 2001/06/14. doi: 10.1016/s0171-2985(01)80017-6. PubMed PMID: 11402502.
243. Shimizu Y, van Seventer GA, Horgan KJ, Shaw S. Costimulation of proliferative responses of resting CD4+ T cells by the interaction of VLA-4 and VLA-5 with fibronectin or VLA-6 with laminin. J Immunol. 1990;145(1):59-67. Epub 1990/07/01. PubMed PMID: 1972721.
244. Tsukamoto T, Okada S. The use of RetroNectin in studies requiring in vitro HIV-1 infection of human hematopoietic stem/progenitor cells. Journal of virological methods. 2017;248:234-7. Epub 2017/08/10. doi: 10.1016/j.jviromet.2017.08.003. PubMed PMID: 28789988.
245. Ho O, Larsen K, Polacino P, Li Y, Anderson D, Song R, et al. Pathogenic infection of Macaca nemestrina with a CCR5-tropic subtype-C simian-human immunodeficiency virus. Retrovirology. 2009;6:65. doi: 10.1186/1742-4690-6-65. PubMed PMID: 19602283; PubMed Central PMCID: PMCPMC2720380.
246. Martin AP, Ortiz S, Cabalier ME, Frede S, Burgos E, Hliba E, et al. Vascular endothelium express CS-1 fibronectin in allergic contact dermatitis. Journal of cutaneous pathology. 2002;29(6):347-53. Epub 2002/07/24. PubMed PMID: 12135465.
247. Elices MJ, Tsai V, Strahl D, Goel AS, Tollefson V, Arrhenius T, et al. Expression and functional significance of alternatively spliced CS1 fibronectin in rheumatoid arthritis microvasculature. J Clin Invest. 1994;93(1):405-16. Epub 1994/01/01. doi: 10.1172/jci116975. PubMed PMID: 8282813; PubMed Central PMCID: PMCPMC293796.
248. Meek RM, McLellan S, Crossan JF. Dupuytren's disease. A model for the mechanism of fibrosis and its modulation by steroids. The Journal of bone and joint surgery British volume. 1999;81(4):732-8. Epub 1999/08/27. PubMed PMID: 10463754.
249. Kamarajan P, Garcia-Pardo A, D'Silva NJ, Kapila YL. The CS1 segment of fibronectin is involved in human OSCC pathogenesis by mediating OSCC cell spreading, migration, and invasion. BMC cancer. 2010;10:330. Epub 2010/06/29. doi: 10.1186/1471-2407-10-330. PubMed PMID: 20579373; PubMed Central PMCID: PMCPMC3146068.
250. Magnuson VL, Young M, Schattenberg DG, Mancini MA, Chen DL, Steffensen B, et al. The alternative splicing of fibronectin pre-mRNA is altered during aging and in response to growth factors. J Biol Chem. 1991;266(22):14654-62. Epub 1991/08/05. PubMed PMID: 1713586.

251. Rosi E, Beckmann JD, Pladsen P, Rennard SI, Romberger DJ. Modulation of human bronchial epithelial cell IIICS fibronectin mRNA in vitro. The European respiratory journal. 1996;9(3):549-55. Epub 1996/03/01. PubMed PMID: 8730018.

252. Pal S, Schnapp LM. HIV-Infected Lymphocytes Regulate Fibronectin Synthesis by TGF 1 Secretion. The Journal of Immunology. 2004;172(5):3189-95. doi: 10.4049/jimmunol.172.5.3189.

253. Brown BK, Darden, J.M., Tovanabutra,S., Oblander, T., Frost, J., Sanders-Buell, E., de Sousa, M.S., Birx, D.L., McCutchan, F.E. and Polonis, V.R. Biologic and Genetic Characterization of a Panel of 60 Human Immunodeficiency Virus Type 1 Isolates, Representing Clades A, B, C, D, CRF01_AE, and CRF02_AG, for the Development and Assessment of Candidate Vaccines. J Virology 2005;79(10): 6089-101.

254. Gartner S, Markovits P, Markovitz DM, Kaplan MH, Gallo RC, Popovic M. The role of mononuclear phagocytes in HTLV-III/LAV infection. Science. 1986;233(4760):215-9. Epub 1986/07/11. PubMed PMID: 3014648.

255. Cheng-Mayer C, Levy JA. Distinct biological and serological properties of human immunodeficiency viruses from the brain. Annals of neurology. 1988;23 Suppl:S58-61. Epub 1988/01/01. PubMed PMID: 3258140.

256. Lindenbach BD. Measuring HCV infectivity produced in cell culture and in vivo. Methods in molecular biology (Clifton, NJ). 2009;510:329-36. Epub 2008/11/15. doi: 10.1007/978-1-59745-394-3_24. PubMed PMID: 19009272.

257. Julg B, Sok D, Schmidt SD, Abbink P, Newman RM, Broge T, et al. Protective Efficacy of Broadly Neutralizing Antibodies with Incomplete Neutralization Activity against Simian-Human Immunodeficiency Virus in Rhesus Monkeys. J Virol. 2017;91(20). Epub 2017/08/05. doi: 10.1128/jvi.01187-17. PubMed PMID: 28768869; PubMed Central PMCID: PMCPMC5625479.

258. Gautam R, Nishimura Y, Pegu A, Nason MC, Klein F, Gazumyan A, et al. A single injection of anti-HIV-1 antibodies protects against repeated SHIV challenges. Nature. 2016;533(7601):105-9. Epub 2016/04/28. doi: 10.1038/nature17677. PubMed PMID: 27120156; PubMed Central PMCID: PMCPMC5127204.

259. Julg B, Tartaglia LJ, Keele BF, Wagh K, Pegu A, Sok D, et al. Broadly neutralizing antibodies targeting the HIV-1 envelope V2 apex confer protection against a clade C SHIV challenge. Sci Transl Med. 2017;9(406). Epub 2017/09/08. doi: 10.1126/scitranslmed.aal1321. PubMed PMID: 28878010; PubMed Central PMCID: PMCPMC5755978.

260. Shingai M, Donau OK, Plishka RJ, Buckler-White A, Mascola JR, Nabel GJ, et al. Passive transfer of modest titers of potent and broadly neutralizing anti-HIV monoclonal antibodies block SHIV infection in macaques. J Exp Med. 2014;211(10):2061-74. Epub 2014/08/27. doi: 10.1084/jem.20132494. PubMed PMID: 25155019; PubMed Central PMCID: PMCPMC4172223.

261. Saunders KO, Pegu A, Georgiev IS, Zeng M, Joyce MG, Yang ZY, et al. Sustained Delivery of a Broadly Neutralizing Antibody in Nonhuman Primates Confers Long-Term Protection against Simian/Human Immunodeficiency Virus Infection. J Virol. 2015;89(11):5895-903. Epub 2015/03/20. doi: 10.1128/jvi.00210-15. PubMed PMID: 25787288; PubMed Central PMCID: PMCPMC4442454.

262. Hu SL, Abrams K, Barber GN, Moran P, Zarling JM, Langlois AJ, et al. Protection of macaques against SIV infection by subunit vaccines of SIV envelope glycoprotein gp160. Science. 1992;255(5043):456-9. Epub 1992/01/24. PubMed PMID: 1531159.

263. Checkley MA, Luttge BG, Freed EO. HIV-1 envelope glycoprotein biosynthesis, trafficking, and incorporation. J Mol Biol. 2011;410(4):582-608. Epub 2011/07/19. doi: 10.1016/j.jmb.2011.04.042. PubMed PMID: 21762802; PubMed Central PMCID: PMCPMC3139147.

264. Rao M, Peachman KK, Kim J, Gao G, Alving CR, Michael NL, et al. HIV-1 variable loop 2 and its importance in HIV-1 infection and vaccine development. Curr HIV Res. 2013;11(5):427-38. Epub 2013/11/07. PubMed PMID: 24191938; PubMed Central PMCID: PMCPMC4086350.
265. Chand S, Messina EL, AlSalmi W, Ananthaswamy N, Gao G, Uritskiy G, et al. Glycosylation and oligomeric state of envelope protein might influence HIV-1 virion capture by alpha4beta7 integrin. Virology. 2017;508:199-212. Epub 2017/06/05. doi: 10.1016/j.virol.2017.05.016. PubMed PMID: 28577856; PubMed Central PMCID: PMCPMC5526109.
266. Guo W, Cleveland B, Davenport TM, Lee KK, Hu SL. Purification of recombinant vaccinia virus-expressed monomeric HIV-1 gp120 to apparent homogeneity. Protein Expr Purif. 2013;90(1):34-9. doi: 10.1016/j.pep.2013.04.009. PubMed PMID: 23665667; PubMed Central PMCID: PMCPMC3718289.
267. Drillien R, Spehner D, Kirn A. Host range restriction of vaccinia virus in Chinese hamster ovary cells: relationship to shutoff of protein synthesis. J Virol. 1978;28(3):843-50. Epub 1978/12/01. PubMed PMID: 310474; PubMed Central PMCID: PMCPMC525809.
268. Ramsey-Ewing A, Moss B. Recombinant protein synthesis in Chinese hamster ovary cells using a vaccinia virus/bacteriophage T7 hybrid expression system. J Biol Chem. 1996;271(28):16962-6. Epub 1996/07/12. PubMed PMID: 8663285.
269. Jelicic K, Cimbro R, Nawaz F, Huang da W, Zheng X, Yang J, et al. The HIV-1 envelope protein gp120 impairs B cell proliferation by inducing TGF-beta1 production and FcRL4 expression. Nat Immunol. 2013;14(12):1256-65. doi: 10.1038/ni.2746. PubMed PMID: 24162774; PubMed Central PMCID: PMCPMC3870659.
270. Stanley P, Narasimhan S, Siminovitch L, Schachter H. Chinese hamster ovary cells selected for resistance to the cytotoxicity of phytohemagglutinin are deficient in a UDP-N-acetylglucosamine--glycoprotein N-acetylglucosaminyltransferase activity. Proc Natl Acad Sci U S A. 1975;72(9):3323-7. Epub 1975/09/01. PubMed PMID: 1059116; PubMed Central PMCID: PMCPMC432984.
271. Elbein AD, Tropea JE, Mitchell M, Kaushal GP. Kifunensine, a potent inhibitor of the glycoprotein processing mannosidase I. J Biol Chem. 1990;265(26):15599-605. Epub 1990/09/15. PubMed PMID: 2144287.
272. Raska M, Takahashi K, Czernekova L, Zachova K, Hall S, Moldoveanu Z, et al. Glycosylation patterns of HIV-1 gp120 depend on the type of expressing cells and affect antibody recognition. J Biol Chem. 2010;285(27):20860-9. Epub 2010/05/05. doi: 10.1074/jbc.M109.085472. PubMed PMID: 20439465; PubMed Central PMCID: PMCPMC2898351.
273. Mackett M, Smith GL, Moss B. General method for production and selection of infectious vaccinia virus recombinants expressing foreign genes. J Virol. 1984;49(3):857-64. Epub 1984/03/01. PubMed PMID: 6321770; PubMed Central PMCID: PMCPMC255547.
274. Hu SL, Kosowski SG, Dalrymple JM. Expression of AIDS virus envelope gene in recombinant vaccinia viruses. Nature. 1986;320(6062):537-40. Epub 1986/04/10. doi: 10.1038/320537a0. PubMed PMID: 3008002.
275. Chakrabarti S, Robert-Guroff M, Wong-Staal F, Gallo RC, Moss B. Expression of the HTLV-III envelope gene by a recombinant vaccinia virus. Nature. 1986;320(6062):535-7. Epub 1986/04/10. doi: 10.1038/320535a0. PubMed PMID: 3008001.
276. Cooney EL, Collier AC, Greenberg PD, Coombs RW, Zarling J, Arditti DE, et al. Safety of and immunological response to a recombinant vaccinia virus vaccine expressing HIV envelope glycoprotein. Lancet (London, England). 1991;337(8741):567-72. Epub 1991/03/09. PubMed PMID: 1671940.
277. Cooney EL, McElrath MJ, Corey L, Hu SL, Collier AC, Arditti D, et al. Enhanced immunity to human immunodeficiency virus (HIV) envelope elicited by a combined vaccine regimen

consisting of priming with a vaccinia recombinant expressing HIV envelope and boosting with gp160 protein. Proc Natl Acad Sci U S A. 1993;90(5):1882-6. Epub 1993/03/01. PubMed PMID: 8446603; PubMed Central PMCID: PMCPMC45984.

278. Graham BS, Gorse GJ, Schwartz DH, Keefer MC, McElrath MJ, Matthews TJ, et al. Determinants of antibody response after recombinant gp160 boosting in vaccinia-naive volunteers primed with gp160-recombinant vaccinia virus. The National Institute of Allergy and Infectious Diseases AIDS Vaccine Clinical Trials Network. J Infect Dis. 1994;170(4):782-6. Epub 1994/10/01. PubMed PMID: 7930718.

279. Pialoux G, Excler JL, Riviere Y, Gonzalez-Canali G, Feuillie V, Coulaud P, et al. A prime-boost approach to HIV preventive vaccine using a recombinant canarypox virus expressing glycoprotein 160 (MN) followed by a recombinant glycoprotein 160 (MN/LAI). The AGIS Group, and l'Agence Nationale de Recherche sur le SIDA. AIDS Res Hum Retroviruses. 1995;11(3):373-81. Epub 1995/03/01. doi: 10.1089/aid.1995.11.373. PubMed PMID: 7598771.

280. Nitayaphan S, Pitisuttithum P, Karnasuta C, Eamsila C, de Souza M, Morgan P, et al. Safety and immunogenicity of an HIV subtype B and E prime-boost vaccine combination in HIV-negative Thai adults. J Infect Dis. 2004;190(4):702-6. Epub 2004/07/24. doi: 10.1086/422258. PubMed PMID: 15272397.

281. Garcia-Arriaza J, Perdiguero B, Heeney J, Seaman M, Montefiori DC, Labranche C, et al. Head-to-Head Comparison of Poxvirus NYVAC and ALVAC Vectors Expressing Identical HIV-1 Clade C Immunogens in Prime-Boost Combination with Env Protein in Nonhuman Primates. J Virol. 2015;89(16):8525-39. Epub 2015/06/05. doi: 10.1128/jvi.01265-15. PubMed PMID: 26041302; PubMed Central PMCID: PMCPMC4524234.

282. Cox WI, Tartaglia J, Paoletti E. Induction of cytotoxic T lymphocytes by recombinant canarypox (ALVAC) and attenuated vaccinia (NYVAC) viruses expressing the HIV-1 envelope glycoprotein. Virology. 1993;195(2):845-50. Epub 1993/08/01. doi: 10.1006/viro.1993.1442. PubMed PMID: 8337851.

283. Pejchal R, Doores KJ, Walker LM, Khayat R, Huang PS, Wang SK, et al. A potent and broad neutralizing antibody recognizes and penetrates the HIV glycan shield. Science. 2011;334(6059):1097-103. Epub 2011/10/15. doi: 10.1126/science.1213256. PubMed PMID: 21998254; PubMed Central PMCID: PMCPMC3280215.

284. Chakrabarti S, Sisler JR, Moss B. Compact, synthetic, vaccinia virus early/late promoter for protein expression. BioTechniques. 1997;23(6):1094-7. Epub 1998/01/09. PubMed PMID: 9421642.

285. Rasmussen RA, Ong H, Song R, Chenine AL, Ayash-Rashkovsky M, Hu SL, et al. Efficacy of a multigenic protein vaccine containing multimeric HIV gp160 against heterologous SHIV clade C challenges. Aids. 2007;21(14):1841-8. Epub 2007/08/28. doi: 10.1097/QAD.0b013e32828684ea. PubMed PMID: 17721091.

286. Guttman M, Varadi C, Lee KK, Guttman A. Comparative glycoprofiling of HIV gp120 immunogens by capillary electrophoresis and MALDI mass spectrometry. Electrophoresis. 2015;36(11-12):1305-13. Epub 2015/03/27. doi: 10.1002/elps.201500054. PubMed PMID: 25809283; PubMed Central PMCID: PMCPMC4544863.

287. Campbell MP, Royle L, Radcliffe CM, Dwek RA, Rudd PM. GlycoBase and autoGU: tools for HPLC-based glycan analysis. Bioinformatics (Oxford, England). 2008;24(9):1214-6. Epub 2008/03/18. doi: 10.1093/bioinformatics/btn090. PubMed PMID: 18344517.

288. Darc M, Hait SH, Soares EA, Cicala C, Seuanez HN, Machado ES, et al. Polymorphisms in the alpha4 integrin of neotropical primates: insights for binding of natural ligands and HIV-1 gp120 to the human alpha4beta7. PLoS One. 2011;6(9):e24461. Epub 2011/09/14. doi:

10.1371/journal.pone.0024461. PubMed PMID: 21912696; PubMed Central PMCID: PMCPMC3166318.

289. Reitano KN, Kottilil S, Gille CM, Zhang X, Yan M, O'Shea MA, et al. Defective plasmacytoid dendritic cell-NK cell cross-talk in HIV infection. AIDS Res Hum Retroviruses. 2009;25(10):1029-37. Epub 2009/10/03. doi: 10.1089/aid.2008.0311. PubMed PMID: 19795986; PubMed Central PMCID: PMCPMC2828160.

290. Alvarez Y, Tuen M, Shen G, Nawaz F, Arthos J, Wolff MJ, et al. Preferential HIV infection of CCR6+ Th17 cells is associated with higher levels of virus receptor expression and lack of CCR5 ligands. J Virol. 2013;87(19):10843-54. doi: 10.1128/JVI.01838-13. PubMed PMID: 23903844; PubMed Central PMCID: PMCPMC3807416.

291. He X, Mokili JL, Hong K, Chen J, Wei J, Xin R, et al. Conservancy of the alpha4beta7 integrin mimotope in the V2 domain of HIV type 1 CRF07_BC compared to subtype B' strains in China. AIDS Res Hum Retroviruses. 2011;27(10):1127-33. Epub 2011/03/23. doi: 10.1089/aid.2011.0007. PubMed PMID: 21417760.

292. Mota TM, Murray JM, Center RJ, Purcell DF, McCaw JM. Application of a case-control study design to investigate genotypic signatures of HIV-1 transmission. Retrovirology. 2012;9:54. Epub 2012/06/27. doi: 10.1186/1742-4690-9-54. PubMed PMID: 22731404; PubMed Central PMCID: PMCPMC3419081.

293. Richardson SI, Gray ES, Mkhize NN, Sheward DJ, Lambson BE, Wibmer CK, et al. South African HIV-1 subtype C transmitted variants with a specific V2 motif show higher dependence on alpha4beta7 for replication. Retrovirology. 2015;12:54. Epub 2015/06/25. doi: 10.1186/s12977-015-0183-3. PubMed PMID: 26105197; PubMed Central PMCID: PMCPMC4479312.

294. Gorny MK, Pan R, Williams C, Wang XH, Volsky B, O'Neal T, et al. Functional and immunochemical cross-reactivity of V2-specific monoclonal antibodies from HIV-1-infected individuals. Virology. 2012;427(2):198-207. Epub 2012/03/10. doi: 10.1016/j.virol.2012.02.003. PubMed PMID: 22402248; PubMed Central PMCID: PMCPMC3572902.

295. Zolla-Pazner S, deCamp AC, Cardozo T, Karasavvas N, Gottardo R, Williams C, et al. Analysis of V2 antibody responses induced in vaccinees in the ALVAC/AIDSVAX HIV-1 vaccine efficacy trial. PLoS One. 2013;8(1):e53629. Epub 2013/01/26. doi: 10.1371/journal.pone.0053629. PubMed PMID: 23349725; PubMed Central PMCID: PMCPMC3547933.

296. Shen G, Upadhyay C, Zhang J, Pan R, Zolla-Pazner S, Kong XP, et al. Rationally Targeted Mutations at the V1V2 Domain of the HIV-1 Envelope to Augment Virus Neutralization by Anti-V1V2 Monoclonal Antibodies. PLoS One. 2015;10(10):e0141233. Epub 2015/10/23. doi: 10.1371/journal.pone.0141233. PubMed PMID: 26491873; PubMed Central PMCID: PMCPMC4619609.

297. Pan R, Gorny MK, Zolla-Pazner S, Kong XP. The V1V2 Region of HIV-1 gp120 Forms a Five-Stranded Beta Barrel. J Virol. 2015;89(15):8003-10. Epub 2015/05/29. doi: 10.1128/jvi.00754-15. PubMed PMID: 26018158; PubMed Central PMCID: PMCPMC4505664.

298. Torres OB, Matyas GR, Rao M, Peachman KK, Jalah R, Beck Z, et al. Heroin-HIV-1 (H2) vaccine: induction of dual immunologic effects with a heroin hapten-conjugate and an HIV-1 envelope V2 peptide with liposomal lipid A as an adjuvant. NPJ vaccines. 2017;2:13. Epub 2017/12/22. doi: 10.1038/s41541-017-0013-9. PubMed PMID: 29263870; PubMed Central PMCID: PMCPMC5604742 that is jointly owned by the US Army and the US Department of Health and Human Services. Other authors declare no conflicts.

299. Powell RLR, Totrov M, Itri V, Liu X, Fox A, Zolla-Pazner S. Plasticity and Epitope Exposure of the HIV-1 Envelope Trimer. J Virol. 2017;91(17). Epub 2017/06/16. doi: 10.1128/jvi.00410-17. PubMed PMID: 28615206; PubMed Central PMCID: PMCPMC5553165.

300. Santangelo PJ, Cicala C, Byrareddy SN, Ortiz KT, Little D, Lindsay KE, et al. Early treatment of SIV+ macaques with an alpha4beta7 mAb alters virus distribution and preserves CD4(+) T cells in later stages of infection. Mucosal Immunol. 2017. Epub 2018/01/19. doi: 10.1038/mi.2017.112. PubMed PMID: 29346349.

301. Girard A, Jelicic K, Van Ryk D, Rochereau N, Cicala C, Arthos J, et al. Neutralizing and Targeting Properties of a New Set of alpha4beta7-Specific Antibodies Are Influenced by Their Isotype. Journal of acquired immune deficiency syndromes (1999). 2017;75(1):118-27. Epub 2017/02/09. doi: 10.1097/qai.0000000000001307. PubMed PMID: 28177967.

302. Martinelli E, Tharinger H, Frank I, Arthos J, Piatak M, Jr., Lifson JD, et al. HSV-2 infection of dendritic cells amplifies a highly susceptible HIV-1 cell target. PLoS Pathog. 2011;7(6):e1002109. Epub 2011/07/09. doi: 10.1371/journal.ppat.1002109. PubMed PMID: 21738472; PubMed Central PMCID: PMCPMC3128120.

303. Martinelli E, Veglia F, Goode D, Guerra-Perez N, Aravantinou M, Arthos J, et al. The frequency of alpha(4)beta(7)(high) memory CD4(+) T cells correlates with susceptibility to rectal simian immunodeficiency virus infection. Journal of acquired immune deficiency syndromes (1999). 2013;64(4):325-31. Epub 2013/06/26. doi: 10.1097/QAI.0b013e31829f6e1a. PubMed PMID: 23797688; PubMed Central PMCID: PMCPMC3815485.

304. Goode D, Truong R, Villegas G, Calenda G, Guerra-Perez N, Piatak M, et al. HSV-2-driven increase in the expression of alpha4beta7 correlates with increased susceptibility to vaginal SHIV(SF162P3) infection. PLoS Pathog. 2014;10(12):e1004567. Epub 2014/12/19. doi: 10.1371/journal.ppat.1004567. PubMed PMID: 25521298; PubMed Central PMCID: PMCPMC4270786.

305. Goode D, Aravantinou M, Jarl S, Truong R, Derby N, Guerra-Perez N, et al. Sex hormones selectively impact the endocervical mucosal microenvironment: implications for HIV transmission. PLoS One. 2014;9(5):e97767. Epub 2014/05/17. doi: 10.1371/journal.pone.0097767. PubMed PMID: 24830732; PubMed Central PMCID: PMCPMC4022654.

306. Hait SH, Darc M, Machado ES, Soares EA, Sprinz E, Soares MA. Conservation of the alpha4beta7 lymphocyte homing receptor in HIV-infected patients with distinct transmission routes and disease progression profiles. AIDS Res Hum Retroviruses. 2014;30(5):493-7. Epub 2014/01/07. doi: 10.1089/aid.2013.0248. PubMed PMID: 24387749.

307. Lu X, Li Z, Li Q, Jiao Y, Ji Y, Zhang H, et al. Preferential loss of gut-homing alpha4beta7 CD4(+) T cells and their circulating functional subsets in acute HIV-1 infection. Cellular & molecular immunology. 2016;13(6):776-84. Epub 2015/08/19. doi: 10.1038/cmi.2015.60. PubMed PMID: 26277899; PubMed Central PMCID: PMCPMC5101442.

308. Joag VR, McKinnon LR, Liu J, Kidane ST, Yudin MH, Nyanga B, et al. Identification of preferential CD4+ T-cell targets for HIV infection in the cervix. Mucosal Immunol. 2016;9(1):1-12. Epub 2015/04/16. doi: 10.1038/mi.2015.28. PubMed PMID: 25872482.

309. Sivro A, Schuetz A, Sheward D, Joag V, Yegorov S, Liebenberg LJ, et al. Integrin alpha4beta7 expression on peripheral blood CD4(+) T cells predicts HIV acquisition and disease progression outcomes. Sci Transl Med. 2018;10(425). Epub 2018/01/26. doi: 10.1126/scitranslmed.aam6354. PubMed PMID: 29367348.

310. Sattentau Q. HIV's gut feeling. Nat Immunol. 2008;9(3):225-7. Epub 2008/02/21. doi: 10.1038/ni0308-225. PubMed PMID: 18285769.

311. Johnson RP. How HIV guts the immune system. N Engl J Med. 2008;358(21):2287-9. Epub 2008/05/24. doi: 10.1056/NEJMcibr0802134. PubMed PMID: 18499575.

312. Cicala C, Arthos J, Fauci AS. HIV-1 envelope, integrins and co-receptor use in mucosal transmission of HIV. Journal of translational medicine. 2011;9 Suppl 1:S2. Epub 2011/02/10. doi:

10.1186/1479-5876-9-s1-s2. PubMed PMID: 21284901; PubMed Central PMCID: PMCPMC3105502.

313. Wilen CB, Tilton JC, Doms RW. HIV: cell binding and entry. Cold Spring Harbor perspectives in medicine. 2012;2(8). Epub 2012/08/22. doi: 10.1101/cshperspect.a006866. PubMed PMID: 22908191; PubMed Central PMCID: PMCPMC3405824.

314. McKinnon LR, Kaul R. Quality and quantity: mucosal CD4+ T cells and HIV susceptibility. Curr Opin HIV AIDS. 2012;7(2):195-202. Epub 2012/02/09. doi: 10.1097/COH.0b013e3283504941. PubMed PMID: 22314505.

315. O'Connell RJ, Excler JL. HIV vaccine efficacy and immune correlates of risk. Curr HIV Res. 2013;11(6):450-63. Epub 2013/09/17. PubMed PMID: 24033301.

316. Cicala C, Arthos J. Virion attachment and entry: HIV gp120 Env biotinylation, gp120 Env, or integrin ligand-binding assay. Methods in molecular biology (Clifton, NJ). 2014;1087:3-12. Epub 2013/10/26. doi: 10.1007/978-1-62703-670-2_1. PubMed PMID: 24158809.

317. Girard A, Rochereau N, Roblin X, Genin C, Paul S. [Targeting and role of alpha4beta7 integrin in the pathophysiology of IBD and HIV infection]. Medecine sciences : M/S. 2015;31(10):895-903. Epub 2015/10/21. doi: 10.1051/medsci/20153110016. PubMed PMID: 26481029.

318. Pham HT, Mesplede T. The latest evidence for possible HIV-1 curative strategies. Drugs in context. 2018;7:212522. Epub 2018/03/03. doi: 10.7573/dic.212522. PubMed PMID: 29497452; PubMed Central PMCID: PMCPMC5824924.

319. Arthos J, Cicala C, Nawaz F, Byrareddy SN, Villinger F, Santangelo PJ, et al. The Role of Integrin alpha4beta7 in HIV Pathogenesis and Treatment. Current HIV/AIDS reports. 2018;15(2):127-35. Epub 2018/02/27. doi: 10.1007/s11904-018-0382-3. PubMed PMID: 29478152; PubMed Central PMCID: PMCPMC5882766.

320. Ransohoff RM. Natalizumab and PML. Nature neuroscience. 2005;8(10):1275. Epub 2005/09/29. doi: 10.1038/nn1005-1275. PubMed PMID: 16189528.

321. Howell AL, Taylor TH, Miller JD, Groveman DS, Eccles EH, Zacharski LR. Inhibition of HIV-1 infectivity by low molecular weight heparin. Results of in vitro studies and a pilot clinical trial in patients with advanced AIDS. International journal of clinical & laboratory research. 1996;26(2):124-31. Epub 1996/01/01. PubMed PMID: 8856366.

322. Gellibert F, de Gouville AC, Woolven J, Mathews N, Nguyen VL, Bertho-Ruault C, et al. Discovery of 4-{4-[3-(pyridin-2-yl)-1H-pyrazol-4-yl]pyridin-2-yl}-N-(tetrahydro-2H- pyran-4-yl)benzamide (GW788388): a potent, selective, and orally active transforming growth factor-beta type I receptor inhibitor. Journal of medicinal chemistry. 2006;49(7):2210-21. Epub 2006/03/31. doi: 10.1021/jm0509905. PubMed PMID: 16570917.

323. Bonafoux D, Lee WC. Strategies for TGF-beta modulation: a review of recent patents. Expert opinion on therapeutic patents. 2009;19(12):1759-69. Epub 2009/11/27. doi: 10.1517/13543770903397400. PubMed PMID: 19939191.

324. Hawinkels LJ, Ten Dijke P. Exploring anti-TGF-beta therapies in cancer and fibrosis. Growth factors (Chur, Switzerland). 2011;29(4):140-52. Epub 2011/07/02. doi: 10.3109/08977194.2011.595411. PubMed PMID: 21718111.

325. Vincenti F, Fervenza FC, Campbell KN, Diaz M, Gesualdo L, Nelson P, et al. A Phase 2, Double-Blind, Placebo-Controlled, Randomized Study of Fresolimumab in Patients With Steroid-Resistant Primary Focal Segmental Glomerulosclerosis. Kidney international reports. 2017;2(5):800-10. Epub 2017/12/23. doi: 10.1016/j.ekir.2017.03.011. PubMed PMID: 29270487; PubMed Central PMCID: PMCPMC5733825.

326. Theron AJ, Anderson R, Rossouw TM, Steel HC. The Role of Transforming Growth Factor Beta-1 in the Progression of HIV/AIDS and Development of Non-AIDS-Defining Fibrotic Disorders.

Frontiers in immunology. 2017;8:1461. Epub 2017/11/23. doi: 10.3389/fimmu.2017.01461. PubMed PMID: 29163528; PubMed Central PMCID: PMCPMC5673850.

Vita

David Alan Plotnik was born in Pullman, Washington. In 2003 he earned a Bachelor of Natural Health Sciences and a Master of Acupuncture and Oriental Medicine from Bastyr University in Kenmore, Washington. From 2005 to 2012 he was employed as a scientist in the Radiation Oncology Department at the University of Washington. In 2011 he earned a second Bachelor's degree in Molecular, Cellular, and Developmental Biology from the University of Washington. In 2012 he joined the Department of Pharmaceutics at the University of Washington as a Ph.D student, and worked in the laboratory of Dr. Shiu-Lok Hu from 2012 to 2018 to complete his Ph.D.